

**The Modelling of a
Falling Sludge Bed Reactor
using AQUASIM**

Neil E. Ristow

**Department of Chemical Engineering
University of Cape Town
Rondebosch, 7701
South Africa**

submitted 20 October 1999

**This dissertation is submitted for the degree of Master
of Science at the University of Cape Town**

The copyright of this thesis vests in the author. No quotation from it or information derived from it is to be published without full acknowledgement of the source. The thesis is to be used for private study or non-commercial research purposes only.

Published by the University of Cape Town (UCT) in terms of the non-exclusive license granted to UCT by the author.

ACKNOWLEDGEMENTS

I would like to thank the following groups and individuals for their input, guidance, patience and funding:

The Water Research Commission for the project funding

Professor P. Rose, K. Wittington-Jones and C. Corbett from Rhodes University, Department of Biochemistry and Microbiology, for operational data, discussion on the model development, and assessment of the simulated data

Dr M.R. Kosseva for the extensive collection of papers

A.W. Breed, C. Corbett, C. Erasmus, S. Jahren and J. van Rensburg for proof reading of the report

Professor G. Hansford for the project supervision

J. van Rensburg for financial assistance, moral support, understanding, and maintaining an element of the real world and sanity in my life

SUMMARY

This dissertation details the modelling of a Falling Sludge Bed Reactor (FSBR) using AQUASIM. This study is one of the first of a series of projects investigating the design and use of this novel bioreactor for enhanced hydrolysis of particulate organic matter. The main feature of this bioreactor is the increased solids retention time obtained by allowing the solid matter to settle into three valleys, while the aqueous phase exits with a relatively short retention time.

The main aim of this project was to identify the state of the art regarding mathematical modelling of anaerobic digestion and biological sulfate reduction, to select rate equations from the literature that would simulate the various interactions taking place in the FSBR being fed a mixture of organic matter and acid mine drainage, and to investigate the trends obtained from the an AQUASIM model of the system. This would then serve as a basis for further projects, which would include identification of the enzymatic interactions in the FSBR, kinetic studies of critical processes not available in the current literature, and the development of a more complex mathematical model that would include factors other than the biological processes.

The FSBR was the first in a series of bioreactors that were operated on site at the Grootvlei Gold Mine (Pty) Ltd by Rhodes University, Department of Biochemistry and Microbiology. The overall process involved the removal of sulfate and heavy metals from acid mine drainage (AMD). Specific to the FSBR, sewage sludge was being hydrolysed, with the hydrolysis products being used as the carbon source and electron donor for the bioreduction of sulfate to sulfide. The main aim of the FSBR was to maximise the hydrolysis of the particulate organic feed. The majority of the sulfate reduction took place in the baffled reactor, which followed the FSBR in the treatment process.

In order to achieve the objectives of the project, the literature was surveyed to identify the processes taking place inside the FSBR. These would include the anaerobic digestion of particulate organic matter, in this case primary settled sewage sludge, and the sulfate reducing reactions which compete with the anaerobic digesting bacteria for soluble organic products.

These processes, together with their rate equations and kinetic constants, were included in a mathematical model. AQUASIM was used to integrate the rate equations extracted from the literature. AQUASIM was designed for the identification and simulation of aquatic systems, and has been used extensively for simulating wastewater treatment processes, but this is the first time it has been used for anaerobic digestion and biological sulfate reduction. The current model configures AQUASIM to include sulfate reduction, and simulates the flow patterns characteristic of the FSBR.

The reaction scheme or mechanism used in the model has been chosen from literature, and includes a total of nine reactions. These are hydrolysis, fermentation, anaerobic oxidation, acetogenesis, acetogenic sulfidogenesis, acetoclastic methanogenesis, acetoclastic sulfidogenesis, hydrogenotrophic methanogenesis and hydrogenotrophic sulfidogenesis.

For each of these reactions, a rate equation was chosen. These rate equations include terms for acetic acid inhibition, sulfide inhibition, and both sulfate and organic substrate limitation for sulfate reducing bacteria. The result is that the model will predict the anaerobic digestion of organic matter, both soluble and particulate, in the presence or absence of sulfate.

The results of the literature survey show that there is an extensive amount of kinetic data available for anaerobic digestion and sulfate reduction. The most important consideration in selecting kinetic data is that the sulfate reducing bacteria outcompete anaerobic digesting bacteria when there is sufficient sulfate in the system. Therefore, although a rigorous statistical analysis of the data was not performed, values of the kinetic constants were chosen so that the sulfate reducing bacteria will dominate in the system. Values were chosen from a published mathematical model that was successfully used to model a sulfate reducing system being fed soluble complex organic matter. The bioreactor was operated at an ambient temperature of 15°C, while the kinetic constants available in the literature were measured at 35°C. The kinetic constants were adjusted to predict the performance of the bioreactor at 15°C by reducing the maximum specific growth rates and the hydrolysis rate constants by 4.

Acid-base equilibria were included in the model for acetic acid dissociation and hydrogen sulfide dissociation. A constant pH of 7 was chosen, since the model did not predict the pH in the system. The vapour-liquid equilibria were also not included in the model.

In order to predict the concentration variations in the FSBR, the total volume was divided into nine compartments, inter-linked by liquid flow streams and solid settling streams. This allowed for the model to predict the increased solid retention times found in the pilot-plant operation of the FSBR.

The pilot plant was analysed with the aim of improving the hydrolysis of the particulate organic matter and observing the sulfate reduction taking place. Therefore, total COD measurements and sulfate measurements were made at various operating conditions and at various points in the FSBR. These concentrations were used to identify three steady state operating points for use in calibrating and verifying the model. A summary of the three steady-state operating points is shown in Table 1.

Table 1: Summary of the steady state operating data

Feed COD: SO ₄ ratio	Feed Sulfate Concentration (g.m ⁻³)	Feed COD Concentration (gCOD.m ⁻³)	Effluent Sulfate Concentration (g.m ⁻³)
2 : 1	1718 ± 107	3390 ± 238	970 ± 41
1.5 : 1	1777 ± 27	2646 ± 24	1496 ± 172
3 : 1	1604 ± 101	4728 ± 557	820 ± 171

The three total COD measurements made in the valleys of the FSBR were used to calibrate the settling coefficients in the model. These values are shown in Table 2.

Table 2: Total COD measurements from each of the three valleys when operating at a COD: SO₄ ratio of 2

	Concentration 1 (gCOD.m ⁻³)	Concentration 2 (gCOD.m ⁻³)	Average (gCOD.m ⁻³)	% Variation
Valley 1	59631	64001	61816 ± 2185	3.53
Valley 2	45612	54489	50050 ± 4438	8.87
Valley 3	40276	67035	53655 ± 13379	24.9

The model was able to predict the total COD of the sludge in each of the three valleys, to within 3% of the measured values, as well as being able to predict the overall sulfate conversion across the bioreactor to within 34% of the measured value. Results of this calibration are shown in Table 3.

Table 3: Comparison of measured and simulated concentrations to calibrate the settling coefficients in the model

Sample point	Measured value	Simulated value	% deviation
valley 1 (gCOD.m ⁻³)	61816	61500	0.46
valley 2 (gCOD.m ⁻³)	50050	50900	1.67
valley 3 (gCOD.m ⁻³)	53655	52000	3.07
effluent sulfate concentration	970 mg.l ⁻¹	1300 mg.l ⁻¹	34.0

Two other operating conditions were used to verify the model. The model was able to predict the overall sulfate conversion to within 28% of the measured value for the first operating condition, and 1% of the measured value for the second operating condition. The results of the verification of the model are shown in Table 4.

Table 4: Comparisons of measured values to simulated values for verification of the model

COD:SO₄²⁻	2 : 1	1.33 : 1	2.82 : 1
COD in (gCOD.m⁻³) (meas.)	3390	2646	4728
sulfate in (mg.l⁻¹) (meas.)	1718	1777	1604
sulfate out (mg.l⁻¹) (meas.)	970	1496	820
simulated sulfate out (mg.l⁻¹)	1300	1481	1048
% deviation in sulfate out	34.0	1.00	27.8

The aim of the FSBR in the biological process treating acid mine drainage is to hydrolyse the complex organic substrate feed, so that the sulfate reducing bacteria can use the soluble products in the baffled reactor which follows. The aim of adding mine water to the FSBR is to ensure the presence of sulfate. In this way, the sulfate reducing bacteria will not be sulfate limited, and any soluble substrate that is available will be used by the sulfate reducing bacteria, instead of the methane producing bacteria. In this way, none of the feed COD will be wasted on methane formation.

The aim of the model was to predict trends in the bioreactor performance while changing the operating conditions, in order to propose operating conditions that will

improve the bioreactor performance. Operating conditions that could be changed are the hydraulic retention time (HRT), the sludge recycle ratio (SRR), the COD: SO_4^{2-} ratio. Varying the feed flow rate changes the HRT. Varying the recycle flow rate changes the SRR. Varying the concentration of the COD entering the bioreactor changes the COD: SO_4^{2-} ratio.

The fate of the particulate COD entering the FSBR is of minor importance compared to the hydrolysis conversion taking place. However, methane formation and biomass production would decrease the amount of COD available for sulfate reduction in the down-stream processes. Therefore, the fraction of COD leaving the FSBR as particulate COD, soluble COD, methane, biomass, or consumed for sulfate reduction was monitored.

The most important operating parameter is the HRT, since this determines the size of the bioreactor. The model was used to simulate an HRT of between 0.5 and 2.5 days, maintaining a constant recycle pump rate of $48 \text{ m}^3 \cdot \text{d}^{-1}$ and a feed COD: SO_4^{2-} ratio of 2.

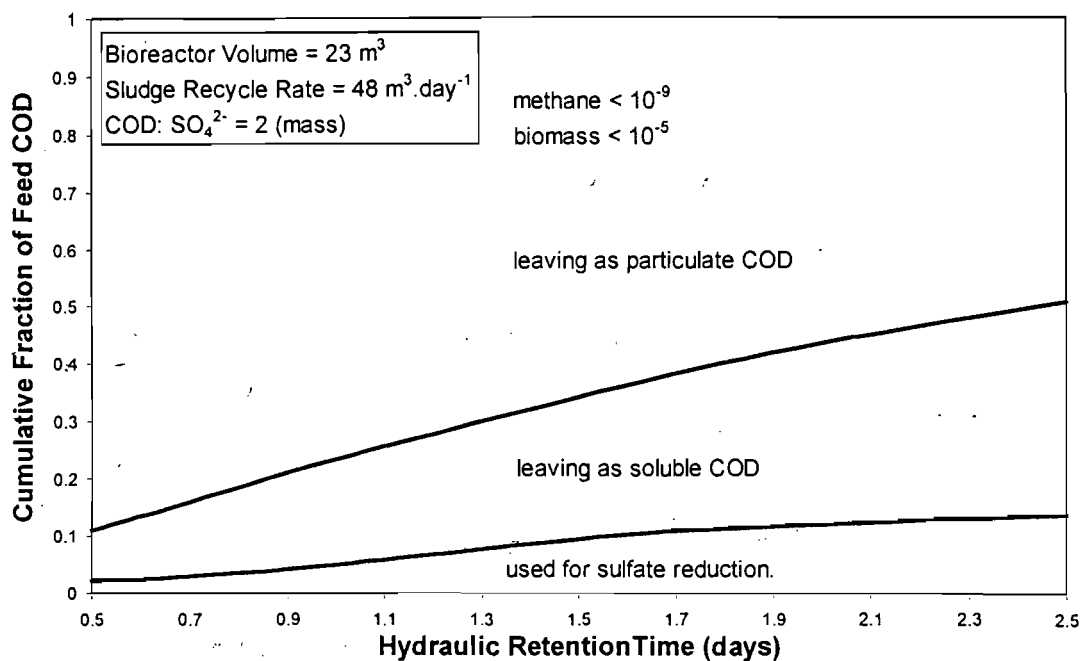


Figure 1: Model predictions of the fraction of the feed COD that is leaving the bioreactor as particulate COD, soluble COD, biomass, methane and sulfide, as the feed to the bioreactor is varied, varying the hydraulic retention time (COD: SO_4^{2-} = 2)

Figure 1 shows that the model predicts that the fraction of the feed COD leaving as particulate COD decreases with an increase in the HRT. This results in more soluble COD being produced. This would then result in more organic substrate available for sulfate reduction. However, the fraction used for sulfate reduction does not increase

as fast as the particulate COD fraction decreases. The result is that more soluble COD is leaving the FSBR. The model also predicts that an insignificant amount of biomass and methane are leaving the FSBR. The model therefore predicts that an increase in the HRT would improve the performance of the FSBR.

The SRR is defined as the ratio of the total sludge recycle flow rate to the total feed rate. For the simulations, the SRR was varied between 0.25 and 4. Figure 2 shows that the model predicts that a SRR of greater than 1 has little effect on the fraction of the feed COD that is leaving the FSBR as particulate COD, as soluble COD, and being used for sulfate reduction. In fact, an extreme SRR of 10 was simulated, and the almost ten-fold increase in SRR resulted in an insignificant increase in the bioreactor performance. There is very little biomass and methane produced.

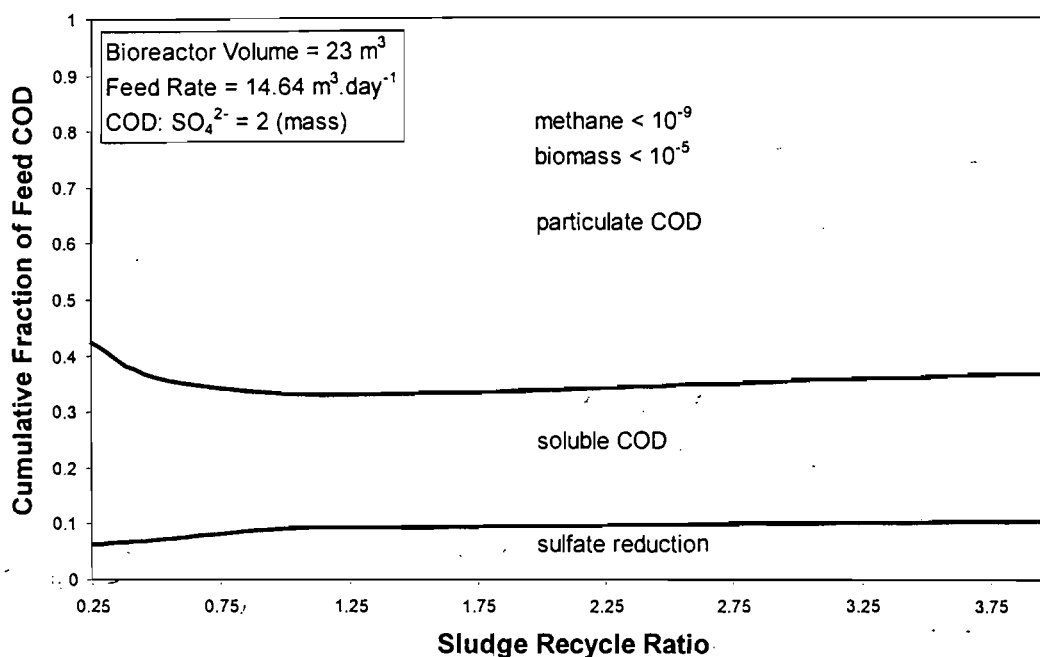


Figure 2: Model prediction of the fraction of the feed COD leaving the FSBR as particulate COD, soluble COD, biomass, methane, or used for sulfide reduction, as a function of the SRR (HRT = 1.57; COD: SO_4^{2-} = 2)

However, at an SRR below 1, there is a change in the simulated trends. The fraction of the feed COD leaving as particulate COD decreases, together with a change in the COD being used for sulfate reduction. One explanation for this trend is that at these low sludge recycle rates, there is less particulate matter in the feed, since less is being recycled. Less particulate matter then has to settle out of the top of the FSBR and less is being washed out. This means that the particulate matter will have an increased retention time, and will allow for greater hydrolysis. However, this could not

be verified during the pilot plant operational period. Reduced SRR means reduced operating costs, which would be beneficial to the overall mine water treatment costs.

Finally, the model was used to predict the affect of the COD: SO_4^{2-} ratio on the performance of the FSBR. The COD: SO_4^{2-} ratio was changed by changing the COD concentration of the feed stream. Figure 3 shows that the model predicts that the majority of the feed COD leaves the bioreactor as particulate COD. The fraction of the feed COD that is leaving as soluble COD increases with an increase in the COD: SO_4^{2-} ratio, while the fraction of the feed COD being used for sulfate reduction is decreasing with an increase in the COD: SO_4^{2-} ratio. The fraction of the feed COD being used to produce biomass and methane is insignificant.

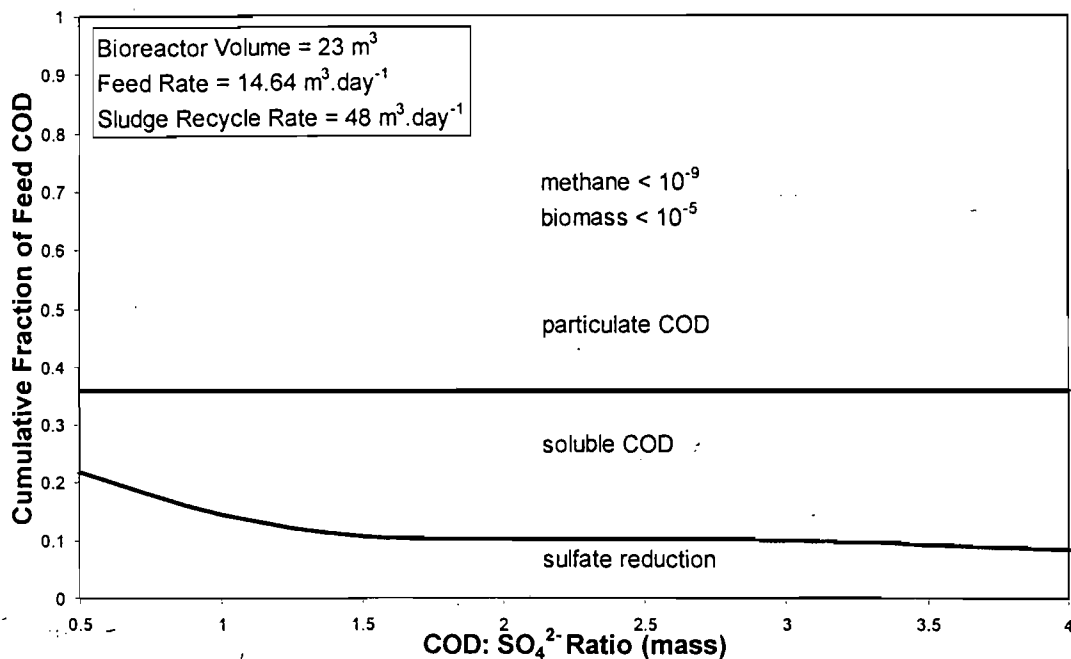


Figure 3: Model prediction of the fraction of feed COD that is leaving the bioreactor as either particulate COD, soluble COD, biomass, methane or sulfide, at various COD: SO_4^{2-} ratios (HRT = 1.57; SRR = 3.28)

An increase in the COD: SO_4^{2-} ratio does not increase the fraction of the feed particulate organic matter that is hydrolysed, but results in more soluble COD being produced, which can then be fed to the baffled reactor to be used for sulfate reduction. However, at high organic loading rates, the increased levels of hydrogen partial pressure lead to certain of the bioreactions becoming thermodynamically non-spontaneous. Unfortunately, the model does not predict this affect, and therefore cannot give the maximum organic loading rate that can be used before the process fails.

Therefore, to improve the pilot FSBR performance, an increase in the HRT would increase the amount of particulates that are hydrolysed. A decrease in the SRR would have little effect on the fraction of the particulates that are hydrolysed, but some recycle is necessary to contact the sulfate in the top section of the reactor with the biomass in the valleys. Finally, a higher COD: SO_4^{2-} ratio would result in more soluble COD being produced, but the limit for the organic loading rate has not been determined.

Determining this limit, as well as a greater understanding of the process taking place inside the FSBR, and kinetic data for these processes, would be valuable for the improved performance and scale up of the FSBR.

A sensitivity analysis was performed on selected kinetic parameters and the operating parameters used in the model. The results show that the model output is most sensitive to the hydrolysis kinetic constants. Therefore, experimental analysis of the hydrolysis rate is critical. Also, the model is most sensitive to the settling coefficients. The value of these coefficients was determined from the total COD measurement in each of the three valleys (Table 2). Therefore, these measurements should be made under more controlled environments and more frequently, in order to accurately predict the settling of the solids.

The investigation has shown that the reaction scheme and rate equations available in the literature are able to predict the reactions occurring in the bioreactor. However, the kinetic constants available are for higher temperatures than the temperature at which the FSBR pilot plant was being operated. The methods used to adjust these parameters are simplistic, general and probably crude, and the temperature dependence of the bacterial reactions needs to be determined experimentally, if further work is to be done at these low temperatures. However, due to the biological reactions being exothermic, a larger scale FSBR would automatically have a higher temperature. This higher temperature would increase the rate of the bioreactions, and would lead to improved bioreactor performance.

There is also evidence that the addition of the AMD to the sewage sludge increases the rate of anaerobic digestion or hydrolysis of the particulate organic matter. Further investigation is required to determine the compound responsible for this acceleration, and the extent of this acceleration.

To improve the predictive power of the model, the solution chemistry of the bioreactor can be included. This would allow for the calculation of the pH variations inside the FSBR, which in turn affect the concentration of the inhibitory undissociated acetic

acid and hydrogen sulfide. Another possibility would be to include vapour-liquid equilibria to the model, so that the production of methane, hydrogen sulfide and carbon dioxide to the vapour space could be predicted.

Further kinetic studies need to be done on the influence of the sulfate concentration on biological reactions, since sulfate reducing bacteria systems fail at sulfate concentrations greater than about 10 mg.l^{-1} .

Inhibition due to sulfide needs to be clarified. The mechanism needs to be clarified, since the reports on sulfide inhibition can be contradictory. A model for simulating sulfide inhibition then needs to be determined, since the first order equation used in this study is not satisfactory.

Acetic acid inhibition of sulfate reducing bacteria has not been investigated. MPB are sensitive to changes in the pH, since this increases the concentration of the inhibitory acetic acid. Since the SRB are less sensitive to low pH than the MPB, they must also be less sensitive to acetic acid. However, a build up of acetic acid in systems degrading ethanol could be due to the acetic acid inhibiting the acetoclastic methanogens and acetoclastic sulfidogens. Acetic acid is possibly affecting the different bacteria differently, and studies need to be conducted to determine this.

The identification of the need for the above future studies shows the shortcomings or limits of the model. However, in view of the ability of the model to predict the bioreactor performance, the model is adequate in determining the affects of varying the operational parameters, and these modifications could possibly be a minor improvement.

CONTENTS

	Page
Acknowledgements	i
Summary	ii
Contents	xi
List of Tables	xiv
List of Figures	xv
Nomenclature	xviii
Glossary	xx
1. Introduction and Background	1
1.1 Introduction	1
1.2 Acid Mine Drainage	3
1.3 Formation of Acid Mine Drainage	4
1.4 Affects of Acid Mine Drainage	4
1.5 Treating Acid Mine Drainage	5
1.6 The Pilot Plant	7
2. Kinetics of Anaerobic Digestion and Sulfate Reduction	10
2.1 Hydrolysis	12
2.2 Fermentation/Acidogenesis	14
2.3 Anaerobic Oxidation	16
2.4 Acetogenic Sulfidogenesis	16
2.5 Acetogenesis	18
2.6 Methanogenesis	19
2.6.1 Acetoclastic Methanogenesis	20
2.6.2 Hydrogenotrophic Methanogenesis	21
2.7 Sulfidogenesis	22
2.7.1 Acetoclastic Sulfidogenesis	22
2.7.2 Hydrogenotrophic Sulfidogenesis	23
2.8 Hydrogen Partial Pressure	23
2.9 Summary	25

3. AQUASIM as a Simulation Tool	28
4. Model Formulation and Development	30
4.1 Organic Feed Composition	31
4.2 Reaction Scheme	32
4.3 Biological Rate Equations	33
4.3.1 Hydrolysis of Proteins, Lipids and Carbohydrates	34
4.3.2 Fermentation	35
4.3.3 Anaerobic Oxidation	35
4.3.4 Acetogenic Sulfidogenesis	36
4.3.5 Acetogenesis	36
4.3.6 Acetoclastic Methanogenesis	36
4.3.7 Hydrogenotrophic Methanogenesis	37
4.3.8 Acetoclastic Sulfidogenesis	37
4.3.9 Hydrogenotrophic Sulfidogenesis	37
4.4 Acid-Base Equilibria of Inhibitory Compounds	38
4.5 Kinetic Constants	39
4.6 Reactor configuration	44
4.7 Model Omissions	48
5. Model Calibration	49
5.1 Pilot Plant Operating Data	49
5.2 Steady State Operating Points	52
5.3 Calibration of Settling Coefficients	57
5.4 Model Verification	60
6. Simulated Trends and Discussion	62
6.1 Affects of Hydraulic Retention Time	62
6.2 Affects of Sludge Recycle Ratio	67
6.3 Affects of COD: SO ₄ ratio	72
7. Sensitivity Analysis	78
8. Conclusions	81

9. Future Work	83
9.1 Temperature affects	83
9.2 Affects of sulfate and sulfide on hydrolysis	84
9.3 Solution chemistry	84
9.4 Liquid vapour mass transfer	85
9.5 Kinetic studies	85
10. References	86

Appendices

Appendix A: Kinetic Inhibition Models	96
Appendix B: Results of the Sensitivity Analysis	99
Appendix C: AQUASIM Code and User Tips	101
Appendix D: Tables of Literature Kinetic Constants	138

LIST OF TABLES

Table Number	Table Title	Page
Table 1:	The composition of primary municipal sludge as given by Eastman and Ferguson (1981)	31
Table 2:	Rate equations, kinetic constants and stoichiometry for hydrolysis	34
Table 3:	Kinetic parameters used in the model	41
Table 4:	A summary of the reactions, rate equations, stoichiometry, and kinetic constants used in the model	42
Table 5:	Pilot plant operating data for the month of November 1998, giving the sulfate concentration (g.m^{-3}) and COD concentration (gCOD.m^{-3}) of the feed and effluent of the FSBR, for two COD: SO_4 ratios (2 and 1.5)	50
Table 6:	Total COD measurements from each of the three valleys when operating at a COD: SO_4 ratio of 2	51
Table 7:	Pilot plant operating data for the month of March 1999, giving the sulfate concentration (g.m^{-3}), and COD concentration (gCOD.m^{-3}) of the feed and effluent of the FSBR, for a COD: SO_4 ratio of 3	52
Table 8:	Summary of the steady state operating data	57
Table 9:	Comparison of measured and simulated concentrations to calibrate the settling coefficients in the model	59
Table 10:	Comparisons of measured values to simulated values for verification of the model	60
Table 11:	Results of the sensitivity analysis performed on the kinetic parameters from the model, showing the kinetic parameter that causes the greatest influence (absolute difference, highest 10 values) on the output parameters	80
Table 12:	Results of the sensitivity analysis performed on the operating parameters from the model, showing the operating parameter that causes the greatest influence (absolute difference, highest 10 values) on the output parameters	80

LIST OF FIGURES

Figure Number	Figure Title	Page
Figure 1:	The negative affects of acid mine drainage on the ecosystem	5
Figure 2:	Schematic representation of the process developed by Rhodes University for treating AMD	8
Figure 3:	A schematic representation of the FSBR	9
Figure 4:	The reaction scheme used in the model to describe anaerobic digestion and sulfate reduction	11
Figure 5:	The logical structure of AQUASIM	29
Figure 6:	Procedure used in developing the model	30
Figure 7:	The dimensions and configuration on the FSBR pilot plant	44
Figure 8:	The FSBR divided into 9 compartments for the AQUASIM model	45
Figure 9:	The flow of water and soluble substrates through the FSBR	45
Figure 10:	The flow of solids in the FSBR	46
Figure 11:	The flow patterns taking place in one section of the reactor, and the subsequent representation of this section in AQUASIM	47
Figure 12:	The AQUASIM representation of the FSBR showing the compartments and the connecting streams	47
Figure 13:	Pilot plant operating data for the month of November 1998, identifying steady state input data (COD: SO ₄ ratio = 2); average COD concentration = 3390 gCOD.m ⁻³ , average sulfate concentration is 1718 g.m ⁻³ , between days 12 and 19	53
Figure 14:	Pilot plant operating data for the month of November 1998, identifying steady state input data (COD: SO ₄ ratio = 1.5); average COD concentration = 2646 gCOD.m ⁻³ , average sulfate concentration is 1777 g.m ⁻³ , between days 5 and 11	54
Figure 15:	Pilot plant operating data for the month of March 1999, identifying steady state input data (COD: SO ₄ ratio = 3); average COD concentration = 4728 gCOD.m ⁻³ , average sulfate concentration is 1604 g.m ⁻³ , between days 1 and 11	54
Figure 16:	Pilot plant effluent sulfate concentrations for the first identified operating steady state (feed COD = 3390 gCOD.m ⁻³ , feed sulfate = 1718 g.m ⁻³ , COD: SO ₄ ²⁻ = 2), showing the steady state effluent sulfate concentration (average = 970 g.m ⁻³ ± 41)	55

Figure 17:	Pilot plant effluent sulfate concentrations for the second identified operating steady state (feed COD = 2646 gCOD.m ⁻³ , feed sulfate = 1777 g.m ⁻³ , COD: SO ₄ ²⁻ = 1.5), showing the steady state effluent sulfate concentration (average = 1496 g.m ⁻³ ± 172)	56
Figure 18:	Pilot plant effluent sulfate concentrations for the third identified operating steady state (feed COD = 4728 gCOD.m ⁻³ , feed sulfate = 1604 g.m ⁻³ , COD: SO ₄ ²⁻ = 3), showing the steady state effluent sulfate concentration (average = 820 g.m ⁻³ ± 171)	56
Figure 19:	AQUASIM output graph of the total COD in four of the AQUASIM compartments as the simulation approaches steady state (COD: SO ₄ ratio = 2, feed COD = 3400 gCOD.m ⁻³ , feed sulfate = 1700 g.m ⁻³)	59
Figure 20:	Model predictions of the fraction of the feed COD that is leaving the bioreactor as particulate COD, soluble COD, biomass, methane and sulfide, as the feed to the bioreactor is varied, varying the hydraulic retention time (COD: SO ₄ ²⁻ = 2)	63
Figure 21:	Model predictions of the fraction of the feed particulate COD that is being hydrolysed, as the feed to the bioreactor is varied, varying the hydraulic retention time (COD: SO ₄ ²⁻ = 2)	65
Figure 22:	Model predictions of the sulfate conversion when varying the hydraulic retention time (COD: SO ₄ ²⁻ = 2)	65
Figure 23:	Model predictions of the terms for substrate limitation, sulfate limitation, sulfide inhibition, and the product of the three terms, for the acetogenic sulfidogens, as the feed to the bioreactor is varied, varying the hydraulic retention time (COD: SO ₄ ²⁻ = 2)	66
Figure 24:	Model prediction of the fraction of the feed COD leaving the FSBR as particulate COD, soluble COD, biomass, methane, or used for sulfide reduction, as a function of the SRR (HRT = 1.57; COD: SO ₄ ²⁻ = 2)	69
Figure 25:	Model prediction of the fraction of the hydrolysis conversion as a function of the SRR (HRT = 1.57; COD: SO ₄ ²⁻ = 2)	70
Figure 26:	Model prediction of the fraction of sulfate converted as a function of the SRR (HRT = 1.57; COD: SO ₄ ²⁻ = 2)	71
Figure 27:	Model prediction of the effluent methane concentration, indicating methane production, as a function of the SRR (HRT = 1.57; COD: SO ₄ ²⁻ = 2)	71
Figure 28:	Model prediction of the fraction of feed COD that is leaving the bioreactor as either particulate COD, soluble COD, biomass, methane or sulfide, at various COD: SO ₄ ²⁻ ratios (HRT = 1.57; SRR = 3.28)	73
Figure 29:	Model prediction of the fraction of hydrolysis of the feed COD at various COD: SO ₄ ²⁻ ratios (HRT = 1.57; SRR = 3.28)	74
Figure 30:	Model prediction of the sulfate conversion at various COD: SO ₄ ²⁻ ratios, together with the three measured concentrations used for the model calibration and verification (HRT = 1.57; SRR = 3.28)	75

- Figure 31: Model prediction of the concentration of methane leaving the bioreactor, indicating methane production, at various COD: SO_4^{2-} ratios (HRT = 1.57; SRR = 3.28) 76
- Figure 32: Model predictions of the terms for substrate limitation, sulfate limitation, sulfide inhibition, and the product of the three terms, for the acetogenic sulfidogens, as the COD: SO_4^{2-} ratio of feed to the bioreactor is varied (HRT = 1.57; SRR = 3.28) 77
-

NOMENCLATURE

Symbol	Description	Units
[3-EPh]	3-ethylphenol concentration	g COD. m ⁻³
[Ac ⁻]	acetate concentration	g COD. m ⁻³
[COD _p]	particulate COD concentration	g COD. m ⁻³
[COD _{p,n}]	non-degradable particulate COD concentration	g COD. m ⁻³
[COD _s]	soluble COD concentration	g COD. m ⁻³
C _{be}	bulk liquid enzyme concentration	g. m ⁻³
C _x	bacterial concentration	g VSS. m ⁻³
[H ⁺]	hydrogen ion concentration	g COD. m ⁻³
[H ₂]	hydrogen concentration	g COD. m ⁻³
[H ₂] _T	threshold hydrogen concentration	g COD. m ⁻³
[HAc]	undissociated acetic acid concentration	g COD. m ⁻³
[HLac]	undissociated lactic concentration	g COD. m ⁻³
[HPri]	undissociated propionic acid concentration	g COD. m ⁻³
[H ₂ S]	undissociated hydrogen sulfide concentration	g COD. m ⁻³
k _d	cell death rate coefficient	day ⁻¹
k _h	first order hydrolysis coefficient	day ⁻¹
K _{3-EPh}	3-ethylphenol inhibition constant	g COD. m ⁻³
K _{H⁺}	hydrogen ion inhibition constant	g. m ⁻³
K _{HAc}	undissociated acetic acid inhibition constant	g COD. m ⁻³
K _{H₂S}	undissociated hydrogen sulfide inhibition constant	g COD. m ⁻³

K_{NH_3}	undissociated ammonia inhibition constant	g. m^{-3}
K_{OH^-}	hydroxide ion inhibition constant	g. m^{-3}
K_S	organic substrate half saturation constant	g COD. m^{-3}
$K_{\text{SO}_4^{2-}}$	sulfate half saturation constant	g. m^{-3}
K_{VFA}	undissociated volatile fatty acid inhibition constant	g COD. m^{-3}
m	maintenance coefficient	day^{-1}
m, n, p	exponential constants	
$[\text{NH}_3]$	ammonia concentration	g. m^{-3}
pH_{LL}	pH lower limit	
pH_{UL}	pH upper limit	
$[\text{SO}_4^{2-}]$	sulfate concentration	g. m^{-3}
$[\text{VFA}]$	volatile fatty acid concentration	g COD. m^{-3}
x_C	settling coefficient	
Y_{SX}	growth yield coefficient	g VSS. g COD^{-1}
$Y_{\text{SX}}^{\text{max}}$	maximum yield coefficient	g VSS. g COD^{-1}
z_0	2000 x hydrogen partial pressure	g COD. m^{-3}
μ	specific bacterial growth rate	day^{-1}
μ_{max}	maximum specific growth rate	day^{-1}
v	Michaelis-Menten substrate utilisation rate	$\text{g COD. m}^{-3} \cdot \text{day}^{-1}$
v_{max}	maximum Michaelis-Menten substrate utilisation rate	$\text{g COD. m}^{-3} \cdot \text{day}^{-1}$

GLOSSARY

Abbreviation	Description
AMD	acid mine drainage
acetogenic	produces acetate from longer chain fatty acids
acetoclastic	using acetate as the organic substrate
acidogenic	produces acetate and other volatile fatty acids
a-MPB	acetoclastic methane producing bacteria
a-SRB	acetoclastic sulfate reducing bacteria
COD	chemical oxygen demand
FSBR	falling sludge bed reactor
HRT	hydraulic retention time
hydrogenotrophic	using hydrogen as the organic electron donor
h-MPB	hydrogenotrophic methane producing bacteria
h-SRB	hydrogenotrophic sulfate reducing bacteria
methanogenesis	methane producing
MPB	methane producing bacteria
p-SRB	acetogenic sulfate reducing bacteria growing on propionate
SRB	sulfate reducing bacteria
SRR	sludge recycle ratio
sulfidogenic	hydrogen sulfide producing
TDS	total dissolved solids
VSS	volatile suspended solids

1. INTRODUCTION AND BACKGROUND

1.1 Introduction

This dissertation details the modelling of a Falling Sludge Bed Reactor (FSBR) using AQUASIM. This study is one of the first of a series of projects investigating the design and use of this novel bioreactor for enhanced hydrolysis of particulate organic matter. The main feature of this bioreactor is the increased solids retention time obtained by allowing the solid matter to settle into three valleys, while the aqueous phase exits with a relatively short retention time.

The main aim of this project was to identify the state of the art regarding mathematical modelling of anaerobic digestion and biological sulfate reduction, to select rate equations from the literature that would simulate the various interactions taking place in the FSBR being fed a mixture of organic matter and acid mine drainage, and to investigate the trends obtained from the an AQUASIM model of the system. This would then serve as a basis for further projects, which would include identification of the enzymatic interactions in the FSBR, kinetic studies of critical processes not available in the current literature, and the development of a more complex mathematical model that would include factors other than the biological processes.

The FSBR was the first in a series of bioreactors that were operated on site at the Grootvlei Gold Mine (Pty) Ltd by Rhodes University, Department of Biochemistry and Microbiology. The overall process involved the removal of sulfate and heavy metals from acid mine drainage (AMD). Specific to the FSBR, sewage sludge was being hydrolysed, with the hydrolysis products being used as the carbon source and electron donor for the bioreduction of sulfate to sulfide. The main aim of the FSBR was to maximise the hydrolysis of the particulate organic feed. The majority of the sulfate reduction took place in the baffled reactor, which follows the FSBR in the treatment process.

In order to achieve the objectives of the project, the literature was surveyed to identify the processes taking place inside the FSBR. These would include the anaerobic digestion of particulate organic matter, in this case primary settled sewage

sludge, and the sulfate reducing reactions which compete with the anaerobic digesting bacteria for soluble organic products.

These processes, together with their rate equations and kinetic constants, were included in a mathematical model. AQUASIM was used to integrate the rate equations extracted from the literature. AQUASIM was designed for the identification and simulation of aquatic systems, and has been used extensively for simulating wastewater treatment processes, but this is the first time it has been used for anaerobic digestion and biological sulfate reduction.

This dissertation gives some background to the problem of acid mine drainage. Topics such as the extent of the problem of contaminated water in South Africa, the causes of AMD, the impact AMD has on the environment and available treatment technologies are discussed. The advantages of active processes compared to passive processes are discussed, as well as the use of organic waste materials as opposed to bulk chemicals as the organic substrate and electron donor.

The results of an extensive literature survey on the kinetics of anaerobic digestion and biological sulfate reduction are given, with a view of defining the state of the art regarding the modelling of these processes. This also gives an insight into the mechanisms of anaerobic digestion of particulate organic matter, the role that the hydrogen concentration plays in the system, and most importantly, the competition between sulfate reducing bacteria and methane producing bacteria for the organic substrate.

A brief introduction to AQUASIM is given, and the ability of AQUASIM to model bacterial sulfate reduction is discussed. Advantages and disadvantages of using AQUASIM to model a system of this kind are given and discussed.

The model development is given, which states the reaction scheme used, the rate equations chosen for each of the reactions in the reaction scheme, and the kinetic parameters used in the model. The reaction scheme, rate equations and kinetic constants were then incorporated into AQUASIM.

The use of AQUASIM to model the characteristic flow patterns found in the FSBR is shown. The settling of the solid particles gives a velocity profile different to that of the liquid flow. By using a number of compartments linked by both water flow streams and settling solids streams, the velocity profile due to the recycle and the solids settling of the various components in the bioreactor can be simulated. This enabled the model to predict the distribution of biomass and particulate organic matter inside the bioreactor, while also predicting the sulfate conversion.

The model was then used to predict the trends found in the bioreactor performance when the operating parameters were changed. The main aim of the FSBR was to maximise the amount of particulate organic matter that was hydrolysed. However, the soluble products formed from this hydrolysis reaction can be used to form methane, in competition with the sulfate reducing bacteria. Therefore, the sulfate containing mine water is added to this bioreactor, so that the sulfate reducing bacteria will not be sulfate limited, and can compete successfully with the methane producing bacteria for any soluble organic products formed.

The effects of the hydraulic retention time, the sludge recycle ratio and the feed COD: SO_4^{2-} ratio on the performance of the bioreactor, according to the model, are shown and discussed.

Areas in which further work is required in order to improve the predictability of the model are defined and discussed. These suggestions arose partly from the literature survey and partly from observations made while operating the pilot plant.

1.2 Acid Mine Drainage

In South Africa, the supply of sufficient quantities of water for domestic and industrial use is threatened both from a quantity and a quality point of view. It has been predicted that the South African supply and demand curves for water will converge before 2020 (Bekker, 1982). This can be attributed to the fact that South Africa is a semi-arid country with limited water resources. Therefore, in order to overcome the predicted water shortages, more effluents originating from domestic, industrial and mining sources will have to be treated for reuse before disposal (Toerien, 1987). Mineralisation is currently one of the most important water quality problems in South Africa (Heynike, 1981). Sulfate will be an important contributing factor to these increasing TDS concentrations. The treatment of sulfate polluted water will contribute considerably to the quality of South Africa's surface water, as sulfate is directly responsible for the mineralisation of receiving waters. Some of the problems associated with high sulfate concentrations include corrosion, transferring of tastes to drinking water, scaling of pipes, boilers and heat exchangers, and facilitating biocorrosion.

A potential new local sulfur source that could be exploited is biological sulfur production from industrial and mining effluents. Industrial effluents can be reused after treatment for sulfur recovery, which is a desirable development in view of the

limited water supplies. In addition, heavy metals can also be recovered from suitable effluents.

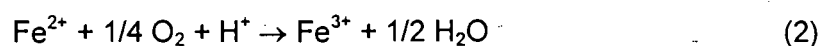
1.3 Formation of Acid Mine Drainage

The biological and physico-chemical processes giving rise to pyrite oxidation, acid formation and heavy metal solubilisation are comprehensively reviewed elsewhere (Kuenen and Robertson, 1992; Pronk and Johnson, 1992; Robb, 1994; Johnson, 1995).

At pH > 4, pyrite is mainly oxidised by oxygen dissolved in water:

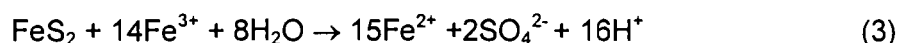


The ferrous iron produced in this reaction is released into the water where it is oxidised to ferric iron:



Due to the production of hydrogen ions in the above processes, the pH will decrease.

At a pH < 4, the ferric iron reacts with pyrite:



The overall effect of the above reactions is an increase in the sulfate concentration due to the dissolving and oxidation of sulfide precipitates, an increase in the dissolved metals concentration, and a decrease in pH.

AMD is recognised as a multi-factor pollutant and the importance of each factor varies within and between affected systems. The main factors are high acidity (pH = 2 - 3), high levels of metals (Al = 50 - 2000 mg.l⁻¹; Fe = 10 - 6700 mg.l⁻¹; Zn = 10 - 100 mg.l⁻¹), high sulfate concentration (3 - 30 g.l⁻¹), and high total dissolved solids (TDS = 1800 - 45000 mg.l⁻¹) (Christensen *et al.*, 1996).

1.4 Affects of Acid Mine Drainage

AMD results in both direct and indirect pressures on the organisms within the ecosystem. These affects can be characterised as chemical, physical, biological and ecological. The overall impact is the elimination of species. This simplifies the food chain, thereby reducing ecological stability (Gray, 1997). The affects of AMD are summarised in the Figure 1.

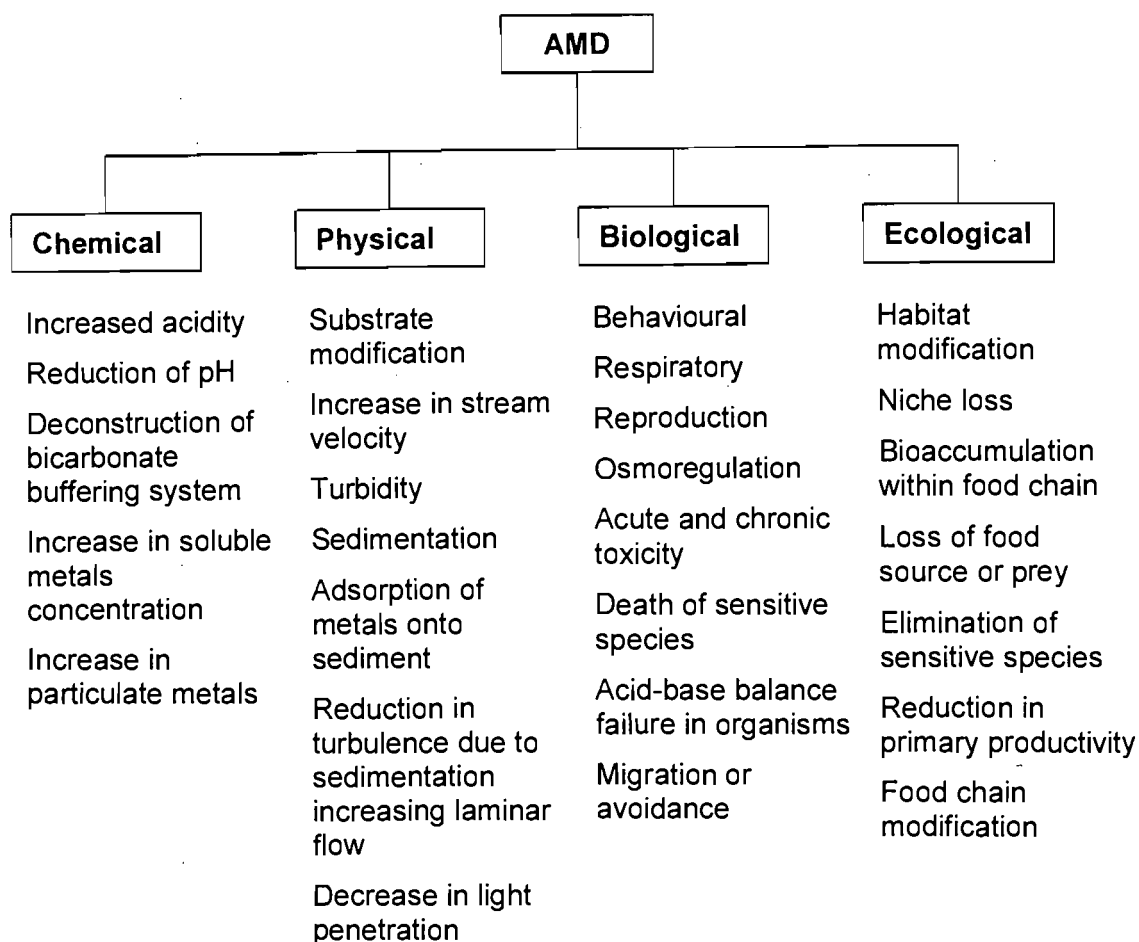
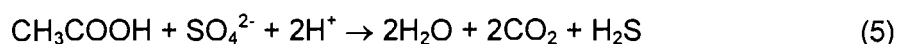
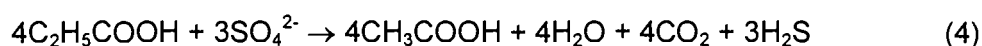


Figure 1: The negative affects of acid mine drainage on the ecosystem (after Gray 1997)

1.5 Treating Acid Mine Drainage

AMD may be treated chemically or biologically. Biological approaches to AMD treatment have been reviewed by Kuenen and Robertson (1992), Gadd and White (1993), Johnson (1995), Salomons (1995), Ledin and Pedersen (1996), and Cidu *et al.* (1997). Sulfate reducing bacteria are particularly effective in treating AMD since they reduce the sulfate component, produce sulfide, which forms insoluble precipitates with the metal ions present, and neutralise the solution by consuming protons (Barton and Tomei, 1995). The following are some reactions that have been identified as being performed by SRB:



Biological systems may be active or passive. The use of wetlands for the treatment of AMD is a passive technology, which has developed rapidly in recent years (Johnson, 1995; van Zyl, 1996). This technology provides a low operational cost approach to long term management of the problem.

Active technologies make use of bioreactors and rely in the main on the high SRB growth rates and the precipitation of metal sulfides. Although numerous SRB reactor design studies have been reported (De Walle, 1979; Chian and De Walle, 1983; Riviera, 1983; Maree *et al.*, 1987; Umita *et al.*, 1988; Buisman *et al.*, 1989; Maree and Hill, 1989; Barnes, 1991; Herrera *et al.*, 1991; Grobicki and Stuckey, 1992; van Houten *et al.*, 1994), scale-up applications of active AMD treatment technologies have been limited. The successful operation of a SRB process at the Budelco Zinc Refinery, The Netherlands, has been reported (Scheeren *et al.*, 1993).

Compost beds and open pit reactors, fed organic waste materials, provide an intermediate position between active and passive systems (Kalin *et al.*, 1991; Devorak *et al.*, 1992; Bèchard *et al.*, 1993; Kuyucak and St-Germain, 1994). These processes allow the control advantages of active processes on the systems, but have lower operating costs.

In spite of the type of biological AMD process technology used, the singular factors constraining the biological treatment approach are the reactor configuration used, the cost of the construction, and the cost and availability of the carbon source (or electron donor) for the microbial reduction processes. Carbon sources which have been evaluated for active bacterial sulfate reduction include sewage sludge (Butlin *et al.*, 1956; Pipes, 1960; Burgess and Wood, 1961; Conradie and Grutz, 1973), animal waste slurries (Ueki *et al.*, 1988), lactate and cheese whey (Oleszkiewicz and Hilton, 1986; Herrera *et al.*, 1991), molasses (Maree and Hill, 1989), ethanol and methanol (Postgate, 1984; Braun and Stolp, 1985; Szwezyk and Pfennig, 1990) and producer gas (Du Preez *et al.*, 1992; van Houten *et al.*, 1994).

In general, electron donors available in large quantities can be divided into two groups, namely organic waste materials and bulk chemicals. The use of organic waste materials is generally accompanied by additional pollution of the wastewater and therefore a supplementary treatment process is needed to produce a clean effluent. Products of the anaerobic digestion of organic wastes form substrates that are common for different groups of bacteria, for example, sulfate reducing bacteria and methane producing bacteria will compete for acetate and hydrogen. This results

in competition between these groups for the substrate, and limits the amount available for sulfate reduction.

The use of relatively pure, fully degradable chemicals offers a number of substantial advantages (van Houten, 1996). Firstly, no remaining pollution exists and therefore no supplementary treatment is required. Secondly, pure chemicals have a well-defined composition, making it easier to predict and describe the biodegradation and sulfate reduction. Possible compounds, all of which are relatively cheap, include ethanol, methanol and synthesis gas. Ethanol is a cheaper substrate for small-scale plants, but synthesis gas becomes cheaper at larger scales (van Houten, 1996).

However, in the South African context, sewage is possibly the most cost effective organic electron donor. The treatment of the sewage in conjunction with AMD is an advantage, as there is no longer a need to treat the sewage independently. Although the science of sewage treatment is advanced, this is still an attractive proposition. There is also evidence that the presence of either sulfate or sulfide increases the rate of degradation of the sewage, and this influence is currently under investigation (personal correspondence with P. Rose, Rhodes University).

1.6 The Pilot Plant

In order to allow mining operations at the far East Rand Mining Basin to continue, the Grootvlei Gold Mine (Pty) Ltd is currently discharging approximately 110×10^6 l.d⁻¹ of AMD into the Blesbokspruit Wetland. This wetland has been designated to the list of Wetlands of International Importance in terms of the RAMSAR Convention in October 1986. At present, a number of different treatment processes are being developed and tested on site in order to find the most cost effective way of treating the AMD.

On site, the mine water first enters a high-density sludge process, where the AMD is neutralised, and the metal hydroxides are precipitated. The neutralised mine water is then pumped to the various pilot scale treatment plants, where the sulfate component is treated.

Rhodes University Department of Biochemistry and Microbiology has designed and is investigating the use of a pilot scale falling sludge bed reactor (FSBR), in which treated mine water is mixed with primary settled sewage sludge. The organic feed acts as the electron donor for the sulfate reduction. The flow diagram of the process proposed by Rhodes University is illustrated in Figure 2.

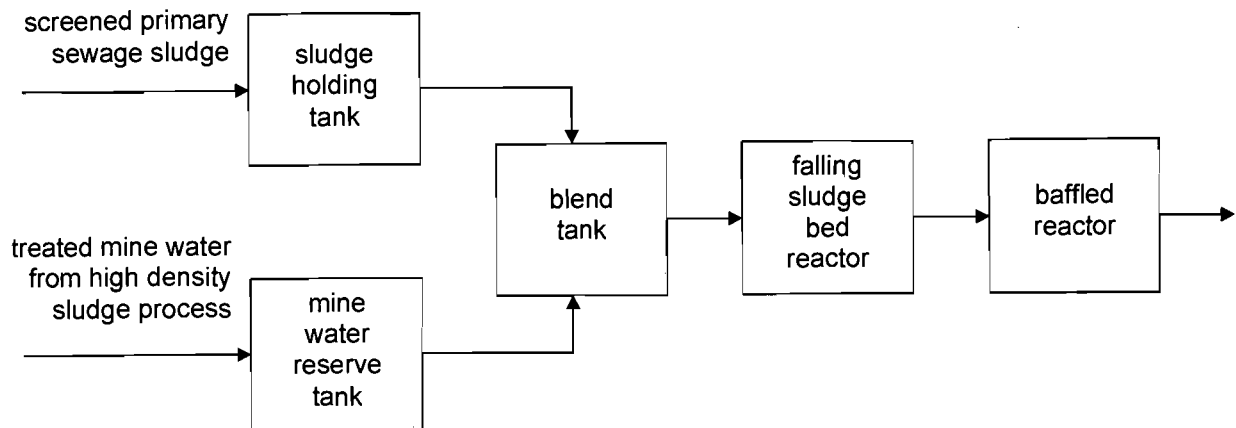


Figure 2: Schematic representation of the process developed by Rhodes University for treating AMD

The FSBR was designed and constructed by Rhodes University. The novel design ensures a high solids retention time, which increases the bacterial concentration, and allows for enhanced hydrolysis of the particulate organic feed.

At the time of writing this dissertation, no official documentation was available from Rhodes University regarding the construction and operation of the pilot plant. All information below was obtained from the many visits to both Rhodes University and the Grootvlei pilot plant, and the information was obtained from personal correspondence with Professor P. Rose, C. Corbett and K. Wittington-Jones.

The FSBR was constructed from a rectangular container (6m x 2.5m x 2.5m). Six rectangular plates were welded into the base of this container to form three valleys (Figure 3). The total working volume was 23 m³. The feed entered at a constant rate of 610 l.h⁻¹ (14.64 m³.d⁻¹), which allows for less than two days hydraulic retention time, and had an average sulfate concentration of 1700 mg.l⁻¹. The primary settled sewage sludge, obtained from Erwat (East Rand Water Care Company, Bapsfontein Road, Kempton Park, South Africa, +27 11 929 7000), was delivered weekly, and was obtained from the underflow of the primary settler from the domestic sewage works. The total chemical oxygen demand (COD) of the sewage was determined for each batch delivered to the pilot plant, and the flow rate was adjusted to give the reactor inlet the required COD: SO₄²⁻ (mass) ratio. The feed and recycle streams were pumped into the reactor through a downward facing nozzle. Recycle streams were drawn from the base of the three valleys via a pump. The pump had a total capacity of 2000 l.h⁻¹ and pumped from each of the valleys for fixed times, namely 60, 30 and 10 seconds from valleys 1, 2 and 3 respectively.

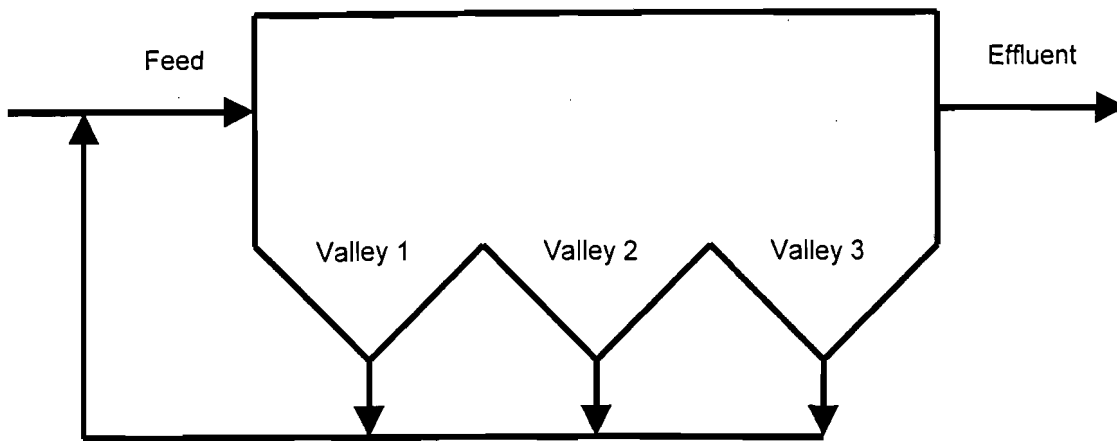


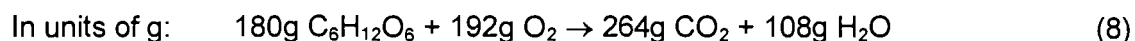
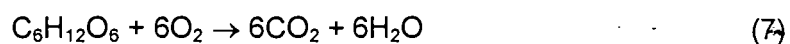
Figure 3: A schematic representation of the FSBR

The following section of the dissertation show the results of a literature survey on the mechanisms, rate equations and kinetic parameters involved in the anaerobic digestion of complex organic matter and bacterial sulfate reduction.

2. KINETICS OF ANAEROBIC DIGESTION AND SULFATE REDUCTION

The results of an extensive literature survey into anaerobic digestion and sulfate reduction are summarised below. A major finding of the literature review is that to date, no work has been published on sulfate reduction when the organic feed consists of either complex or particulate organic matter. However, it was possible to formulate a reaction scheme, which describes the anaerobic digestion of particulate organic matter based on published information. The sulfate reducing steps, based on units of COD instead of moles, were included in this reaction scheme to represent the sulfate reduction. The reaction scheme shows the transfer of the chemical oxygen demand (COD) during the anaerobic digestion of particulate COD in the presence of sulfate. The reaction scheme is shown in Figure 4. It can be divided into nine reactions or biological processes, as indicated and labelled in the figure.

The chemical oxygen demand of a compound is defined as the amount of oxygen required to oxidise all of the components of the compound to their lowest oxidative state. Therefore, all carbon must be oxidised to carbon dioxide, all sulfur species to sulfate, all nitrogen species to nitrate, and all hydrogen species to water. Values of COD have been published extensively for various compounds (as gCOD/g), or can be derived. For example, for glucose, the following process takes place:



Therefore, 192g O₂ are required for 180g C₆H₁₂O₆, giving glucose a COD value of 1.0667 gCOD.g⁻¹.

To date, the steps listed in Figure 4 have been described by means of rate equations ranging from simple first order kinetics to complex multi-substrate limiting, multi-inhibited Michaelis-Menten kinetics. In an attempt to relate the models presented in the literature to the reaction scheme, the models have been grouped according to the dominant processes shown in Figure 4. What follows is a brief summary of each author's contribution to a process, and finally a summary of each process is given.

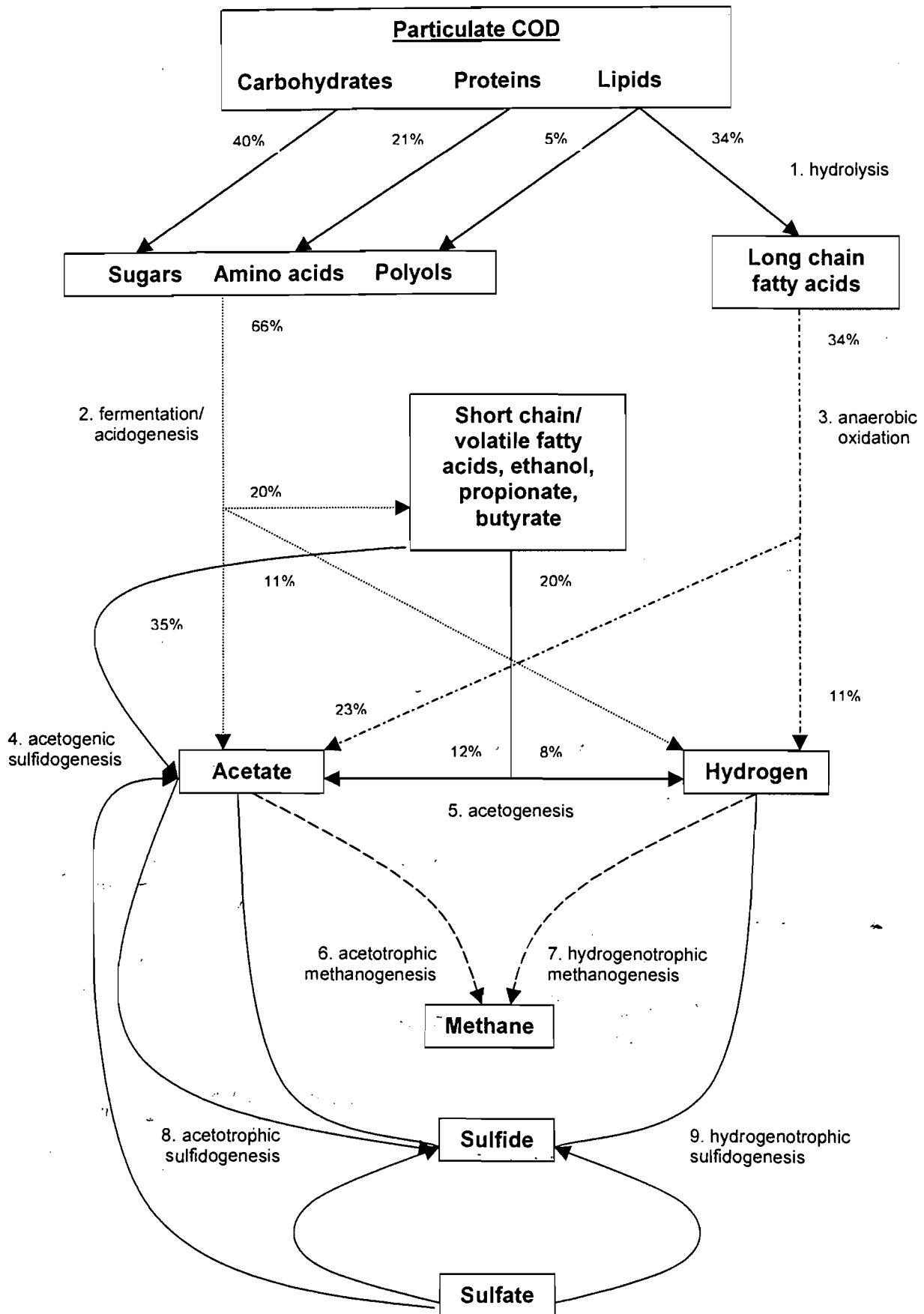


Figure 4: The reaction scheme used in the model to describe anaerobic digestion and sulfate reduction (Modified from Gujer and Zehnder, 1983)

2.1 Hydrolysis

The process whereby particulate organic material is broken into monomers or dimers is known as hydrolysis. Because particulate material cannot pass through the bacteria cell wall, the bacteria tend to form a layer over the surface of the particle, and then secrete enzymes which solubilise the polymers. The fermentative bacteria then absorb these soluble products. The reaction is complex and happens extracellularly.

The rate of hydrolysis is affected by temperature, pH, bacterial concentration, particle size, type of organic and soluble product concentration, and is generally the rate limiting step in the anaerobic digestion of particulate organic matter.

Although early work by Hill and Barth (1977), on the anaerobic digestion of animal waste, resulted in the formulation of a mathematical model based on inhibited Michaelis-Menten/ Monod kinetics, most subsequent work has modelled hydrolysis using simpler first order kinetics.

A number of researchers suggested that the rate of hydrolysis can be described as first order with respect to the particulate organic matter concentration (Eastman and Ferguson, 1981; Gujer and Zehnder, 1983; Henze and Harremoës, 1983; Bryers, 1985; Pavlostathis and Giraldo-Gomez, 1991), namely:

$$-r_{\text{COD}_p} = k_h[\text{COD}_p] \quad (9)$$

Substrates used ranged from primary domestic sludge (Eastman and Ferguson, 1981; Pavlostathis and Giraldo-Gomez, 1991), to organic solids (Gujer and Zehnder, 1983; Bryers, 1985), to wastewater (Henze and Harremoës, 1983). The hydrolysis rate constant in Equation 9 is a function of the conditions used. Gujer and Zehnder (1983) report it as a function of temperature and pH. At 28°C, the hydrolysis rate constant for the organic component of solid municipal waste has been reported to be (Hamelers *et al.*, 1998):

$$k_h = (1.95 \text{ pH} - 6.94) \times 10^{-3} \quad (10)$$

Equation 10 predicts that the rate of hydrolysis will increase with an increase in the pH of the system. Ray *et al.* (1989) extended the first order model to include two particulate components, one of which degraded at a rate that was two orders of magnitude greater than the other. This took into account the two fractions of particulate organic matter that have been identified (readily biodegradable COD and slowly biodegradable COD).

Other variations in the first order models include a product inhibition term, where high concentrations of soluble COD inhibit the hydrolysis of the particulate COD (Barthakur *et al.*, 1991):

$$-r_{\text{COD}_p} = k_h([\text{COD}_p] - [\text{COD}_s]) \quad (11)$$

Shimizu *et al.* (1993) suggested a similar expression in which the rate of hydrolysis is dependent on the concentration of degradable particulate organic matter only, and the non-degradable fraction is subtracted from the total concentration:

$$-r_{\text{COD}_p} = k_h([\text{COD}_p] - [\text{COD}_{p,n}]) \quad (12)$$

Jain *et al.* (1992) suggested a similar rate equation in which the rate of hydrolysis was first order with respect to the bulk enzyme concentration rather than the COD concentration:

$$-r_{\text{COD}_p} = k_h C_{be} \quad (13)$$

In Equation 13, the bulk enzyme concentration is calculated from:

- i) rate of biomass growth on soluble substrate
- ii) rate of enzyme production from microorganisms
- iii) rate of mass transfer of enzymes to the bulk liquid

It is clear that Equation 13 is an attempt to relate biomass concentration and activity to the rate at which hydrolysis occurs. Eliosov and Argaman (1995) directly included the active biomass concentration in the first order model:

$$-r_{\text{COD}_p} = k_h[\text{COD}_p].C_x \quad (14)$$

In order to model the rate of hydrolysis, several factors need to be taken into account. The most important of these is the type of particulate feed being fed to the system. This is further effected by the temperature and the pH of the system, and the biomass concentration in the system. The rate of hydrolysis should therefore be modelled using a first order rate equation with respect to the concentration of the particulate organic matter, where the kinetic constant is selected for the correct temperature, pH and biomass concentration, or as a function of these three factors.

For the model, a rate equation was used for the degradation of each of the components of the primary settled sewage sludge. These equations were first order with respect to the three components, namely proteins, carbohydrates and lipids, with kinetic constants chosen for each of these from O'Rourke (1968).

2.2 Fermentation/Acidogenesis

Fermentation is the process in which long chain soluble monomers or dimers, such as carbohydrates and amino acids, are reduced to short chain volatile fatty acids, such as acetic acid, propionic acid, butyric acid, lactic acid and ethanol, or longer chain fatty acids. Fermentative bacteria, or acidogens, are generally faster growing than the other bacteria involved in anaerobic digestion, and are more resistant to inhibition than the other bacteria. For this reason, fermentation has sometimes been omitted from model development, since it will not limit the rate of the overall process, and will have little influence on the system.

When included in the model development, most workers have chosen to describe fermentation kinetics by means of either Michaelis-Menten or Monod kinetics. The simplest form of the Monod equation relates the bacterial specific growth rate to the substrate concentration as follows:

$$\mu = \frac{\mu_{\max}}{1 + \frac{K_s}{[\text{COD}_s]}} \quad (15)$$

The rate of substrate utilisation can then be determined using Equation 16.

$$r_s = \frac{\mu \cdot C_x}{Y_{sx}} \quad (16)$$

The rate of increase in biomass concentration is then given Equation 17.

$$r_x = \mu \cdot C_x - k_d \cdot C_x \quad (17)$$

To date, simple Monod kinetics have been used to describe the fermentation kinetics of a number of substrates, under a range of operating conditions (Gujer and Zehnder, 1983; Bryers, 1985; Pavlostathis and Giraldo-Gomez, 1991; Buffiere *et al.*, 1995; Jeyaseelan, 1997; Wu *et al.*, 1998).

Similar to the Monod equation in form is the Michaelis-Menten equation, which Yu and Pinder (1993) chose to describe the rate of lactose degradation:

$$v = \frac{v_{\max}}{1 + \frac{K_s}{[\text{COD}_s]}} \quad (18)$$

Although the Monod equation and the Michaelis-Menten equation are similar in form, they have been derived from two different aspects of biological reactions. The Monod equation is empirical, and refers to the observed relation between the substrate

concentrations and the microbial reaction rate. The Michaelis-Menten equation was derived from a specific enzyme mechanism and specific reaction scheme, and is mathematically rigorous. However, the values of the kinetic constants used in the Monod equation and Michaelis-Menten equation are mathematically related, and these reactions and kinetic constants have been used interchangeably in the literature.

Several researchers have suggested that, under certain conditions, fermentation kinetics are best described by inhibited Monod kinetics models. Moletta *et al.* (1986) and Kiely *et al.* (1997) proposed that the fermentation kinetics of organic wastes were uncompetitively inhibited by acetic acid, according to Equation 19:

$$\mu = \frac{\mu_{\max}}{1 + \frac{K_s}{[\text{COD}_s]} + \frac{[\text{HAc}]}{K_{\text{HAc}}}} \quad (19)$$

Equation 19 was further modified by Costello *et al.* (1991) to account for inhibition by both pH and dissolved hydrogen gas:

$$\mu = \frac{\mu_{\max}}{1 + \frac{K_s}{[\text{COD}_s]} + \frac{[\text{HAc}]}{K_{\text{HAc}}}} = \frac{-r_s \cdot Y_{\text{SX}}}{C_x} \cdot \left(\frac{1}{1 + zn} \right)^{-1} \left(\frac{\text{pH} - \text{pH}_{\text{LL}}}{\text{pH}_{\text{UL}} - \text{pH}_{\text{LL}}} \right)^{-M} \quad (20)$$

Costello *et al.* (1991) also added terms to the model to predict the formation of certain products of the degradation of glucose under conditions of high dissolved hydrogen concentrations. Since hydrogen is a product of some of these reactions, the reactions that produce less or no hydrogen would be favoured under conditions of high dissolved hydrogen concentrations. This is discussed further in Section 2.8.

Denopoulou *et al.* (1988) found that the affect of high concentrations of volatile fatty acids resulted in noncompetitive inhibition of bacterial growth according to:

$$\mu = \frac{\mu_{\max}}{\left(1 + \frac{K_s}{[\text{COD}_s]} \right) \left(1 + \frac{[\text{VFA}]}{K_{\text{VFA}}} \right)} \quad (21)$$

Kalyuzhnyi and Fedorovich (1998) developed a Monod based model to demonstrate the competition between SRB and MPB in anaerobic reactors, which included a first order term for the inhibition of fermentation due to sulfide:

$$\mu = \frac{\mu_{\max}}{1 + \frac{K_s}{[\text{COD}_s]} \left(1 - \frac{[\text{H}_2\text{S}]}{K_{\text{H}_2\text{S}}} \right)} \quad (22)$$

The rate of fermentation is never rate limiting, and could be excluded from the model. However, if included, a modified Monod equation should be used. This rate equation should include a switch function to account for high hydrogen concentrations, if necessary. Although acetic acid does not inhibit this reaction, a competitive inhibition term was included in the model, as used by Costello *et al.* (1991), and a sulfide inhibition term as used by Kalyuzhnyi and Fedorovich (1998).

2.3 Anaerobic Oxidation

Anaerobic oxidation refers to the process whereby the long chain fatty acids from the hydrolysis of the lipid fraction of particulate organic matter are anaerobically oxidised to acetic acid and hydrogen. Although the rate of anaerobic oxidation has been extensively discussed by Gujer and Zehnder (1983), little emphasis has been placed on this reaction in the literature, as it follows roughly the same kinetics and reaction scheme as the fermentative bacteria. For this reason, most workers have used the Monod equation to describe the rate at which anaerobic oxidation takes place (O'Rourke, 1968; Novak and Carlson, 1970; Pavlostathis and Giraldo-Gomez, 1991). To date, it has been included in most models in the acidogenic step.

In the model developed in this study, the Monod equation was used for this reaction, with a first order sulfide inhibition term (Equation 22).

2.4 Acetogenic Sulfidogenesis

Sulfate reducing bacteria are considered to be capable of growing on more varied substrates than methane producing bacteria, such as propionate, butyrate, lactate and ethanol, and have been reported to prefer these to acetate (Oude Elferink *et al.*, 1994). Sulfate reducing bacteria are able to degrade short chain volatile fatty acids, excluding acetic acid, as well as other substrates such as ethanol. The process has acetic acid and hydrogen sulfide as its products, and is therefore named acetogenic sulfidogenesis. However, the degradation of more complex substrates, such as sugars and amino acids, has not been reported.

As in the case of previously discussed steps in anaerobic digestion and bacterial sulfate reduction, a number of researchers have used basic forms of the Monod equations to describe the kinetics of acetogenic sulfidogenesis (Heyes and Hall, 1983; Chen *et al.*, 1994; Laanbroek *et al.*, 1984), or the Michaelis-Menten equations (Harada *et al.*, 1994).

In contrast to most researchers, Szewzyk and Pfennig (1990) and Okabe *et al.* (1992) chose to use the Pirt equation (Pirt, 1975) to describe the kinetics of acetogenic sulfidogenesis for SRB grown on ethanol and lactate, respectively. The Pirt equation relates the rate of substrate utilisation to the growth rate via the yield and maintenance coefficients:

$$-r_s = \frac{r_x}{Y_{SX}} + mC_x \quad (23)$$

This can therefore be used in conjunction with Monod kinetics to give (Szewzyk and Pfennig, 1990):

$$r_s = \frac{\mu_{\max} \cdot C_x}{Y_{SX}^{\max} \left(1 + \frac{K_s}{[VFA]} \right)} + mC_x \quad (24)$$

Specific to the Pirt equation, the maximum yield, Y_{SX}^{\max} , differs from Y_{SX} , but the maintenance coefficient, m , and the dilution rate, D relate the two yield coefficients as follows:

$$\frac{1}{Y_{SX}} = \frac{1}{Y_{SX}^{\max}} + \frac{m}{D} \quad (25)$$

Reis *et al.* (1992) proposed a model that included terms that accounted for product inhibition by both sulfide and acetic acid:

$$\frac{\mu}{\mu_{\max}} = \frac{\left(1 - \frac{[H_2S]}{K_{H_2S}} \right)^n}{\left(1 + \left(\frac{[HAc]}{K_{HAc}} \right)^p \right)} \quad (26)$$

In addition, Reis *et al.* (1992) found that the affect of pH range was adequately described by means of a competitive inhibition model:

$$\mu = \frac{\mu_{\max}}{1 + \frac{[H^+]}{K_H} + \frac{K_{OH}}{[H^+]}} \quad (27)$$

As in the case of fermentation, a number of researchers have found the kinetics of acetogenic sulfidogenesis to be inhibited by sulfide. The reported forms of inhibition have ranged from noncompetitive inhibition (Okabe *et al.*, 1995), to uncompetitive inhibition (Maillecheruvu and Parkin, 1996), to first order inhibition (Kalyuzhnyi and

Fedorovich, 1998). These inhibition terms are discussed further in Appendix A, and their effect on the rate equation at varying inhibitor concentrations is illustrated.

A topic of many studies on bacterial sulfate reduction has been the affects of the feed organic substrate to sulfate ratio (Laanbroek *et al.*, 1984; Isa *et al.*, 1986; Yoda *et al.*, 1987; Bhattacharya, Uberoi and Dronamraju, 1996). In cases of a high organic substrate to sulfate ratio, methanogenesis dominates, while when sulfate is in excess, sulfidogenesis predominates. To account for these variations in the available substrates, Konishi *et al.* (1996) and Kalyuzhnyi and Fedorovich (1998) used a dual substrate form of the Monod equation, although Kalyuzhnyi and Fedorovich (1998) also included a term for sulfide inhibition, similar to Equation 22:

$$\mu = \frac{\mu_{\max}}{\left(1 + \frac{K_{\text{HLac}}}{[\text{HLac}]}\right) \left(1 + \frac{K_{\text{SO}_4^{2-}}}{[\text{SO}_4^{2-}]}\right)} \quad (28)$$

According to Equation 28, the bacteria will be limited at low concentrations of both organic substrate and sulfate.

Acetogenic sulfidogenesis should only be included in models that deal with long chain fatty acid degradation in the presence of SRB. The rate equation used in the model was a two-limiting substrate Monod type equation, for sulfate and the organic substrate, and included a first order sulfide inhibition term.

2.5 Acetogenesis

This is the reaction that degrades short chain fatty acids such as propionic acid, butyric acid, or longer chain fatty acids, as well as other intermediates such as ethanol, to acetic acid and hydrogen, in the absence of sulfate, or in competition with the acetogenic sulfidogenic bacteria. Obligate hydrogen producing bacteria, or acetogens, have been extensively studied because of the importance of this particular step on the overall process. By producing acetic acid, the pH of the bioreactor will drop, suppressing other biological reactions that prefer higher pH than the acetogens. Also, the production of hydrogen in the system inhibits the formation of acetic acid, thereby inhibiting the anaerobic digestion, and resulting in process failure (see Section 2.8). It also produces the two substrates used for methanogenesis, which is accepted as the rate-controlling step in the absence of hydrolysis.

Even in spite of the above factors, simple rate equations have still been used to model this step, such as first order (Shimizu *et al.*, 1993; Hamelers *et al.*, 1998), the Monod equation (Eastman and Ferguson, 1981; Gujer and Zehnder, 1983; Bryers, 1985; Pavlostathis and Giraldo-Gomez, 1991; Buffiere *et al.*, 1995), or the Michaelis-Menten equation (Kasper and Wuhrmann, 1978; Ahring and Westermann, 1987; Lin *et al.*, 1989).

Henze and Harremoes (1983) used Equation 19 for uncompetitive acetic acid inhibition. Hill and Barth (1977) used Equation 19 to describe acetogenesis, except that the inhibitory substance was the total volatile fatty acid concentration, rather than acetic acid. Thiele and Zeikus (1988) and Costello *et al.* (1991) used a non-competitive model (Equation 21), although Costello *et al.* (1991) included terms for hydrogen inhibition and pH inhibition for the degradation of lactic acid. For propionic acid and butyric acid, Costello *et al.* (1991) used a competitive inhibition model, again with terms for hydrogen inhibition and pH inhibition:

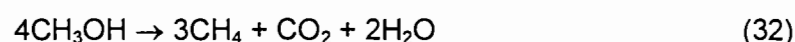
$$\mu = \frac{\mu_{\max}}{1 + \frac{K_s}{[\text{VFA}] \left(1 + \frac{[\text{HAc}]}{K_{\text{HAc}}} \right)}} \quad (29)$$

Kalyuzhnyi and Fedorovich (1998) used Equation 22 to describe the inhibition of acetogenesis by sulfide.

Acetogenesis is not affected by high acetic acid concentrations. However, a term for noncompetitive inhibition by acetic acid was included in the model, as given by Costello *et al.* (1991), and first order sulfide inhibition term from Kalyuzhnyi and Fedorovich (1998).

2.6 Methanogenesis

Methanogenesis is the process whereby low molecular weight substrates are degraded to form methane. The following reactions take place:



Methanogenesis is the final step in anaerobic digestion, and is generally the rate-limiting step when hydrolysis does not occur in the system. Approximately 70% of all methane is formed from acetate cleavage or acetoclastic methanogenesis (Equation 30), whereas the production of methane from methanol (Equation 32) is seldom

observed. For this reason, methanogenesis is often modelled as a single final step, the rate of which is equivalent to the rate of acetate cleavage, i.e. acetoclastic methanogenesis.

2.6.1 Acetoclastic Methanogenesis

As stated above, the majority of methane is formed from acetate cleavage, and this process is often the rate-limiting step in the anaerobic digestion of soluble organics. Although acetoclastic methanogenesis has been described using simple first order kinetics (Ray *et al.*, 1989; Shimizu *et al.*, 1993), most researchers have chosen to model the kinetics using either simple Monod (Henze and Harremoës, 1983; Gujer and Zehnder, 1983; Bryers, 1985; Thiele and Ziekus, 1988; Pavlostathis and Giraldo-Gomez, 1991; Buffiere *et al.*, 1995; Jeyaseelan, 1997; Wu *et al.*, 1998) or Michaelis-Menten kinetics (Kasper and Wuhrmann, 1978; Ahring and Westermann, 1987; Lin *et al.*, 1989). Although most researchers have adequately described acetoclastic methanogenesis by means of the basic Monod equation, methanogenesis is inhibited by all of the following: VFA, NH_3 , 3-ethylphenol, pH and sulfide.

Andrews and Graef (1971), Moletta *et al.* (1986) and Fox and Suidan (1990) found that acetoclastic methanogenesis could be described by means of the Monod equation, modified to account for uncompetitive inhibition (Equation 19) by acetic acid, VFA and 3-ethylphenol respectively, where as Hill and Barth (1977) and Kiely *et al.* (1997) found that the specific growth rate of methanogens was inhibited by both volatile fatty acids and ammonia:

$$\mu = \frac{\mu_{\max}}{1 + \frac{K_s}{[\text{HAC}]} + \frac{[\text{VFA}]}{K_{\text{VFA}}} + \frac{[\text{NH}_3]}{K_{\text{NH}_3}}} \quad (33)$$

On the other hand, Costello *et al.* (1991) used the Monod equation with a pH inhibition term and a hydrogen inhibition term, similar to Equation 20, to describe the rate of methane formation from acetate.

Kalyuzhnyi and Fedorovich (1998) included a first order term for sulfide inhibition in the rate equation describing methanogenesis from acetate. The specific growth rate of the methanogens could be described by Equation 22.

The rate equation for acetoclastic methanogenesis was modelled using a Monod equation with a term for first order sulfide inhibition. Acetic acid inhibition should have been included here, but was erroneously omitted.

2.6.2 Hydrogenotrophic Methanogenesis

The growth of methanogens using hydrogen as substrate (Equation 31) has been described using simple Monod (Gujer and Zehnder, 1983; Bryers, 1985; Pavlostathis and Giraldo-Gomez, 1991; Buffiere *et al.*, 1995) and Monod kinetics modified to account for pH (Costello *et al.*, 1991) and sulfide inhibition (Kalyuzhnyi and Fedorovich, 1998). Costello *et al.* (1991) used an equation similar to the form of Equation 20, whereas Kalyuzhnyi and Fedorovich (1998) used an equation analogous to Equation 22. In addition to Monod kinetics, hydrogenotrophic methanogenesis has also been modelled using both single (Ahring and Westermann, 1987) and inhibited Michaelis-Menten kinetics (Giraldo-Gomez *et al.*, 1992).

Giraldo-Gomez *et al.* (1992) proposed that the rate of hydrogen utilisation could be modelled using the Michaelis-Menten equation modified to include threshold concentration of hydrogen, which is the concentration below which no substrate is consumed:

$$v = \frac{v_{\max}([H_2] - T)}{K'_s + ([H_2] - T)} \quad (34)$$

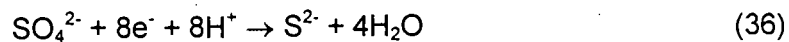
In addition, they suggested that there are two pools of hydrogen in bacterial aggregates; the internal pool where hydrogen is produced during acetogenesis, and the external pool where hydrogen is in equilibrium with the atmosphere, and that when mass transfer limitations exist, the apparent half saturation constant is given by:

$$K'_s = \frac{K_s}{\eta} \quad (35)$$

As mentioned before, this step has been omitted from most anaerobic digestion models, including those describing the inhibition of methanogenesis by acetic acid, VFA, ammonia and 3-ethylphenol. Therefore, there is no literature on the inhibition of the hydrogenotrophic methanogens by these compounds. Therefore, for the model proposed in this study, the rate was described using the Monod equation with a term for first order sulfide inhibition (Equation 22).

2.7 Sulfidogenesis

Sulfidogenesis is the process in which sulfate is reduced to sulfide by the SRB.



The two electron donors discussed below are acetic acid and hydrogen. Acetoclastic sulfidogenesis refers to the above reaction when acetate is the electron donor (Equation 5). Hydrogenotrophic sulfidogenesis refers to the utilisation of hydrogen as the electron donor (Equation 6). These two reactions occur due to different groups of bacteria.

Methanogens tend to adhere to carrier particles or aggregates more effectively than SRB, and will therefore dominate in systems close to washout (Isa *et al.*, 1986; Harada *et al.*, 1994; Shin *et al.*, 1996). SRB present in aggregates are due to entrapment, rather than attachment, and thus bioreactors can be designed to favour one reaction over the other.

The organic electron donor to sulfate ratio has an affect on the competition between SRB and MPB for dominance (Isa *et al.*, 1986; Oude Elferink *et al.*, 1994; Bhattacharya, Uberoi and Dronamraju, 1996). At COD: sulfate ratios greater than 10, MPB tend to be the dominant species in the system. At ratios less than 1, SRB tend to dominate. At ratios between these two limits, both SRB and MPB are present in the system.

A product of sulfate reduction is sulfide. Sulfide in the undissociated form is toxic, malodourous, and corrosive (Oude Elferink *et al.*, 1994), and inhibits the growth of all bacteria. However, SRB are more resistant to sulfide than MPB (Maillecheruvu and Parkin 1996).

2.7.1 Acetoclastic Sulfidogenesis

Acetoclastic sulfidogens are generally slower growing than hydrogenotrophic sulfidogens, but will outcompete the acetoclastic methanogens for acetate in the absence of longer chain fatty acids. When longer chain fatty acids are present, these are preferred by the SRB (Oude Elferink *et al.*, 1994; Maillecheruvu and Parkin 1996).

Once again, the rate equations describing acetoclastic sulfidogenesis vary from simple Monod (Gupta *et al.*, 1994; Bhattacharya *et al.*, 1996) or Michaelis-Menten kinetics (Isa *et al.*, 1986; Harada *et al.*, 1994; Shin *et al.*, 1996). Maillecheruvu and

Parkin (1996) used Equation 19 for the uncompetitive inhibition of the Monod equation due to sulfide rather than acetic acid. Kalyuzhnyi and Fedorovich (1998) included a first order inhibition term for sulfide, as well as a two limiting substrate Monod equation for sulfate and acetate:

$$\mu = \frac{\mu_{\max}}{\left(1 + \frac{K_s}{[\text{HAc}]}\right) \left(1 + \frac{K_{\text{SO}_4^{2-}}}{[\text{SO}_4^{2-}]}\right)} \left(1 - \frac{[\text{H}_2\text{S}]}{K_{\text{H}_2\text{S}}}\right) \quad (37)$$

Equation 37 was used in the model to predict the rate of the acetoclastic sulfidogens.

2.7.2 Hydrogenotrophic Sulfidogenesis

Hydrogenotrophic sulfidogens control the concentration of dissolved hydrogen in a sulfate reducing system. They have a higher affinity for hydrogen than the hydrogenotrophic methanogens, and tend to keep the concentration below the thermodynamic limit, at which methanogenesis becomes non-spontaneous, in order to starve the methanogens (Kristjansson *et al.*, 1982). The other consequence of this control regards the degradation of sugars and long chain fatty acids, where under high and low concentrations of dissolved hydrogen, different products are formed (Costello *et al.*, 1991).

The growth of these SRB has been described using single Michaelis-Menten kinetics (Kristjansson *et al.*, 1982; Isa *et al.*, 1986; Harada *et al.*, 1994; Shin *et al.*, 1996). Maillecheruvu and Parkin (1996) used Equation 19 for the uncompetitive inhibition of the Monod equation due to sulfide rather than acetic acid, while Kalyuzhnyi and Fedorovich (1998) again used Equation 37.

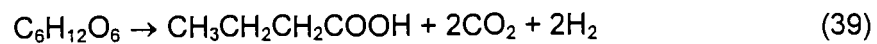
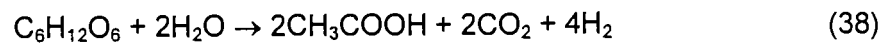
Equation 37 was once again used in the model, with hydrogen as the organic substrate, for the rate of hydrogenotrophic sulfidogenesis.

2.8 Hydrogen Partial Pressure

In the anaerobic treatment of organic waste materials, the partial pressure of hydrogen plays an important role. The regulatory effect that the partial pressure of hydrogen has on anaerobic digestion systems has been studied (Kasper and Wuhrmann, 1978; Mosey, 1983; Harper and Pohland, 1986; Costello *et al.*, 1991). The majority of the work has been done using known organic substrates, such as

glucose (Mosey, 1983; Harper and Pohland, 1986; Costello *et al.*, 1991) and propionate (Kasper and Wuhrmann, 1978).

In the degradation of complex soluble organic matter, several catabolic pathways are available to the bacteria. The majority of these reactions produce a volatile fatty acid and hydrogen. The following reactions are involved in the degradation of glucose:



Similar reactions exist for the degradation of other intermediary products of anaerobic digestion. Under conditions of low hydrogen partial pressure, the formation of acetic acid from glucose gives the fermentative bacteria the most energy (Equation 38), and would be favoured. However, under conditions of high hydrogen partial pressure, this reaction would be the least favoured of the three, since 4 moles of hydrogen are produced for each mole of glucose consumed, while for the others, hydrogen is either produced in smaller quantities (Equation 39) or is consumed (Equation 40). For Equation 38, at high hydrogen partial pressures, there is a positive change in the Gibb's Free Energy, and this reaction becomes non-spontaneous. The overall effect of the hydrogen partial pressure is that the ratio of the products of the biological degradation of glucose will change with a change in hydrogen partial pressure.

For sulfate reducing systems, the hydrogen partial pressure is also regulatory, in that the acetogenic reactions become non-spontaneous at high hydrogen partial pressures, while the hydrogenotrophic sulfidogenic and methanogenic reactions become non-spontaneous at low hydrogen partial pressures. The lower limit for the sulfidogens is also lower than for the methanogens, and the sulfidogens tend to maintain the hydrogen partial pressure below the methanogenic limit, to eliminate the competition for the organic substrate between the two groups of bacteria.

The hydrogen partial pressure found in natural ecosystems at steady state can be between 6 and 400 Pa (Oude Elferink *et al.*, 1994). This implies that a large range of partial pressure can be accommodated by anaerobic systems, at steady state. However, the failure of anaerobic digestion systems normally occurs due to a shock increase in the organic loading rate to the system. Under these conditions, the partial pressure of hydrogen will increase, causing certain reactions to become non-spontaneous. This in turn results in a build up of volatile fatty acids, which decreases the pH of the system. Overall system failure results in a low pH with a high volatile fatty acid concentration.

Little work has been done to model the effects of hydrogen partial pressure on anaerobic digestion systems, especially in the presence of sulfate reducing bacteria. Mosey (1983) and Costello *et al.* (1991) included terms for hydrogen inhibition in the degradation of glucose, as well as for the stoichiometry of formation of the products, so that the model would correctly predict the formation of certain long and short chain fatty acids at various hydrogen partial pressures. However, no work has been done on modelling an anaerobic digestion system when the organic feed contains particulates, or complex waste products.

2.9 Summary

The review shows that the literature contains a variety of rate equations that have been used to describe anaerobic digestion and sulfate reduction. Many different reaction schemes or mechanisms exist for describing the degradation pathways of particulate and complex soluble organic materials. The choice of a particular reaction scheme has often determined the complexity and form of the rate equations used to model the system. These rate equations also differ for the different processes, where some processes include terms for inhibition where other processes are not inhibited. However, the following summary indicates that an anaerobic system degrading particulate organic matter can be modelled using Figure 4, with a choice of rate equation according to the following guidelines.

The rate of **hydrolysis** is the rate-limiting step in the anaerobic digestion of particulate organic matter. It is affected by temperature, pH, hydrolytic fermentative bacterial concentration, particle size, type of organic matter and the soluble product concentration. However, since this step has been studied widely, it is possible to choose a first order rate constant for a particular feed at a specified temperature and pH. In the case of a particulate feed that consists of a variety of different components, more than one equation, with different rate constants, can be used to model this reaction.

Another point often discussed about hydrolysis is the two fractions of particulate organic matter, namely readily biodegradable COD (RBCOD), and slowly biodegradable COD (SBCOD). Ray *et al.* (1989) used two rate equations for the hydrolysis step of the model, with varying rates. However, for this model, kinetic constants are available for the degradation of each of the components of primary settled sewage sludge, and these components degrade at different rates, thereby

facilitating the differential degradation of the readily and slowly degradable particulate COD.

The overall lack of literature data for **anaerobic oxidation**, and the ability of mathematical models to predict rates of anaerobic digestion while omitting it specifically from the reaction scheme, suggests that this process does not contribute significantly to the overall kinetics of the anaerobic digestion of complex organic matter.

Fermentative bacteria or acidogens are faster growing than other anaerobic digesting bacteria, and are more resistant to contamination and toxicity than the other types of bacteria. For this reason, **fermentation or acidogenesis** is seldom rate limiting, hence it has been left out of many kinetic models. This reaction forms acetic acid, which inhibits biological reactions when at high concentrations. However, in instances of high acetic acid, and thus process failure, this reaction would not fail. However, the hydrogen partial pressure does affect the stoichiometry of this process, depending on the organic feed, and could be included in the modelling of a system operating at high organic loading rates.

Acetogenesis is an important step in anaerobic digestion since it produces acidity which lowers the pH, inhibiting the methane producing bacteria, and also produces hydrogen, which has a regulatory effect on the preferred production of fatty acid species. The role of hydrogen in controlling this step has been discussed (Harper and Pohland 1985), and if the hydrogen concentration exceeds either of the upper or lower limits, switch function terms should be included to model this. In the presence of sulfate-reducing bacteria, sulfide inhibition terms should be included.

For all sulfate-reducing bacteria, a two-limiting-substrate Monod-type equation should be used in the model. Sulfide inhibition terms should also always be included. **Acetogenic sulfidogenesis** has only recently been identified as a step in sulfate reduction. The SRB are able to use more complex organic substrates than acetate, while MPB are limited to acetate and hydrogen. It has been shown that the SRB prefer to grow on these longer chain volatile fatty acids rather than on acetate. However, the build-up of acetate in these systems is often observed (Personal correspondence with C. Erasmus), suggesting that acetoclastic sulfidogenesis is rate limiting rather than acetogenic sulfidogenesis. However, production of sulfide inhibits all biological reactions, and product inhibition of this reaction by sulfide is expected. As this process also produces acetate, acetic acid inhibition is possible, since acetic acid is inhibitory to anaerobic digestion systems.

Acetoclastic methanogenesis is one of the most important reactions in methanogenic systems, since approximately 70% of all methane produced is by acetate cleavage. It is the rate limiting step in the anaerobic digestion of soluble organic feeds, and operating conditions are normally adjusted to optimise the rate of this reaction. However, it can be inhibited by acetic acid and sulfide, and has an optimum pH of greater than 7, since both acetate and hydrogen sulfide are mostly in their undissociated forms at this pH, and are therefore un-inhibiting. Other workers have modelled this step with a term for acetic acid inhibition. These models also included ammonia inhibition, which could be included in a model for nitrification and denitrification, or where high levels of nitrogenous compounds are expected. A term for sulfide inhibition should be included if sulfate reduction is taking place.

Hydrogenotrophic methanogenesis has not been studied as extensively as acetate cleavage, but is said to be important to anaerobic systems, since the hydrogen concentration regulates the rate of production of the volatile fatty acids. The Gibb's Free Energy for the biological degradation reactions has been plotted as a function of hydrogen partial pressure (Harper and Pohland, 1986), and this shows the 'operating window' for the hydrogen partial pressure in which all biological reactions will proceed spontaneously. Since these bacteria use hydrogen for growth, they control the concentration in the anaerobic digestion system, thereby controlling the system. At low partial pressures of hydrogen, this step would be inhibited. A switch function describing this could be included in the model if low concentrations of hydrogen were being predicted.

Hydrogenotrophic sulfidogenesis controls the hydrogen concentration in a sulfate reducing system, as well as producing the inhibitory hydrogen sulfide, since they outcompete the MPB for hydrogen, and can maintain the concentration below that at which the MPB can grow successfully.

In general, SRB outcompete MPB for substrate, and should dominate in a co-culture of anaerobic digesting and sulfate reducing bacteria. However, MPB tend to form agglomerates more effectively, as well as immobilise on the reactor packing more effectively. Therefore, in a reactor operating close to washout, the MPB should predominate over the SRB. It has also been shown that the feed organic substrate to sulfate ratio affects the population ratios inside the bioreactor. The explanation for this could be that the SRB have two limiting substrates and that if either the organic substrate or the sulfate concentration is limiting, these bacteria would not compete effectively.

3. AQUASIM AS A SIMULATION TOOL

The program AQUASIM was designed for the identification and simulation of aquatic systems in the laboratory, in technical plants and in nature. The program is a tool that performs four main tasks: simulation, identifiability analysis, parameter estimation and uncertainty analysis. It has been applied to a number of biological systems, the majority of these involving denitrification of activated sludge. In this study, for the first time, AQUASIM was applied to a bacterial sulfate reduction process.

Aquatic systems can generally be divided into a number of zones with well-defined transport processes in which spatial interactions are essential, but where the interactions with other zones are limited to a small number of well defined interfaces. These zones are called compartments. The description of an aquatic system is based on a division of the system into such compartments. Although the introduction of specific types of compartments limits the generality of the approach, it does allow for the selection of efficient numerical algorithms according to the type of partial differential equation used to describe the transport process (Reichert 1994).

AQUASIM makes use of the following compartments: mixed reactor, biofilm reactor, advective-diffusive reactor, saturated soil column, river section and lake compartment. The compartments can be linked with advective links, in which water flows between two compartments, or diffusive links, in which some diffusive layer exists, such as a membrane or gas-liquid or liquid-solid interface.

For each of the compartments, the processes taking place inside need to be defined. These processes make use of a number of variables of various descriptions, according to AQUASIM. State variables refer to concentrations of the components, while constant variables refer to values of the kinetic parameters of the processes, or equilibrium constants. Formula variables allow for the definition of one variable as a function of another. Figure 5 shows the logical structure of AQUASIM systems.

There are a number of advantages of using AQUASIM to model the FSBR. The program is relatively easy to use. It does not require knowledge of a programming language. The mathematical algorithms used in the calculation of the simultaneous rate equations are complex and rigorous, but require no input from the user, except to define the variables, state the rate equation, and the reaction stoichiometry. The

reactor compartments allow for the calculation of complex reactions in complex systems, if the system has been defined accurately by the user. It has ability to model equilibrium reactions such as acid-base equilibria, liquid-gas equilibria, and diffusion through biofilms. All of these advantages allow for AQUASIM to be used in a number of applications.

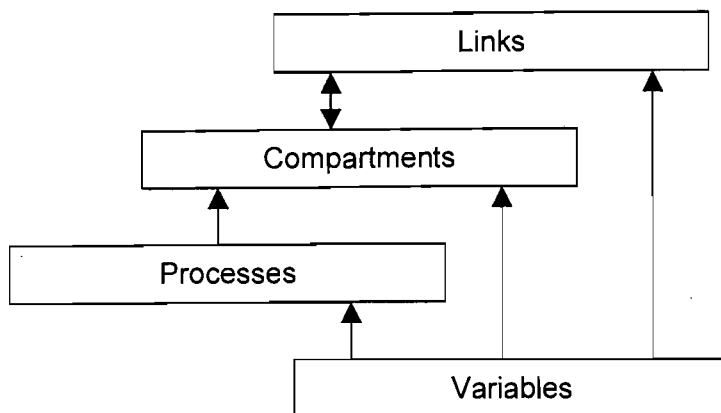


Figure 5: The logical structure of AQUASIM

The main drawback of AQUASIM is the absence of a database, requiring that the user define all kinetic and equilibrium constants. This can be done with relative ease when modelling only the bacterial interactions in a reactor. However, when the equilibrium reactions taking place in an aquatic system are included in the model, the model can become excessively complex. For example, if ferrous iron is added to the solution, the equilibria between the ferrous ion and the hydroxide ion only are numerous, since they form a number of complexes. Two equilibrium equations would need to be included for each of these equilibria. However, some of these equilibria are kinetically controlled, and these kinetics would then also need to be added.

Programmes that have been developed to model solution chemistry do exist, and it would seem more reasonable to utilise one of these packages to model the solution chemistry, instead of using AQUASIM. However, for the modelling of the bacterial systems, ignoring the solution chemistry, AQUASIM has many advantages, and the use is justified.

4. MODEL FORMULATION AND DEVELOPMENT

Figure 6 shows the steps used in developing and calibrating the model. The following sections of the report discuss each of these steps individually.

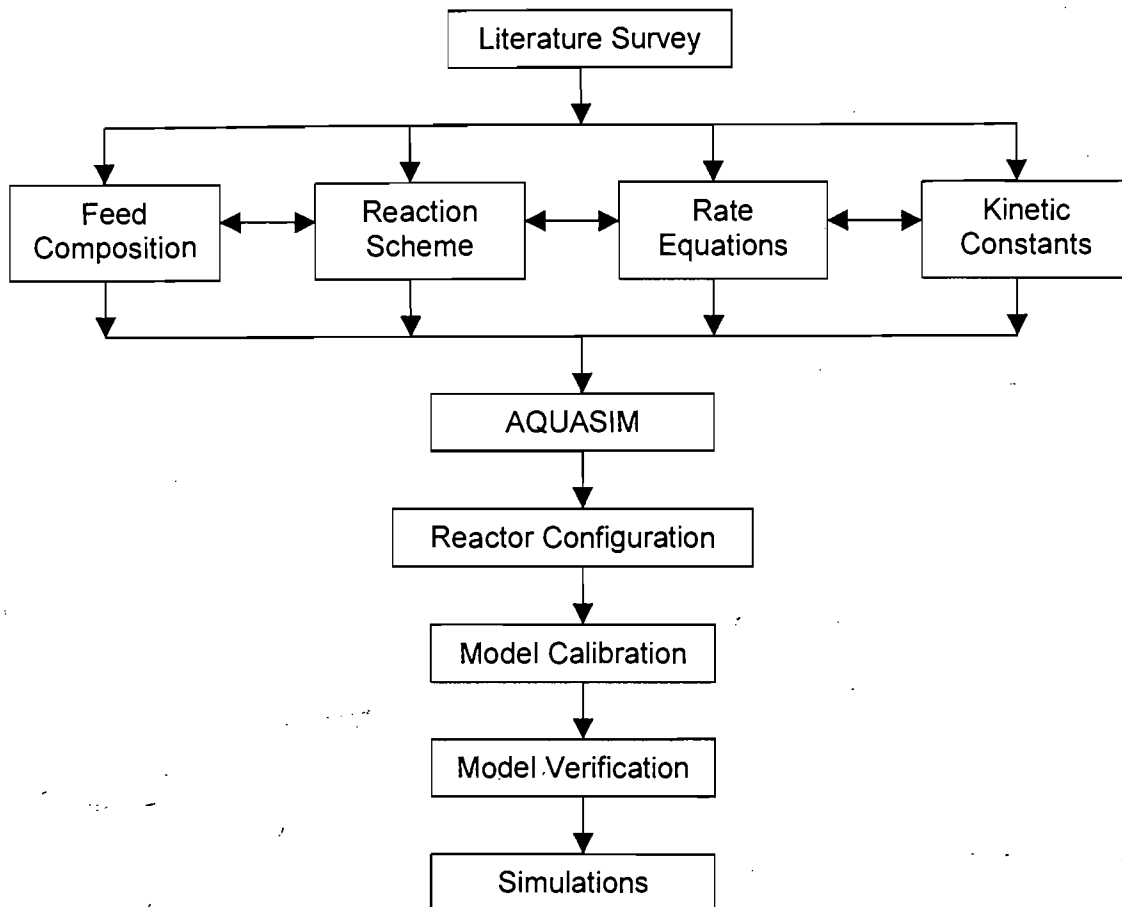


Figure 6: Procedure used in developing the model

Figure 6 shows the order in which the model development proceeded. The operating conditions of the pilot plant defined the boundaries of the project. The literature was surveyed in order to get a model to predict the FSBR performance. A reaction scheme for the anaerobic digestion of particulate organic matter in the presence of sulfate and sulfate reducing bacteria needed to be defined from the literature. The composition of the organic feed also needed to be determined from the literature, since this was not defined from the pilot plant analysis.

Once this reaction scheme had been chosen, it was then necessary to choose a rate equation that would predict the rate of each reaction in the scheme, and the

interactions between the various groups of bacteria. Once again, the conditions of the pilot plant would determine the choice of rate equation since for example terms for sulfide inhibition would need to be included that would not be included in an anaerobic digestion model in the absence of sulfate and sulfate reducing bacteria.

Finally, the choice of kinetic constants needed to be made. This choice is mostly affected by the temperature and pH of the system, or in the case of hydrolysis, the particular feed being used.

The following sections describe the choices made from the literature regarding the organic feed composition, the reaction scheme, the rate equations and finally the kinetic constants that are used in this study.

4.1 Organic Feed Composition

Pavlostathis and Giraldo-Gomez (1991) compared the typical composition of primary municipal sludge and activated sludge, as given by five separate authors. The composition of primary municipal sludge was given by O'Rourke (1968), Eastman and Ferguson (1981) and Higgins *et al.* (1982). Further inspection of these compositions showed that the ratios of the various components varied considerably. The composition given by Eastman and Ferguson (1981) was used initially, and on further correspondence with Rhodes University, this choice was confirmed as being relatively accurate for the actual feed to the pilot plant. Table 1 shows these values.

Table 1: The composition of primary municipal sludge as given by Eastman and Ferguson (1981)

Feed component	% of total feed COD
ash	25.4
VSS consisting of:	74.6
lipids	21.0
cellulose	19.9
protein	28.7
volatile fatty acids	5.0

The ash component was assumed to have a COD value, but would pass through the system as an inert substance. Ratios given in Table 1 were used to define the composition of the organic feed to the bioreactor in the model.

4.2 Reaction Scheme

Although the reviewing of the reaction schemes used in mathematical models in the literature was not discussed in the results of the literature survey, the complexity of the processes involved in these models varied considerably. The simplest reaction schemes used for anaerobic digestion processes consisted of as little as one rate controlling reaction (hydrolysis or acetoclastic methanogenesis), or up to six separate processes. When sulfate reduction takes place in the same system, the number of processes increases due to the competition between the sulfate reducing bacteria and the anaerobic digestion bacteria for organic substrate. To enable all these competitive processes to take place in the model, the production and consumption of the organic substrates for the competitive groups of bacteria needs to be included in the reaction scheme.

The reaction scheme used in the model is given in Figure 4, including the following reactions: hydrolysis, fermentation, anaerobic oxidation, acetogenesis, acetogenic sulfidogenesis, acetoclastic methanogenesis, hydrogenotrophic methanogenesis, acetoclastic sulfidogenesis, hydrogenotrophic sulfidogenesis. This allows for the competition between the sulfate reducing bacteria and the anaerobic digestion bacteria for propionate, acetate and hydrogen.

A rate equation was chosen for each of these reactions, and these are described in Section 4.3. The stoichiometry chosen for the complex organic matter degradation was chosen from Figure 4, as percentage COD, as given by Gujer and Zehnder (1983). However, for the sulfate reducing and methane producing reactions, the actual stoichiometric equations are known (SRB: Equations 4 to 6; MPB: Equations 28 to 30). These processes are competing for the same organic substrate. The equation for each of these reactions, as given in units of moles, was converted to units of gCOD, in order to be consistent with the units of the stoichiometry in Figure 4.

4.3 Biological Rate Equations

The model used in this study was based on a combination of parts of three mathematical models presented in the literature. The model development started with the model by Kalyuzhnyi and Fedorovich (1998), since this model described the degradation of complex soluble organic matter (sucrose), the competition between the sulfate reducing bacteria and the anaerobic digestion bacteria for propionate, acetate and hydrogen, and included terms for sulfate substrate limitation, organic substrate limitation, and undissociated hydrogen sulfide inhibition. The second model that was considered from the literature was that proposed by Costello *et al.* (1991), which included terms for acetic acid inhibition, hydrogen partial pressure regulation and pH inhibition of the various bacterial reactions. Finally, first order rate equations for the hydrolysis of the various components of primary settled sludge were considered based on the work by O'Rourke (1968).

The model development started with the Kalyuzhnyi and Fedorovich (1998) model, and the O'Rourke (1998) hydrolysis reactions. Once an initial model had been developed, the simulations showed high concentrations of acetic acid. It was then decided to include terms from the model by Costello *et al.* (1991) for acetic acid inhibition.

The rate equations chosen for each of the reactions listed in the previous section are described below. For hydrolysis, the rate equations are first order with respect to the particulate organic substrate concentration, and independent of any biomass concentration. However, all other reactions are catalysed by bacteria, and therefore two equations are needed for each reaction. The first of these equations (Equation 41) gives the rate at which substrate is being utilised, and is dependent on the biomass concentration catalysing that particular reaction. This concentration can be determined from the second equation (Equation 42), which gives the rate of growth of the biomass using the specific substrate. These two equations are linked by the cell yield coefficient. Common to both the substrate utilisation rate and the biomass growth rate for a particular bacterial species is the specific growth rate, μ . The following sections give the various equations used to calculate μ for each of the bacterial species, but all of these are then substituted into Equations 41 and 42 in the model, giving the substrate utilisation rate and the biomass growth rate for each group.

The substrate utilisation rate in all the reactions is given by the following reaction:

$$r_s = \frac{\mu \cdot C_x}{Y_{sx}} \quad (41)$$

The growth rate of the bacteria is given by the following equation, which does not include the term for cell maintenance or death:

$$r_x = \mu \cdot C_x \quad (42)$$

4.3.1 Hydrolysis of Proteins, Lipids and Cellulose

A hydrolysis rate constant was chosen for each of the particulate components. As is consistent with most models presented in the literature, the rate of hydrolysis of each of these components was first order with respect to the concentration of each of the species. The stoichiometry used in the model shows all the cellulose and protein being degraded to sugars and amino acids, which are indistinguishable to the model, while the lipids degrade to long chain fatty acids and polyols (grouped with the sugars and amino acids). Kinetic constants for each of these processes were chosen from O'Rourke (1968), who did work on the affects of temperature and pH on hydrolysis. The constants were chosen as the value for a 10 day solids retention time at 35°C for each of the components. The rates of hydrolysis for each of the components in the feed are given in Table 2. Table 2 includes a value for the first order kinetic constant at two temperatures (see Section 4.5), as well as the stoichiometry.

Table 2: Rate equations, kinetic constants and stoichiometry for hydrolysis

Substrate	Rate equation	k_h (d ⁻¹)	k_h (d ⁻¹)	Stoichiometry
		(35°C)	(15°C)	
lipids	$r_{lipids} = k_{h_{lipids}} \cdot [lipids]$	0.17	0.0425	lipids: -1 fatty acids: 1
proteins	$r_{proteins} = k_{h_{protein}} \cdot [protein]$	0.15	0.0375	proteins: -1 sugars, amino acids: 1
cellulose	$r_{cellulose} = k_{h_{cellulose}} \cdot [cellulose]$	0.21	0.0525	cellulose: -1 sugars, amino acids: 1

4.3.2 Fermentation

Amino acids and sugars are degraded to propionic acid and other intermediary products, acetic acid and hydrogen by fermentative or acidogenic bacteria. The equation for the specific growth rate of these bacteria includes a term for non-competitive acetic acid inhibition, as given by Costello *et al.* (1991), and a term for sulfide inhibition, as given by Kalyuzhnyi and Fedorovich (1998). The specific growth rate is based on the Monod equation, and is given as follows:

$$\mu = \frac{\mu_{\max}}{\left(1 + \frac{K_S}{[SAA]}\right) \left(1 + \frac{[HAc]}{K_{HAc}}\right)} \left(1 - \frac{[H_2S]}{K_{H_2S}}\right) \quad (43)$$

4.3.3 Anaerobic Oxidation

Anaerobic oxidation of the long chain fatty acids to acetic acid and hydrogen is performed by anaerobically oxidising bacteria. In the model published by Kalyuzhnyi and Fedorovich (1998), rate equations were given for the anaerobic digestion and sulfate reduction in systems fed with sucrose, propionic acid and acetic acid. This reaction was not included in the model because no long chain fatty acids were present in the feed. However, since the rate equations for the rest of the processes were based on this model, the term for sulfide inhibition was included in this step with the same form as used in the other rate equations. The value for the sulfide inhibition constant was chosen according to the values for the other reactions. The specific growth rate for these bacteria is as follows:

$$\mu = \frac{\mu_{\max}}{\left(1 + \frac{K_S}{[FA]}\right)} \left(1 - \frac{[H_2S]}{K_{H_2S}}\right) \quad (44)$$

4.3.4 Acetogenic Sulfidogenesis

The specific growth rate of the acetogenic sulfidogenic bacteria includes a term for sulfide inhibition, as well as being dependent on both the organic substrate concentration and the sulfate concentration, as given by Kalyuzhnyi and Fedorovich (1998). This also adds to the completeness of the model, in that it predicts the absence of sulfate reduction in the absence of sulfate. The specific growth rate of the acetogenic sulfidogenic bacteria is given as follows:

$$\mu = \frac{\mu_{\max}}{\left(1 + \frac{K_S}{[HPr]}\right) \left(1 + \frac{K_{SO_4^{2-}}}{[SO_4^{2-}]}\right)} \left(1 - \frac{[H_2S]}{K_{H_2S}}\right) \quad (45)$$

4.3.5 Acetogenesis

The volatile fatty acid component of the feed was divided into two equal fractions, which the model identifies as acetic acid and propionic acid. The propionic acid concentration represents all longer chain fatty acids, as well as other intermediary products such as ethanol. The propionic acid concentration used to calculate the rate of acetogenesis originates from both the rate of addition of propionic acid in the feed stream as well as from the anaerobic digestion of the more complex components of the feed as shown in Figure 4. The equation for the specific growth rate of the acetogenic bacteria includes a term for competitive acetic acid product inhibition, as given by Costello *et al.* (1991), and a term for sulfide inhibition, as given by Kalyuzhnyi and Fedorovich (1998):

$$\mu = \frac{\mu_{\max}}{1 + \frac{K_S}{[HPf]} \left(1 + \frac{[HAc]}{K_{HAc}}\right)} \left(1 - \frac{[H_2S]}{K_{H_2S}}\right) \quad (46)$$

4.3.6 Acetoclastic Methanogenesis

Acetoclastic methanogenesis or acetate cleavage is the reaction where acetate is converted into methane and carbon dioxide. The specific growth rate of the methanogens includes a term for sulfide inhibition, as follows:

$$\mu = \frac{\mu_{\max}}{\left(1 + \frac{K_S}{[HAc]}\right)} \left(1 - \frac{[H_2S]}{K_{H_2S}}\right) \quad (47)$$

4.3.7 Hydrogenotrophic Methanogenesis

Hydrogenotrophic methanogenic bacteria use hydrogen and carbon dioxide to form methane. The specific growth rate of these methanogens is similar to that of the other methanogens, as follows:

$$\mu = \frac{\mu_{\max}}{\left(1 + \frac{K_S}{[H_2]}\right)} \left(1 - \frac{[H_2S]}{K_{H_2S}}\right) \quad (48)$$

4.3.8 Acetoclastic Sulfidogenesis

Acetoclastic sulfidogenic bacteria use acetate and sulfate as substrates to form hydrogen sulfide. Kalyuzhnyi and Fedorovich (1998) included a term for sulfide inhibition and for organic substrate limitation and sulfate limitation. The equation for the specific growth rate is as follows:

$$\mu = \frac{\mu_{\max}}{\left(1 + \frac{K_S}{[HAc]}\right) \left(1 + \frac{K_{SO_4^{2-}}}{[SO_4^{2-}]}\right)} \left(1 - \frac{[H_2S]}{K_{H_2S}}\right) \quad (49)$$

4.3.9 Hydrogenotrophic Sulfidogenesis

Hydrogenotrophic sulfidogenic bacteria use hydrogen and sulfate to form hydrogen sulfide. Dual substrate limitation terms for hydrogen and sulfate are included in the equation for the specific growth rate, as well as a sulfide inhibition term, as follows:

$$\mu = \frac{\mu_{\max}}{\left(1 + \frac{K_S}{[H_2]}\right) \left(1 + \frac{K_{SO_4^{2-}}}{[SO_4^{2-}]}\right)} \left(1 - \frac{[H_2S]}{K_{H_2S}}\right) \quad (50)$$

At this stage it is apparent that the rate equations used in the model are not consistent with the conclusions drawn from the literature survey, and are not of the best form to be used in a mathematical model. The conclusions in the literature survey indicate that the rate of hydrolysis is dependent on the temperature, the biomass concentration, the pH and the particulate organic matter concentration. For this study, terms for acetic acid inhibition were included in the fermentation and

acetogenesis processes, while the literature survey clearly concludes that the methanogens are most susceptible to high concentrations of acetic acid. The sulfide inhibition terms were first order, which could allow the rate equation to become negative at high concentrations of undissociated hydrogen sulfide. This is critical since the anaerobic digestion processes are more sensitive to hydrogen sulfide inhibition and would have a zero rate at high sulfide concentrations, while the sulfate reducing bacteria would continue to produce sulfide at these high concentrations. The sulfide concentration would then exceed the value of the sulfide inhibition constant for these reactions, for which the model would calculate a negative rate, and reactants would be formed from products in the simulations. Therefore, the model does not consist of the most rigorous rate equations.

4.4 Acid-Base Equilibria of Inhibitory Compounds

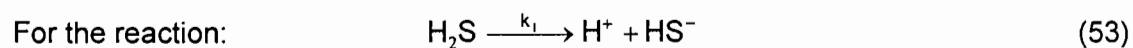
Undissociated hydrogen sulfide is inhibitory to all biological reactions, while undissociated acetic acid is inhibitory to some of the reactions. These concentrations had to be calculated from the model. From the stoichiometry of the sulfate reducing reactions, it can be taken that one mole of sulfide is formed for every mole of sulfate reduced. The biological sulfate reducing reactions have a stoichiometry such that 96 g of sulfate form 64 gCOD dissociated sulfide. To calculate the concentration of undissociated sulfide, the pH of the system was assumed to be constant at 7. The equilibrium concentrations were then calculated in AQUASIM using the equilibrium constant (Ramachandra Roa and Hepler, 1976), as follows:

$$K_a = \frac{[\text{HS}^-][\text{H}^+]}{[\text{H}_2\text{S}]} = 0.75 \times 10^{-7} \quad (54)$$

For any dynamic equilibrium reaction, two processes are taking place simultaneously, although the overall process shows no change. This is the case for all acid-base equilibria, vapour-liquid equilibria, and precipitation equilibria. For example, the equilibrium relating to Equation 51 can be written as:



If the rate of dissociation of the H_2S molecule is first order with respect to the H_2S concentration, it can be written as follows:



The rate of reaction is:
$$r_{\text{HS}^-} = k_1 [\text{H}_2\text{S}] \quad (54)$$

Assuming the same for the formation of H₂S:



the rate of reaction is: $r_{\text{H}_2\text{S}} = k_2 [\text{H}^+][\text{HS}^-]$ (56)

At equilibrium, the rates of the two reactions are equal, and then:

$$k_1[\text{H}_2\text{S}] = k_2 [\text{H}^+][\text{HS}^-] \quad (57)$$

Rearranging, we get Equation 51, which defines the ratio between the two kinetic constants.

$$K_a = \frac{[\text{HS}^-][\text{H}^+]}{[\text{H}_2\text{S}]} = \frac{k_1}{k_2} \quad (58)$$

Then, by assuming a constant pH in the system of 7, one kinetic constant can be arbitrarily set ($k_1 = 10^5$), so that the overall rate of the reaction is far greater than the rates of the biological reactions, and therefore equilibrium concentrations would be calculated immediately. The same algorithm was used for the acetate/ acetic acid equilibrium, using the equilibrium constant at 15°C (Weist, 1977):

$$K_a = \frac{[\text{Ac}^-][\text{H}^+]}{[\text{HAc}]} = 1.745 \times 10^{-5} \quad (59)$$

The value of k_1 was set at 10^6 , since the value of K_a is bigger than for the sulfide equilibrium, and by elevating the reaction rate constant, the rate of the reverse reaction will still be sufficiently higher than the biological reactions to ensure equilibrium values are obtained. This method of calculating equilibrium values of acid-base equilibria has been reported (Musvoto *et al.*, 1997).

4.5 Kinetic Constants

The selection of kinetic constants from the literature is critical in order to get the correct interactions between the various groups of bacteria. Appendix D contains tabulated kinetic constants from the literature. These constants have not been summarised in any way, but have been converted to a common set of units. From these tables, it can be seen that the values of the various parameters are dependent on the organic substrate, the temperature of the system under investigation, the type of bioreactor used in the system, the pH, and even constants measured under these identical conditions vary from one researcher to the other.

As an example, the degradation of propionate takes place according to two possible reactions, acetogenesis and acetogenic sulfidogenesis. From the summary of the literature survey (Section 2.9), it is expected that the sulfate reducing bacteria would outcompete the acetogenic bacteria for the organic substrate, since they have a greater affinity for the substrate, and are able to grow faster under non-limiting conditions. Therefore, the two kinetic constants, μ_{\max} and K_S are critical. The value of μ_{\max} should be greater for the sulfidogens, while the value of K_S should be smaller. Specifically for the value of μ_{\max} , from Appendix D, there are three values published for the acetogenic sulfidogens, and twenty values published for the acetogens, growing on propionate. For the sulfidogens, the values range from 0.81 to 3.65, with an average of 2.40. For the acetogens, the values range from 0.05 to 1.2, with an average of 0.31. These ranges overlap. Therefore, if values of μ_{\max} were randomly chosen from various published values, a value could possibly be chosen for the sulfidogens that is lower than the value for the acetogens, and the model would predict incorrect interactions.

Therefore, in order to get the correct ratios of the various kinetic constants, values from a single existing model were chosen for the model used in this study. Once again, the majority of the values were chosen from the model presented by Kalyuzhnyi and Fedorovich (1998). Values for the hydrolysis reactions were chosen from O'Rourke (1968), and for the anaerobic oxidation of long chain fatty acids from Novak and Carlson (1970). The sulfide inhibition constant for the anaerobic oxidation processes was estimated from the constants for the other processes, since Kalyuzhnyi and Fedorovich (1998) did not include this step in their model. Therefore, since Kalyuzhnyi and Fedorovich (1998) were able to predict the correct interactions between the anaerobic digestion bacteria and the sulfate reducing bacteria, the model developed in this study should also be able to predict these interactions.

However, kinetic constants in the literature are given for laboratory temperatures of 35°C, while the ambient temperature of the system under investigation was roughly 15°C. The kinetic parameters chosen from the literature therefore needed to be converted to these lower temperatures. This conversion was done using a rule of thumb, where the half saturation constant is not strongly dependent on temperature, the yield coefficient is slightly dependent on temperature, but this variation can be ignored, and the maximum specific growth rate is largely dependent on temperature. The dependence is roughly that the specific growth rate will double for a 10 to 15°C increase in temperature. To apply this rule of thumb, the maximum specific growth

rate constants and hydrolysis rate constants were all divided by 4, reducing the rate equations from 35°C to 15°C, as required.

Table 3 lists the kinetic constants for each of the biological reactions according to the group of biomass taking part in the reactions. The values for μ_{\max} are given at both the published temperatures and the reduced values used in the model.

Table 3: Kinetic Parameters used in the model

Bacteria	μ_{\max} (35°C) d ⁻¹	μ_{\max} (15°C) d ⁻¹	K_S gCOD.m ⁻³	K_{HAc} gCOD.m ⁻³	$K_{SO_4^{2-}}$ gCOD.m ⁻³	K_{H_2S} gCOD.m ⁻³	Y_{XS} gVSS gCOD
fermenters	8.0	2.0	28	604		550	0.043
anaerobic oxidisers	0.55	0.1375	1.816			550	0.11
acetogens	0.16	0.04	247	181		215	0.018
p-SRB	0.81	0.2025	295		7.4	285	0.035
a-MPB	0.24	0.06	56			285	0.026
h-MPB	1.0	0.25	0.13			215	0.018
a-SRB	0.51	0.1275	24		19.2	285	0.041
h-SRB	5.0	1.25	0.05		0.9	550	0.077

Table 4 gives a summary of the reactions, their rate equations, the stoichiometry, and the kinetic constants used in the model, at a temperature of 15°C, as used for the model calibration and verification.

Table 4: A summary of the reactions, rate equations, stoichiometry and kinetic constants used in the model

Process	Reaction	Rate Equation	Constants	Stoichiometry	References
hydrolysis of proteins	proteins → amino acids	$r_{\text{proteins}} = k_{h,\text{protein}} [\text{protein}]$	$k_{h,\text{protein}} = 0.0375 \text{ d}^{-1}$	proteins: -1 SAA: 1	O'Rourke (1968)
hydrolysis of lipids	lipids → long chain fatty acids	$r_{\text{lipids}} = k_{h,\text{lipids}} [\text{lipids}]$	$k_{h,\text{lipids}} = 0.0425 \text{ d}^{-1}$	lipids: -1 FA: 1	O'Rourke (1968)
hydrolysis of cellulose	cellulose → sugars	$r_{\text{cellulose}} = k_{h,\text{cellulose}} [\text{cellulose}]$	$k_{h,\text{cellulose}} = 0.0525 \text{ d}^{-1}$	cellulose: -1 SAA: 1	O'Rourke (1968)
fermentation	sugars + amino acids → propionate + acetate + hydrogen	$-r_{\text{Sf}} = \frac{\mu_{\text{max},f} C_f}{Y_f \left(1 + \frac{K_{\text{Sf}}}{[\text{SAA}]} \right) \left(1 + \frac{[\text{HAC}]}{K_{\text{if,HAC}}} \right) \left(1 - \frac{[\text{H}_2\text{S}]}{K_{\text{if,H}_2\text{S}}} \right)}$	$\mu_{\text{max},f} = 2.0 \text{ day}^{-1}$ $K_{\text{Sf}} = 28 \text{ gCOD.m}^{-3}$ $Y_f = 0.043 \text{ gVSS.gCOD}^{-1}$ $K_{\text{if,H}_2\text{S}} = 550 \text{ g S.m}^{-3}$ $K_{\text{if,HAC}} = 604 \text{ gCOD.m}^{-3}$	SAA: -66 HAC: 35 HPR: 20 H ₂ : 11	Kinetic constants and sulfide inhibition from Kalyuzhnyi and Fedorovich (1998) Acetate inhibition equation and constant from Costello <i>et al.</i> (1991)
growth of fermenting bacteria	sugars + amino acids → biomass	$r_{\text{Xf}} = \frac{\mu_{\text{max},f} C_f}{\left(1 + \frac{K_{\text{Sf}}}{[\text{SAA}]} \right) \left(1 + \frac{[\text{HAC}]}{K_{\text{if,HAC}}} \right) \left(1 - \frac{[\text{H}_2\text{S}]}{K_{\text{if,H}_2\text{S}}} \right)}$	$\mu_{\text{max},f} = 2.0 \text{ day}^{-1}$ $K_{\text{Sf}} = 28 \text{ gCOD.m}^{-3}$ $Y_f = 0.043 \text{ gVSS.gCOD}^{-1}$ $K_{\text{if,H}_2\text{S}} = 550 \text{ g S.m}^{-3}$ $K_{\text{if,HAC}} = 604 \text{ gCOD.m}^{-3}$	SAA: -1/Y _f C _f : 1	Kinetic constants and sulfide inhibition from Kalyuzhnyi and Fedorovich (1998) Acetate inhibition equation and constant from Costello <i>et al.</i> (1991)
anaerobic oxidation	long chain fatty acids → acetate + hydrogen	$-r_{\text{So}} = \frac{\mu_{\text{max},o} C_o}{Y_o \left(1 + \frac{K_{\text{So}}}{[\text{FA}]} \right) \left(1 - \frac{[\text{H}_2\text{S}]}{K_{\text{lo}}} \right)}$	$\mu_{\text{max},o} = 0.1375 \text{ day}^{-1}$ $K_{\text{So}} = 1.816 \text{ gCOD.m}^{-3}$ $Y_o = 0.11 \text{ gVSS.gCOD}^{-1}$ $K_{\text{lo}} = 550 \text{ g S.m}^{-3}$	FA: -34 HAC: 23 H ₂ : 11	Kinetic constants from Novak and Carlson (1970) Estimated sulfide inhibition constant
growth of oxidisers	long chain fatty acids → biomass	$r_{\text{Xo}} = \frac{\mu_{\text{max},o} C_o}{1 + \frac{K_{\text{So}}}{[\text{FA}]} \left(1 - \frac{[\text{H}_2\text{S}]}{K_{\text{lo}}} \right)}$	$\mu_{\text{max},o} = 0.1375 \text{ day}^{-1}$ $K_{\text{So}} = 1.816 \text{ gCOD.m}^{-3}$ $Y_o = 0.11 \text{ gVSS.gCOD}^{-1}$ $K_{\text{lo}} = 550 \text{ g S.m}^{-3}$	FA: -1/Y _o C _o : 1	Kinetic constants from Novak and Carlson (1970) Estimated sulfide inhibition constant
aceticlastic sulfidogenesis	propionate + sulfate → acetate + sulfide	$-r_{\text{Sps}} = \frac{\mu_{\text{max},ps} C_{\text{ps}}}{Y_{\text{ps}} \left(1 + \frac{K_{\text{S,ps}}}{[\text{HPR}]} \right) \left(1 + \frac{K_{\text{S,SO}_4}}{[\text{SO}_4^{2-}]} \right) \left(1 - \frac{[\text{H}_2\text{S}]}{K_{\text{ips}}} \right)}$	$\mu_{\text{max},ps} = 0.2025 \text{ day}^{-1}$ $K_{\text{S,ps}} = 295 \text{ gCOD.m}^{-3}$ $Y_{\text{ps}} = 0.035 \text{ gVSS.gCOD}^{-1}$ $K_{\text{ips}} = 285 \text{ g S.m}^{-3}$ $K_{\text{S,SO}_4} = 7.4 \text{ gCOD.m}^{-3}$	HPR: -224 SO ₄ ²⁻ : -144 HAC: 128 HS ⁻ : 93	Kinetic constants and sulfide inhibition from Kalyuzhnyi and Fedorovich (1998)
growth of aceticlastic sulfidogens	propionate + sulfate → biomass	$r_{\text{Xps}} = \frac{\mu_{\text{max},ps} C_{\text{ps}}}{\left(1 + \frac{K_{\text{S,ps}}}{[\text{HPR}]} \right) \left(1 + \frac{K_{\text{S,SO}_4}}{[\text{SO}_4^{2-}]} \right) \left(1 - \frac{[\text{H}_2\text{S}]}{K_{\text{ips}}} \right)}$	$\mu_{\text{max},ps} = 0.2025 \text{ day}^{-1}$ $K_{\text{S,ps}} = 295 \text{ gCOD.m}^{-3}$ $Y_{\text{ps}} = 0.035 \text{ gVSS.gCOD}^{-1}$ $K_{\text{ips}} = 285 \text{ g S.m}^{-3}$ $K_{\text{S,SO}_4} = 7.4 \text{ gCOD.m}^{-3}$	HPR: -1/Y _{ps} p-SRB: 1	Kinetic constants and sulfide inhibition from Kalyuzhnyi and Fedorovich (1998)
acetogenesis	propionate → acetate + hydrogen	$-r_{\text{Sa}} = \frac{\mu_{\text{max},a} C_a}{Y_a \left(1 + \frac{K_{\text{S,a}}}{[\text{HPR}]} \right) \left(1 + \frac{[\text{HAC}]}{K_{\text{ia,HAC}}} \right) \left(1 - \frac{[\text{H}_2\text{S}]}{K_{\text{ia,H}_2\text{S}}} \right)}$	$\mu_{\text{max},a} = 0.04 \text{ day}^{-1}$ $K_{\text{S,a}} = 247 \text{ gCOD.m}^{-3}$ $Y_a = 0.018 \text{ gVSS.gCOD}^{-1}$ $K_{\text{ia,H}_2\text{S}} = 215 \text{ g S.m}^{-3}$ $K_{\text{ia,HAC}} = 181 \text{ gCOD.m}^{-3}$	HPR: -7 HAC: 4 H ₂ : 3	Kinetic constants and sulfide inhibition from Kalyuzhnyi and Fedorovich (1998) Acetate inhibition equation and constant from Costello <i>et al.</i> (1991)

growth of acetogens	propionate → biomass	$r_{Xa} = \frac{\mu_{\max,a} C_a}{\left(1 + \frac{K_{S,a}}{[HPI]}\right) \left(1 + \frac{[HAC]}{K_{Ia,HAC}}\right)} \left(1 - \frac{[H_2S]}{K_{Ia,H_2S}}\right)$	$\begin{aligned} \mu_{\max,a} &= 0.04 \text{ day}^{-1} \\ K_{S,a} &= 247 \text{ gCOD.m}^{-3} \\ Y_a &= 0.018 \text{ gVSS.gCOD}^{-1} \\ K_{i,H_2S} &= 215 \text{ g S.m}^{-3} \\ K_{i,HAC} &= 181 \text{ gCOD.m}^{-3} \end{aligned}$	HPR: -1/Y _a C _a : 1	Kinetic constants and sulfide inhibition from Kalyuzhnyi and Fedorovich (1998) Acetate inhibition equation and constant from Costello et al. (1991)
acetoclastic methanogenesis	acetate → methane	$-r_{Sam} = \frac{\mu_{\max,am} C_{am}}{Y_{am} \left(1 + \frac{K_{S,am}}{[HAC]}\right)} \left(1 - \frac{[H_2S]}{K_{Iam}}\right)$	$\begin{aligned} \mu_{\max,am} &= 0.06 \text{ day}^{-1} \\ K_{S,am} &= 56 \text{ gCOD.m}^{-3} \\ Y_{am} &= 0.026 \text{ gVSS.gCOD}^{-1} \\ K_{i,am} &= 285 \text{ g S.m}^{-3} \end{aligned}$	HAC: -64 CH ₄ : 64	Kinetic constants and sulfide inhibition from Kalyuzhnyi and Fedorovich (1998)
growth of acetoclastic methanogens	acetate → biomass	$r_{Xam} = \frac{\mu_{\max,am} C_{am}}{1 + \frac{K_{S,am}}{[HAC]}} \left(1 - \frac{[H_2S]}{K_{Iam}}\right)$	$\begin{aligned} \mu_{\max,am} &= 0.06 \text{ day}^{-1} \\ K_{S,am} &= 56 \text{ gCOD.m}^{-3} \\ Y_{am} &= 0.026 \text{ gVSS.gCOD}^{-1} \\ K_{i,am} &= 285 \text{ g S.m}^{-3} \end{aligned}$	HAC: -1/Y _{am} a-MPB: 1	Kinetic constants and sulfide inhibition from Kalyuzhnyi and Fedorovich (1998)
hydrogenotrophic methanogenesis	hydrogen → methane	$-r_{Shm} = \frac{\mu_{\max,hm} C_{hm}}{Y_{hm} \left(1 + \frac{K_{S,hm}}{[H_2]}\right)} \left(1 - \frac{[H_2S]}{K_{Ihm}}\right)$	$\begin{aligned} \mu_{\max,hm} &= 0.25 \text{ day}^{-1} \\ K_{S,hm} &= 0.13 \text{ gCOD.m}^{-3} \\ Y_{hm} &= 0.018 \text{ gVSS.gCOD}^{-1} \\ K_{i,hm} &= 215 \text{ g S.m}^{-3} \end{aligned}$	H ₂ : -48 CH ₄ : 48	Kinetic constants and sulfide inhibition from Kalyuzhnyi and Fedorovich (1998)
growth of hydrogenotrophic methanogens	hydrogen → biomass	$r_{Xhm} = \frac{\mu_{\max,hm} C_{hm}}{1 + \frac{K_{S,hm}}{[H_2]}} \left(1 - \frac{[H_2S]}{K_{Ihm}}\right)$	$\begin{aligned} \mu_{\max,hm} &= 0.25 \text{ day}^{-1} \\ K_{S,hm} &= 0.13 \text{ gCOD.m}^{-3} \\ Y_{hm} &= 0.018 \text{ gVSS.gCOD}^{-1} \\ K_{i,hm} &= 215 \text{ g S.m}^{-3} \end{aligned}$	H ₂ : -1/Y _{hm} h-MPB: 1	Kinetic constants and sulfide inhibition from Kalyuzhnyi and Fedorovich (1998)
acetoclastic sulfidogenesis	acetate + sulfate → sulfide	$-r_{Sas} = \frac{\mu_{\max,as} C_{as}}{Y_{as} \left(1 + \frac{K_{S,as}}{[HAC]}\right) \left(1 + \frac{K_{S,SO_4}}{[SO_4^{2-}]}\right)} \left(1 - \frac{[H_2S]}{K_{Ias}}\right)$	$\begin{aligned} \mu_{\max,as} &= 0.1275 \text{ day}^{-1} \\ K_{S,as} &= 24 \text{ gCOD.m}^{-3} \\ Y_{as} &= 0.041 \text{ gVSS.gCOD}^{-1} \\ K_{i,as} &= 285 \text{ g S.m}^{-3} \\ K_{S,SO_4} &= 19.2 \text{ gCOD.m}^{-3} \end{aligned}$	HAC: -64 SO ₄ ²⁻ : -96 HS ⁻ : 62	Kinetic constants and sulfide inhibition from Kalyuzhnyi and Fedorovich (1998)
growth of acetoclastic sulfidogens	acetate + sulfate → biomass	$r_{Xas} = \frac{\mu_{\max,as} C_{as}}{\left(1 + \frac{K_{S,as}}{[HAC]}\right) \left(1 + \frac{K_{S,SO_4}}{[SO_4^{2-}]}\right)} \left(1 - \frac{[H_2S]}{K_{Ias}}\right)$	$\begin{aligned} \mu_{\max,as} &= 0.1275 \text{ day}^{-1} \\ K_{S,as} &= 24 \text{ gCOD.m}^{-3} \\ Y_{as} &= 0.041 \text{ gVSS.gCOD}^{-1} \\ K_{i,as} &= 285 \text{ g S.m}^{-3} \\ K_{S,SO_4} &= 19.2 \text{ gCOD.m}^{-3} \end{aligned}$	HAC: -1/Y _{as} a-SRB: 1	Kinetic constants and sulfide inhibition from Kalyuzhnyi and Fedorovich (1998)
hydrogenotrophic sulfidogenesis	hydrogen + sulfate → sulfide	$-r_{Shs} = \frac{\mu_{\max,hs} C_{hs}}{Y_{hs} \left(1 + \frac{K_{S,hs}}{[H_2]}\right) \left(1 + \frac{K_{S,SO_4}}{[SO_4^{2-}]}\right)} \left(1 - \frac{[H_2S]}{K_{Ihs}}\right)$	$\begin{aligned} \mu_{\max,hs} &= 1.25 \text{ day}^{-1} \\ K_{S,hs} &= 0.05 \text{ gCOD.m}^{-3} \\ Y_{hs} &= 0.077 \text{ gVSS.gCOD}^{-1} \\ K_{i,hs} &= 550 \text{ g S.m}^{-3} \\ K_{S,SO_4} &= 0.9 \text{ gCOD.m}^{-3} \end{aligned}$	H ₂ : -48 SO ₄ ²⁻ : -96 HS ⁻ : 62	Kinetic constants and sulfide inhibition from Kalyuzhnyi and Fedorovich (1998)
growth of hydrogenotrophic sulfidogens	hydrogen + sulfate → biomass	$r_{Xhs} = \frac{\mu_{\max,hs} C_{hs}}{\left(1 + \frac{K_{S,hs}}{[H_2]}\right) \left(1 + \frac{K_{S,SO_4}}{[SO_4^{2-}]}\right)} \left(1 - \frac{[H_2S]}{K_{Ihs}}\right)$	$\begin{aligned} \mu_{\max,hs} &= 1.25 \text{ day}^{-1} \\ K_{S,hs} &= 0.05 \text{ gCOD.m}^{-3} \\ Y_{hs} &= 0.077 \text{ gVSS.gCOD}^{-1} \\ K_{i,hs} &= 550 \text{ g S.m}^{-3} \\ K_{S,SO_4} &= 0.9 \text{ gCOD.m}^{-3} \end{aligned}$	H ₂ : -1/Y _{hs} h-SRB: 1	Kinetic constants and sulfide inhibition from Kalyuzhnyi and Fedorovich (1998)

4.6 Reactor Configuration

The FSBR was constructed from a rectangular shipping container, and has the dimensions and configuration as described in Section 1.6.

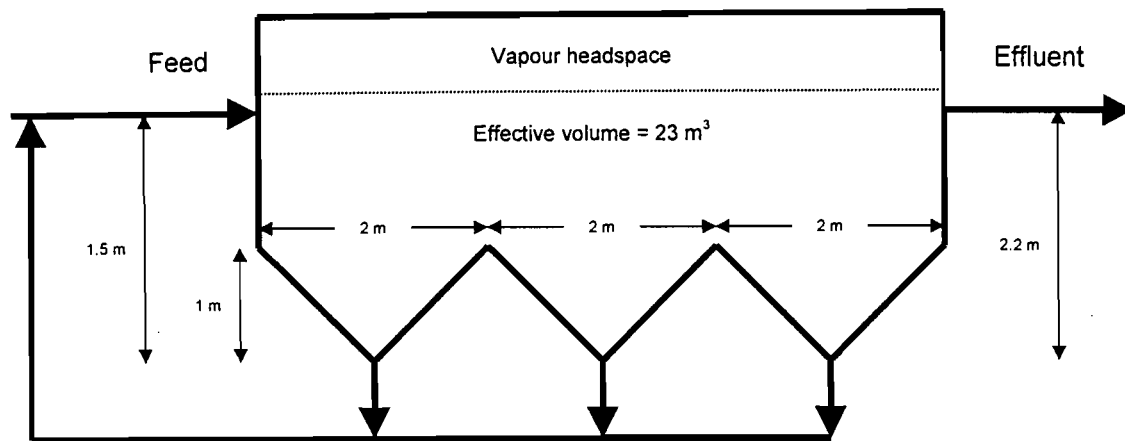


Figure 7: The dimensions and configuration on the FSBR pilot plant

The Falling Sludge Bed Reactor (FSBR) is a unique design specifically for heterogeneous systems. The solid fractions are able to settle into each of the three valleys, forming a high solids density bed, while the liquid fraction flows across the top of the system. The shape and operation of the FSBR allows for a higher solids recycle rate, and therefore longer solids residence time, while the hydraulic residence time is considerably smaller. The challenge in modelling the FSBR is that there is a concentration profile in both the horizontal and vertical directions. There is an increase in biomass and particulate organic matter concentration from the top to the bottom of the bioreactor, while substrate concentrations tend to decrease with an increase in reactor depth. There is also a distribution of biomass between the three valleys, due to the recycle from each valley, as well as the differential settling of larger particulates into the first valley, due to their higher settling velocity. The soluble substrate concentrations decrease along the length of the FSBR, as the reaction conversion increases.

The model made use of the mixed reactor compartment from AQUASIM, which means that the composition of the effluent stream from the reactor is identical to the composition at each point in the reactor. Because the composition changes at the various points in the FSBR, the entire volume was divided into compartments, each represented by a mixed reactor, in order to represent these varying compositions.

The FSBR was divided into nine separate reactors in the model, as shown by the dotted lines in Figure 8. This configuration allows for approximate plug flow of the liquid and dissolved components across the top of the reactor (compartments 1 to 6, Figure 8), with settling of the solids into the three valleys (compartments 7 to 9, Figure 8).

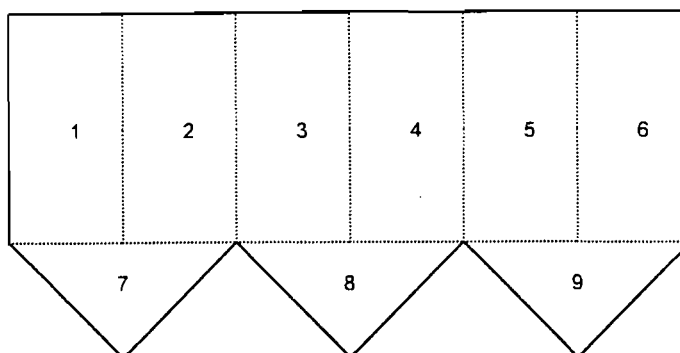


Figure 8: The FSBR divided into 9 compartments for the AQUASIM model

The model makes use of three different streams to represent the different flow patterns in the reactor. The first stream type is the flow of water, with the dissolved compounds and the particulates, from the inlet compartment to the outlet, and to the three valleys due to the recycle. This is illustrated in Figure 9. The flow rates to each of the valleys is dependent on the recycle pump capacity, as discussed in Section 1.6.

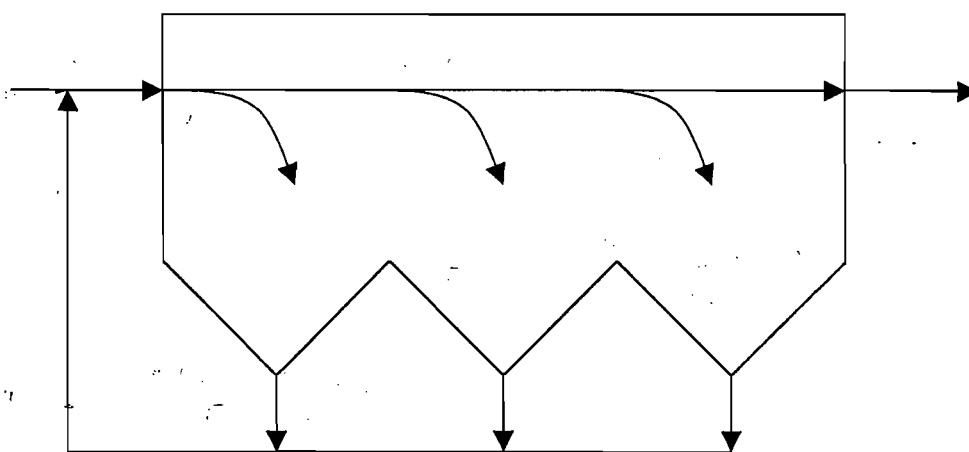


Figure 9: The flow of water and soluble substrates through the FSBR

A greater amount of liquid flow is expected in the first of the three valleys because of the longer time that the recycle pump draws from this valley, compared to the other two valleys. The flow of water into each valley was modelled as being equal to the rate at which the recycle pump is drawing water from each.

The second type of stream used in the model shows the settling of the particulates into the valleys. This velocity profile is superimposed on the liquid flow, due to the differential forces of gravity on the particulates. This is shown in Figure 10. The larger particles will settle faster than the smaller ones, and therefore preferentially into the first of the three valleys. However, this overall affect is probably more due to the higher recycle and liquid flow rate from the first valley, than to the FSBR acting as a settling basin.

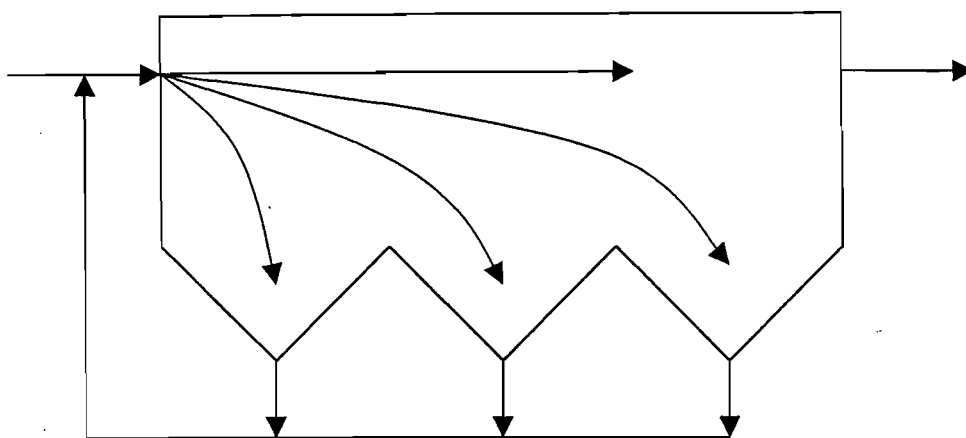


Figure 10: The flow of solids in the FSBR

The final stream used in the model represents the overflow of particulate matter from one valley to the next. This is due to the filling of the first valley caused by the immediate settling of the majority of the particulates, thereby causing the sludge bed to overflow to the adjacent valley. It is also partially due to the liquid movement across the top of the valleys, possibly causing the particles to spill into the next valley. However, this is modelled as purely a solid flux from one valley to the next.

Figure 11 shows the flow patterns taking place in one section of the reactor, and the subsequent representation of this section in AQUASIM. The model makes the assumption that the solids present in the bioreactor have no volume, and that concentrations calculated in the compartments of the model are for the entire volume.

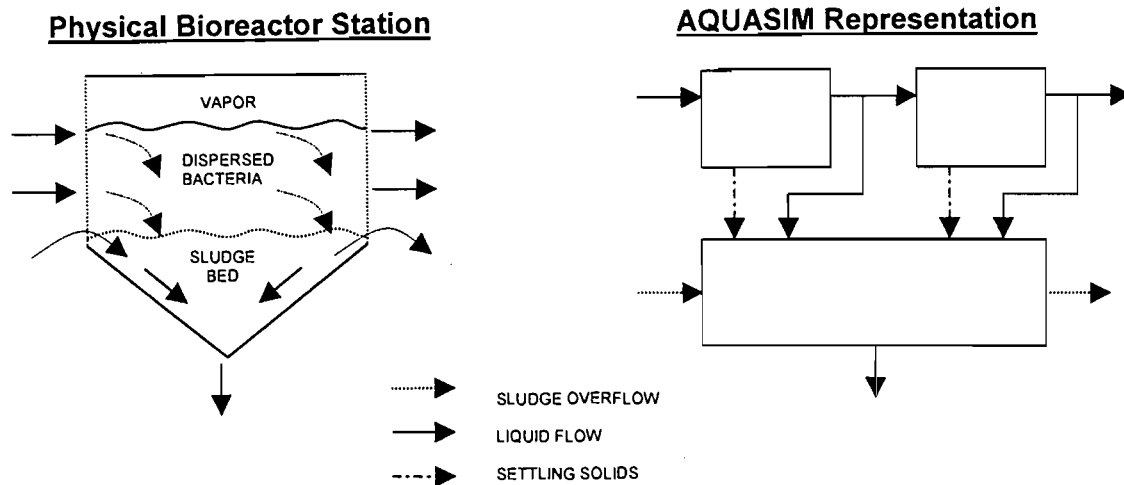


Figure 11: The flow patterns taking place in one section of the reactor, and the subsequent representation of this section in AQUASIM

To summarise, the flow patterns found in the FSBR are due to the recycle of the sludge as well as to the settling of the solids due to gravity. The overall affect is a high solids residence time and high biomass concentrations in the three valleys, which allows for a relatively short hydraulic residence time. The complete reactor configuration used in the model is shown in Figure 12, and this can be compared to the physical FSBR configuration, shown in Figure 3.

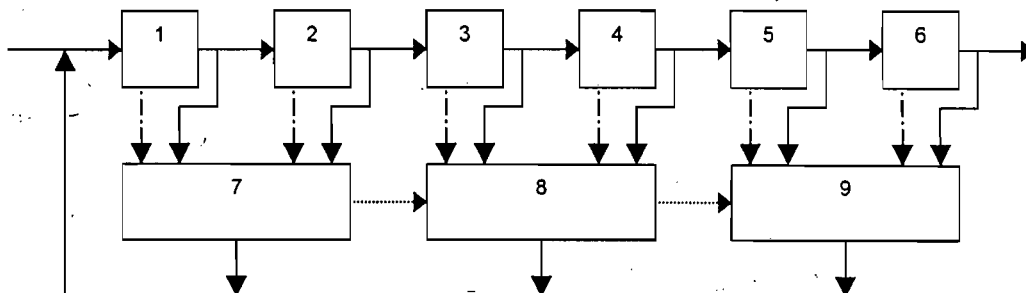


Figure 12: The AQUASIM representation of the FSBR showing the compartments and the connecting streams

The number in each of the reactors in Figure 12 refers to the compartment in the reactor as shown in Figure 8, while the connecting streams are identical to those shown in Figure 11.

4.7 Model Omissions

Chapter 5 discusses some of the difficulties in operating and analysing the FSBR. Difficulties arise from sampling and analysis of these samples due to the dynamic flow patterns found in the bioreactor. These variations further complicate the modelling of such a process, since errors in the measured data are expected to be significant.

In developing the model of the FSBR, certain assumptions were made and certain processes were ignored. These omissions were made since this model was the first model developed of the FSBR, and would be used as a basis for further models of this process. The use of AQUASIM for this modelling exercise was also being investigated, specifically for the biological processes taking place. Further models would be developed using more sophisticated computer software, in which these various calculations would be performed automatically.

The first omission was the calculation of the pH variations in the various compartments of the bioreactor. Although acid base equilibria were calculated, a constant pH of 7 was assumed for the entire bioreactor. However, with the production of acetic acid and hydrogen sulfide, the acidity and alkalinity of the system would change for both the microenvironments around the bacterium or solid organic matter particle, as well as for the spatial variations found in the FSBR.

The second important omission is the diffusion of gaseous products from the liquid phase to the vapour phase. The production of carbon dioxide, and possibly methane, would result in bubbles of these gases being formed at all points in the bioreactor, but especially in the three valleys, where the biomass concentration is the highest. These bubbles would strip the hydrogen sulfide from the liquid phase, reducing the inhibitory effect of this specie.

When using more sophisticated computer modelling packages, these processes are taken into account automatically, and their omission in this model, where the main aim is to identify the microbial processes, is therefore not critical.

5. MODEL CALIBRATION AND VERIFICATION

5.1 Pilot Plant Operating Data

The pilot plant was operated under various conditions with the aim of improving the performance and overall conversion of the treatment of acid mine drainage. The results of the FSBR pilot-plant study were more inclined towards determining the strong points of the FSBR design, whether it is a useful bioreactor design for the purpose of sludge hydrolysis, and understanding the operation of such as bioreactor. Therefore, obtaining experimental data for the purpose of modelling the system was not a priority. Overall conversion factors were of more importance to the operators than critically analysing the compositions of the various streams. For example, the total COD was measured rather than determining the concentration of each of the volatile fatty acids, the proteins, carbohydrates, lipids, or other organic compounds in the system. Quantification of the stripping of hydrogen sulfide was not performed, where this is an area that is critical in developing a mathematical model of the system. Minor observations such as spatial variations of pH were also not performed, resulting in little data being available. This made the task of modelling the system difficult, since the available calibration data was not specific to each of the many variables used in the model. The system was therefore under-specified in terms of calibrating the model.

Data from the pilot plant is presented in Table 5. The major objective of the FSBR pilot-plant operators was to increase the hydrolysis of the particulate organic matter, while monitoring the amount of the solubilised COD being used for sulfate reduction in the various bioreactors making up the pilot plant system. Therefore, Table 5 shows the COD and sulfate concentrations in the feed and leaving the FSBR. This data was obtained for the month of November 1998, and consisted of two operating conditions. The COD: SO₄ ratio was changed from 2 to 1.5 for one week of the month (5th to the 11th), and then back to 2 for the remainder of the month.

Table 5: Pilot plant operating data for the month of November 1998, giving the sulfate concentration (g.m^{-3}) and COD concentration (gCOD.m^{-3}) of the feed and effluent of the FSBR, for two COD: SO_4 ratios (2 and 1.5)

Date	COD: SO_4 ratio	Feed		Effluent	
		Sulfate	COD	Sulfate	COD
98.11.02	1.98	1704	3369	1428	1983
98.11.03	1.98	1861	3682	1224	1756
98.11.04	1.97	1996	3923	1512	1863
98.11.05	1.49	1804	2664	1529	1754
98.11.09	1.49	1754	2622	1324	1607
98.11.10	1.49	1785	2651	1592	1540
98.11.11	1.50	1767	2649	1539	1367
98.11.12	1.99	1650	3283	1468	1776
98.11.13	1.97	1826	3596	1344	1578
98.11.16	1.97	1639	3234	1004	1512
98.11.17	1.98	1819	3606	929	1663
98.11.18	1.96	1611	3152	956	1362
98.11.19	1.96	1766	3468	989	1407
98.11.23	1.99	2094	4168	1122	1649
98.11.24	1.99	1890	3768	1097	1282
98.11.25	1.98	1863	3690	1228	1603
98.11.26	1.99	1819	3611	948	1707
98.11.27	1.99	1934	3858	1353	1759
98.11.30	1.97	2049	4039	858	2048

There are many sources of error involved in measuring the concentrations of the sulfate and COD for such a system. The major source of error is the difficulty and inaccuracy involved in measuring the COD of particulates. Obtaining a representative sample of the sludge is critical, and difficult, and the composition of the particulates also differs considerably, resulting in two identically sized particles from the same sample giving different COD data. Also, measuring sulfate concentrations is complicated by the presence of the organic matter as well as the presence of ferrous and ferric ions in the solution (personal correspondence with C. Corbett). Therefore, inaccuracies are expected in the operating data in Table 5.

For the latter half of the month, two sets of data were obtained for the total COD in each of the three valleys of the FSBR, when operating at a COD: SO_4 ratio of 2. This

data would enable the settling of the solids inside the FSBR to be modelled in AQUASIM, and would allow for the calibration of the settling coefficients.

The difficulties in obtaining a representative sample of such a heterogeneous system were discussed earlier, and since the solids concentration in the three valleys is higher than in the feed, the expected errors in the measured values would be greater. Secondly, the concentration of particulates in a valley would be dependent on the recycle pump cycle, as discussed in Section 1.6. To reiterate, the recycle pump operated at a constant capacity of 2000 l.h⁻¹, but pumped alternatively from each of the three valleys for different lengths of time (60, 30 and 10 seconds from valleys 1, 2 and 3 respectively). Therefore, the concentration of particulate organic matter in each of the three valleys would be dependent on the alternating cycle of the recycle pump.

Table 6: Total COD measurements from each of the three valleys when operating at a COD: SO₄ ratio of 2

	Concentration 1 (gCOD.m ⁻³)	Concentration 2 (gCOD.m ⁻³)	Average (gCOD.m ⁻³)	% Variation
Valley 1	59631	64001	61816 ± 2185	3.53
Valley 2	45612	54489	50050 ± 4438	8.87
Valley 3	40276	67035	53655 ± 13379	24.9

Table 6 shows that the variation in the measured COD is insignificant for valleys 1 and 2 (< 10%), while valley 3 varied appreciably more (nearly 25%). However, these average values are critical to the model calibration, and average values as given in Table 6 were used to calibrate the settling of the solids.

A second set of operating data was obtained for a third operating condition where the feed COD: SO₄ ratio was set to 3. The data was obtained from March 1999, which was when the pilot plant was disassembled. Once again, data for the sulfate and COD concentrations entering and leaving the FSBR are given in Table 7.

The data for the three operating conditions (COD: SO₄ ratios of 2, 1.5 and 3 respectively) allowed for the model to be calibrated, using one set of steady state data, and verified using the other two sets of steady state data.

Table 7: Pilot plant operating data for the month of March 1999, giving the sulfate concentration (g.m^{-3}) and COD concentration (gCOD.m^{-3}) of the feed and effluent of the FSBR, for a COD: SO_4 ratio of 3

Date	COD: SO_4 ratio	Feed		Effluent	
		Sulfate	COD	Sulfate	COD
99.03.01	2.95	1630	4801	938	1022
99.03.02	2.95	1676	4943	990	1467
99.03.03	2.91	1672	4862	801	1578
99.03.04	3.01	1687	5285	930	1550
99.03.05	2.91	1653	4826	708	1603
99.03.08	2.90	1516	4409	885	1476
99.03.09	2.86	1560	4470	649	1207
99.03.10	2.94	1537	4520	715	1272
99.03.11	2.95	1503	4434	762	1121

5.2 Steady State Operating Points

In order to identify a steady state operating point, the pilot plant operating data should be relatively constant for a minimum of three hydraulic retention times (3×1.57 days). To determine the criteria for constant data, several factors should be taken into account. The first of these is the difficulty and inaccuracy involved in measuring the COD of particulates, and the sulfate concentration, as discussed in Section 5.1. Therefore, the COD and sulfate data points from the pilot plant were allowed a 10% variation when considering steady state.

Determining a steady state operating point is made easier by plotting the data versus time (Figure 13 for Table 5, Figure 15 for Table 7). Figure 13 highlights data from day 12 to day 19 (8 days, >5 residence times) as been adequately constant according to the criteria stated above and thus a steady state point. The 10% variations in the average values of the COD and sulfate concentrations over this time are also plotted, and the data points all lie within these limits. The average total COD concentration of the feed for that time period was 3390 gCOD.m^{-3} (± 238), while the average sulfate concentration in the feed was 1718 g.m^{-3} (± 107). This gave an average COD: SO_4^{2-} ratio of 1.97:1.

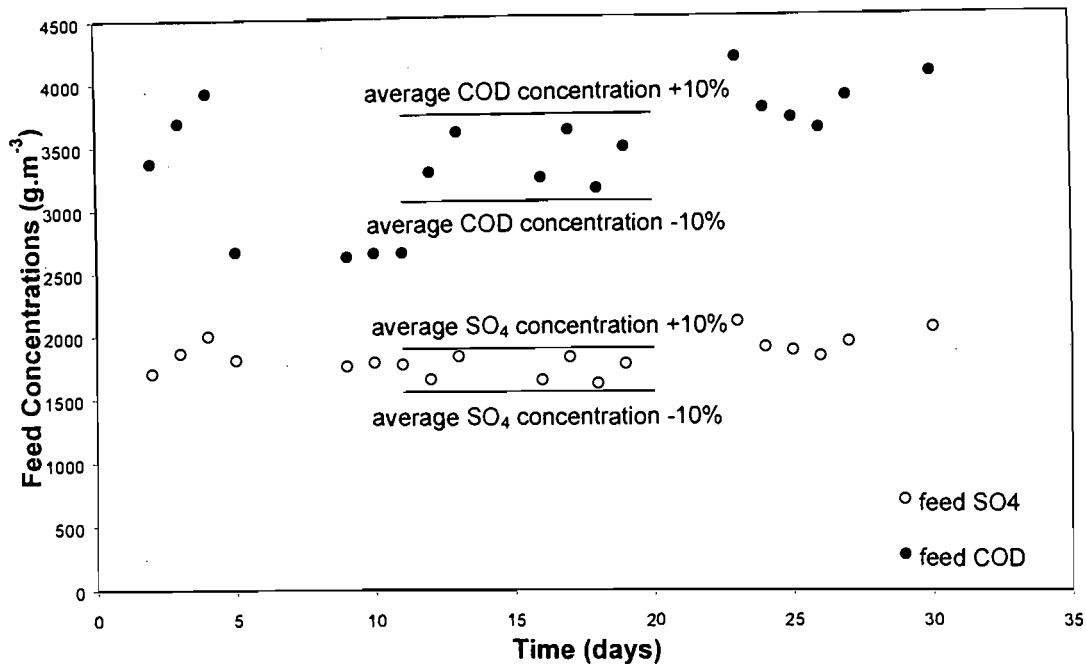


Figure 13: Pilot plant operating data for the month of November 1998, identifying steady state input data (COD: SO₄²⁻ ratio = 2); average COD concentration = 3390 gCOD.m⁻³, average sulfate concentration is 1718 g.m⁻³, between days 12 and 19

Figure 14 focuses on days 5 to 11 (7 days, 4.5 residence times) from Figure 13, when the pilot plant was being run at a COD: SO₄²⁻ ratio of about 1.5. Once again, the 10% variation in the measured data is plotted on the graph, and all data points lie within this allowable error range. This has been identified as a second steady state operating point, where the average COD concentration of the feed for that time period was 2646 gCOD.m⁻³ (± 24), while the average sulfate concentration in the feed was 1777 g.m⁻³ (± 27). This gave an average COD: SO₄²⁻ ratio of 1.49.

Figure 15 shows the data from Table 7 for the third steady state operating point, for days 1 to 11 (11 days, 7 residence times), with only one data point outside the 10% allowable error variation (COD concentration, day 4). This was identified as the third steady state operating point, where the average COD concentration of the feed for that time period was 4728 gCOD.m⁻³ (± 557), while the average sulfate concentration in the feed was 1604 g.m⁻³ (± 101). This gave an average COD: SO₄²⁻ ratio of 2.95.

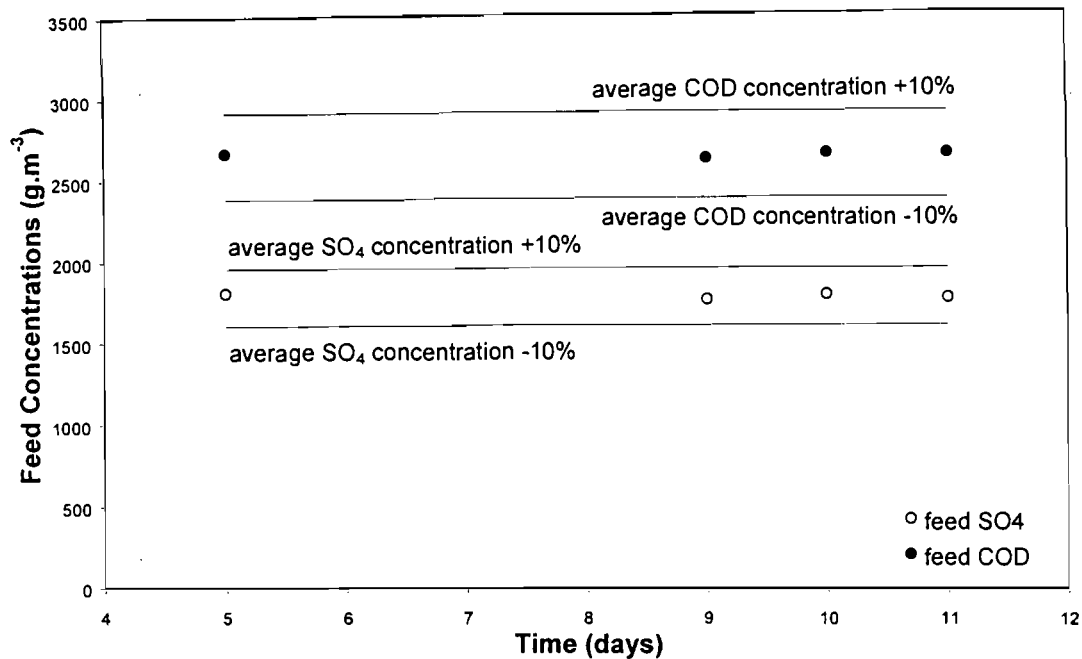


Figure 14: Pilot plant operating data for the month of November 1998, identifying steady state input data (COD: SO₄ ratio = 1.5); average COD concentration = 2646 gCOD.m⁻³, average sulfate concentration is 1777 g.m⁻³, between days 5 and 11

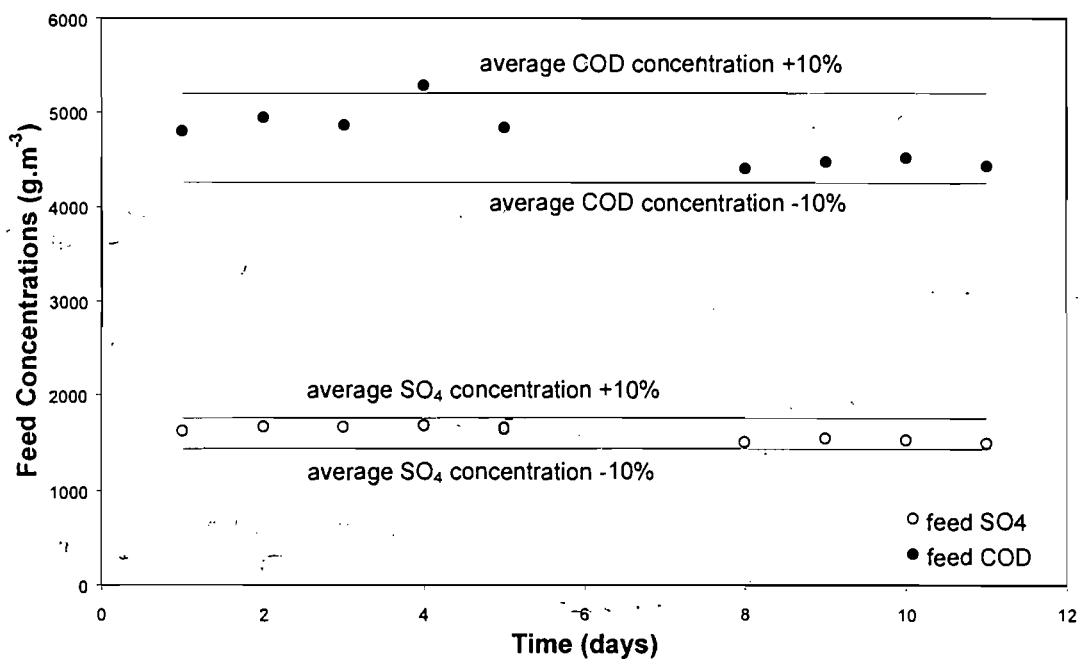


Figure 15: Pilot plant operating data for the month of March 1999, identifying steady state input data (COD: SO₄ ratio = 3); average COD concentration = 4728 gCOD.m⁻³, average sulfate concentration is 1604 g.m⁻³, between days 1 and 11.

For each of the steady states identified in Figures 13 to 15, the steady state effluent sulfate concentration was measured. Due to the complex interactions and processes taking place inside the FSBR, a greater variation in the effluent concentrations would be expected than the variations found in the feed concentrations. Figure 16 shows the changes in the effluent sulfate concentration over the steady state time period of Figure 13 (COD: $\text{SO}_4^{2-} = 2$)

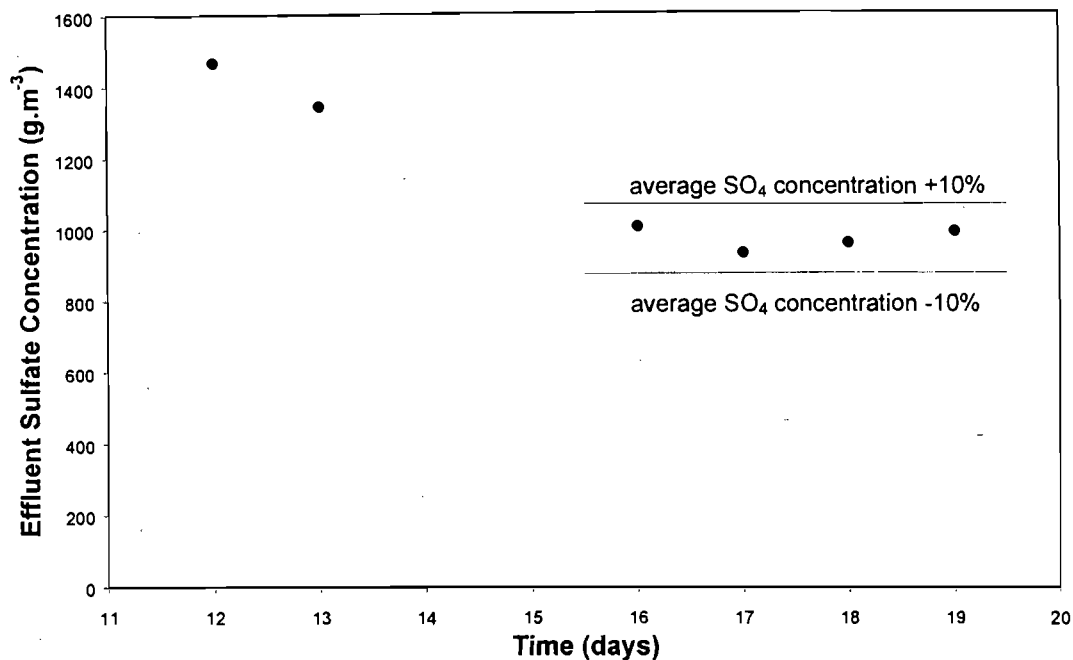


Figure 16: Pilot plant effluent sulfate concentrations for the first identified operating steady state (feed COD = 3390 gCOD.m^{-3} , feed sulfate = 1718 g.m^{-3} , COD: $\text{SO}_4^{2-} = 2$), showing the steady state effluent sulfate concentration (average = $970 \text{ g.m}^{-3} \pm 41$)

The effluent sulfate concentration shown in Figure 16 decreases from day 12 to day 16, after which it reaches a steady state. The average effluent sulfate concentration for these four days (days 16 to 19) is $970 \text{ g.m}^{-3} (\pm 41)$. This average was used as to further verify the calibration of the model.

Similarly, the sulfate concentrations corresponding to the steady state identified in Figure 14 (COD: $\text{SO}_4^{2-} = 1.5$) are plotted in Figure 17. The average effluent sulfate concentration for these four data points was $1496 \text{ g.m}^{-3} (\pm 172)$. One data point lay outside the 10% allowable error range (day 9), but was included in the average value.

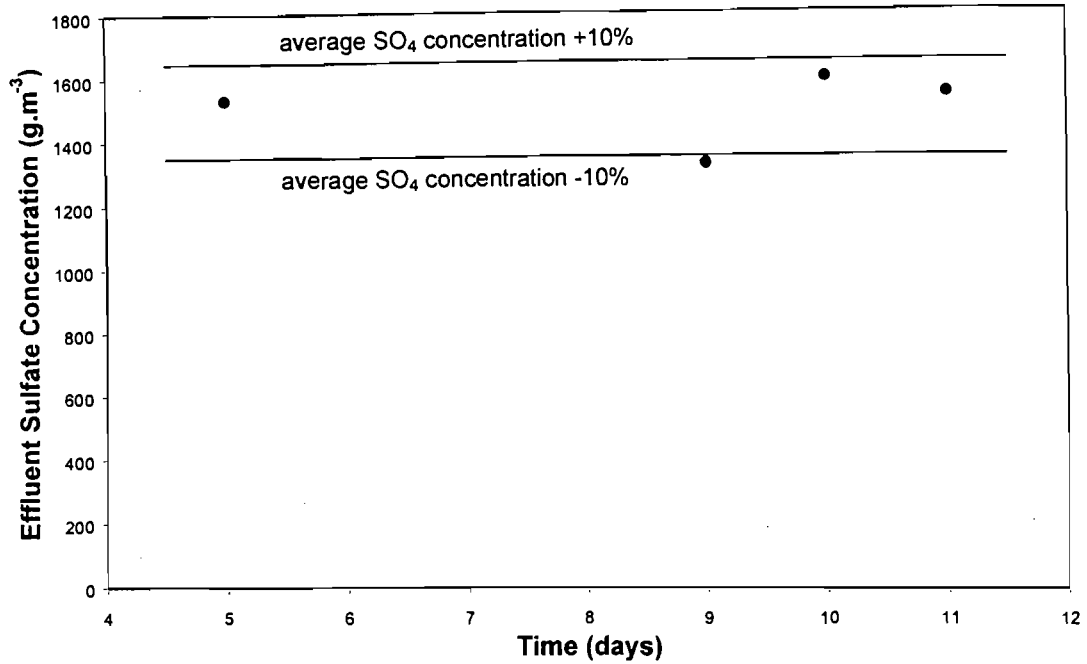


Figure 17: Pilot plant effluent sulfate concentrations for the second identified operating steady state (feed COD = 2646 gCOD.m⁻³, feed sulfate = 1777 g.m⁻³, COD: SO₄²⁻ = 1.5), showing the steady state effluent sulfate concentration (average = 1496 g.m⁻³ ± 172)

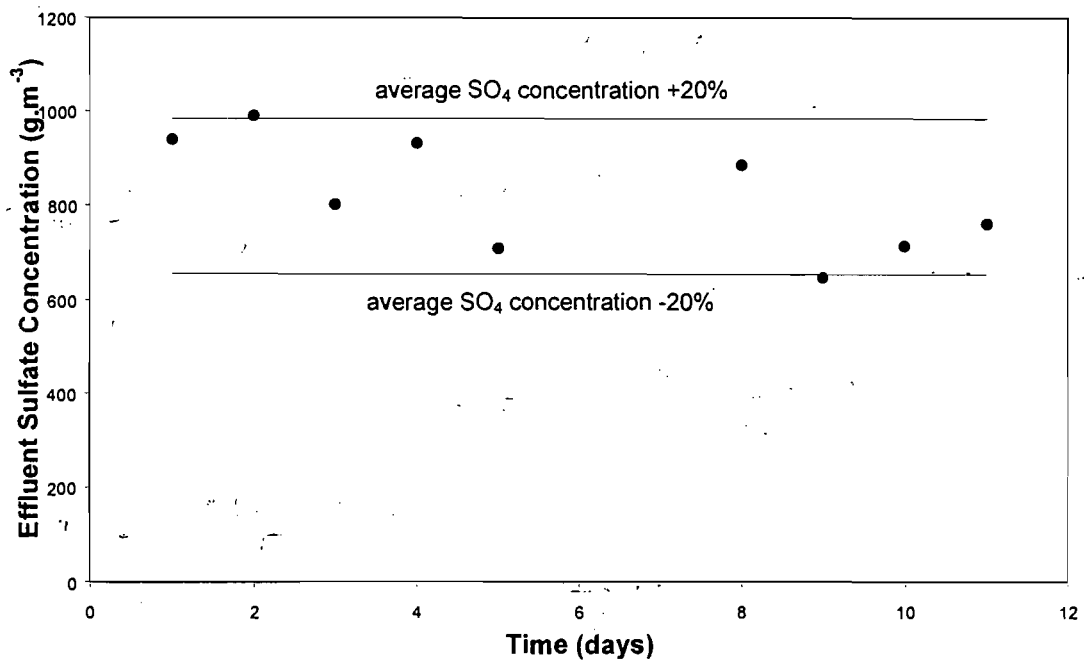


Figure 18: Pilot plant effluent sulfate concentrations for the third identified operating steady state (feed COD = 4728 gCOD.m⁻³, feed sulfate = 1604 g.m⁻³, COD: SO₄²⁻ = 3), showing the steady state effluent sulfate concentration (average = 820 g.m⁻³ ± 171)

The third steady state identified in Figure 15 had an average effluent sulfate concentration of 820 g.m^{-3} (± 171). For this steady state, the absolute error value was in the same range as for the other sulfate average values, but due to the lower sulfate concentrations, the percentage error is greater than 20% (Figure 18). All of the data points shown in Figure 18 were used to calculate the average sulfate concentration. The three steady state operating points are summarised in Table 8.

Table 8: Summary of the steady state operating data

Feed COD: SO ₄ ratio	Feed Sulfate Concentration (g.m ⁻³)	Feed COD Concentration (gCOD.m ⁻³)	Effluent Sulfate Concentration (g.m ⁻³)
2 : 1	1718 ± 107	3390 ± 238	970 ± 41
1.5 : 1	1777 ± 27	2646 ± 24	1496 ± 172
3 : 1	1604 ± 101	4728 ± 557	820 ± 171

5.3 Calibration of Settling Coefficients

In order to simulate the COD concentrations in each of the three valleys, the settling functions in AQUASIM were calibrated according to the average total COD values in Table 6. The operational parameters were set as for the first steady state (feed COD = 3400 gCOD.m^{-3} , feed SO₄²⁻ = 1700 g.m^{-3} , COD: SO₄²⁻ = 2). The first assumption made in calibrating the model is that no anaerobic digestion or sulfate reduction takes place prior to entering the reactor, i.e. in the storage tanks or the blend tank. By assuming this, the feed to the reactor could be estimated from the literature, and was accepted as being constant over a period of time. This assumption was made knowing that the organic feed has a residence time of between 1 and 7 days in the storage and blend tanks before entering the FSBR, and that anaerobic digestion of this feed takes place over this time.

The aim was to calibrate the settling coefficients (αC_i) in the model in order to predict the correct total COD concentrations in each of the three valleys, thereby predicting the settling of the solids. Once these values had been calibrated, they would remain constant for the remainder of the simulations.

The formula AQUASIM uses to calculate the mass flux streams is a function of the discharge, Q ($\text{m}^3.\text{day}^{-1}$), from the compartment, the concentration of the particles in the compartment, C_{particle} (kg.m^{-3}), and some settling coefficient, αC_i (no units), which determines the fraction of the particles leaving the compartment that will be

transferred to another compartment independent of the water flow. The discharge from a compartment is calculated as the sum of the flow rates of all the streams entering the compartment. The particle concentration inside the compartment is calculated as for a completely mixed reactor, and is the same in the product stream.

$$\text{mass flux} = Q \cdot C_{\text{particle}} \cdot xC_i \quad (60)$$

It is the settling coefficient (xC_i) that was varied in AQUASIM in order to predict the distribution of particulates in the valleys.

Figure 12 shows that there are eight mass flux streams used in the model. The settling coefficients are not different for all eight streams. The initial guess for these coefficients was based on the understanding that more solids settle into the first valley (valley 1) than into the other two (valleys 2 and 3). This is due to the inlet being directly above the first valley, and any large particles present in the feed will settle into this valley. Also, the recycle pump draws for a longer time from the first valley, and therefore more particles will flow into this valley than into the other two. Therefore, the settling coefficient from the first two compartments (compartments 1 and 2 in Figure 12) were the same, and bigger than the settling coefficients from the other four compartments (compartments 3 to 6), which were all the same.

After initial simulations were performed, it was necessary to include mass flux streams from valley 1 to valley 2, and from valley 2 to valley 3. This resulted in a higher concentration of total COD in each of the three valleys. These two settling coefficients were varied so that the correct distribution of total COD could be predicted in each of the valleys.

Figure 19 shows the AQUASIM simulation output of the total COD concentrations in four of the compartments used in the model (see Figure 12). The model predicted a steady state after 100 days. This is not unreasonable in comparison to the pilot plant, since the model was not seeded as the pilot plant was. The same steady state was reached in the same simulation time when the integration step size (step size = 10, number of steps = 30) was one order of magnitude less (step size = 1, number of steps = 300), indicating that the solution obtained was not step size variant. Further changes in the numerical parameters in AQUASIM (maximum internal step size, maximum integration order, number of co-diagonals of the Jacobian matrix, maximum number of internal time steps for one external time step) also had no effect on the steady state obtained, indicating that the steady states were not dependent on the calculation options.

Figure 19 shows the variations in the total COD concentration for four compartments in the model. This illustrates the affect of using the mass flux streams to predict the distribution of the particulate matter. Table 9 compares the simulated steady state concentrations from Figure 19 with the measured data. Table 9 shows that the model accurately predicts the total COD measured in each of the three valleys. Furthermore, the effluent sulfate concentration predicted by the model was within 34% of the measured value for these operating conditions.

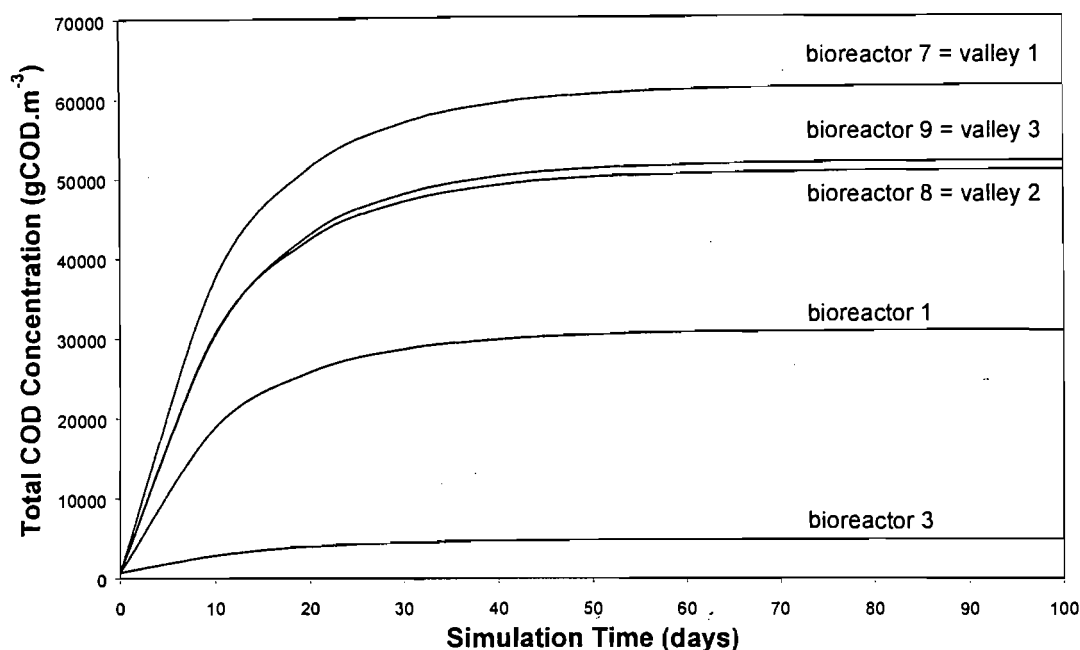


Figure 19: AQUASIM output graph of the total COD in four of the AQUASIM compartments as the simulation approaches steady state (COD: SO_4 ratio = 2, feed COD = 3400 gCOD.m^{-3} , feed sulfate = 1700 g.m^{-3})

Table 9: Comparison of measured and simulated concentrations to calibrate the settling coefficients in the model

Sample point	Measured value	Simulated value	% deviation
valley 1 (gCOD.m^{-3})	61816	61500	0.46
valley 2 (gCOD.m^{-3})	50050	50900	1.67
valley 3 (gCOD.m^{-3})	53655	52000	3.07
effluent sulfate concentration	970 mg.l^{-1}	1300 mg.l^{-1}	34.0

The change in simulated total COD values obtained from varying one of the settling coefficients showed that these coefficients were not independent of each other, and when accurately predicting the total COD in one of the valleys, a change in one

coefficient changed the total COD obtained in all the valleys. This is not surprising, since mass flux streams connect the valleys, and the total COD in each valley is recycled to the feed, so that all AQUASIM compartments are interconnected and will be affected. However, the fact that the model predicted an effluent sulfate concentration that was believable, if not precisely accurate, means that the trends predicted by the model can be expected to be realistic.

The rate equations and kinetic constants in Table 4 were not changed in order to calibrate the model. The only adjustment made to the kinetic constants from the literature was to reduce the value of the maximum specific growth rate and hydrolysis rate constant due to the changes in operating temperatures between the system for which the data were published and the pilot plant in this study (Section 4.5).

5.4 Model Verification

Unfortunately, more data for this operating point was not available to further verify the model. The other two steady-state points in Table 8 could be used to get some indication of whether the model is predicting realistic results, and these two operating conditions were simulated using the same settling coefficients used in calibrating the model. The only change was made to the feed COD and sulfate concentrations. Table 10 compares the simulated data to the measured data for these two operating conditions.

Table 10: Comparisons of measured values to simulated values for verification of the model

COD:SO₄²⁻	2 : 1	1.33 : 1	2.82 : 1
COD in (gCOD.m⁻³) (meas.)	3390	2646	4728
sulfate in (mg.l⁻¹) (meas.)	1718	1777	1604
sulfate out (mg.l⁻¹) (meas.)	970	1496	820
simulated sulfate out (mg.l⁻¹)	1300	1481	1048
% deviation in sulfate out	34.0	1.00	27.8

Table 10 shows that the model accurately predicts the performance of the FSBP pilot plant at these operating conditions. The rate equations and kinetic constants used are therefore adequate in modelling the bioreactions taking place in the FSBP, while the correct solids retention is being predicted, since the correct biomass concentration is allowing for the correct sulfate conversion to take place.

Unfortunately, the pilot plant was no longer in operation once the model had been developed, and transient data could not be obtained from the pilot plant to further verify the model. Therefore, no comparison can be made between the time it took for the pilot FSBR to reach a significant change in steady state, to the time it took AQUASIM to simulate the change.

An attempt was made to simulate the change in COD: SO₄ ratio from 1.5 to 2 for day 12 in Table 5. From Figure 16, the effluent sulfate concentration reached a steady state after 4 days. The same steady state was predicted only after 90 days in AQUASIM, indicating that AQUASIM is unable to accurately predict these transient changes in the pilot plant operation.

The model was then used to predict the bioreactor performance under different operating conditions. Although the temperature dependence of biological reactions is certainly not linear, the adjustment of the kinetic constants seems to be accurate enough in modelling the system. Although it would seem logical to use the kinetic constants as presented in the literature in order to prevent inaccuracies caused by the linear change, the predicted values from the model would be unrealistic compared to the performance of the pilot plant, and would not have any value. At 35°C, the model predicts hydrolysis conversions of greater than 90%, while the sulfate conversion is greater than 85%. The levels of sulfide inhibition at these high sulfate conversions were also unrealistic. Therefore, the parameters were not changed from those used to calibrate and verify the model.

6. SIMULATED TRENDS AND DISCUSSION

The simulated trends obtained from varying the operational parameters of the FSBR are now presented and discussed below. In order to offer operational changes necessary to improve the performance of the bioreactor, the aim of the bioreactor needs to be reiterated. The aim of the FSBR is to hydrolyse as much of the particulate feed as possible. This needs to be accomplished while producing as little methane as possible, in as small a reactor as possible, with as little recycle and other operating costs as possible.

The following sections show the simulated trends obtained from varying the hydraulic retention time, the sludge recycle rate, and the COD: SO_4^{2-} ratio independently. The important trends to observe would be the amount of particulate feed that is leaving the bioreactor as particulates, the amount that is leaving as soluble COD, the amount of biomass produced, the amount leaving as methane, and finally the amount that has been used for sulfate reduction.

6.1 Affects of Hydraulic Retention Time

In order to obtain simulated trends from various hydraulic retention times (HRT), the feed rate to the bioreactor was varied. Although the feed pump capacity at the pilot plant is only $14.64 \text{ m}^3 \cdot \text{d}^{-1}$, the simulations were performed at feed rates of up to $46 \text{ m}^3 \cdot \text{d}^{-1}$, resulting in a 0.5 day HRT. A maximum HRT of 2.5 days was simulated, requiring a feed rate of $9.2 \text{ m}^3 \cdot \text{d}^{-1}$.

By changing the feed rate, the sludge recycle rate (SRR - to be defined later) is also changed. Ultimately, the total feed to the full-scale treatment process will be fixed, and the aim of the simulations was to determine the optimum HRT, so that the correct bioreactor volume could be designed and constructed. However, to change the total reactor volume in the model would be more tedious than changing the feed rate. It was therefore hoped that the simultaneous affects of changing the HRT and simultaneously the SRR are not too different than changing the HRT independently, and the trends found are treated as changes in HRT only.

The model gives the concentrations of the various components leaving the bioreactor as particulate COD, biomass, soluble COD, methane, or that has been used for sulfate reduction and is leaving as a sulfide species. At any HRT, the total COD

entering the bioreactor is known. Figure 20 shows the fraction of the feed leaving as either of these components.

By summing the concentrations of all the five groups of COD that could leave the bioreactor (particulate species, biomass species, sulfide species, soluble species, methane) as groups, and then dividing these total group concentrations by the total COD entering, the fraction of the total COD entering that is leaving as each of these groups can be calculated.

In order to improve the performance of the bioreactor, the fraction that is leaving as particulate COD and as methane needs to be minimised, while the ratios between the fractions leaving as sulfide, soluble COD or biomass is of secondary importance. Figure 20 shows that the model predicts that an increase in the HRT will decrease the fraction of the product stream that is particulate COD. The fraction of the COD leaving as methane and as biomass is insignificant compared to the other groups, and these points don't even appear in Figure 20. The fraction leaving as sulfide increases significantly from a HRT of 0.5 until around 1.7, when the amount seems to remain constant. The fraction leaving as soluble COD increases substantially as the HRT is increased across the whole range.

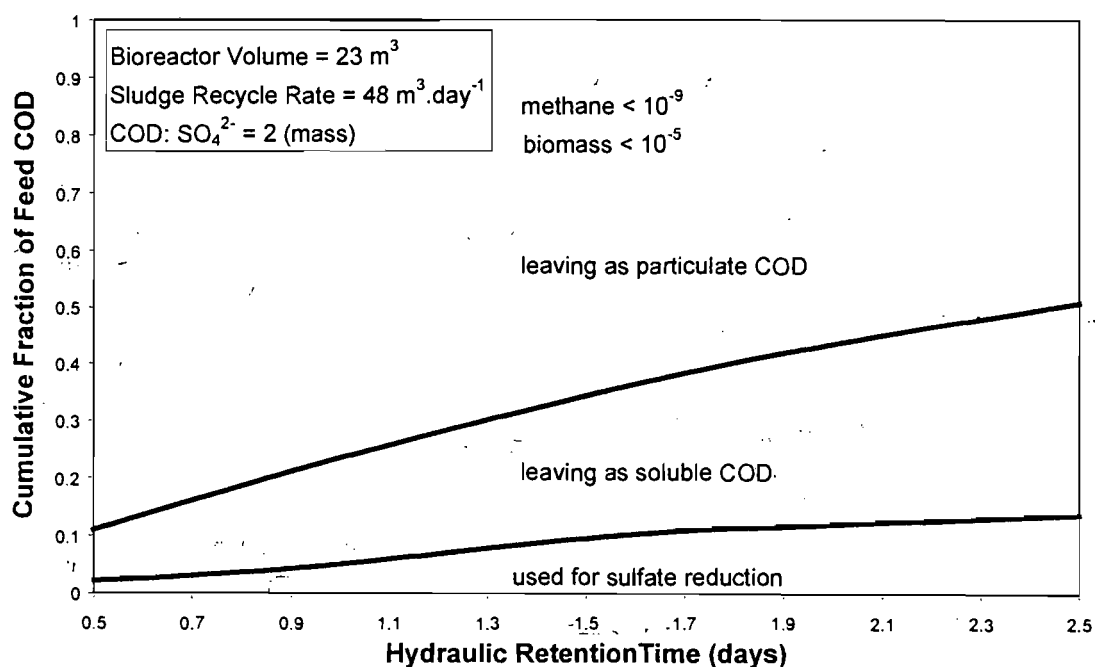


Figure 20: Model predictions of the fraction of the feed COD that is leaving the bioreactor as particulate COD, soluble COD, biomass, methane and sulfide, as the feed to the bioreactor is varied, varying the hydraulic retention time (COD: $\text{SO}_4^{2-} = 2$)

The decrease in the fraction leaving as particulate COD could be expected since the rate of hydrolysis is first order with respect to the particulate COD concentration, and

an increase in the HRT would allow for an increased reaction time, which would in turn lead to greater reaction conversion.

Figure 20 indicated that the model predicted that the fraction of the feed COD leaving the bioreactor as methane is insignificant ($<10^{-9}$). The model in fact predicts that the greatest concentration of methane produced in the system is $2.7 \times 10^{-5} \text{ gCOD.m}^{-3}$ at a HRT of 1.57 days. This is favourable in the bioreactor operation, in that there is very little of the COD is being wasted on methane production.

It can be seen from Figure 20 that the fraction of the feed COD that is leaving as sulfide is substantial, compared to methane. The idea of adding sulfate to the bioreactor to prevent methane formation is therefore justified, since the sulfate reducing bacteria outcompete the methane-producing bacteria for the organic substrate. The fraction of the COD that is leaving the bioreactor as sulfide also increases with an increase in the HRT. However, the trend seems to level off at HRT greater than approximately 1.6 days. It would be expected that the sulfate conversion would increase with an increase in HRT for many reasons. The first is that the amount of particulates being hydrolysed increases, increasing the amount of available organic substrate. Secondly, the increased HRT increases the reaction time available to the sulfate reducing bacteria, and more sulfate conversion would be expected.

Figure 21 shows the model predictions of the fraction of the feed particulate COD that is being hydrolysed as a function of the HRT. It can be seen that the hydrolysed fraction increases from about 10% at a HRT of 0.5 days, to about 50% at a HRT of 2.5 days. The trend in Figure 21 is not linear, and a maximum fraction of hydrolysis could be expected at a higher HRT. However, the higher the HRT, the greater the bioreactor volume is required. Low values of HRT are therefore favourable to avoid high capital costs in constructing the bioreactor. There is thus a trade off between the amount of particulates that will be hydrolysed and the cost of the bioreactor.

Figure 22 shows the predicted trend in the sulfate conversion as the HRT is varied. It can be seen that the sulfate conversion increases with an increase in the HRT. The shape of the curve however does not resemble any of the other trends so far predicted. There seems to be an inflection point in the sulfate conversion at a HRT of about 1.5 days.

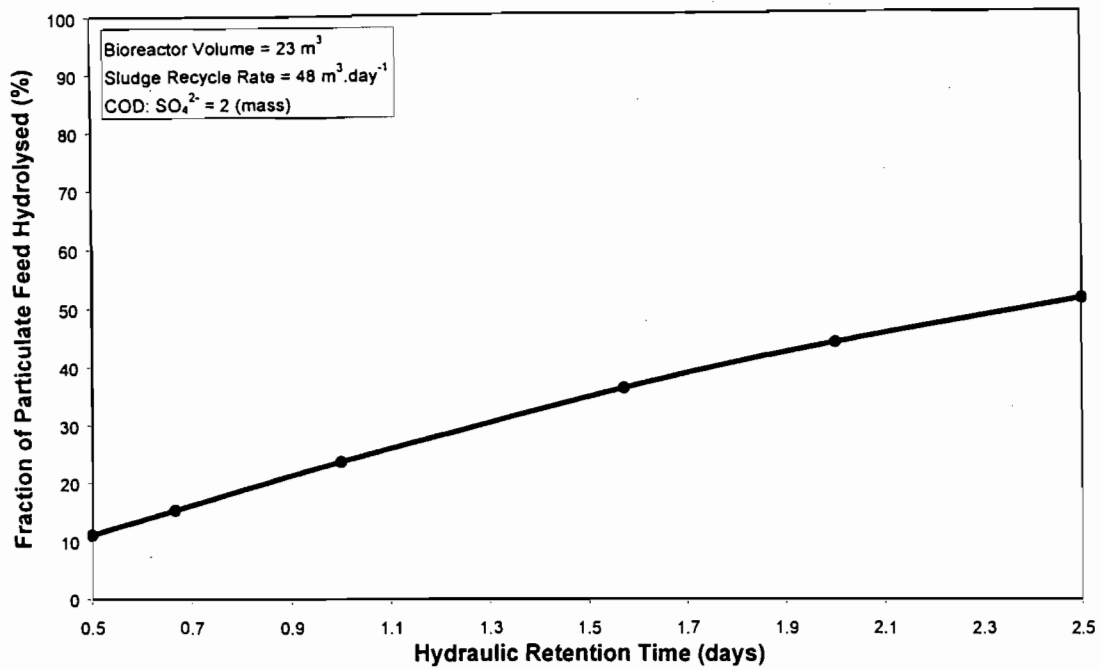


Figure 21: Model predictions of the fraction of the feed particulate COD that is being hydrolysed, as the feed to the bioreactor is varied, varying the hydraulic retention time (COD: SO₄²⁻ = 2)

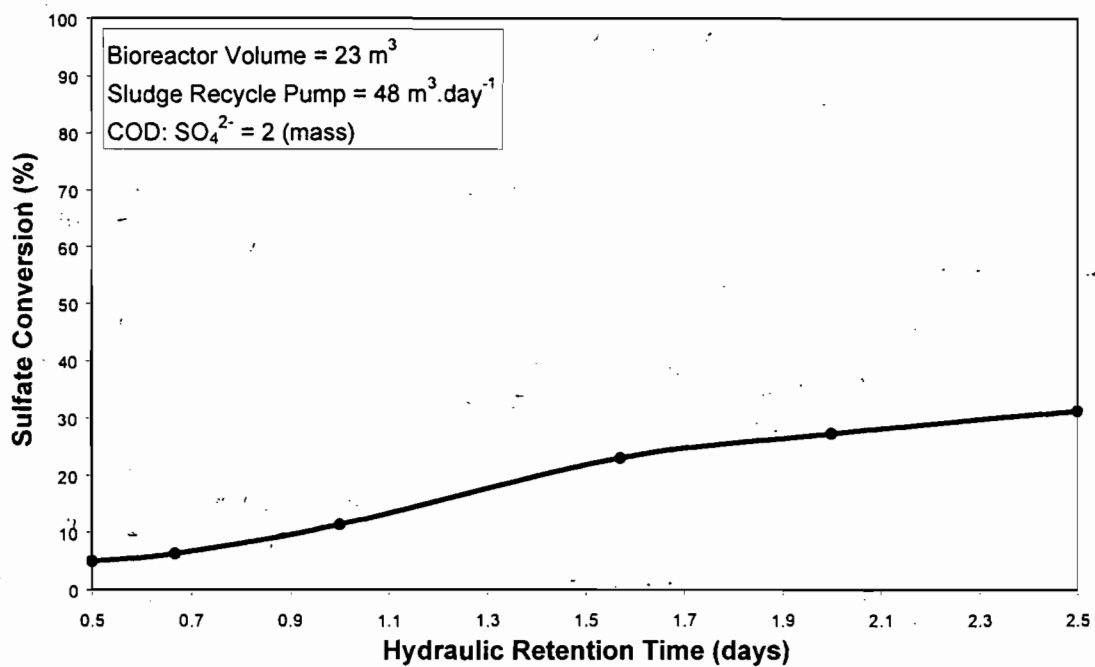


Figure 22: Model predictions of the sulfate conversion when varying the hydraulic retention time (COD: SO₄²⁻ = 2)

In an attempt to explain this inflection point, the rate equation for the specific growth rate of the p-SRB will be used (Equation 45). Equation 45 can be rewritten to separate the terms for organic substrate limitation, sulfate substrate limitation, and sulfide inhibition, as in Equation 61:

$$\frac{\mu}{\mu_{\max}} = \left(\frac{[\text{HPr}]}{K_S + [\text{HPr}]} \right) \left(\frac{[\text{SO}_4^{2-}]}{K_{\text{SO}_4^{2-}} + [\text{SO}_4^{2-}]} \right) \left(1 - \frac{[\text{H}_2\text{S}]}{K_{\text{H}_2\text{S}}} \right) \quad (61)$$

This equation suggests that when the concentration of propionate is much higher than the value of the half saturation constant, the term for organic substrate limitation will be close to 1, and will not effect the value of the specific growth rate in Equation 61. Similarly, when the sulfate concentration is much higher than the half saturation constant for sulfate, this term will be close to 1, and not effect the specific growth rate. When the concentration of undissociated hydrogen sulfide is much smaller than the sulfide inhibition constant, the term for sulfide inhibition will be close to 1 and not effect the specific growth rate. If all three of the above terms are close to 1, the specific growth rate will be equal to the maximum specific growth rate for the bacteria. Therefore, by calculating the value for each of these terms individually, and then the product of the three terms, the term most affecting the specific growth rate can be determined.

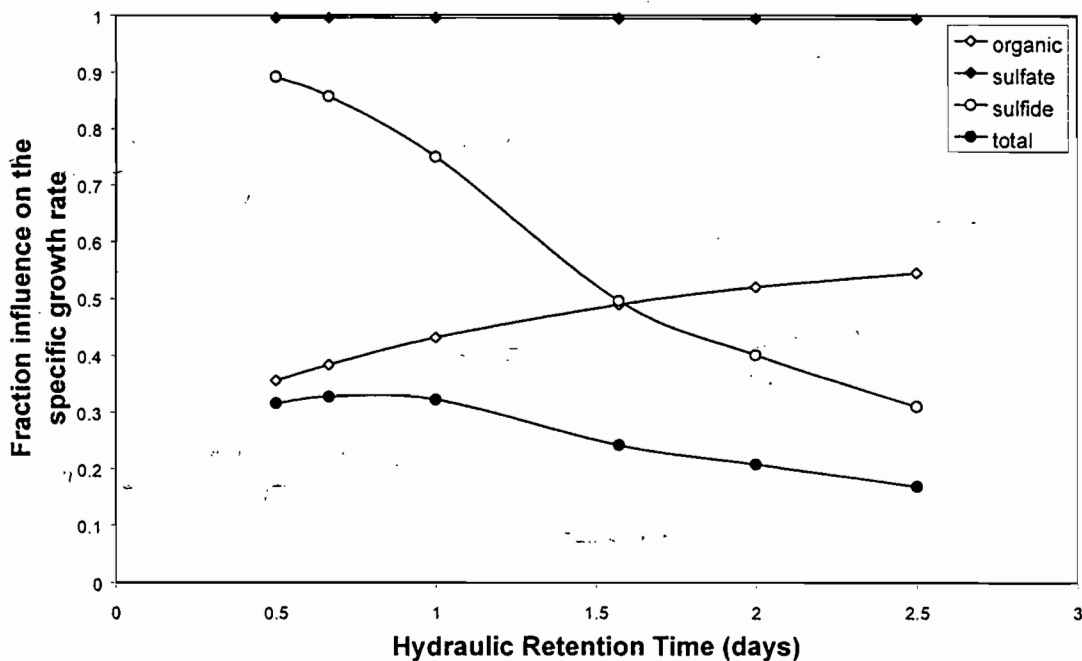


Figure 23: Model predictions of the terms for substrate limitation, sulfate limitation, sulfide inhibition, and the product of the three terms, for the acetogenic sulfidogens, as the feed to the bioreactor is varied by varying the hydraulic retention time (COD: $\text{SO}_4^{2-} = 2$)

Figure 23 is a plot of the terms for substrate limitation, sulfate limitation, sulfide inhibition, and the product of the three terms, for the acetogenic sulfidogens, as predicted by the model, as the HRT is varied. Figure 23 shows that the values for the sulfate limitation are close to 1 throughout the simulations, suggesting that the bacteria are never sulfate limited. The value for the organic substrate limitation increases with an increase in the HRT. This would be expected, as more hydrolysis is taking place as the HRT is increased, resulting in more soluble COD being formed. Figure 20 showed that the fraction of the feed COD leaving the bioreactor as soluble COD increased with an increase in HRT. This would then suggest that the propionate concentration would increase, resulting in less substrate limitation of the p-SRB.

Thirdly, the sulfide inhibition term decreases with an increase in the HRT. This would be expected since the sulfate conversion increases (Figure 22), resulting in more sulfide being produced. As this value increases, the bacteria become more inhibited.

However, what is important to the discussion is the fact that the model predicts that the term most affecting the specific growth rate is the organic substrate limitation term, at a HRT of less than 1.5 days, while it is the sulfide inhibition term at a HRT of greater than 1.5 days.

Therefore, as the sulfate conversion increases with an increase in the HRT, forming more sulfide, the bacteria become sulfide inhibited. The rate of hydrolysis is not affected by the sulfide concentration in the model, and forms more soluble COD at higher hydraulic retention times. Thus more soluble substrate is being formed, but the bacteria are becoming more inhibited, and the soluble COD accumulates. This explains the increase in the fraction of the feed COD leaving the bioreactor as soluble COD, shown in Figure 20.

6.2 Affects of Sludge Recycle Ratio

One of the main features of the FSBR is the high solids density in each of the three valleys, with the subsequent recycle of this high-density sludge back to the feed stream. The classical definition of recycle ratio is a fraction of the effluent stream being fed back to the feed stream. For the FSBR, the sludge recycle ratio (SRR) is defined as the total volumetric flow rate of the combined recycle streams as a ratio of the total volumetric flow rate of the feed stream. This is shown in Figure 3.

The sludge recycle ratio is then defined as:

$$\text{SRR} = \frac{R_{\text{TOTAL}}}{\text{Feed}} \quad (62)$$

In AQUASIM, the various flows of both solids and liquid streams are dependent on the recycle stream, since this determines the liquid flow in the FSBP. Figure 11 illustrates the various flows taking place in the FSBP, and the way that AQUASIM has been used to represent these streams.

AQUASIM calculates the flow rate of the liquid streams across the top of the reactor using a mass balance. The total flow of water into each of the compartments is equal to the total flow out. The solid lines in Figure 11 represent the liquid flow. Between the six top compartments, the liquid stream is split, and this split stream flows to the compartments below. The flow rate of each of these streams is set by the flow rate of liquid from each of the bottom compartments. These flow rates are in turn set by the total flow of the recycle pump, since the pump draws from each of these compartments for a set time. However, in AQUASIM, this is represented by a constant, but reduced, flow rate, rather than being switched on and off.

However, the dotted lines representing solids flow do not depend directly on the recycle pump rate. These are calculated from the total discharge from a compartment, which will be influenced by the recycle flow rate (Section 5.3). For example, the protein fraction that will settle out of the first top compartment to the first valley is calculated as the product of the discharge from the compartment, the concentration of protein in the compartment, and settling coefficient.

Therefore, the model will predict the settling of solids into the bottom three compartments even in the absence of a recycle flow rate. However, there will be no flow from one bottom compartment to the next, as there is no discharge from these compartments. There will also be no flow of solids back into the top six compartments. For these reasons, the recycle flow rate can not be set to 0 in the model, since the hydrodynamic flow patterns in the FSBP will not be simulated.

The total recycle pump capacity can be varied to determine the effects of the SRR on the performance of the FSBP. At the pilot plant, the recycle pump had a capacity of 2000 l.h⁻¹ (48 m³.d⁻¹), while the feed flow rate was 610 l.h⁻¹ (14.64 m³.d⁻¹), giving a SRR of 3.28. To obtain simulated trends from varying the SRR, the capacity of the recycle pump was varied. A minimum SRR of 0.25 was simulated, needing a recycle pump capacity of 3.66 m³.d⁻¹, while simulated trends up to a maximum SRR of 4 are shown.

Figure 24 shows the model prediction of the fraction of the feed COD that is leaving the FSBR as particulate COD, soluble COD, biomass, methane, or used for sulfide reduction, as a function of the SRR.

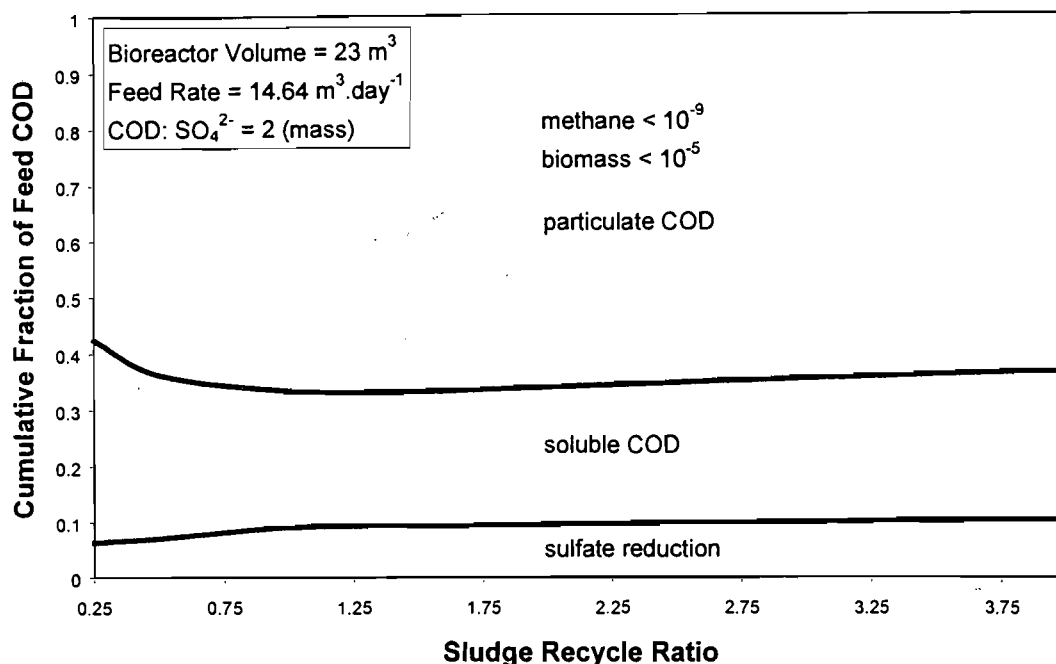


Figure 24: Model prediction of the fraction of the feed COD leaving the FSBR as particulate COD, soluble COD, biomass, methane, or used for sulfide reduction, as a function of the SRR (HRT = 1.57; COD: SO_4^{2-} = 2)

Figure 24 shows that the model predicts that a SRR of greater than 1 has little effect on the fractions of the various groups. In fact, an extreme SRR of 10 was simulated, and the increase in bioreactor performance with a ten-fold increase in SRR was insignificant. There is very little biomass ($<10^{-5}$) and methane produced ($<10^{-9}$), as in Figure 20.

However, at a SRR below 1, there is a change in the simulated trends. The fraction of the feed COD leaving as particulate COD suddenly decreases drastically, together with a change in the COD being used for sulfate reduction. The trend was simulated for a SRR value of 0.25, but at lower values, AQUASIM experience calculation errors! Although the calculation options were varied, now solution was obtained. These variations included increasing the maximum internal step size for the integration, increasing the maximum integration order to 5, increasing the number of co-diagonals of the Jacobian matrix, and the number of internal time steps for each external time step. These changes would allow AQUASIM the greatest opportunity of converging after a calculation loop, and thus obtaining a solution. Unfortunately, AQUASIM user support was not able to help in solving this problem, and thus a minimum SRR of 0.25 was simulated.

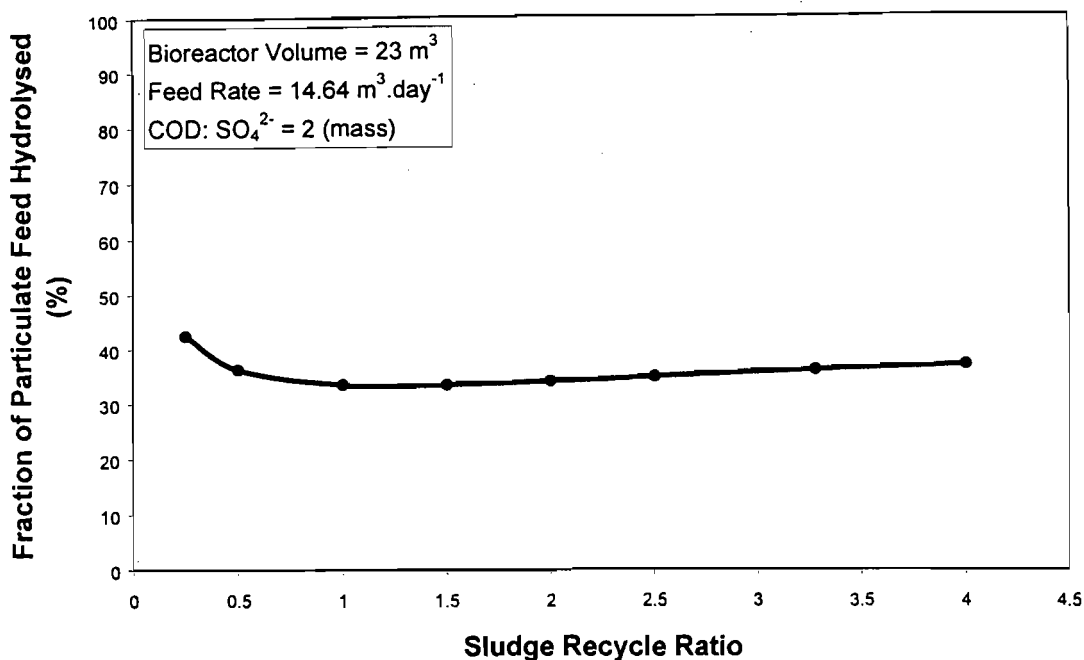


Figure 25: Model prediction of the fraction of the hydrolysis conversion as a function of the SRR (HRT = 1.57; COD: SO_4^{2-} = 2)

Figure 25 shows the fraction of the feed particulate COD that is being hydrolysed, as a function of the SRR. Figure 25 indicates a slight increase in the fraction being hydrolysed for SRR values greater than 1, but at SRR values below 1, there is a sudden increase in the fraction being hydrolysed. A possible explanation for this is that at lower recycle ratios, there is less of the high density sludge being mixed with the feed, resulting in a lower concentration of particulates in the inlet compartment. There are then fewer solids that have to settle out of this liquid stream into the high solids density compartments below, with fewer not settling sufficiently, and being washed out of the bioreactor with the effluent stream. This would result in a higher solids retention time than at higher solids recycle ratios, where more solids would be washed out unhydrolysed. With a higher reaction time available, greater solids hydrolysis is possible.

With greater solids hydrolysis taking place, more sulfate conversion would be expected, since there is more organic substrate available. However, Figure 24 shows that the fraction of the feed COD being used for sulfate reduction actually decreases at SRR values of less than 1.

Figure 26 shows the sulfate conversion as a function of the SRR. At SRR values greater than 1, there is a slight increase in the amount of sulfate converted. However, there is a decline in the sulfate conversion for values of SRR of less than 1.

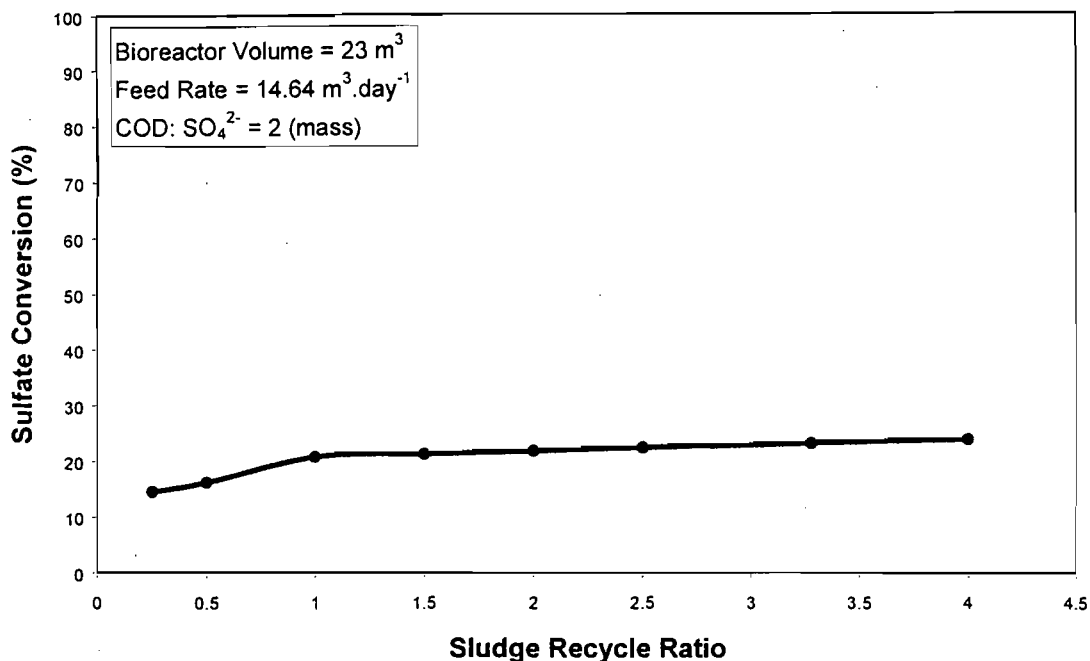


Figure 26: Model prediction of the fraction of sulfate converted as a function of the SRR (HRT = 1.57; COD: $\text{SO}_4^{2-} = 2$).

Figure 27 shows the concentration of methane in the bioreactor outlet as a function of the SRR. There is a definite increase in the amount of methane being produced as the SRR increases, but this concentration is still very small compared to the amount of sulfide being produced (see Figure 24).

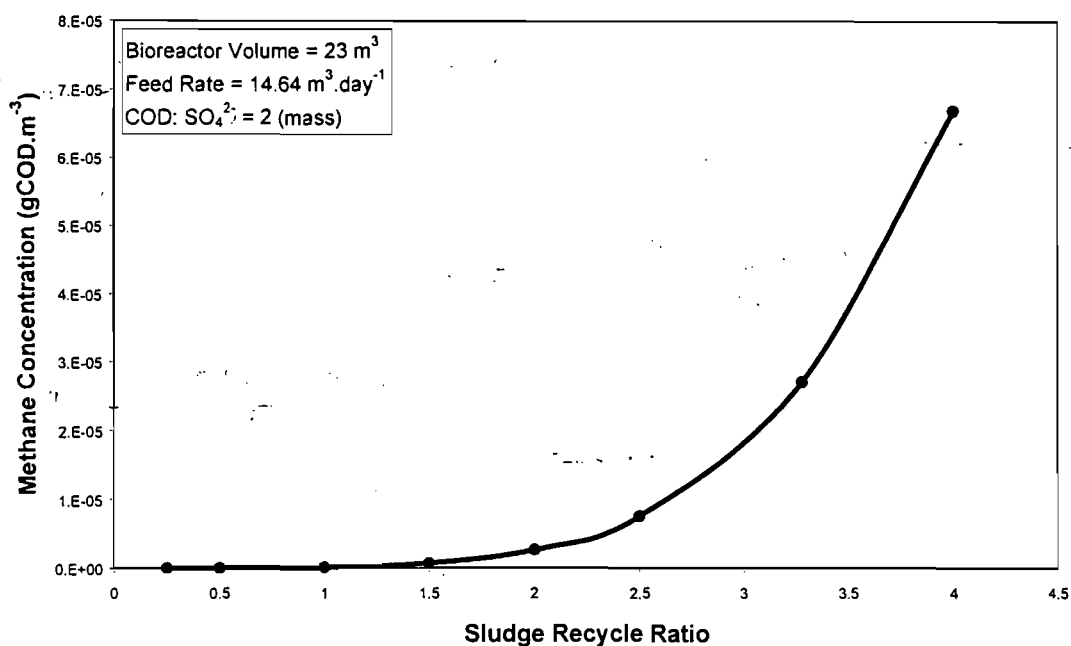
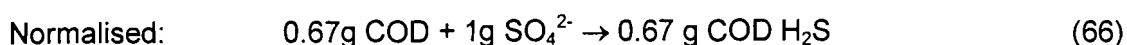
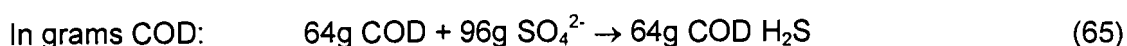
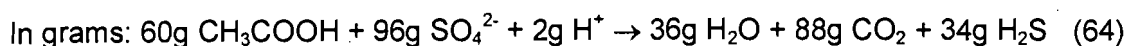
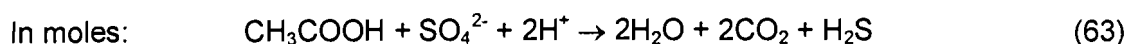


Figure 27: Model prediction of the effluent methane concentration, indicating methane production, as a function of the SRR (HRT = 1.57; COD: $\text{SO}_4^{2-} = 2$).

6.3 Affects of COD: SO₄²⁻ Ratio

Theoretically, in anaerobic systems, a COD: SO₄²⁻ ratio of 0.67 will result in all of the sulfate being reduced to sulfide, using all the available COD. For example, in the reaction where acetate is used as the organic electron donor, conversion of the units of the stoichiometric reaction gives the following:



This does not take the production of biomass into account. However, the aim of the FSBR is not to reduce all the sulfate added to the bioreactor, but rather to hydrolyse as much of the particulate COD being added as possible. The soluble products from this bioreactor enter a baffled reactor, where the majority of the sulfate reduction takes place. The characteristics and advantages of a baffled reactor will not be discussed here, but it is apparently more suited to biological sulfate reduction than the FSBR. The performance of the FSBR allows for high solids retention, rather than intimate contact of the soluble substrates with the biomass.

The point of adding sulfate to the feed of the first reactor is to enable the sulfate reducing bacteria to use any propionate, acetate or hydrogen that might be produced for sulfate reduction, instead of the methane producing bacteria converting this to methane. The aim of the simulations is therefore to predict the maximum amount of particulate organic matter that can be added with the minimum amount of sulfate, so that the production of methane is avoided, while the hydrolysis of the particulate organic matter is maximised.

The rate of hydrolysis is increased in the presence of sulfate and sulfate reducing bacteria. This was observed during the operation of the pilot plant. The exact affect that the sulfate concentration has on the rate of hydrolysis is unknown at this point, and therefore the model cannot predict this affect. The model can only be used to predict the affect of the COD: SO₄²⁻ ratio on the competition between the methanogens and the sulfate reducing bacteria.

The affect of the hydrogen partial pressure on anaerobic digestion systems has been discussed earlier in the report, and mention was made of process failure at high organic loading rates. However, the affects of the hydrogen partial pressure were not included in the model, since the reaction scheme used in the model was more

general than would be needed to compute the hydrogen partial pressure affects. For example, the exact reaction stoichiometry would be needed for all reactions involving hydrogen, in order to calculate the Gibb's Free Energy change for the reaction. This would require the concentration of each of the reactants and products at any time during the simulation, to determine the spontaneity of the reaction, and the ratio of products formed. This would drastically increase the complexity of the model. Hydrogen partial pressure affects have therefore been omitted. The model predictions will therefore become more uncertain at high organic loading rates, where the hydrogen partial pressure would be expected to increase. A maximum COD: SO_4^{2-} ratio of 4 was used, giving an organic feed rate of $100 \text{ g COD}\cdot\text{d}^{-1}$.

Figure 28 shows the model prediction of the fraction of the feed COD that is leaving the FSBR as particulate COD, soluble COD, biomass, methane, or that has been consumed during sulfate reduction.

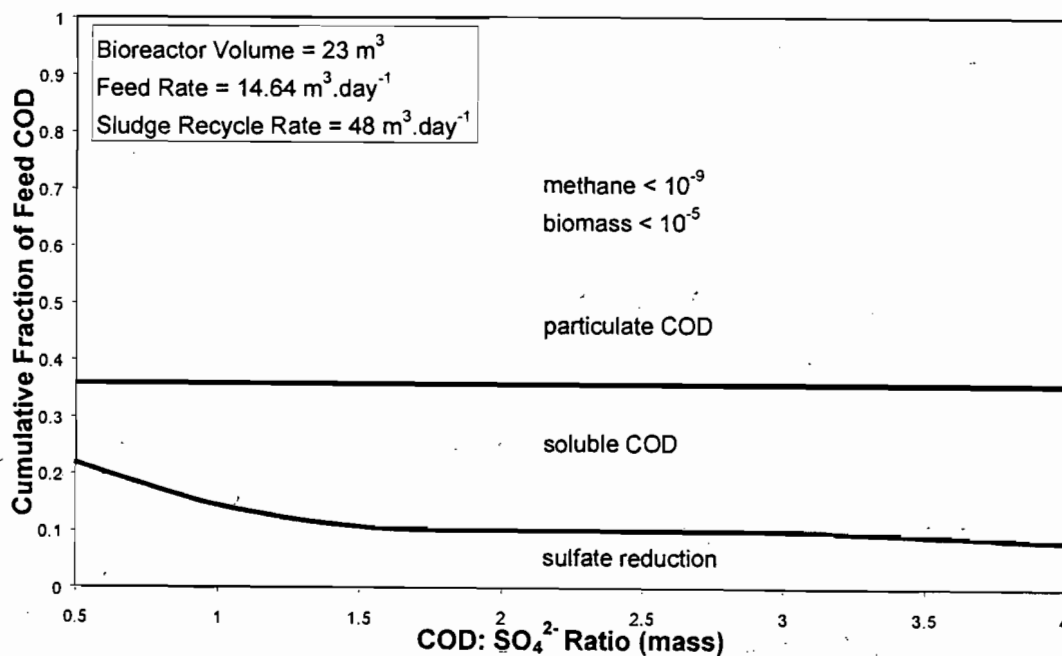


Figure 28: Model prediction of the fraction of feed COD that is leaving the bioreactor as either particulate COD, soluble COD, biomass, methane or sulfide, at various COD: SO_4^{2-} ratios (HRT = 1.57; SRR = 3.28)

Figure 28 shows that the majority of the feed COD is leaving the bioreactor still as particulate COD. Figure 28 also shows that the fraction of the feed COD that is leaving as soluble COD is increasing with an increase in the COD: SO_4^{2-} ratio, while the fraction of the feed COD being used for sulfate reduction is decreasing with an increase in the COD: SO_4^{2-} ratio.

The fraction of the feed COD being used to produce biomass and methane is of such minor quantities that these fractions do not appear in Figure 28. This suggests that very little methane is being produced ($<10^{-7}$), and that very little biomass is being produced ($<10^{-3}$).

Once again, the effects of sulfate on the rate of hydrolysis are not known, and not included in the model. Therefore, the only factor effecting the rate of hydrolysis is the concentration of the particulate COD and the available reaction time. Figure 29 shows the model prediction of the fraction of the feed particulate COD that is hydrolysed, as a function of the COD: SO_4^{2-} ratio. The model predicts that as more particulate COD is added to the bioreactor, more is leaving the bioreactor, with the same fraction being hydrolysed.

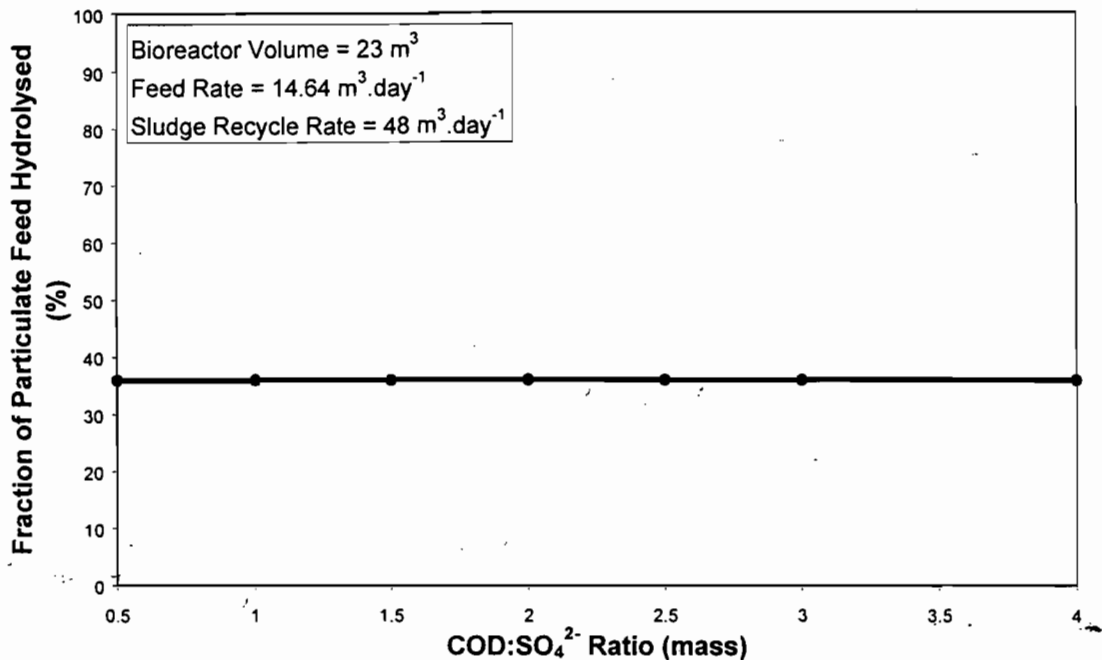


Figure 29: Model prediction of the fraction of hydrolysis of the feed COD at various COD: SO_4^{2-} ratios (HRT = 1.57; SRR = 3.28)

An increase in the COD: SO_4^{2-} ratio is a result of more COD being added, since the SO_4^{2-} concentration is constant. The rate of hydrolysis is first order with respect to the particulate COD concentration. Therefore, at higher feed concentrations, the rate of hydrolysis would increase. The higher reaction rate would cause greater conversion of the reactants for the same reaction time (HRT). The overall result is that more soluble COD is produced with an increase in the COD: SO_4^{2-} ratio.

In fact, Figure 29 shows that the fraction of the feed particulate COD that is hydrolysed is constant. Therefore, the variations in reactant concentration in the feed and the subsequent variations in the reaction rate result in the same fraction of

and the subsequent variations in the reaction rate result in the same fraction of hydrolysis. The model therefore predicts that the COD: SO_4^{2-} ratio does not effect the fraction of the feed particulate COD that is hydrolysed in the bioreactor. However, it does allow for greater amounts of soluble COD to be produced. This would be beneficial to the second bioreactor in the process following the FSBR, in that there would now be more substrate available for sulfate reduction in this bioreactor. It would also mean that there is more soluble substrate available for sulfate reduction and methane production in the FSBR.

Figure 30 shows the predicted sulfate conversion taking place in the bioreactor. Also plotted in Figure 30 are the measured sulfate conversion points from the pilot plant FSBR. The sulfate conversion does increase with an increase in the COD: SO_4^{2-} ratio. However, Figure 28 shows that the fraction of the total feed COD being used for sulfate reduction does not increase with an increase in the COD: SO_4^{2-} ratio. This means that although the amount of sulfate reduced does increase with an increase in the COD: SO_4^{2-} ratio, the sulfate reducing bacteria are effected by something other than the organic substrate concentration.

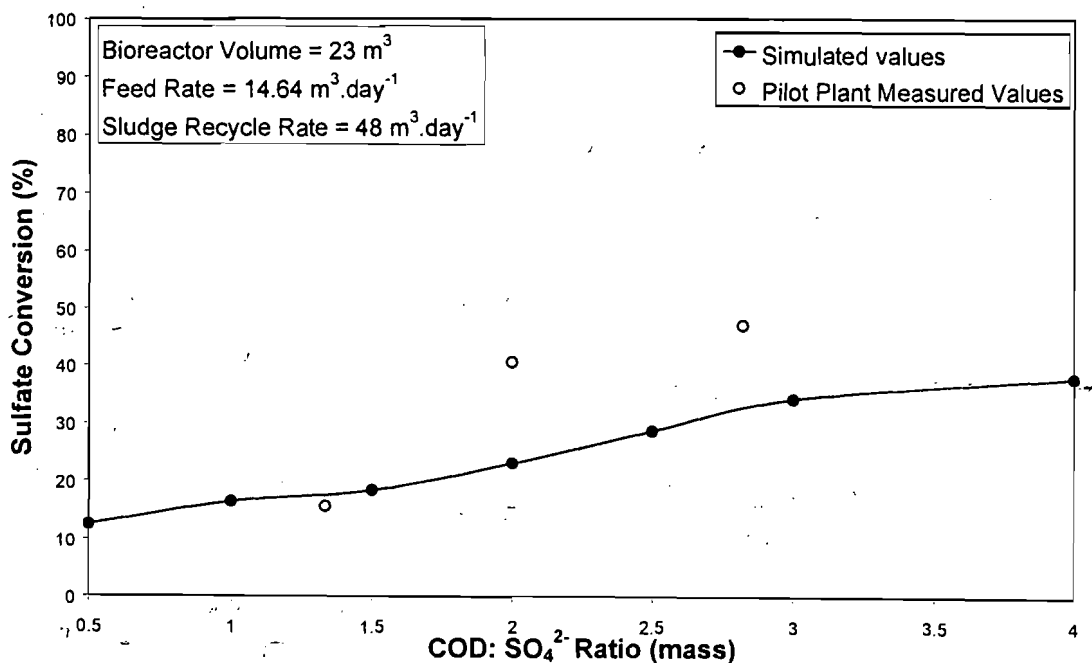


Figure 30: Model prediction of the sulfate conversion at various COD: SO_4^{2-} ratios, together with the three measured concentrations used for the model calibration and verification (HRT = 1.57; SRR = 3.28)

Figure 31 illustrates the predicted concentration of methane produced in the system. It shows that a maximum methane production occurs at a COD: SO_4^{2-} ratio of 1, but results in an effluent concentration of less than 2×10^{-4} g COD. m^{-3} . This means that

very little methane is being produced in the system, and that less is being produced at higher COD: SO_4^{2-} ratios, even as the soluble COD concentration increases.

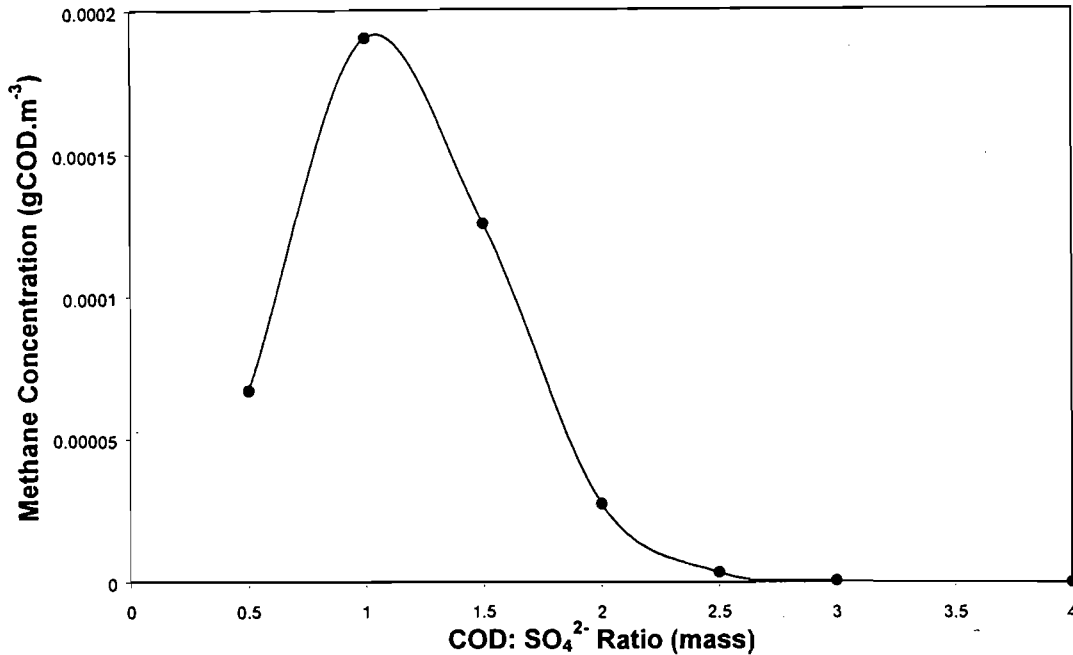


Figure 31: Model prediction of the concentration of methane leaving the bioreactor, indicating methane production, at various COD: SO_4^{2-} ratios (HRT = 1.57; SRR = 3.28)

In order to explain the inactivity of the bacteria at these higher COD: SO_4^{2-} ratios, the specific growth rate is divided into terms for substrate limitation and other inhibition terms. For the acetogenic sulfidogens, Equation 61 was again calculated for each COD: SO_4^{2-} ratio, as well as each of the three terms, namely organic substrate limitation, sulfate substrate limitation and undissociated sulfide inhibition.

Figure 32 is a plot of each of these individual effects on the specific growth rate, as well as the overall effect of each of these combined. Figure 32 shows that the sulfate limitation is close to 1 at all COD: SO_4^{2-} ratios, suggesting that the sulfate concentration is never substrate limiting. Figure 32 also shows that the value for the organic substrate limitation increases significantly with an increase in the COD: SO_4^{2-} ratio. This means that the organic substrate is becoming less limiting at higher COD: SO_4^{2-} ratios. This would be expected, as we have seen previously that the soluble COD concentration in the system increases with an increase in the COD: SO_4^{2-} ratio.

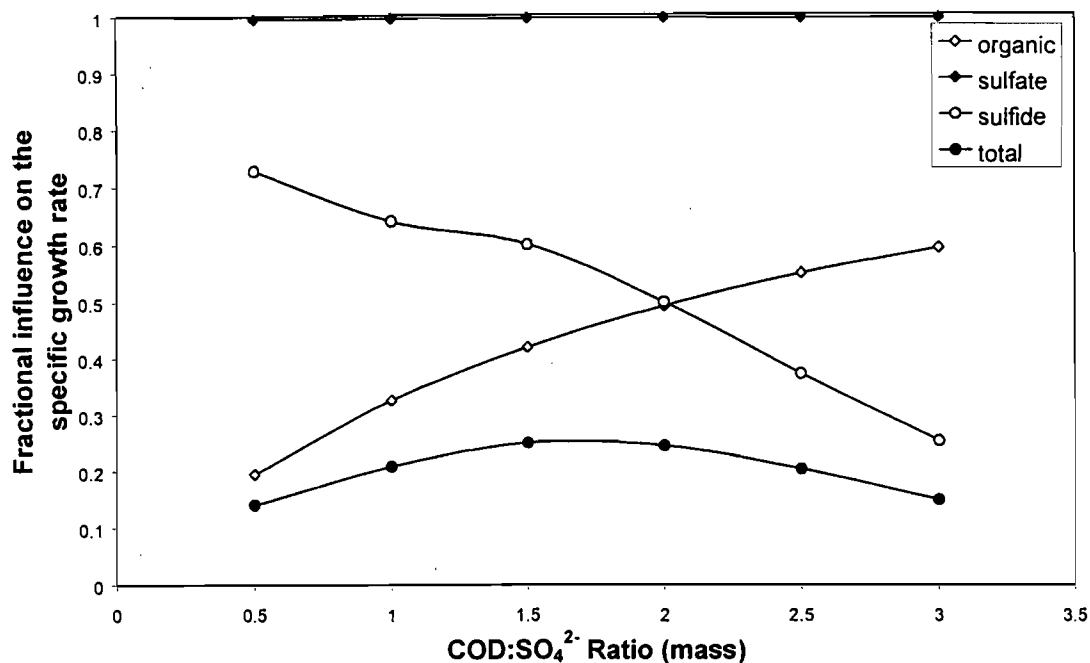


Figure 32: Model predictions of the terms for substrate limitation, sulfate limitation, sulfide inhibition, and the product of the three terms, for the acetogenic sulfidogens, as the COD: SO₄²⁻ ratio of feed to the bioreactor is varied (HRT = 1.57; SRR = 3.28)

Figure 32 shows that the sulfide inhibition value decreases with an increase in the COD: SO₄²⁻ ratio. This indicates that the bacteria are becoming more inhibited by the undissociated hydrogen sulfide. This would indicate an increase in the undissociated hydrogen sulfide concentration, which would be expected, as Figure 30 shows an increase in the sulfate conversion with an increase in the COD: SO₄²⁻ ratio, which produces undissociated hydrogen sulfide. Finally, Figure 32 shows that for a COD: SO₄²⁻ ratio of less than two, the bacteria are mostly effected by organic substrate limitation, while at COD: SO₄²⁻ ratios greater than 2, they are mostly effected by the sulfide inhibition.

A similar trend is observed for the other sulfate reducing bacteria, as well as for the methane-producing bacteria. This suggests that at low COD: SO₄²⁻ ratios, the bacteria are competing for the organic substrate, while at higher COD: SO₄²⁻ ratios, the bacteria are more inhibited by the undissociated hydrogen sulfide concentration. The model predicts that the sulfate reducing bacteria are less effected by the undissociated hydrogen sulfide than the methane producing bacteria, as well as competing more effectively for the available organic substrate, resulting in an insignificant amount of methane being produced.

7. SENSITIVITY ANALYSIS

In order to identify the model parameters that influence on the simulated outputs the most, a sensitivity analysis was performed on the model. This could have been done in two ways. The first method is mathematically rigorous, and requires taking the partial derivative of each output state variable (sulfate concentration, protein concentration, etc.) with respect to each constant variable (kinetic parameters, operational parameters, etc.). These results can be set up in a matrix, and the values in the matrix with the highest absolute values would correspond to the parameters that effect the model outputs the most.

The second method would require a full understanding of the system, and identification of the critical processes. The kinetic parameters relevant to these processes would be varied, simulations performed with these changed parameters, and the resulting changes in the output variables would identify the parameters that affect the model outputs the most.

The second method was used for this study. By understanding the processes involved in the anaerobic digestion of particulate organic matter in the presence of sulfate reducing bacteria, hydrolysis and acetoclastic sulfidogenesis were identified as critical steps. This was done following the results of the literature survey, where it was concluded that hydrolysis is the rate-limiting step in an anaerobic digestion process being fed particulate organic matter (Section 2.1), while acetoclastic methanogenesis is rate limiting when the feed to the process is soluble (Section 2.6.1). Also, Section 2.7.1 states that the acetoclastic sulfidogens will outcompete the acetoclastic methanogens for acetate. Therefore hydrolysis and acetoclastic sulfidogenesis will be the two critical biological processes in the FSBR.

The hydrolysis process was modelled using three rate equations, one each for the hydrolysis of protein, lipids, and carbohydrates. Each of these rate equations consists of one kinetic constant, as shown in Table 2. The acetoclastic sulfidogenesis rate equation depends on five kinetic parameters, as shown in Table 4.

To perform the sensitivity analysis, these kinetic parameters were increased and decreased by one order of magnitude (0.1 becomes 1 and 0.01) and a simulation performed with these new values, keeping all other parameters unchanged. The

results of the simulations were grouped consistently with those of Chapter 6, where the outputs of interest are the fractions of COD leaving as particulate COD, soluble COD, biomass, methane and used for sulfate reduction. It is the fraction variation in each of these parameters that was used to determine the parameter to which the model is most sensitive.

Similarly, the operational parameters were varied by 10%, since a larger variation would be unreasonable to the operation of the pilot plant, and would be outside the believable range used to calibrate the model. The operational parameters that have been changed are the feed COD concentration, feed sulfate concentration, recycle rate, feed rate, and the feed COD: SO_4 ratio, and the settling of the solids. The result of varying the recycle rate, feed rate, and the feed COD: SO_4 ratio was the topic of Chapter 6, where the model predicted that the pilot plant operation was most sensitive to the hydraulic retention time.

Table 11 shows the, according to a ten-fold variation in the kinetic parameters. Table 12 shows the ten greatest variations in the grouped outputs according to a 10% variation in the feed concentrations and the settling coefficients (See Appendix B).

Table 11 shows that the first order rate constant for protein hydrolysis has the greatest influence on the particulate COD concentration leaving the bioreactor, according to the model. Table 11 shows that all of the hydrolysis rate constants have a larger influence on the output of the model than the acetoclastic sulfidogenesis kinetic parameters. This is expected, since the aim of the FSBR is to hydrolyse the particulate organic matter, and the settling and recycle of the solid fraction allows for greater solids residence times, and thus greater solids concentrations. The value of the hydrolysis rate constants, and in fact the form of the hydrolysis rate equation, is therefore the most critical factor in modelling the FSBR, and these two choices will have the most influence on the predictability of the model.

Table 12 shows that the settling coefficients and the feed COD have most influence on the outputs of the model, and that the output most affected by the variation in the operating parameters is once again the particulate COD concentration, indicating the hydrolysis is the most critical process in the FSBR.

Therefore, in order to improve the predictability of future mathematical models, critical areas for research and analysis are the measuring of the hydrolysis rate constant and rate equation, accurately measuring the feed COD, and measuring the total COD in each of the three valleys, as discussed in Section 5.3, for the correct calibration of the settling coefficients.

Table 11: Results of the sensitivity analysis performed on the kinetic parameters from the model, showing the kinetic parameter that causes the greatest influence (absolute difference, highest 10 values) on the output parameters

Parameter	Old value	New value	Δ VSS (gVSS.m ⁻³)	Δ SO ₄ (gCOD.m ⁻³)	Δ COD _s (gCOD.m ⁻³)	Δ COD _p (gCOD.m ⁻³)	Δ CH ₄ (gCOD.m ⁻³)
$k_{n_{protein}}$ (d ⁻¹)	0.0375	0.375	1.91 10 ⁻⁴	3.63 10 ⁻²	1.49 10 ⁻¹	2.00 10⁻¹	7.13 10 ⁻⁹
$k_{n_{protein}}$ (d ⁻¹)	0.0375	0.375	1.91 10 ⁻⁴	3.63 10 ⁻²	1.49 10⁻¹	2.00 10 ⁻¹	7.13 10 ⁻⁹
$k_{n_{lipids}}$ (d ⁻¹)	0.0425	0.425	5.02 10 ⁻⁴	4.87 10 ⁻²	8.41 10 ⁻²	1.42 10⁻¹	9.89 10 ⁻⁹
$k_{n_{cellulose}}$ (d ⁻¹)	0.0525	0.525	1.11 10 ⁻⁴	2.28 10 ⁻²	9.23 10 ⁻²	1.26 10⁻¹	7.77 10 ⁻⁹
$k_{n_{protein}}$ (d ⁻¹)	0.0375	0.00375	1.08 10 ⁻⁴	1.85 10 ⁻²	9.48 10 ⁻²	1.25 10⁻¹	3.64 10 ⁻⁸
$K_{l_{as}}$ (g S.m ⁻³)	285	2850	3.19 10 ⁻⁴	9.64 10 ⁻²	1.08 10⁻¹	0	1.00 10 ⁻⁸
$k_{n_{cellulose}}$ (d ⁻¹)	0.0525	0.00525	9.08 10 ⁻⁵	1.63 10 ⁻²	7.76 10 ⁻²	1.04 10⁻¹	2.85 10 ⁻⁸
$k_{n_{lipids}}$ (d ⁻¹)	0.0425	0.00425	3.49 10 ⁻⁴	2.31 10 ⁻²	6.89 10 ⁻²	9.83 10⁻²	9.37 10 ⁻⁸
$K_{l_{as}}$ (g S.m ⁻³)	285	2850	3.19 10 ⁻⁴	9.64 10⁻²	1.08 10 ⁻¹	0	1.00 10 ⁻⁸
$k_{n_{protein}}$ (d ⁻¹)	0.0375	0.00375	1.08 10 ⁻⁴	1.85 10 ⁻²	9.48 10⁻²	1.25 10 ⁻¹	3.64 10 ⁻⁸

Table 12: Results of the sensitivity analysis performed on the operating parameters from the model, showing the operating parameter that causes the greatest influence (absolute difference, highest 10 values) on the output parameters

Parameter	Old value	New value	Δ VSS (gVSS.m ⁻³)	Δ SO ₄ (gCOD.m ⁻³)	Δ COD _s (gCOD.m ⁻³)	Δ COD _p (gCOD.m ⁻³)	Δ CH ₄ (gCOD.m ⁻³)
xC ₁	0.467	0.5137	1.4910 ⁻⁴	2.02 10 ⁻²	5.83 10 ⁻²	8.54 10⁻²	8.41 10 ⁻⁹
feed COD	3400	3060	7.41 10 ⁻⁵	9.47 10 ⁻³	3.72 10 ⁻²	6.44 10⁻²	2.29 10 ⁻⁸
xC ₁	0.467	0.4203	1.20 10 ⁻⁴	1.60 10 ⁻²	4.26 10 ⁻²	6.38 10⁻²	9.72 10 ⁻⁹
xC ₁	0.467	0.5137	1.4910 ⁻⁴	2.02 10 ⁻²	5.83 10⁻²	8.54 10 ⁻²	8.41 10 ⁻⁹
feed COD	3400	3740	5.99 10 ⁻⁵	8.17 10 ⁻³	3.02 10 ⁻²	5.27 10⁻²	2.45 10 ⁻⁹
xC ₁	0.467	0.4203	1.20 10 ⁻⁴	1.60 10 ⁻²	4.26 10⁻²	6.38 10 ⁻²	9.72 10 ⁻⁹
feed COD	3400	3060	7.41 10 ⁻⁵	9.47 10 ⁻³	3.72 10⁻²	6.44 10 ⁻²	2.29 10 ⁻⁸
feed COD	3400	3740	5.99 10 ⁻⁵	8.17 10 ⁻³	3.02 10⁻²	5.27 10 ⁻²	2.45 10 ⁻⁹
xC ₁	0.467	0.5137	1.4910 ⁻⁴	2.02 10⁻²	5.83 10 ⁻²	8.54 10 ⁻²	8.41 10 ⁻⁹
xC ₁	0.467	0.4203	1.20 10 ⁻⁴	1.60 10⁻²	4.26 10 ⁻²	6.38 10 ⁻²	9.72 10 ⁻⁹

8. CONCLUSIONS

The main aim of this project was to identify the state of the art regarding mathematical modelling of anaerobic digestion and biological sulfate reduction, to select rate equations from the literature that would simulate the various interactions taking place in the Falling Sludge Bed Reactor (FSBR) being fed a mixture of primary settled sewage sludge and acid mine drainage, and to investigate the trends obtained from the an AQUASIM model of the system.

The results of the literature survey showed that so far no mathematical model has been developed for the anaerobic digestion of particulate organic matter and simultaneous biological sulfate reduction. Rate equations have been developed for both anaerobic digestion and sulfate reduction, and these can be applied to the system in this study. However, kinetic constants to be used in these rate equations are not uniform, and depend on many experimental factors. The most critical dependence is on temperature, and there is a lack of data for these biological reactions at reduced temperatures.

The mathematical model developed in this study focussed on the biological processes taking place in the FSBR, and omitted vapour-liquid equilibria, acid-base equilibria and other factors such as hydrogen partial pressure affects. It is therefore a simplification of the biological reality. The results of the simulations would be able to predict trends in the operation of the pilot plant, rather than accurate concentrations.

The pilot plant operating data showed variations and inaccuracies that were taken into account when calibrating and verifying the pilot-plant operation. These inaccuracies further confirmed that exact values from the simulations were meaningless, and the predicted trends only were of importance. The hydraulic retention time (HRT), sludge recycle ratio (SRR) and COD: SO_4^{2-} ratio were varied in order to obtain predicted trends.

The model predicts that the performance of the FSBR is mainly dependent on the HRT. The model predicts that an increase in the HRT increases the amount of particulate COD that is hydrolysed, which is the primary aim of the FSBR. Secondly, at the SRR and COD: SO_4^{2-} ratio used, the model predicts that the production of methane is insignificant, resulting in more soluble COD being available for sulfate

reduction in the baffled reactor. Thirdly, the model predicts that the amount of biomass produced is also insignificant. The overall effect is that an increase in the HRT would improve the performance of the FSBR.

The model predicts that the SRR has very little effect on the bioreactor performance when the ratio varies from 1 to 10. However, at SRR values below 1, there is an increase in the bioreactor performance with a decrease in the SRR. At these low SRR, the flow patterns in the FSBR differ compared to higher SRR, and the FSBR is acting more as a settler than a completely mixed reactor. Unfortunately, the pilot plant cannot verify these trends. However, the model-predicted trend does show that the recycle pump capacity can be reduced from $48 \text{ m}^3 \cdot \text{d}^{-1}$ to $15 \text{ m}^3 \cdot \text{d}^{-1}$, saving on operational costs, without jeopardising the bioreactor performance.

Finally, the model predicts that the COD: SO_4^{2-} ratio does not effect the fraction of the feed particulate COD that is solubilised. However, for the same HRT and SRR, when more particulate COD is added to the FSBR, the same fraction is hydrolysed, resulting in more soluble COD being produced.

The model predicts that the methane production in the FSBR is negligible, even at high COD: SO_4^{2-} ratios, suggesting that sufficient sulfate is being added to the FSBR to allow the sulfate reducing bacteria to outcompete the methane producing bacteria for the available organic substrate.

The results of the sensitivity analysis identified hydrolysis as the rate-limiting step, and the hydrolysis kinetic constants were most critical to the performance of the model. Therefore, critical experimental evaluation of these kinetic constants and rate equations are most important in developing an improved model of the FSBR.

9. FUTURE WORK

The current investigation has identified the following areas that require further investigation, in order to improve the predictability of the model for more accurate predictions of the pilot plant performance. The identification of these areas consequently shows the shortcomings or limitations of the model.

9.1 Temperature Affects

The effects of temperature on the system need to be quantified if further work is to be attempted at these low temperatures. The kinetic constants available were measured at 35°C, while the pilot plant was operating at between 15°C and 20°C. The rule of thumb stating that the rate of a biological reaction will double with a 10-15°C increase in temperature is merely a guideline. Chaudhry and Beg (1997) gave the following equations for the temperature dependence of methanogens and denitrifiers, between 20 and 45°C:

For denitrifiers:
$$\mu_t = \mu_{20} \theta^{(t-20)} \quad (67)$$

where $\theta = 1.1$

For methanogens:
$$\frac{r_{x,T_1}}{r_{x,T_2}} = e^{\kappa(T_1 - T_2)} \quad (68)$$

where $\kappa = 0.9 - 1.0$

Middleton and Lawrence (1977) gave the following Arrhenius type equations for the temperature dependence of the kinetic parameters of sulfate reducing bacteria growing on acetate:

$$k = (0.695)(10^7) \left(10^{\frac{-1790}{T}} \right) \quad (69)$$

$$K_S = (1.65)(10^{-39}) \left(10^{\frac{12082}{T}} \right) \quad (70)$$

where T is the temperature in °K.

What Equations 67 – 70 show is that the temperature dependence is not linear, and that it affects more than the specific growth rate of the bacteria. It also shows that the temperature dependences are different for different groups of bacteria. It is therefore necessary to either measure the kinetic constants at the specified temperatures, or to determine the temperature dependence of each bacterial species. It is also important that the temperature range should cover that under which the reactor might operate.

9.2 Affects of Sulfate and Sulfide on Hydrolysis

The effect of either sulfate or sulfide concentration on the rate of hydrolysis has been discussed previously in this report (Section 8.3). Rhodes University, Department of Biochemistry and Microbiology, state that there is evidence that the rate of hydrolysis is accelerated due to the presence of sulfate, sulfide, or sulfate reducing bacteria in the system. This is of paramount importance, since if either the sulfate or the sulfide effect the rate of hydrolysis, these could be added to waste water treatment plants in order to accelerate the rate of hydrolysis, which is traditionally the rate-limiting step in the anaerobic digestion of particulates. It would also effect the predictability of the model, in that more hydrolysis would be expected at higher sulfate or sulfide concentrations. The optimum amount of AMD added to the FSBR could then be determined, in order to maximise the amount of particulates that are hydrolysed, as well as eliminating methanogenesis.

9.3 Solution Chemistry

The solution chemistry of the system should be included in the model. This would include the pH variations throughout the reactor. The model now assumes a constant pH of 7. However, the production of fatty acids and hydrogen sulfide would change the acidity and alkalinity of the system. The sulfate reducing reactions also use protons, increasing the pH of the system. These pH variations change the sulfide equilibrium, producing more undissociated hydrogen sulfide, which is inhibitory to the bacterial growth. It also changes the acetate equilibrium, which increases the concentration of the inhibitory acetic acid.

9.4 Liquid-Vapour Mass Transfer

The mass transfer of substances such as sulfide, methane and hydrogen and carbon dioxide between the liquid and the gas volume should also be included, to determine the concentration of the gas phase leaving the reactor.

The model that has been developed is therefore the start of a more extensive model. Once this model has been developed, it could be applied to the anaerobic digestion of various organic substrates, in the presence or absence of sulfate.

9.5 Kinetic Studies

Further kinetic studies that need to be performed are mostly in the areas of the affect of sulfate and sulfide on the anaerobic digestion processes. There is little published data on sulfide inhibition, and the kinetic mechanism of sulfide inhibition is not understood. Studies on the mechanism and extent of sulfide inhibition need to be performed, so that the best rate-equation terms for sulfide inhibition can be determined.

The upper limits of sulfate concentration that can be treated by sulfate reducing bacteria also needs to be determined. There is evidence that at sulfate concentrations greater than 10 mg.l^{-1} , for bacteria growing on ethanol and acetate, the systems need long adaptation phases, and sometimes do not reduce sulfate at all (personal correspondence with S. Moosa, C. Erasmus and J. Moon). However, activation of the bacteria at these high sulfate concentrations does occur, but the reason for the delay is not understood. Also, there is little data on sulfate limitation of sulfate reducing bacteria.

There is therefore a possibility of sulfate inhibition of both sulfate-reducing bacteria and other anaerobic bacteria, as well as sulfide inhibition.

Finally, acetic acid inhibition of anaerobic digestion systems has been modelled extensively. However, acetic acid inhibition of sulfate reducing systems has not been investigated. The fact that sulfate-reducing systems have an optimum pH less than the optimum pH for methanogenic systems suggests that acetic acid inhibition is less inhibitory to the sulfate reducing bacteria. If so, a decrease in the pH of a sulfate reducing system would increase the concentration of undissociated acetic acid, which would give the sulfate reducing bacteria an added advantage over the methane producing bacteria.

10. REFERENCES

- Ahring, B.K. and Westermann, P. 1987. Kinetics of butyrate and hydrogen metabolism in a thermophilic, anaerobic, butyrate degrading triculture. *Applied and Environmental Microbiology* **53**(2): 434 – 439.
- Andrews, J.F. and Graef, S.P. 1971. Dynamic modelling and simulation of the anaerobic digestion process. *Anaerobic Biological Treatment Processes: Advances in Chemistry* **105**:126–160.
- Barnes, L.J., Janssen, F.J., Scheeren, P.J.H., Versteegh, J.H. and Koch, R.O. 1991. Simultaneous microbial removal of sulfate and heavy metals from wastewater. First European Metals Conference, Bruxelles, Belgium.
- Barthakur, A., Bora, M. and Singh, H.D. 1991. Kinetic model for substrate utilisation and methane production in the anaerobic digestion of organic feeds. *Biotechnol. Prog.* **17**(4): 369 – 376.
- Barton, L.L. and Tomei, F.A. 1995. Characteristics and activities of sulfate reducing bacteria. In: Barton L.L. (Ed) *Sulfate Reducing Bacteria* (p 1-22). Plenum Press, New York.
- Béchar, G., Rajan, S. and Gould, W.D. 1993. Characterisation of a microbial process for the treatment of acid mine drainage. In: A.E. Torma, M.L. Apel, and C.L. Brierly (eds), *Biohydrometallurgical Technologies* p 277 – 286 The Minerals, Metals and Materials Society.
- Bekker, J.L. 1982. Water use in South Africa and estimated future needs. *Civ. Engr. S. Afr.* Dec: 653.
- Bhattacharya, S.K., Uberoi, V. and Dronamraju, M.M. 1996. Interaction between acetate fed sulfate reducers and methanogens. *Wat. Res.* **30**(10): 2239 – 2249.
- Bhattacharya, S.K., Qu, M. and Madura, R.L. 1996. Effects of nitrobenzene and zinc on acetate utilising methanogens. *Wat. Res.* **30**(12): 3099 – 3105.
- Braun, M. and Stolp, H. 1985. Degradation of methanol by a sulfate reducing bacterium. *Arch. Microbiol.* **58**: 786 – 793.

- Bryers, J.D. 1985. Structural modelling of the anaerobic digestion of biomass particulates. *Biotechnology and Bioengineering* **27**: 638 – 649.
- Buffiere, P., Steyer, J-P., Fonade, C. and Moletta, R. 1995. Comprehensive modelling of methanogenic biofilms in fluidised bed systems: Mass transfer limitations and multisubstrate aspects. *Biotechnology and Bioengineering* **28**: 725 – 736.
- Buffiere, P., Steyer, J-P., Fonade, C. and Moletta R. 1998. Mixing and phase hold-ups variations due to gas production in anaerobic fluidised bed digesters: Influence on reactor performance. *Biotechnology and Bioengineering* **60**(1): 36 – 43.
- Buisman, C.J.N., Post, R., Ijspeert, P., Geraats, G. and Lettinga, G. 1989. Biotechnological processes for sulfide removal with sulfur reclamation. *Acta Biotechnol.* **9**: 255 – 267.
- Burgess, S.G. and Wood, L.B. 1961. Pilot plant studies in production of sulfur from sulfate enriched sewage sludge. *J. Sci. Food Agric.* **12**: 326 – 341.
- Butlin, K.R., Selwyn, S.C. and Wakerley, D.S. 1956. Sulfide production from sulfate enriched sewage sludges. *J. Appl. Bacteriol.* **19**: 3 – 15.
- Chaundry, M.A.S. and Beg, S.A. 1997. Modelling of simultaneous methanogenesis and denitrification in an upflow packed bed biofilm reactor. *J. Chem. Technol. Biotechnol.* **70**: 267 – 277.
- Chen, C.I., Mueller, R.F. and Griebe T. 1994. "Kinetic analysis of microbial sulfate reduction by *Desulfivibrio desulfuricans* in an anaerobic upflow porous media biofilm reactor. *Biotechnology and Bioengineering* **43**(4): 267 – 274.
- Chian, E.S.K. and De Walle, F.B. 1983. Removal of heavy metals from a fatty acid wastewater with a complete mixed anaerobic filter. 920 - 927. In: Proceedings 38th Industrial Waste Conference, Purdue University, West Lafayette, IN.
- Christensen, B., Laake, M. and Lien, T. 1996. Treatment of acid mine water by sulfate reducing bacteria: results from a bench scale experiment. *Wat. Res.* **30**(7): 1617 – 1624.
- Cidu, R., Caboi, R., Fanfani, L. and Frau, F. 1997. Acid drainage from sulfides hosting gold mineralisation. *Environmental Geology* **30**(3/4): 231 – 237.

- Conradie, P.J.A. and Grutz, P.W.E. 1973. The treatment of acid mine waste in a mixture with sewage sludge in an anaerobic digester. Report to the Chamber of Mines (File No. w6/534/3). National Institute for Water Research, Pretoria.
- Costello, D.J., Greenfield, P.F. and Lee, P.L. 1991. Dynamic modelling of a single stage high rate anaerobic reactor. *Wat. Res.* **25**(7): 847 – 871.
- Denopoulou, G., Sterritt, R.M. and Lester, J.N. 1988. Anaerobic acidogenesis of a complex wastewater: II, Kinetics of growth, inhibition and product formation. *Biotechnology and Bioengineering* **31**: 969 – 978.
- Devorak, D.A., Hedin, R.S. and Edenborn, H.M. 1992. Treatment of metal - containing water using bacterial sulfate reduction: results from pilot plant reactors. *Biotech. Bioeng.* **40**: 609 – 616.
- De Walle, F.B., Chian, E.S.K. and Brush, J. 1979. Heavy metal removal with completely mixed anaerobic filter. *J. Water Poll. Control Fed.* **51**: 22 – 36.
- Du Preez, L.A., Odendaal, J.P., Maree, J.P. and Ponsonby, M. 1992. Biological removal of sulfate from industrial effluents using producer gas as an energy source. *Environ. Technol.* **13**: 875 – 882.
- Eastman, J.A. and Ferguson, J.F. 1981. Solubilisation of particulate organic carbon during the acid phase of anaerobic digestion. *JWPCF* **53**(3): 352 – 366.
- Eliosov, B. and Argaman, Y. 1995. Hydrolysis of particulate organics in activated sludge systems. *Wat. Res.* **29**(1): 155 – 163.
- Florencio, L., Field, J.A. and Lettinga G. 1995. Substrate competition between methanogens and acetogens during the degradation of methanol in UASB reactors. *Wat. Res.* **29**(3): 915 – 922.
- Fox, P. and Suidan, M.T. 1990. Batch tests to determine activity distribution and kinetic parameters for acetate utilisation in expanded bed anaerobic reactors. *Applied and Environmental Microbiology* **56**(4): 887 – 894.
- Gadd, G.M. and White, C. 1993. Microbial treatment of metal pollution – a working biotechnology? *TIBTECH* **11**: 353 – 359.
- Giraldo-Gomez, E., Goodwin, S. and Switzenbaum, M.S. 1992. Influence of mass transfer limitations on determination of the half saturation constant for hydrogen uptake in a mixed culture CH₄-producing enrichment. *Biotech. Bioeng.* **40**: 768 – 776.

- Gray, N.F. 1997. Environmental impact and remediation of AMD: a management problem. *Environmental Geology* **30**(1/2): 62 – 71.
- Grobicki, A and Stuckey, D.C. 1992. Hydrodynamic characteristics of the anaerobic baffled reactor. *Wat. Res.* **23**(3): 371 – 378.
- Gujer, W. and Zehnder, A.J.B. 1983. Conversion processes in anaerobic digestion. *Wat. Sci. Tech.* **15**: 127 – 167.
- Gupta, A., Flora, J.R.V., Sayles, G.D. and Suidan, M.T. 1994. Methanogenesis and sulfate reduction in chemostats. *Wat. Res.* **28**(4): 795 – 803.
- Gupta, M., Sharma, D., Suidan, M.T. and Sayles, G.D. 1996. Biotransformation rates of chloroform under anaerobic conditions. *Wat. Res.* **30**(6): 1377 – 1394.
- Hamelers, B., Scharff, H., Veeken, A. and Kalyuzhnyi, S. 1998. Inhibition of anaerobic hydrolysis of biowastes by pH and VFA: Experimental observations and simulations. Unpublished Paper.
- Harada, H., Uemura, S. and Momonoj, K. 1994. Interaction between sulfate reducing bacteria and methane producing bacteria in UASB reactors fed with low strength wastes containing different levels of sulfate. *Wat. Res.* **28**(2): 355 – 367.
- Harper, S.R. and Pohland, F.G. 1986. Recent developments in hydrogen management during anaerobic biological wastewater treatment. *Biotech. Bioeng.* **28**(4): 585 – 602.
- Henze, M., Harremoës, P. 1983. Anaerobic treatment of wastewater in fixed film reactors – A literature review. *Wat. Sci. Tech.* **15**: 1 – 101.
- Herrera, L.J., Hernández, P., Ruiz and Gantenbein, S. 1991. *Desulfovibrio desulfuricans* growth kinetics. *Environ. Toxicol. Water Qual.* **6**: 225 – 238.
- Heyes, R.H., Hall, R.J. 1983. Kinetics of two subgroups of propionate-using organisms in anaerobic digestion. *Applied and Environmental Microbiology* **46**(3): 710 – 715.
- Heynike, J.J.C. 1981. The economic effect of the mineral content present in the Vaal River water on the community of the PWV complex. Report of the Water Research Commission, Pretoria.
- Higgins, A.J., Kaplovsky, A.J. and Hunter, J.V. (1982). Organic composition aerobic, anaerobic and compost-stabilised sludges. *JWPCF* **54**: 466-473.
- Hill, D.T., Barth, C.L. 1977. A dynamic model for simulation of animal waste digestion. *JWPCF* October: 2129 – 2143, Technical Contribution No. 1318.

- Hoh, C.Y. and Cord-Ruwisch, R. 1996. A practical kinetic model that considers endpoint inhibition in anaerobic digestion processes by including the equilibrium constant. *Biotech. Bioeng* **51**: 597 – 604.
- Ingvorsen, K. and Jørgensen, B.B. 1984. Kinetics of sulfate uptake by freshwater and marine species of *Desulfovibrio*. *Arch. Microbiol.* **139**: 61 – 66
- Ingvorsen, K., Zehnder, A.J.B. and Jørgensen, B.B. 1984. Kinetics of sulfate and acetate uptake by *Desulfobacter postgatei*. *Applied and Environmental Microbiology* **47**(2): 403 – 408.
- Isa, Z., Grusenmeyer, S. and Verstraete, W. 1986. Sulfate reduction relative to methane production in high-rate anaerobic digestion. *Applied and Environmental Microbiology* **51**(3): 572 – 587.
- Jain, S., Lala, A.K., Bhatia, S.K. and Kudchadker, A.P. 1992. Modelling of hydrolysis controlled anaerobic digestion. *J. Chem. Tech. Biotechnol.* **53**: 337 – 344.
- Jeyaseelan, S. 1997. A simple mathematical model for anaerobic digestion process. *Wat. Sci. Tech.* **35**(8): 185 – 191.
- Johnson, D.B. 1995. Acidophilic microbial communities: candidates for bioremediation of acidic mine effluents. *Int. Biodet. and Biodeg.* :41 – 58.
- Kalin, M., Scribailo, R.W. and Wheeler, W.N. 1991. Acid mine drainage amelioration in natural bog systems. 61 – 77. In: *Proceedings of the Seventh Annual General Meeting of BIOMINET*. November, Mississauga, Ontario, Canada.
- Kalyuzhnyi, S.V. and Fedorovich, V.V. 1998. Mathematical modelling of competition between sulfate reduction and methanogenesis in anaerobic reactors. *Biodegradation* **9**: 187 – 199.
- Kasper, H.F. and Wuhrmann, K. 1978. Kinetic parameters and relative turnovers of some important catalytic reactions in digesting sludge. *Applied and Environmental Microbiology* **36**(1): 1 – 7.
- Kiely, G., Tayfur, G., Dolan, C. and Tanji, K. 1997. Physical and mathematical modelling of anaerobic digestion of organic wastes. *Wat. Res.* **31**(3): 534 – 540.
- Kristjansson, J.K., Schönheit, P. and Thauer, R.K. 1982. Different K_S values for hydrogen of methanogenic bacteria and sulfate reducing bacteria: An explanation for the apparent inhibition of methanogenesis by sulfate. *Arch. Microbiol.* **131**: 278 – 282.

- Konishi, Y., Yoshida, N. and Asai, S. 1996. Desorption of hydrogen sulfide during batch growth of the sulfate reducing bacterium *Desulfovibrio desulfuricans*. *Biotechnol. Prog.* **12**: 322 – 330.
- Kuenen, J.G. and Robertson, L.A. 1992. The use of natural bacterial populations for the treatment of sulfur containing wastewater. *Biodegradation* **3**: 239 – 254.
- Kuyucak, N. and St-Germain, P. 1994. Evaluation of sulfate reducing bacteria and related process parameters for developing a passive treatment method. 287 – 303. In: *Proceedings of the Biomineral Bioprocessing II Conference*, Snowbird, Utah.
- Laanbroek, H.J., Geerligs, H.J., Sijtsma, L. and Veldkamp, H. 1984. Competition for sulfate and ethanol among *Desulfobacter*, *Desulfobulbus* and *Desulfovibrio* species isolated from industrial sediments. *Applied and Environmental Microbiology* **47**(2): 329-334.
- Ledin, M. and Pederson, K. 1996. The environmental impact of mine wastes – Roles of microorganisms and their significance in treatment of mine wastes. *Earth – Science Reviews* **41**: 67 – 108
- Lettinga, G. 1995. *Anaerobic digestion and wastewater treatment systems*. *Antonie van Leeuwenhoek* **67**: 3 – 28.
- Lin, C.Y., Noike, T., Furumai, H. and Matsumoto, J. 1989. A kinetic study of the methanogenesis process in anaerobic digestion. *Wat. Sci. Tech.* **21**: 175 – 186.
- Maillacheruvu, K.Y. and Parkin, G.F. 1996. Kinetics of growth, substrate utilisation, and sulfide toxicity for propionate, acetate and hydrogen utilisers in anaerobic systems. *Water Environment Research* **58**(7): 1099 – 1106.
- Maree, J.P. and Hill, E. 1989. Biological removal of sulfate from industrial effluents and concomitant production of sulfur. *Wat. Sci. Tech.* **21**: 265 – 276.
- Maree, J.P., Gerber, A. and Hill, E. 1987. An integrated process for biological treatment of sulfate containing industrial effluents. *JWPCF* **59**: 1069 – 1074.
- Middleton, A.C. and Lawrence, A.W. 1977. Kinetics of microbial sulfate reduction. *JWPCF* **6**: 1659 – 1670.
- Moletta, R., Verrier, D. and Albanac, G. 1986. Dynamic modelling of anaerobic digestion. *Wat. Res.* **20**(4): 427 – 434.

- Mosey, F.E. 1983. Mathematical modelling of the anaerobic digestion process: Regulatory mechanisms for the formation of short-chain volatile fatty acids from glucose. *Wat. Sci. Tech.* **15**: 209 – 232.
- Musvoto, E.V., Wentzel, M.C., Loewenthal, R.E. and Ekama, G.A. 1997. Kinetic-based model for mixed weak acid / base systems. *Water SA* **23**(4): 311 – 322.
- Nielsen, P.H. 1987. Biofilm dynamics and kinetics during high-rate sulfate reduction under anaerobic conditions. *Applied and Environmental Microbiology* **1**: 27 – 32.
- Novak, J.T. and Carlson, D.A. 1970. The kinetics of anaerobic long chain fatty acid degradation. *JWPCF* **42**: 1932 – 1943.
- O'Flaherty, V., Mahony, T., O'Kennedy, R. and Colleran E. 1998. Effect of pH on growth kinetics and sulfide toxicity thresholds of a range of methanogenic, syntrophic and sulfate reducing bacteria. *Process Biochemistry* **33** (5).
- Oleszkiewicz, J.A. and Hilton, B.L. 1986. Anaerobic treatment of high sulfate wastes. *Canadian Journal of Civil Engineering* **13**: 423 – 428.
- Okabe, S., Nielsen, P.H. and Characklis, W.G. 1992. Factors affecting microbial sulfate reduction by *Desulfovibrio desulfuricans* in continuous culture: limiting nutrients and sulfate concentration. *Biotech. Bioeng.* **40**: 725 – 734.
- Okabe, S., Nielsen, P.H., Jones, W.L. and Characklis, W.G. 1995. Sulfide product inhibition of *Desulfovibrio desulfuricans* in batch and continuous cultures. *Wat. Res.* **29**(2): 571 – 578.
- O'Rourke, J.T. 1968. Kinetics of anaerobic treatment at reduced temperatures. Dissertation, Department of Civil Engineering, Stanford University.
- Oude Elferink, S.J.W.H., Visser, A., Hulshoff Pol, L.W. and Stams, A.J.M. 1994. Sulfate reduction in methanogenic bioreactors. *FEMS Microbiology reviews* **15**: 119 – 136.
- Pavlostathis, S.G. and Giraldo-Gomez, E. 1991. Kinetics of anaerobic treatment. *Wat. Sci. Tech.* **24**(8): 35 – 59.
- Pipes, O.W. 1960. Sludge digestion by sulfate reducing bacteria. Proceedings of the 15th Ind. Waste Conf., Purdue University, Lafayette, Indiana.
- Pirt, S.J. 1975. Principles of microbe and cell cultivation. Blackwell. Oxford.
- Postgate, J.R. 1984. The sulfate reducing bacteria. Cambridge University Press, Cambridge.

- Pronk, J.T. and Johnson, D.B. 1992. Oxidation and reduction of iron by acidophilic bacteria. *Geomicrobiology Journal* **10**: 153 – 171.
- Ramachandra, R.S. and Hepler, L.G. 1976. Equilibrium constants and thermodynamics of ionisation of aqueous hydrogen sulfide. *Hydrometallurgy* **2**: 293 – 299.
- Ray, B.T., Huang, J-C. and Dempsey, B.A. 1989. Sludge digestion by anaerobic fluidised beds. II: Kinetic model. *Journal of Environmental Engineering* **115(6)**: 1156 – 1170.
- Reichert, P. 1994. AQUASIM – A tool for simulation and data analysis of aquatic systems. *Wat. Sci. Tech.* **30(2)**: 21 – 30.
- Reis, M.A.M., Almeida, J.S., Lemos, P.C. and Carrondo, M.J.T. 1992. Effect of hydrogen sulfide on growth of sulfate-reducing bacteria. *Biotech. Bioeng.* **40**: 593 – 600.
- Riviera, A.L. 1983. Heavy metal removal in a packed-bed, anaerobic upflow bioreactor. *J. Water Poll. Control Fed.* **61**: 1576 – 1587.
- Robb, G.A. 1994. Environmental consequences of coalmine closure. *The geographical Journal* **106**: 33 – 40.
- Robinson, J.A. and Teidje, J.M. 1984. Competition between sulfate reducing and methanogenic bacteria for H₂ under resting and growing conditions. *Arch. Microbiol.* **137**: 26 – 32.
- Salomons, W. 1995. Environmental impact of heavy metals derived from mining activities: processes, prediction, prevention. *J. Geochemical Exploration* **52**: 5 – 23.
- Scheeren, P.J.H., Koch, R.O. and Buisman, C.J.N. 1993. Geohydrological containment system and microbial water treatment plan for metal-contaminated ground water at 50. 373 – 384. *Proceedings of the Budelco International Symposium – World Zinc, '93 Proceedings.*
- Shimizu, T., Kudo, K. and Nasu, Y. 1993. Anaerobic waste activated sludge digestion- A bioconversion mechanism and kinetic model. *Biotech. Bioeng.* **41(11)**: 1082 – 1091.
- Shin, H.S., Oh, S.E. and Bae, B.U. 1996. Competition between SRB and MPB according to temperature change in the anaerobic treatment of tannery wastes containing high sulfate. *Environmental Technology* **17**: 361 – 370.

- Stucki, G., Hanselmann, K.W. and Hurzeler, R.A. 1993. Biological sulfuric acid transformation: Reactor design and process optimisation *Biotech. Bioeng* **41**: 303 – 315.
- Szewzyk, R. and Pfennig, N. 1990. Competition for ethanol between sulfate reducing and fermenting bacteria. *Arch Microbiol* **153**: 470 – 477.
- Thiele, J.H. and Zeikus, J.G. 1988. The anion-exchange substrate shuttle process: a new approach to two-stage biomethanation of organic and toxic wastes. *Biotech. Bioeng* **31**(4): 521 – 535.
- Toerien, D.F. and Maree, J.P. 1987. Reflections on anaerobic process biotechnology and its impact on water utilisation in South Africa. *Water SA* **13**: 137 – 144.
- Traore, A.S., Fardeau, M-L., Hatchikian, C.E., Le Gall, J. and Belaich J-P. 1983. Energetics of growth of defined mixed culture of *Desulfovibrio vulgaris* and *Methanosarcina barkeri*: Interspecies hydrogen transfer in batch and continuous cultures. *Applied and Environmental Microbiology* **46**(5): 1152 – 1156.
- Uberoi, V and Bhattacharya, S.K. 1997. Effects of chlorophenols and nitrophenols on the kinetics of propionate degradation in sulfate reducing anaerobic systems. *Environmental Science and Technology* **31**(6): 1607 – 1614.
- Ueki, K., Kotaka, K., Itoh, K. and Ueki, A. 1988. Potential availability of anaerobic treatment with digester slurry of animal waste for the reclamation of acid mine water containing sulfate and heavy metals. *J. Ferment. Technol.* **66**: 43 – 50.
- Umita, T., Nenov, V., Omura, T., Aizawa, J. and Onuma, M. 1988. Biological ferrous iron oxidation with fluidised bed reactor. *Water Pollution Control in Asia*: 479 – 485.
- van Houten, R.T., Hulshoff Pol, L.W. and Lettinga, G. 1994. Biological sulfate reduction using gas-lift reactors fed with hydrogen and carbon dioxide as energy and carbon source. *Biotech. Bioeng* **44**: 586 – 594.
- van Zyl, H.C. 1996. Environmental systems in Amcoal. *Mining Environment Managemant* March: 18 – 21.
- Vavilin, V.A., Rytov, S.V. and Lokshina, L.Y. 1996. A description of hydrolysis kinetics in anaerobic degradation of particulate organic matter. *Bioresource Technology* **56**: 229 – 237.

- Wang, Y-T., Suidan, M.T. and Rittman, B.E. 1986. Kinetics of methanogens in an expanded bed reactor. *Journal of Environmental Engineering* **112**(1): 155 – 170.
- Wu, C., Huang, J. and Jih, C. 1998. Consecutive reaction kinetics involving distributed fraction of methanogens in fluidised-bed bioreactors. *Biotech. Bioeng* **57**(3): 367 – 379.
- Yoda, M., Kitagawa, M. and Miyaji, Y. 1987. Long term competition between sulfate-reducing and methane-producing bacteria for acetate in anaerobic biofilm. *Wat. Res.* **21**(12): 1547 – 1556.
- Yu, J. and Pinder, K.L. 1993. Intrinsic fermentation kinetics of lactose in acidogenic biofilms. *Biotech. Bioeng* **41**: 479 – 488.
- Zellner, G., Neudorfer, F. and Diekmann, H. 1994. Degradation of lactate by an anaerobic culture in a fluidised-bed reactor. *Wat. Res.* **28**(6): 1337 – 1340.
- Weist, R.C. 1977. *Handbook of chemistry and physics*. 58th Edition.

APPENDIX A

The biological reactions in the model have been described using a number of different modified Monod equations. The modifications to the Monod equation have been necessitated due to the complexities of the system. As discussed in Section 4.3, all of the bacterial equations are inhibited by the undissociated hydrogen sulfide, while some of the acid forming bacteria are inhibited by the undissociated acetic acid. Terms such as uncompetitive, non-competitive, competitive and first order inhibition models have been used. The mathematical effects that each of these inhibition models has on the system are now discussed. The various inhibition models are discussed, including their behaviour, and their limitations.

The rate equation for the inhibition models mentioned above are given for the specific growth rate of a species of bacteria using one organic substrate, S (mg.l⁻¹), and being inhibited by the same compound, I (mg.l⁻¹). To be able to demonstrate the affects of both substrate limitation and inhibition, the substrate and inhibitor concentrations need to be varied.

Uninhibited Monod equation:
$$\mu = \frac{\mu_{\max}}{1 + \frac{K_s}{[S]}} \quad (\text{A})$$

Uncompetitive inhibition:
$$\mu = \frac{\mu_{\max}}{1 + \frac{K_s}{[S]} + \frac{[I]}{K_i}} \quad (\text{B})$$

Non-competitive inhibition:
$$\mu = \frac{\mu_{\max}}{\left(1 + \frac{K_s}{[S]}\right) \left(1 + \frac{[I]}{K_i}\right)} \quad (\text{C})$$

Competitive inhibition:
$$\mu = \frac{\mu_{\max}}{1 + \frac{K_s}{[S]} \left(1 + \frac{[I]}{K_i}\right)} \quad (\text{D})$$

First order inhibition:
$$\mu = \frac{\mu_{\max}}{1 + \frac{K_s}{[S]}} \left(1 - \frac{[I]}{K_i}\right) \quad (\text{E})$$

In order to illustrate the affect that the choice of inhibition model has on the system, Equations A to E were plotted as a function of the substrate/ inhibitor concentration. This then shows the effect of the substrate limitation in the absence of the inhibitor, as well as for each of the inhibition models.

The following kinetic parameters were used to calculate the specific growth rate:

$$K_s = 200 \text{ mg.l}^{-1}$$

$$\mu_{\max} = 5 \text{ day}^{-1}$$

$$K_i = 1000 \text{ mg.l}^{-1}$$

These values were then substituted into Equations A – E, while the value of S, and therefore I, was increased. Figure A illustrates the value of the specific growth rate as calculated by Equations A – E for a logarithmic increase in the substrate and inhibitor concentration.

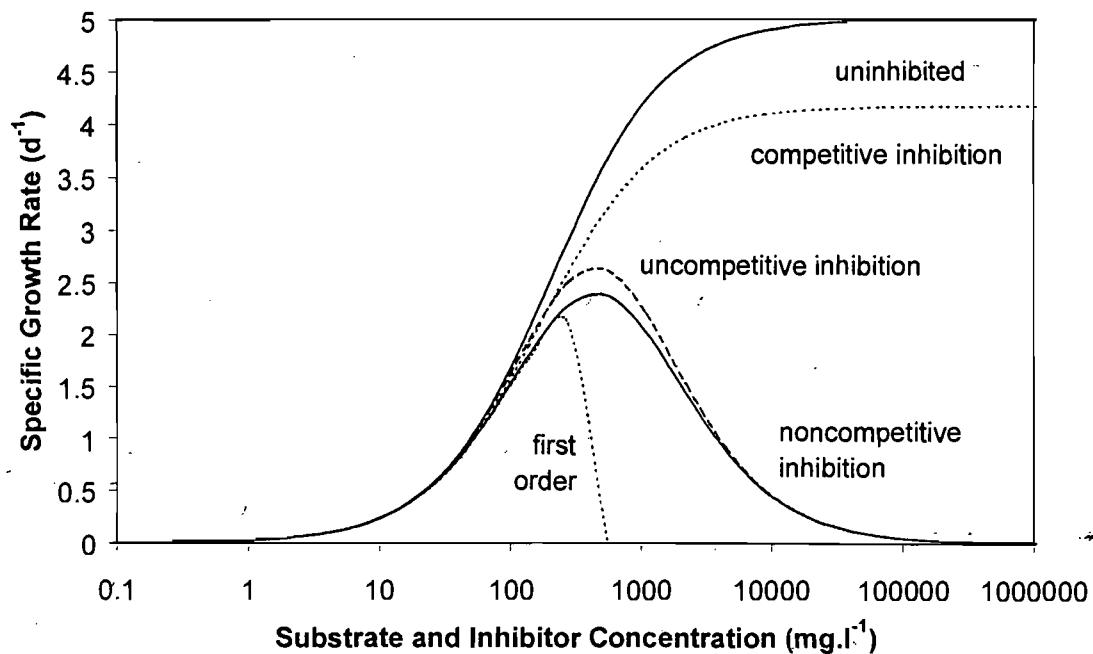


Figure A: The specific growth rate as predicted by the various inhibition models as a function of the substrate and inhibitor concentration, where the substrate is the inhibitor ($K_s = 200 \text{ mg.l}^{-1}$, $\mu_{\max} = 5 \text{ day}^{-1}$, $K_i = 1000 \text{ mg.l}^{-1}$)

Figure A illustrates that the uninhibited Monod equation predicts that the specific growth rate of the bacteria will equal the maximum specific growth rate of the bacteria at high substrate concentrations. For the competitive inhibition model, at high inhibitor concentrations, the specific growth rate becomes a constant fraction of the maximum specific growth rate. The behaviour of the uncompetitive and non-competitive inhibition models does not differ greatly at any inhibitor concentration. What is important is that both of these models will predict that the specific growth rate

will become zero at high inhibitor concentrations. Finally, the first order inhibition model will predict a reaction rate of zero at relatively low inhibitor concentrations.

The uncompetitive inhibition model has been used more regularly than the other inhibition models, especially for acetic acid inhibition of acetogenesis and methanogenesis. This equation has also been used for the inhibition of methanogenesis by undissociated ammonia, as well as the inhibition of acetogenesis and methanogenesis by undissociated hydrogen sulfide. The model predicts that the reaction rate will become 0 at high inhibitor concentrations, and these processes are the critical steps when anaerobic digestion systems fail.

Non-competitive inhibition models have been used less regularly, but show little difference from the uncompetitive inhibition models, and therefore the uncompetitive inhibition models are probably used.

The first order inhibition model gives a sharp decline in the reaction rate at high inhibitor concentrations. This would probably be the case with heavy metal concentrations, or undissociated hydrogen sulfide, where the bacteria are highly sensitive to the inhibitor. However, care should be taken in the model that inhibitor concentrations greater than the value of the inhibition constant are present in the system, as the rate of reaction would be predicted as being negative, and reactants would be generated from products, in the model. This is particularly important when more than one reaction is being inhibited, but the inhibition constants are different. For example, methanogens are more inhibited by undissociated hydrogen sulfide than the sulfate reducing bacteria. At high sulfide concentrations, the methanogenic reactions stop. However, the sulfate reducing reactions continue, because they are not yet completely inhibited. They are however producing more sulfides. When this concentration is greater than the methanogenic inhibition constant value, the rate of methanogenesis becomes negative in the model, and more complex substrates are generated from methane.

The choice of inhibition model therefore depends on the nature of the reaction with respect to the inhibitor.

APPENDIX B: RESULTS OF SENSITIVITY ANALYSIS

Table A: Results (absolute difference) of the sensitivity analysis performed on selected kinetic parameters from the model

Parameter	Old value	New value	Δ VSS (gVSS.m ⁻³)	Δ SO ₄ (gCOD.m ⁻³)	Δ COD _S (gCOD.m ⁻³)	Δ COD _P (gCOD.m ⁻³)	Δ CH ₄ (gCOD.m ⁻³)
$k_{h_{\text{protein}}}$ (d ⁻¹)	0.0375	0.375	1.91 10 ⁻⁴	3.63 10 ⁻²	1.49 10 ⁻¹	2.00 10 ⁻¹	7.13 10 ⁻⁹
$k_{h_{\text{protein}}}$ (d ⁻¹)	0.0375	0.00375	1.08 10 ⁻⁴	1.85 10 ⁻²	9.48 10 ⁻²	1.25 10 ⁻¹	3.64 10 ⁻⁸
$k_{h_{\text{cellulose}}}$ (d ⁻¹)	0.0525	0.525	1.11 10 ⁻⁴	2.28 10 ⁻²	9.23 10 ⁻²	1.26 10 ⁻¹	7.77 10 ⁻⁹
$k_{h_{\text{cellulose}}}$ (d ⁻¹)	0.0525	0.00525	9.08 10 ⁻⁵	1.63 10 ⁻²	7.76 10 ⁻²	1.04 10 ⁻¹	2.85 10 ⁻⁸
$k_{h_{\text{lipids}}}$ (d ⁻¹)	0.0425	0.425	5.02 10 ⁻⁴	4.87 10 ⁻²	8.41 10 ⁻²	1.42 10 ⁻¹	9.89 10 ⁻⁹
$k_{h_{\text{lipids}}}$ (d ⁻¹)	0.0425	0.00425	3.49 10 ⁻⁴	2.31 10 ⁻²	6.89 10 ⁻²	9.83 10 ⁻²	9.37 10 ⁻⁸
$\mu_{\text{max,as}}$ (d ⁻¹)	0.1275	1.275	2.80 10 ⁻⁷	7.01 10 ⁻²	7.36 10 ⁻²	0	9.88 10 ⁻⁹
$\mu_{\text{max,as}}$ (d ⁻¹)	0.1275	0.01275	3.62 10 ⁻⁷	1.45 10 ⁻⁴	2.17 10 ⁻⁴	0	6.47 10 ⁻⁹
$K_{S,\text{as}}$ (gCOD.m ⁻³)	24	240	7.25 10 ⁻⁷	1.09 10 ⁻⁴	1.45 10 ⁻⁴	0	1.44 10 ⁻⁹
$K_{S,\text{as}}$ (gCOD.m ⁻³)	24	2.4	1.09 10 ⁻⁶	7.25 10 ⁻⁵	3.62 10 ⁻⁵	0	2.61 10 ⁻¹⁰
Y_{as} (gVSS.gCOD ⁻¹)	0.041	0.41	1.81 10 ⁻⁶	1.09 10 ⁻⁴	1.09 10 ⁻⁴	0	4.68 10 ⁻⁹
Y_{as} (gVSS.gCOD ⁻¹)	0.041	0.0041	7.23 10 ⁻⁷	5.06 10 ⁻⁴	2.49 10 ⁻³	0	2.72 10 ⁻⁹
$K_{I,\text{as}}$ (g S.m ⁻³)	285	2850	3.19 10 ⁻⁴	9.64 10 ⁻²	1.08 10 ⁻¹	0	1.00 10 ⁻⁸
$K_{I,\text{as}}$ (g S.m ⁻³)	285	28.5	0	1.81 10 ⁻⁴	3.62 10 ⁻⁵	0	1.65 10 ⁻⁷
K_{S,SO_4} (gCOD.m ⁻³)	19.2	192	1.09 10 ⁻⁶	3.62 10 ⁻⁵	2.17 10 ⁻⁴	0	-3.62 10 ⁻¹¹
K_{S,SO_4} (gCOD.m ⁻³)	19.2	1.92	1.09 10 ⁻⁶	0	3.62 10 ⁻⁵	0	-6.52 10 ⁻¹¹

Table B: Results (absolute difference) of the sensitivity analysis performed on selected operational parameters from the model

Parameter	Old value	New value	Δ VSS (gVSS.m ⁻³)	Δ SO ₄ (gCOD.m ⁻³)	Δ COD _S (gCOD.m ⁻³)	Δ COD _p (gCOD.m ⁻³)	Δ CH ₄ (gCOD.m ⁻³)
feed COD	3400	3740	5.99 10 ⁻⁵	8.17 10 ⁻³	3.02 10 ⁻²	5.27 10 ⁻²	2.45 10 ⁻⁹
feed COD	3400	3060	7.41 10 ⁻⁵	9.47 10 ⁻³	3.72 10 ⁻²	6.44 10 ⁻²	2.29 10 ⁻⁸
feed SO ₄	1700	1870	1.09 10 ⁻⁶	1.81 10 ⁻⁴	7.25 10 ⁻⁵	0	3.62 10 ⁻¹¹
feed SO ₄	1700	1530	3.62 10 ⁻⁷	3.62 10 ⁻⁵	3.62 10 ⁻⁵	0	1.81 10 ⁻¹¹
xC ₁	0.467	0.5137	1.4910 ⁻⁴	2.02 10 ⁻²	5.83 10 ⁻²	8.54 10 ⁻²	8.41 10 ⁻⁹
xC ₁	0.467	0.4203	1.20 10 ⁻⁴	1.60 10 ⁻²	4.26 10 ⁻²	6.38 10 ⁻²	9.72 10 ⁻⁹
xC ₂	0.1	0.11	3.28 10 ⁻⁵	3.24 10 ⁻³	8.86 10 ⁻³	5.76 10 ⁻³	9.61 10 ⁻⁹
xC ₂	0.1	0.9	3.03 10 ⁻⁵	3.10 10 ⁻³	8.75 10 ⁻³	5.47 10 ⁻³	5.15 10 ⁻⁹
xC ₃	0.37	0.407	1.70 10 ⁻⁵	2.18 10 ⁻³	6.13 10 ⁻³	8.70 10 ⁻³	4.35 10 ⁻⁹
xC ₃	0.37	0.333	1.63 10 ⁻⁵	2.14 10 ⁻³	6.19 10 ⁻³	9.05 10 ⁻³	4.02 10 ⁻¹⁰
xC ₄	0.31	0.341	8.34 10 ⁻⁶	1.27 10 ⁻³	3.33 10 ⁻³	4.71 10 ⁻³	3.27 10 ⁻⁸
xC ₄	0.31	0.279	9.05 10 ⁻⁶	9.41 10 ⁻⁴	3.22 10 ⁻³	5.07 10 ⁻³	1.48 10 ⁻⁹

APPENDIX C: AQUASIM CODE AND USER TIPS

The kinetic model described in the body of the report is possibly the basis for a more rigorous and complex model. By including the aquatic chemistry and mass transfer between the liquid phase and the vapour phase, the predictability of the model can be improved. The present project is complete, and this appendix is a guide to anyone who might want to run further simulations using the present model, or to use the model as a starting point for a more complex model. The procedure to get AQUASIM to the point where simulations are possible is given, as well as the computer code used in the model.

To reiterate from Section 4, AQUASIM is able to simultaneously integrate a number of differential equations. Once these equations have been defined, the system being modelled has to be divided into a number of compartments, using the predefined compartments in AQUASIM. These compartments allow for the calculation of spatial variations within a compartment. These compartments are then linked with either diffusive or advective links, and the advective links can be either with the water flow, or as a mass flux superimposed on the liquid flow.

The first task in setting up the model in AQUASIM is to define all the variables in the model. Variables can be defined as state variables, constant variables, program variables, real list variable and variable list variables. For the model, only state variables and constant variables were used.

State variables refer to the concentrations of the various components that are dependent on the state of the system. These values will change during the simulation, and are the model outputs in which we are interested. All concentrations need to be defined as state variables, which include the substrate, product and biomass concentrations.

Constant variables are used to define the values of the kinetic constants in the system. The variable name, description, value, and units are required.

The state variables should be included first, followed by the constant variables.

The processes taking place in the system then need to be defined. AQUASIM gives a choice between a dynamic process and an equilibrium process. The equilibrium

process in AQUASIM doesn't seem to work, and the calculation of equilibrium concentrations required that the forward and reverse reaction be defined as dynamic processes with very high reaction rates, with the ratio of their rates equal to the equilibrium constant. This is explained in Section 5.4 of the report.

For the dynamic processes, the inclusion of the reaction rates is similar to a spreadsheet equation, in that it has to be written in one line, without spaces. Hint: write out the equation on a piece of paper first, in a straight line, as required in AQUASIM, so you know where to add in the brackets, etc. AQUASIM will not tell you where the problem is as Excel does. It will just not accept the equation.

The stoichiometry is then defined by choosing the variable from the list, and giving a negative number for a reactant, a positive number for a product. Make sure your stoichiometry is in the correct units.

In the model, use was made of a mixed reactor compartment only. This is a CSTR. AQUASIM needs the user to define the processes taking place in the reactor. You also need to define what variables you want AQUASIM to calculate for that reactor. To do this, choose the mixed reactor compartment as the new compartment, then go to the variables section. Highlight all the variables in the right hand column that you want to be active in that reactor, and press the activate button. You will only be able to activate state variables and program variables.

The next step is to activate the processes that will take place. The same procedure that was used to activate the variables will be required for the processes.

Initial conditions will need to be stated. For a model calculating steady state, these choices are arbitrary. However, a value of greater than 0 needs to be defined for all bacteria species, since these are not present in the feed, and will only be produced if already present, since they catalyse their own growth.

Finally, inputs to the system have to be defined. The water flow required is equal to the feed to the system for the first compartment to the system, but is 0 for the rest of the compartments. These inputs only enter the first compartment in the system, since this is the only feed point. Once the compartment has been defined, duplicates of the compartment, excluding the inputs, will allow for the total 9 compartments to be defined.

To connect the flow of water and sludge between the various compartments, advective and diffusive links can be used. For the model, only advective links were used. Diffusive links refer to mass transfer across a boundary layer. The advective

link refers to water flows, and these represent the flow of water between the compartments. The first link is between the first and second compartments. This is defined simply by choosing compartment 1 as the 'from compart.', while compartment 2 is the 'to compart.'.

Then, to define the flow of water to the valley compartment below, a bifurcation is added. The bifurcation requires that the end compartment be defined, as well as the flow rate. For the first link, the compartment will be compartment 7, while the flow rate is defined as $2/3$ of the recycle rate leaving compartment 7. This will then mean that the flow of water through compartment 7 will be given by the flow of recycle from compartment 7.

To superimpose the settling effects of the solids on the liquid flow, a second bifurcation is added. However, instead of choosing the flux to be with the water flow, it is now defined. The flux of each of the biomass species as well as all the particulate components needs to be defined individually. To add a component, the correct component needs to be chosen, and then the fraction that will settle needs to be defined. In the model, the output of each of the compartments was calculated as a formula variable. A second constant variable was defined, which referred to the fraction of the particulates leaving the above compartment that would settle. This constant had a value of less than 1, and was changed in order to calibrate the model. The total flux of the chosen component is then given as the product of the concentration of the component times the total discharge from the above compartment times the fraction. This is included for all components that will settle.

However, these bifurcation differ between the compartments, allowing for the correct prediction of the particulates in the various compartments.

Once the system has been set up, a dynamic simulation is performed, until steady state is achieved. By increasing the size of the steps of the simulation, the file will be smaller, since less data points will be recorded. This will not effect the results of the simulation. The current model takes about 15 minutes to reach steady state.

To check for steady state, a plot of all the state variables needs to be made. AQUASIM will then plot these values to the screen. If you want to print the graph, you have to list the values to a file, and then open the file in Excel. The data will be given in a number of columns, and by deleting the empty columns, the plot can be made. However, the steady state values were the only important ones for this project, so an example of this plot is not shown here.

To represent the trends from a number of simulations, the data will need to be imported into Excel.

When saving the file, you have to decide if you have more space or time. If space is limited, do not save the calculated states. If time is limiting, save the calculated states.

The computer code that makes up the rest of this appendix is for the model used in the calibration step. The feed pump is set at $14.64 \text{ m}^3 \cdot \text{d}^{-1}$, the recycle pump is set at $48 \text{ m}^3 \cdot \text{d}^{-1}$, and the COD: SO_4 ratio is 2 (HRT = 1.57; SRR = 3.8; COD: $\text{SO}_4^{2-} = 2$). This is the model that formed the basis of the simulations performed for Chapters 6 and 7. For the simulation, the step size was 10, and the number of steps was 30. This did not influence the output of the model, but required less space to save the file than if more steps were calculated. The numerical parameters were left as their default setting, since this once again made no difference to the outcome of the simulations.

The output graphs of importance to this dissertation are the concentrations of all the species leaving the system and the total COD in each of the three valleys. Therefore, these output graphs have been plotted here.

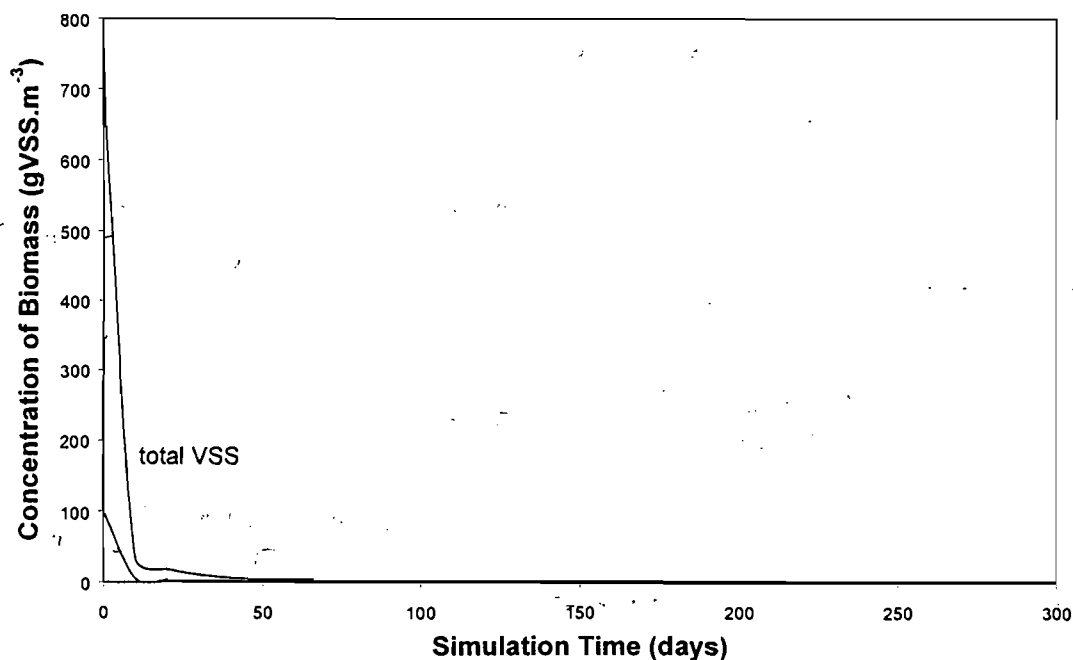


Figure B: AQUASIM simulation output for the total biomass and all individual biomass species concentrations as the system reaches steady state.

AQUASIM allows for the small values to be read off the graph
(HRT = 1.57; SRR = 3.8; COD: $\text{SO}_4^{2-} = 2$)

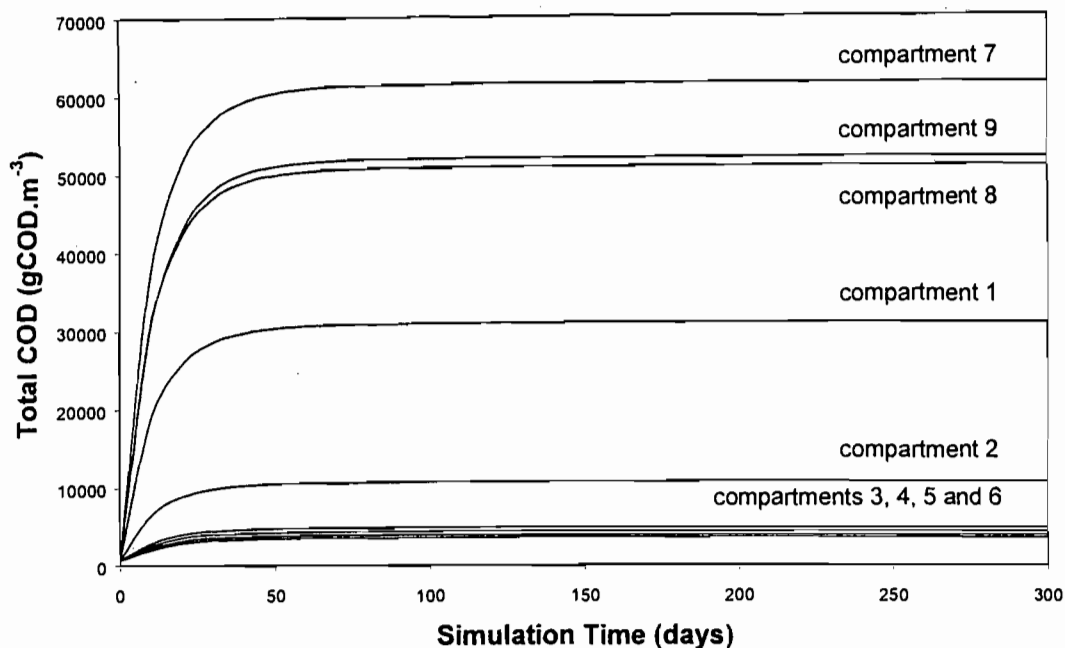


Figure C: AQUASIM simulation output for the total COD in each compartment as the system reaches steady state. AQUASIM allows for the small values to be read off the graph (HRT = 1.57; SRR = 3.8; COD: SO₄²⁻ = 2)

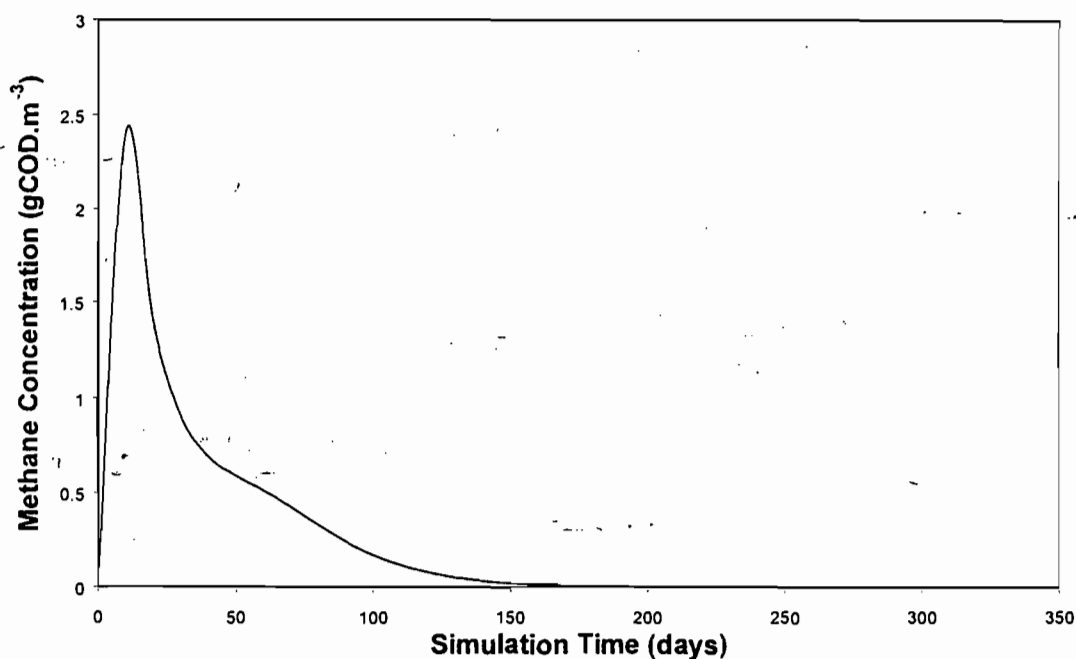


Figure D: AQUASIM simulation output for the methane concentration in the effluent stream as the system reaches steady state. AQUASIM allows for the small values to be read off the graph (HRT = 1.57; SRR = 3.8; COD: SO₄²⁻ = 2)

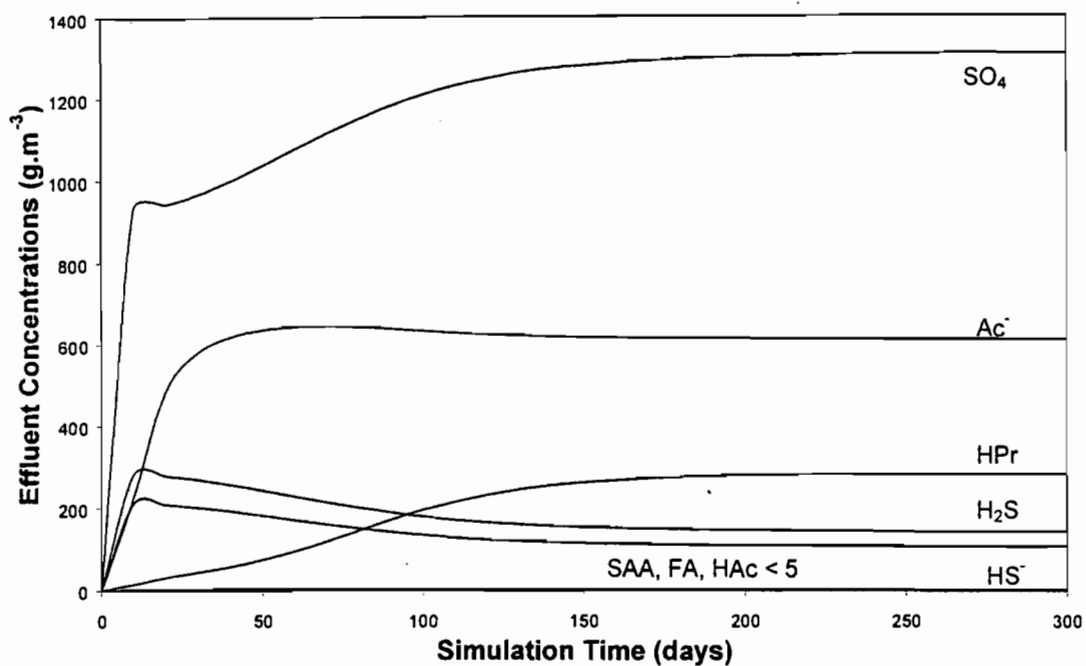


Figure E: AQUASIM simulation output for the effluent concentrations of all soluble organic substrates and sulfate and sulfide concentrations as the system reaches steady state. AQUASIM allows for the small values to be read off the graph (HRT = 1.57; SRR = 3.8; COD: $\text{SO}_4^{2-} = 2$)

 AQUASIM Version 2.0gamma (win/mfc) - Listing of System Definition

 Variables

Ac:	Description:	acetate concentration
	Type:	Dyn. Volume State Var.
	Unit:	gCOD/m ³
	Relative Accuracy:	1e-006
	Absolute Accuracy:	1e-006

Ca:	Description:	acetogenesis biomass
	Type:	Dyn. Volume State Var.
	Unit:	gVSS/m ³
	Relative Accuracy:	1e-006
	Absolute Accuracy:	1e-006

Cam:	Description:	acetoclastic methanogenesis biomass
	Type:	Dyn. Volume State Var.
	Unit:	gVSS/m ³
	Relative Accuracy:	1e-006
	Absolute Accuracy:	1e-006

Cas:	Description:	acetoclastic sulfidogenesis biomass aSRB
	Type:	Dyn. Volume State Var.
	Unit:	gVSS/m ³
	Relative Accuracy:	1e-006
	Absolute Accuracy:	1e-006

cellulose:	Description:	cellulose fraction of particulate C OD
	Type:	Dyn. Volume State Var.
	Unit:	gCOD/m ³
	Relative Accuracy:	1e-006
	Absolute Accuracy:	1e-006

cellulosefeed:	Description:	total cellulose COD in feed stream to bioreactor
	Type:	Formula Variable
	Unit:	gCOD/m ³
	Expression:	0.199*feedCOD

Cf:	Description:	fermentation biomass
	Type:	Dyn. Volume State Var.
	Unit:	gVSS/m ³
	Relative Accuracy:	1e-006
	Absolute Accuracy:	1e-006

CH4:	Description:	methane gas concentration
	Type:	Dyn. Volume State Var.
	Unit:	gCOD/m ³
	Relative Accuracy:	1e-006
	Absolute Accuracy:	1e-006

Chm:	Description:	hydrogenotrophic methanogenesis bio mass
	Type:	Dyn. Volume State Var.
	Unit:	gVSS/m ³

	Relative Accuracy:	1e-006
	Absolute Accuracy:	1e-006

Chs:	Description:	hydrogenotrophic sulfidogenesis bio mass hSRB
	Type:	Dyn. Volume State Var.
	Unit:	gVSS/m ³
	Relative Accuracy:	1e-006
	Absolute Accuracy:	1e-006

Co:	Description:	anaerobic oxidation biomass
	Type:	Dyn. Volume State Var.
	Unit:	gVSS/m ³
	Relative Accuracy:	1e-006
	Absolute Accuracy:	1e-006

CODt:	Description:	total COD in reactor
	Type:	Formula Variable
	Unit:	gCOD/m ³
	Expression:	inert+cellulose+protein+FA+H2+Ac+HP r+SAA+lipids+Ca+Cam+Cas+Cf+Chm+Chs+ Co+HS

Cps:	Description:	acetogenic sulfidogenic biomass
	Type:	Dyn. Volume State Var.
	Unit:	gVSS/m ³
	Relative Accuracy:	1e-006
	Absolute Accuracy:	1e-006

F:	Description:	flow rate of feed stream
	Type:	Constant Variable
	Unit:	m ³ /day
	Value:	14.64
	Standard Deviation:	1
	Minimum:	0
	Maximum:	20
	Sensitivity Analysis:	inactive
	Parameter Estimation:	inactive

FA:	Description:	fatty acid concentration
	Type:	Dyn. Volume State Var.
	Unit:	gCOD/m ³
	Relative Accuracy:	1e-006
	Absolute Accuracy:	1e-006

feedCOD:	Description:	total COD in feed stream to bioreac tor
	Type:	Constant Variable
	Unit:	gCOD/m ³
	Value:	3400
	Standard Deviation:	1
	Minimum:	0
	Maximum:	4000
	Sensitivity Analysis:	inactive
	Parameter Estimation:	inactive

H2:	Description:	hydrogen concentration
	Type:	Dyn. Volume State Var.
	Unit:	gCOD/m ³
	Relative Accuracy:	1e-006
	Absolute Accuracy:	1e-006

H2S:	Description:	undissociated hydrogen sulfide concentration
	Type:	Dyn. Volume State Var.
	Unit:	g S/m ³
	Relative Accuracy:	1e-006
	Absolute Accuracy:	1e-006
HAc:	Description:	Undissociated acetic acid
	Type:	Dyn. Volume State Var.
	Unit:	gCOD/m ³
	Relative Accuracy:	1e-006
	Absolute Accuracy:	1e-006
HAcfeed:	Description:	total HAc COD in feed stream to bio reactor
	Type:	Formula Variable
	Unit:	gCOD/m ³
	Expression:	0.025*feedCOD
HPr:	Description:	volatile fatty acids
	Type:	Dyn. Volume State Var.
	Unit:	gCOD/m ³
	Relative Accuracy:	1e-006
	Absolute Accuracy:	1e-006
HPrfeed:	Description:	total HPr COD in feed stream to bio reactor
	Type:	Formula Variable
	Unit:	gCOD/m ³
	Expression:	0.025*feedCOD
HS:	Description:	dissolved undissociated sulfide concentration
	Type:	Dyn. Volume State Var.
	Unit:	gCOD/m ³
	Relative Accuracy:	1e-006
	Absolute Accuracy:	1e-006
inert:	Description:	inert fraction of particulate COD
	Type:	Dyn. Volume State Var.
	Unit:	gCOD/m ³
	Relative Accuracy:	1e-006
	Absolute Accuracy:	1e-006
inertfeed:	Description:	total inert COD in feed stream to bio reactor
	Type:	Formula Variable
	Unit:	gCOD/m ³
	Expression:	0.254*feedCOD
Khcellulose:	Description:	hydrolysis rate constant for proteins
	Type:	Constant Variable
	Unit:	1/day
	Value:	0.0525
	Standard Deviation:	1
	Minimum:	0
	Maximum:	10
	Sensitivity Analysis:	active
	Parameter Estimation:	inactive

Parameter Estimation: inactive

KIf:	Description:	fermentation inhibition constant
	Type:	Constant Variable
	Unit:	gCOD/m ³
	Value:	550
	Standard Deviation:	1
	Minimum:	0
	Maximum:	600
	Sensitivity Analysis:	active
	Parameter Estimation:	inactive
Kif:	Description:	acetate inhibition constant for fermentation
	Type:	Constant Variable
	Unit:	gCOD/m ³
	Value:	180
	Standard Deviation:	1
	Minimum:	0
	Maximum:	700
	Sensitivity Analysis:	active
	Parameter Estimation:	inactive
KIhm:	Description:	methanogenesis inhibition constant
	Type:	Constant Variable
	Unit:	gCOD/m ³
	Value:	215
	Standard Deviation:	1
	Minimum:	0
	Maximum:	300
	Sensitivity Analysis:	active
	Parameter Estimation:	inactive
KIhs:	Description:	sulfidogenesis inhibition constant
	Type:	Constant Variable
	Unit:	gCOD/m ³
	Value:	550
	Standard Deviation:	1
	Minimum:	0
	Maximum:	600
	Sensitivity Analysis:	active
	Parameter Estimation:	inactive
KIo:	Description:	anaerobic oxidation inhibition constant
	Type:	Constant Variable
	Unit:	gCOD/m ³
	Value:	550
	Standard Deviation:	1
	Minimum:	0
	Maximum:	600
	Sensitivity Analysis:	active
	Parameter Estimation:	inactive
KIps:	Description:	acetogenic sulfidogenesis inhibition constant
	Type:	Constant Variable
	Unit:	gCOD/m ³
	Value:	285
	Standard Deviation:	1
	Minimum:	0

	Maximum:	300
	Sensitivity Analysis:	active
	Parameter Estimation:	inactive

Ksa:	Description:	acetogenesis half saturation constant
	Type:	Constant Variable
	Unit:	gCOD/m ³
	Value:	247
	Standard Deviation:	1
	Minimum:	0
	Maximum:	300
	Sensitivity Analysis:	active
	Parameter Estimation:	inactive

Ksam:	Description:	methanogenesis half saturation constant
	Type:	Constant Variable
	Unit:	gCOD/m ³
	Value:	56
	Standard Deviation:	1
	Minimum:	0
	Maximum:	100
	Sensitivity Analysis:	active
	Parameter Estimation:	inactive

Ksas:	Description:	sulfidogenesis half saturation constant
	Type:	Constant Variable
	Unit:	gCOD/m ³
	Value:	24
	Standard Deviation:	1
	Minimum:	0
	Maximum:	100
	Sensitivity Analysis:	active
	Parameter Estimation:	inactive

Ksasso4:	Description:	sulfidogenesis half saturation constant
	Type:	Constant Variable
	Unit:	gCOD/m ³
	Value:	19.2
	Standard Deviation:	1
	Minimum:	0
	Maximum:	20
	Sensitivity Analysis:	active
	Parameter Estimation:	inactive

Ksf:	Description:	fermentation half saturation constant
	Type:	Constant Variable
	Unit:	gCOD/m ³
	Value:	28
	Standard Deviation:	1
	Minimum:	0
	Maximum:	30
	Sensitivity Analysis:	active
	Parameter Estimation:	inactive

Kshm:	Description:	methanogenesis half saturation constant

Type: Constant Variable
 Unit: gCOD/m³
 Value: 0.13
 Standard Deviation: 1
 Minimum: 0
 Maximum: 1
 Sensitivity Analysis: active
 Parameter Estimation: inactive

Kshs: Description: sulfidogenesis half saturation constant
 Type: Constant Variable
 Unit: gCOD/m³
 Value: 0.05
 Standard Deviation: 1
 Minimum: 0
 Maximum: 1
 Sensitivity Analysis: active
 Parameter Estimation: inactive

Kshso4: Description: sulfidogenesis half saturation constant
 Type: Constant Variable
 Unit: gCOD/m³
 Value: 0.9
 Standard Deviation: 1
 Minimum: 0
 Maximum: 1
 Sensitivity Analysis: active
 Parameter Estimation: inactive

Kso: Description: fermentation half saturation constant
 Type: Constant Variable
 Unit: gCOD/m³
 Value: 1.816
 Standard Deviation: 1
 Minimum: 0
 Maximum: 2000
 Sensitivity Analysis: active
 Parameter Estimation: inactive

Ksps: Description: acetogenic sulfidogenesis half saturation constant
 Type: Constant Variable
 Unit: gCOD/m³
 Value: 295
 Standard Deviation: 1
 Minimum: 0
 Maximum: 300
 Sensitivity Analysis: active
 Parameter Estimation: inactive

Kspso4: Description: acetogenic sulfidogenesis half saturation constant
 Type: Constant Variable
 Unit: gCOD/m³
 Value: 7.4
 Standard Deviation: 1
 Minimum: 0
 Maximum: 20

Sensitivity Analysis: active
Parameter Estimation: inactive

lipids:	Description:	lipid fraction of particulate COD
	Type:	Dyn. Volume State Var.
	Unit:	
	Relative Accuracy:	1e-006
	Absolute Accuracy:	1e-006
lipid_feed:	Description:	total lipid COD in feed stream to bioreactor
	Type:	Formula Variable
	Unit:	gCOD/m ³
	Expression:	0.21*feedCOD
PH2S:	Description:	partial pressure of H2S above reactor
	Type:	Formula Variable
	Unit:	atm
	Expression:	0.0002*H2S
protein:	Description:	protein fraction of particulate COD
	Type:	Dyn. Volume State Var.
	Unit:	gCOD/m ³
	Relative Accuracy:	1e-006
	Absolute Accuracy:	1e-006
proteinfeed:	Description:	total lipid COD in feed stream to bioreactor
	Type:	Formula Variable
	Unit:	gCOD/m ³
	Expression:	0.287*feedCOD
Q:	Description:	discharge from reactors
	Type:	Program Variable
	Unit:	m ³ /d
	Reference to:	Discharge
R1:	Description:	recycle from valley 1
	Type:	Formula Variable
	Unit:	m ³ /day
	Expression:	0.6*Rtotal
R2:	Description:	recycle from valley 2
	Type:	Formula Variable
	Unit:	m ³ /day
	Expression:	0.3*Rtotal
R3:	Description:	recycle from valley 3
	Type:	Formula Variable
	Unit:	m ³ /day
	Expression:	0.1*Rtotal
Rtotal:	Description:	total recycle flow rate
	Type:	Constant Variable
	Unit:	m ³ /day
	Value:	48
	Standard Deviation:	1
	Minimum:	0
	Maximum:	50

	Type:	Constant Variable
	Unit:	l/day
	Value:	2
	Standard Deviation:	1
	Minimum:	0
	Maximum:	100
	Sensitivity Analysis:	active
	Parameter Estimation:	inactive

umaxhm:	Description:	maximum substrate utilisation rate for methanogenesis
	Type:	Constant Variable
	Unit:	l/day
	Value:	0.25
	Standard Deviation:	1
	Minimum:	0
	Maximum:	100
	Sensitivity Analysis:	active
	Parameter Estimation:	inactive

umaxhs:	Description:	maximum substrate utilisation rate for sulfidogenesis
	Type:	Constant Variable
	Unit:	l/day
	Value:	1.25
	Standard Deviation:	1
	Minimum:	0
	Maximum:	10
	Sensitivity Analysis:	active
	Parameter Estimation:	inactive

umaxo:	Description:	maximum substrate utilisation rate for anaerobic oxidation
	Type:	Constant Variable
	Unit:	l/day
	Value:	0.1375
	Standard Deviation:	1
	Minimum:	0
	Maximum:	1
	Sensitivity Analysis:	active
	Parameter Estimation:	inactive

umaxps:	Description:	maximum substrate utilisation rate for acetogenic sulfidogenesis
	Type:	Constant Variable
	Unit:	l/day
	Value:	0.2025
	Standard Deviation:	1
	Minimum:	0
	Maximum:	30
	Sensitivity Analysis:	active
	Parameter Estimation:	inactive

VFAt:	Description:	total titrateable fatty acids
	Type:	Formula Variable
	Unit:	gCOD/m ³
	Expression:	Ac+HPr+FA+HS

VSSt:	Description:	total VSS in reactor
	Type:	Formula Variable
	Unit:	gVSS/m ³

	Expression:	Ca+Cam+Cas+Cf+Chm+Chs+Co
xCl:	Description:	fraction of biomass settled from reactor 1
	Type:	Constant Variable
	Unit:	
	Value:	0.467
	Standard Deviation:	1
	Minimum:	0
	Maximum:	1
	Sensitivity Analysis:	inactive
	Parameter Estimation:	inactive
xC2:	Description:	fraction of biomass settled from reactor 1
	Type:	Constant Variable
	Unit:	
	Value:	0.1
	Standard Deviation:	1
	Minimum:	0
	Maximum:	1
	Sensitivity Analysis:	inactive
	Parameter Estimation:	inactive
xC3:	Description:	fraction of biomass settled from reactor 1
	Type:	Constant Variable
	Unit:	
	Value:	0.37
	Standard Deviation:	1
	Minimum:	0
	Maximum:	1
	Sensitivity Analysis:	inactive
	Parameter Estimation:	inactive
xC4:	Description:	fraction of biomass settled from reactor 1
	Type:	Constant Variable
	Unit:	
	Value:	0.31
	Standard Deviation:	1
	Minimum:	0
	Maximum:	1
	Sensitivity Analysis:	inactive
	Parameter Estimation:	inactive
Ya:	Description:	acetogenesis yield coefficient
	Type:	Constant Variable
	Unit:	gVSS/gCOD
	Value:	0.018
	Standard Deviation:	1
	Minimum:	0
	Maximum:	10
	Sensitivity Analysis:	active
	Parameter Estimation:	inactive
Yam:	Description:	methanogenesis yield coefficient
	Type:	Constant Variable
	Unit:	gVSS/gCOD
	Value:	0.026
	Standard Deviation:	1

Minimum: 0
 Maximum: 10
 Sensitivity Analysis: active
 Parameter Estimation: inactive

Yas: Description: sulfidogenesis yield coefficient
 Type: Constant Variable
 Unit: gVSS/gCOD
 Value: 0.041
 Standard Deviation: 1
 Minimum: 0
 Maximum: 1
 Sensitivity Analysis: active
 Parameter Estimation: inactive

Yf: Description: fermentation yield coefficient
 Type: Constant Variable
 Unit: gVSS/gCOD
 Value: 0.043
 Standard Deviation: 1
 Minimum: 0
 Maximum: 10
 Sensitivity Analysis: active
 Parameter Estimation: inactive

Yhm: Description: methanogenesis yield coefficient
 Type: Constant Variable
 Unit: gVSS/gCOD
 Value: 0.018
 Standard Deviation: 1
 Minimum: 0
 Maximum: 10
 Sensitivity Analysis: active
 Parameter Estimation: inactive

Yhs: Description: sulfidogenesis yield coefficient
 Type: Constant Variable
 Unit: gVSS/gCOD
 Value: 0.077
 Standard Deviation: 1
 Minimum: 0
 Maximum: 1
 Sensitivity Analysis: active
 Parameter Estimation: inactive

Yo: Description: anaerobic digestion yield coefficient
 Type: Constant Variable
 Unit: gVSS/gCOD
 Value: 0.11
 Standard Deviation: 1
 Minimum: 0
 Maximum: 10
 Sensitivity Analysis: active
 Parameter Estimation: inactive

Yps: Description: acetogenic sulfidogenesis yield coefficient
 Type: Constant Variable
 Unit: gVSS/gCOD
 Value: 0.035

Standard Deviation: 1
Minimum: 0
Maximum: 10
Sensitivity Analysis: active
Parameter Estimation: inactive

```

*****
Processes
*****
acetogenesis:  Description:      HPr + 2H2O = HAc + 3H2 + HCO3
                Type:           Dynamic Process
                Rate:           ((umaxa*Ca*HPr)/(Ya*(HPr+(Ksa*(1+(H
                                Ac/Kia))))))*(1-(H2S/KIa))

                Stoichiometry:
                Variable : Stoichiometric Coefficient
                HPr : -7
                Ac : 4
                H2 : 3
-----
acetogenic_sulfidogenesis:
                Description:      4HPr + 3SO4 = 4HAc + 3HS
                Type:           Dynamic Process
                Rate:           (umaxps*HPr*SO4*Cps/(Yps*(Ksps+HPr)
                                *(KspssO4+SO4)))*(1-(H2S/KIps))

                Stoichiometry:
                Variable : Stoichiometric Coefficient
                SO4 : -288
                HS : 186
                HPr : -448
                Ac : 256
-----
acetogenic_sulfidogrow:
                Description:      4HPr + 3SO4 = biomass
                Type:           Dynamic Process
                Rate:           (umaxps*HPr*SO4*Cps/((Ksps+HPr)*(Ks
                                pssO4+SO4)))*(1-(H2S/KIps))

                Stoichiometry:
                Variable : Stoichiometric Coefficient
                SO4 : -1/Yps
                HPr : -1/Yps
                Cps : 1
-----
acetogrow:     Description:      HPr = acetogens
                Type:           Dynamic Process
                Rate:           ((umaxa*Ca*HPr)/(HPr+(Ksa*(1+(HAc/K
                                ia))))))*(1-(H2S/KIa))

                Stoichiometry:
                Variable : Stoichiometric Coefficient
                HPr : -1/Ya
                Ca : 1
-----
Ac_HAc:        Description:      Acetate association
                Type:           Dynamic Process
                Rate:           57.3066*Ac

                Stoichiometry:
                Variable : Stoichiometric Coefficient
                Ac : -1
                HAc : 1
-----
aMethanogenesis:
                Description:      HAc + H2O = CH4 + HCO3
                Type:           Dynamic Process
                Rate:           (umaxam*Cam/(Yam*(1+(Ksam/Ac))))*(1
                                -(H2S/KIam))

                Stoichiometry:
                Variable : Stoichiometric Coefficient
                Ac : -1

```

CH4 : 1

aMethanogrow: Description: HAc = aMPB
 Type: Dynamic Process
 Rate: $(umaxam*Cam/(1+(Ksam/Ac))) * (1 - (H2S/KIam))$
 Stoichiometry:
 Variable : Stoichiometric Coefficient
 Ac : -1/Yam
 Cam : 1

aSulfidogenesis: Description: HAc + SO4 = HS + H2O
 Type: Dynamic Process
 Rate: $((umaxas*Ac*SO4*Cas)/(Yas*(Ksas+Ac)) * (Ksasso4+SO4)) * (1 - (H2S/KIas))$
 Stoichiometry:
 Variable : Stoichiometric Coefficient
 SO4 : -96
 Ac : -64
 HS : 62

aSulfidogrow: Description: HAc = aSRB
 Type: Dynamic Process
 Rate: $((umaxas*Ac*SO4*Cas)/((Ksas+Ac)*(Ksasso4+SO4))) * (1 - (H2S/KIas))$
 Stoichiometry:
 Variable : Stoichiometric Coefficient
 Ac : -1/Yas
 Cas : 1
 SO4 : -1/Yas

cellulosehydrolysis: Description: cellulose = sugars
 Type: Dynamic Process
 Rate: Khcellulose*cellulose
 Stoichiometry:
 Variable : Stoichiometric Coefficient
 cellulose : -1
 SAA : 1

fermengrow: Description: soluble COD = fermentation biomass
 Type: Dynamic Process
 Rate: $(umaxf*Cf*SAA/((SAA+Ksf)*(1+(HAc/Kif)))) * (1 - (H2S/KIf))$
 Stoichiometry:
 Variable : Stoichiometric Coefficient
 SAA : -1/Yf
 Cf : 1

fermentation: Description: sugars, amino acids = acetate + propionate + hydrogen
 Type: Dynamic Process
 Rate: $(umaxf*Cf*SAA/(Yf*(SAA+Ksf)*(1+(HAc/Kif)))) * (1 - (H2S/KIf))$
 Stoichiometry:
 Variable : Stoichiometric Coefficient
 SAA : -66
 Ac : 35
 HPr : 20
 H2 : 11

```

-----
H2S_HS:      Description:      H2S dissociation
              Type:           Dynamic Process
              Rate:           10000*H2S
              Stoichiometry:
                Variable : Stoichiometric Coefficient
                H2S : -1
                HS : 1
-----

HAc_Ac:      Description:      Acetic acid dissociation
              Type:           Dynamic Process
              Rate:           10000*HAc
              Stoichiometry:
                Variable : Stoichiometric Coefficient
                Ac : 1
                HAc : -1
-----

hMethanogenesis:
              Description:      4H2 + HCO3 = CH4 + 3H2O
              Type:           Dynamic Process
              Rate:           (umaxhm*Chm/(Yhm*(1+(Kshm/H2))))*(1
                              -(H2S/KIhm))
              Stoichiometry:
                Variable : Stoichiometric Coefficient
                CH4 : 1
                H2 : -1
-----

hMethanogrow:
              Description:      H2 = hMPB
              Type:           Dynamic Process
              Rate:           (umaxhm*Chm/(1+(Kshm/H2)))*(1-(H2S/
                              KIhm))
              Stoichiometry:
                Variable : Stoichiometric Coefficient
                H2 : -1/Yhm
                Chm : 1
-----

hSulfidogenesis:
              Description:      4H2+ SO4 = HS + 4H2O
              Type:           Dynamic Process
              Rate:           (umaxhs*H2*SO4*Chs/(Yhs*(Kshs+H2))*(
                              Kshsso4+SO4))*(1-(H2S/KIhs))
              Stoichiometry:
                Variable : Stoichiometric Coefficient
                SO4 : -96
                H2 : -48
                HS : 62
-----

hSulfidogrow:
              Description:      H2 = aSRB
              Type:           Dynamic Process
              Rate:           (umaxhs*H2*SO4*Chs/((Kshs+H2)*(Kshs
                              _so4+SO4)))*(1-(H2S/KIhs))
              Stoichiometry:
                Variable : Stoichiometric Coefficient
                Chs : 1
                H2 : -1/Yhs
                SO4 : -1/Yhs
-----

HS_H2S:      Description:      HS association
              Type:           Dynamic Process
              Rate:           13333.3*HS
              Stoichiometry:

```

Variable : Stoichiometric Coefficient
 H2S : 1
 HS : -1

 lipidhydrolysis:

Description: lipids = fatty acids
 Type: Dynamic Process
 Rate: $K_{hlipids} * lipids$
 Stoichiometry:
 Variable : Stoichiometric Coefficient
 lipids : -1
 FA : 1

 oxidation: Description: fatty acids = acetate + hydrogen
 Type: Dynamic Process
 Rate: $(u_{maxo} * C_o / (Y_o * (1 + (K_{so}/FA)))) * (1 - (H_2S/K_{Io}))$
 Stoichiometry:
 Variable : Stoichiometric Coefficient
 FA : -34
 Ac : 23
 H2 : 11

 oxidationgrow: Description: fatty acids = oxidation biomass
 Type: Dynamic Process
 Rate: $(u_{maxo} * C_o / (1 + (K_{so}/FA))) * (1 - (H_2S/K_{Io}))$
 Stoichiometry:
 Variable : Stoichiometric Coefficient
 FA : -1/ Y_o
 Co : 1

 proteinhydrolysis:

Description: proteins = amino acids
 Type: Dynamic Process
 Rate: $K_{hprotein} * protein$
 Stoichiometry:
 Variable : Stoichiometric Coefficient
 protein : -1
 SAA : 1

Initial Conditions:

Variable(Zone) : Initial Condition
 Ca(Bulk Volume) : 100
 Cam(Bulk Volume) : 100
 Cas(Bulk Volume) : 100
 Cf(Bulk Volume) : 100
 Chm(Bulk Volume) : 100
 Chs(Bulk Volume) : 100
 Co(Bulk Volume) : 100
 Cps(Bulk Volume) : 100
 Inflow: 0
 Input Fluxes:
 Volume: 2.6448

bioreactor3: Description:
 Type: Mixed Reactor Compartment
 Compartment Index: 0
 Active Variables: Ca, Cam, Cas, Cf, CH4, Chm, Chs, Co, FA, H2, Ac, HPr, HS, SAA, SO4, H2S, CODt, VSSt, PH2S, VFAt, cellulose, Cps, inert, lipids, protein, Q, HAc
 Active Processes: acetogenesis, acetogrow, aMethanogenesis, aMethanogrow, aSulfidogenesis, aSulfidogrow, fermengrow, fermentation, hMethanogenesis, hMethanogrow, hSulfidogenesis, hSulfidogrow, oxidation, oxidationgrow, acetogenic_sulfidogenesis, cellulosehydrolysis, lipidhydrolysis, proteinhydrolysis, acetogenic_sulfidogrow, HS_H2S, H2S_HS, Ac_HAc, HAc_Ac
 Initial Conditions:
 Variable(Zone) : Initial Condition
 Ca(Bulk Volume) : 100
 Cam(Bulk Volume) : 100
 Cas(Bulk Volume) : 100
 Cf(Bulk Volume) : 100
 Chm(Bulk Volume) : 100
 Chs(Bulk Volume) : 100
 Co(Bulk Volume) : 100
 Cps(Bulk Volume) : 100
 Inflow: 0
 Input Fluxes:
 Volume: 2.6448

bioreactor4: Description:
 Type: Mixed Reactor Compartment
 Compartment Index: 0
 Active Variables: Ca, Cam, Cas, Cf, CH4, Chm, Chs, Co, FA, H2, Ac, HPr, HS, SAA, SO4, H2S, CODt, VSSt, PH2S, VFAt, cellulose, Cps, inert, lipids, protein, Q, HAc
 Active Processes: acetogenesis, acetogrow, aMethanogenesis, aMethanogrow, aSulfidogenesis, aSulfidogrow, fermengrow, fermentation, hMethanogenesis, hMethanogrow, hSulfidogenesis, hSulfidogrow, oxidation, oxidationgrow, acetogenic_sulfidogenesis, cellulosehydrolysis

is, lipidhydrolysis, proteinhydrolysis, acetogenic_sulfidogrow, H2S_HS, HS_H2S, Ac_HAc, HAc_Ac

Initial Conditions:

Variable(Zone) : Initial Condition
 Ca(Bulk Volume) : 100
 Cam(Bulk Volume) : 100
 Cas(Bulk Volume) : 100
 Cf(Bulk Volume) : 100
 Chm(Bulk Volume) : 100
 Chs(Bulk Volume) : 100
 Co(Bulk Volume) : 100
 Cps(Bulk Volume) : 100
 Inflow: 0
 Input Fluxes:
 Volume: 2.6448

bioreactor5: Description: Mixed Reactor Compartment
 Type: 0
 Compartment Index: 0
 Active Variables: Ca, Cam, Cas, Cf, CH4, Chm, Chs, Co, FA, H2, Ac, HPr, HS, SAA, SO4, H2S, CODt, VSSt, PH2S, VFAt, cellulose, Cps, inert, lipids, protein, Q, HAc
 Active Processes: acetogenesis, acetogrow, aMethanogenesis, aMethanogrow, aSulfidogenesis, aSulfidogrow, fermengrow, fermentation, hMethanogenesis, hMethanogrow, hSulfidogenesis, hSulfidogrow, oxidation, oxidationgrow, acetogenic_sulfidogenesis, cellulosehydrolysis, lipidhydrolysis, proteinhydrolysis, acetogenic_sulfidogrow, H2S_HS, HS_H2S, Ac_HAc, HAc_Ac

Initial Conditions:

Variable(Zone) : Initial Condition
 Ca(Bulk Volume) : 100
 Cam(Bulk Volume) : 100
 Cas(Bulk Volume) : 100
 Cf(Bulk Volume) : 100
 Chm(Bulk Volume) : 100
 Chs(Bulk Volume) : 100
 Co(Bulk Volume) : 100
 Cps(Bulk Volume) : 100
 Inflow: 0
 Input Fluxes:
 Volume: 2.6448

bioreactor6: Description: Mixed Reactor Compartment
 Type: 0
 Compartment Index: 0
 Active Variables: Ca, Cam, Cas, Cf, CH4, Chm, Chs, Co, FA, H2, Ac, HPr, HS, SAA, SO4, H2S, CODt, VSSt, PH2S, VFAt, cellulose, Cps, inert, lipids, protein, Q, HAc
 Active Processes: acetogenesis, acetogrow, aMethanogenesis, aMethanogrow, aSulfidogenesis, aSulfidogrow, fermengrow, fermentation, hMethanogenesis, hMethanogrow

ow, hSulfidogenesis, hSulfidogrow,
oxidation, oxidationgrow, acetogeni
c_sulfidogenesis, cellulosehydrolys
is, lipidhydrolysis, proteinhydroly
sis, acetogenic_sulfidogrow, H2S_HS
, HS_H2S, Ac_HAc, HAc_Ac

Initial Conditions:

Variable(Zone) : Initial Condition
Ca(Bulk Volume) : 100
Cam(Bulk Volume) : 100
Cas(Bulk Volume) : 100
Cf(Bulk Volume) : 100
Chm(Bulk Volume) : 100
Chs(Bulk Volume) : 100
Co(Bulk Volume) : 100
Cps(Bulk Volume) : 100
Inflow: 0
Input Fluxes:
Volume: 2.6448

bioreactor7: Description: Mixed Reactor Compartment
Type: 0
Compartment Index: 0
Active Variables: Ca, Cam, Cas, Cf, CH4, Chm, Chs, Co
, FA, H2, Ac, HPr, HS, SAA, SO4, H2
S, CODt, VSSt, PH2S, VFAt, cellulose,
Cps, inert, lipids, protein, Q,
HAc
Active Processes: acetogenesis, acetogrow, aMethanoge
nesis, aMethanogrow, aSulfidogenesi
s, aSulfidogrow, fermengrow, ferment
ation, hMethanogenesis, hMethanogr
ow, hSulfidogenesis, hSulfidogrow,
oxidation, oxidationgrow, acetogeni
c_sulfidogenesis, cellulosehydrolys
is, lipidhydrolysis, proteinhydroly
sis, acetogenic_sulfidogrow, H2S_HS
, HS_H2S, Ac_HAc, HAc_Ac
Initial Conditions:
Variable(Zone) : Initial Condition
Ca(Bulk Volume) : 100
Cam(Bulk Volume) : 100
Cas(Bulk Volume) : 100
Cf(Bulk Volume) : 100
Chm(Bulk Volume) : 100
Chs(Bulk Volume) : 100
Co(Bulk Volume) : 100
Cps(Bulk Volume) : 100
Inflow: 0
Input Fluxes:
Volume: 2.3771

bioreactor8: Description: Mixed Reactor Compartment
Type: 0
Compartment Index: 0
Active Variables: Ca, Cam, Cas, Cf, CH4, Chm, Chs, Co
, FA, H2, Ac, HPr, HS, SAA, SO4, H2
S, CODt, VSSt, PH2S, VFAt, cellulose,
Cps, inert, lipids, protein, Q,
HAc
Active Processes: acetogenesis, acetogrow, aMethanoge

nesis, aMethanogrow, aSulfidogenesi
s, aSulfidogrow, fermengrow, fermen
tation, hMethanogenesis, hMethanogr
ow, hSulfidogenesis, hSulfidogrow,
oxidation, oxidationgrow, acetogeni
c_sulfidogenesis, cellulosehydroly
sis, lipidhydrolysis, proteinhydroly
sis, acetogenic_sulfidogrow, HS_H2S
, H2S_HS, Ac_HAc, HAc_Ac

Initial Conditions:

Variable(Zone) : Initial Condition
Ca(Bulk Volume) : 100
Cam(Bulk Volume) : 100
Cas(Bulk Volume) : 100
Cf(Bulk Volume) : 100
Chm(Bulk Volume) : 100
Chs(Bulk Volume) : 100
Co(Bulk Volume) : 100
Cps(Bulk Volume) : 100
Inflow: 0
Input Fluxes:
Volume: 2.3771

bioreactor9: Description:
Type: Mixed Reactor Compartment
Compartment Index: 0
Active Variables: Ca, Cam, Cas, Cf, CH4, Chm, Chs, Co
, FA, H2, Ac, HPr, HS, SAA, SO4, H2
S, CODt, VSSt, PH2S, VFAt, cellulose,
Cps, inert, lipids, protein, Q,
HAc
Active Processes: acetogenesis, acetogrow, aMethanoge
nesis, aMethanogrow, aSulfidogenesi
s, aSulfidogrow, fermengrow, fermen
tation, hMethanogenesis, hMethanogr
ow, hSulfidogenesis, hSulfidogrow,
oxidation, oxidationgrow, acetogeni
c_sulfidogenesis, cellulosehydroly
sis, lipidhydrolysis, proteinhydroly
sis, acetogenic_sulfidogrow, H2S_HS
, HS_H2S, Ac_HAc, HAc_Ac
Initial Conditions:
Variable(Zone) : Initial Condition
Ca(Bulk Volume) : 100
Cam(Bulk Volume) : 100
Cas(Bulk Volume) : 100
Cf(Bulk Volume) : 100
Chm(Bulk Volume) : 100
Chs(Bulk Volume) : 100
Co(Bulk Volume) : 100
Cps(Bulk Volume) : 100
Inflow: 0
Input Fluxes:
Volume: 2.3771

```

*****
Links
*****
link1:      Type:      Advective Link
           Link Index: 0
           Compartment In: bioreactor1
           Connection In: Outflow
           Compartment Out: bioreactor2
           Connection Out: Inflow
           Bifurcations:
             settling:
               Description:solids settling
               Compartment Out: bioreactor7
               Connection Out: Inflow
               Water Flow: 0
               Mass Fluxes:
                 Variable : Flux
                 Ca : Q*xCl*Ca
                 Cam : Q*xCl*Cam
                 Cas : Q*xCl*Cas
                 cellulose : Q*xCl*cellulose
                 Cf : Q*xCl*Cf
                 Chm : Q*xCl*Chm
                 Chs : Q*xCl*Chs
                 Co : Q*xCl*Co
                 Cps : Q*xCl*Cps
                 inert : Q*xCl*inert
                 lipids : Q*xCl*lipids
                 protein : Q*xCl*protein
             water_flow:
               Description:
               Compartment Out: bioreactor7
               Connection Out: Inflow
               Water Flow: 2*R1/3
-----
link2:      Type:      Advective Link
           Link Index: 0
           Compartment In: bioreactor2
           Connection In: Outflow
           Compartment Out: bioreactor3
           Connection Out: Inflow
           Bifurcations:
             settling:
               Description:solids settling
               Compartment Out: bioreactor7
               Connection Out: Inflow
               Water Flow: 0
               Mass Fluxes:
                 Variable : Flux
                 Ca : Q*xCl*Ca
                 Cam : Q*xCl*Cam
                 Cas : Q*xCl*Cas
                 cellulose : Q*xCl*cellulose
                 Cf : Q*xCl*Cf
                 Chm : Q*xCl*Chm
                 Chs : Q*xCl*Chs
                 Co : Q*xCl*Co
                 Cps : Q*xCl*Cps
                 inert : Q*xCl*inert
                 lipids : Q*xCl*lipids
                 protein : Q*xCl*protein

```

water_flow:
 Description:
 Compartment Out: bioreactor7
 Connection Out: Inflow
 Water Flow: R1/3

link3: Type: Advective Link
 Link Index: 0
 Compartment In: bioreactor3
 Connection In: Outflow
 Compartment Out: bioreactor4
 Connection Out: Inflow
 Bifurcations:
 settling:
 Description:solids settling
 Compartment Out: bioreactor8
 Connection Out: Inflow
 Water Flow: 0
 Mass Fluxes:
 Variable : Flux
 Ca : Q*xC2*Ca
 Cam : Q*xC2*Cam
 Cas : Q*xC2*Cas
 cellulose : Q*xC2*cellulose
 Cf : Q*xC2*Cf
 Chm : Q*xC2*Chm
 Chs : Q*xC2*Chs
 Co : Q*xC2*Co
 Cps : Q*xC2*Cps
 inert : Q*xC2*inert
 lipids : Q*xC2*lipids
 protein : Q*xC2*protein
 water_flow:
 Description:
 Compartment Out: bioreactor8
 Connection Out: Inflow
 Water Flow: R2/2

link4: Type: Advective Link
 Link Index: 0
 Compartment In: bioreactor4
 Connection In: Outflow
 Compartment Out: bioreactor5
 Connection Out: Inflow
 Bifurcations:
 settling:
 Description:solids settling
 Compartment Out: bioreactor8
 Connection Out: Inflow
 Water Flow: 0
 Mass Fluxes:
 Variable : Flux
 Ca : Q*xC2*Ca
 Cam : Q*xC2*Cam
 Cas : Q*xC2*Cas
 cellulose : Q*xC2*cellulose
 Cf : Q*xC2*Cf
 Chm : Q*xC2*Chm
 Chs : Q*xC2*Chs
 Co : Q*xC2*Co
 Cps : Q*xC2*Cps

```

    inert : Q*xC2*inert
    lipids : Q*xC2*lipids
    protein : Q*xC2*protein
water_flow:
  Description:
  Compartment Out: bioreactor8
  Connection Out: Inflow
  Water Flow: R2/2

```

```

link5:      Type:      Advective Link
           Link Index: 0
           Compartment In: bioreactor5
           Connection In: Outflow
           Compartment Out: bioreactor6
           Connection Out: Inflow
           Bifurcations:
             settling:
               Description:solids settling
               Compartment Out: bioreactor9
               Connection Out: Inflow
               Water Flow: 0
           Mass Fluxes:
             Variable : Flux
             Ca : Q*xC2*Ca
             Cam : Q*xC2*Cam
             Cas : Q*xC2*Cas
             cellulose : Q*xC2*cellulose
             Cf : Q*xC2*Cf
             Chm : Q*xC2*Chm
             Chs : Q*xC2*Chs
             Co : Q*xC2*Co
             Cps : Q*xC2*Cps
             inert : Q*xC2*inert
             lipids : Q*xC2*lipids
             protein : Q*xC2*protein
           water_flow:
             Description:
             Compartment Out: bioreactor9
             Connection Out: Inflow
             Water Flow: R3/2

```

```

link6:      Type:      Advective Link
           Link Index: 0
           Compartment In: bioreactor6
           Connection In: Outflow
           Compartment Out:
           Bifurcations:
             settling:
               Description:solids settling
               Compartment Out: bioreactor9
               Connection Out: Inflow
               Water Flow: 0
           Mass Fluxes:
             Variable : Flux
             Ca : Q*xC2*Ca
             Cam : Q*xC2*Cam
             Cas : Q*xC2*Cas
             cellulose : Q*xC2*cellulose
             Cf : Q*xC2*Cf
             Chm : Q*xC2*Chm
             Chs : Q*xC2*Chs

```

Co : $Q \times C2 \times Co$
 Cps : $Q \times C2 \times Cps$
 inert : $Q \times C2 \times inert$
 lipids : $Q \times C2 \times lipids$
 protein : $Q \times C2 \times protein$
 water_flow:
 Description:
 Compartment Out: bioreactor9
 Connection Out: Inflow
 Water Flow: R3/2

link7: Type: Advective Link
 Link Index: 0
 Compartment In: bioreactor7
 Connection In: Outflow
 Compartment Out: bioreactor1
 Connection Out: Inflow
 Bifurcations:
 overflow:
 Description:solids overflow
 Compartment Out: bioreactor8
 Connection Out: Inflow
 Water Flow: 0
 Mass Fluxes:
 Variable : Flux
 Ca : $Q \times C3 \times Ca$
 Cam : $Q \times C3 \times Cam$
 Cas : $Q \times C3 \times Cas$
 cellulose : $Q \times C3 \times cellulose$
 Cf : $Q \times C3 \times Cf$
 Chm : $Q \times C3 \times Chm$
 Chs : $Q \times C3 \times Chs$
 Co : $Q \times C3 \times Co$
 Cps : $Q \times C3 \times Cps$
 inert : $Q \times C3 \times inert$
 lipids : $Q \times C3 \times lipids$
 protein : $Q \times C3 \times protein$

link8: Type: Advective Link
 Link Index: 0
 Compartment In: bioreactor8
 Connection In: Outflow
 Compartment Out: bioreactor1
 Connection Out: Inflow
 Bifurcations:
 overflow:
 Description:solids overflow
 Compartment Out: bioreactor9
 Connection Out: Inflow
 Water Flow: 0
 Mass Fluxes:
 Variable : Flux
 Ca : $Q \times C4 \times Ca$
 Cam : $Q \times C4 \times Cam$
 Cas : $Q \times C4 \times Cas$
 cellulose : $Q \times C4 \times cellulose$
 Cf : $Q \times C4 \times Cf$
 Chm : $Q \times C4 \times Chm$
 Chs : $Q \times C4 \times Chs$
 Co : $Q \times C4 \times Co$
 Cps : $Q \times C4 \times Cps$

inert : Q*xC4*inert
lipids : Q*xC4*lipids
protein : Q*xC4*protein

link9: Type: Advective Link
 Link Index: 0
 Compartment In: bioreactor9
 Connection In: Outflow
 Compartment Out: bioreactor1
 Connection Out: Inflow
 Bifurcations:

 Plot Definitions

Biomass6: Description: biomass concentrations
 Abscissa: Time
 Title: Biomass Concentrations6
 Abscissa Label: Time/ days
 Ordinate Label: gVSS/m³
 Curves:
 Type : Variable [CalcNum,Comp., Zone,Time/Space]
 Value : Ca [0,bioreactor6,Bulk Volume,0]
 Value : Cam [0,bioreactor6,Bulk Volume,0]
 Value : Cas [0,bioreactor6,Bulk Volume,0]
 Value : Cf [0,bioreactor6,Bulk Volume,0]
 Value : Chm [0,bioreactor6,Bulk Volume,0]
 Value : Chs [0,bioreactor6,Bulk Volume,0]
 Value : Co [0,bioreactor6,Bulk Volume,0]
 Value : VSSt [0,bioreactor6,Bulk Volume,0]
 Value : Cps [0,bioreactor6,Bulk Volume,0]

 CH4: Description: Time
 Abscissa: Time
 Title:
 Abscissa Label:
 Ordinate Label:
 Curves:
 Type : Variable [CalcNum,Comp., Zone,Time/Space]
 Value : CH4 [0,bioreactor6,Bulk Volume,0]

 CODtotal: Description: Total COD
 Abscissa: Time
 Title: Total COD
 Abscissa Label:
 Ordinate Label:
 Curves:
 Type : Variable [CalcNum,Comp., Zone,Time/Space]
 Value : CODt [0,bioreactor1,Bulk Volume,0]
 Value : CODt [0,bioreactor2,Bulk Volume,0]
 Value : CODt [0,bioreactor3,Bulk Volume,0]
 Value : CODt [0,bioreactor4,Bulk Volume,0]
 Value : CODt [0,bioreactor5,Bulk Volume,0]
 Value : CODt [0,bioreactor6,Bulk Volume,0]
 Value : CODt [0,bioreactor7,Bulk Volume,0]
 Value : CODt [0,bioreactor8,Bulk Volume,0]
 Value : CODt [0,bioreactor9,Bulk Volume,0]

 concsl: Description: Concentrations1
 Abscissa: Time
 Title: Concentrations1
 Abscissa Label: Time/ days
 Ordinate Label: gCOD/m³
 Curves:
 Type : Variable [CalcNum,Comp., Zone,Time/Space]
 Value : FA [0,bioreactor1,Bulk Volume,0]
 Value : H2 [0,bioreactor1,Bulk Volume,0]
 Value : Ac [0,bioreactor1,Bulk Volume,0]
 Value : HPr [0,bioreactor1,Bulk Volume,0]
 Value : HS [0,bioreactor1,Bulk Volume,0]
 Value : SAA [0,bioreactor1,Bulk Volume,0]
 Value : SO4 [0,bioreactor1,Bulk Volume,0]
 Value : H2S [0,bioreactor1,Bulk Volume,0]

Value : CH4 [0,bioreactor1,Bulk Volume,0]

concs6: Description:
 Abscissa: Time
 Title: Concentrations1
 Abscissa Label: Time/ days
 Ordinate Label: gCOD/m³
 Curves:
 Type : Variable [CalcNum,Comp.,Zone,Time/Space]
 Value : FA [0,bioreactor6,Bulk Volume,0]
 Value : H2 [0,bioreactor6,Bulk Volume,0]
 Value : Ac [0,bioreactor6,Bulk Volume,0]
 Value : HPr [0,bioreactor6,Bulk Volume,0]
 Value : HS [0,bioreactor6,Bulk Volume,0]
 Value : SAA [0,bioreactor6,Bulk Volume,0]
 Value : SO4 [0,bioreactor6,Bulk Volume,0]
 Value : H2S [0,bioreactor6,Bulk Volume,0]
 Value : HAc [0,bioreactor6,Bulk Volume,0]

H2: Description: hydrogen concentration
 Abscissa: Time
 Title: Hydrogen Concentrations
 Abscissa Label: Time
 Ordinate Label: Concentration
 Curves:
 Type : Variable [CalcNum,Comp.,Zone,Time/Space]
 Value : H2 [0,bioreactor1,Bulk Volume,0]
 Value : H2 [0,bioreactor2,Bulk Volume,0]
 Value : H2 [0,bioreactor3,Bulk Volume,0]
 Value : H2 [0,bioreactor4,Bulk Volume,0]
 Value : H2 [0,bioreactor5,Bulk Volume,0]
 Value : H2 [0,bioreactor6,Bulk Volume,0]
 Value : H2 [0,bioreactor7,Bulk Volume,0]
 Value : H2 [0,bioreactor8,Bulk Volume,0]
 Value : H2 [0,bioreactor9,Bulk Volume,0]

HAc: Description:
 Abscissa: Time
 Title:
 Abscissa Label:
 Ordinate Label:
 Curves:
 Type : Variable [CalcNum,Comp.,Zone,Time/Space]
 Value : HAc [0,bioreactor6,Bulk Volume,0]

particulates: Description:
 Abscissa: Time
 Title: particulates
 Abscissa Label:
 Ordinate Label:
 Curves:
 Type : Variable [CalcNum,Comp.,Zone,Time/Space]
 Value : VSSt [0,bioreactor6,Bulk Volume,0]
 Value : protein [0,bioreactor6,Bulk Volume,0]
 Value : cellulose [0,bioreactor6,Bulk Volume,0]
 Value : lipids [0,bioreactor6,Bulk Volume,0]

pSRB: Description:
 Abscissa: Time
 Title:
 Abscissa Label:

Ordinate Label:

Curves:

Type : Variable [CalcNum,Comp.,Zone,Time/Space]
Value : Cas [0,bioreactor6,Bulk Volume,0]

SO4:

Description:

Abscissa: Time

Title: SO4

Abscissa Label: Time/ days

Ordinate Label: gSO4/m³

Curves:

Type : Variable [CalcNum,Comp.,Zone,Time/Space]

Value : SO4 [0,bioreactor1,Bulk Volume,0]

Value : SO4 [0,bioreactor2,Bulk Volume,0]

Value : SO4 [0,bioreactor3,Bulk Volume,0]

Value : SO4 [0,bioreactor4,Bulk Volume,0]

Value : SO4 [0,bioreactor5,Bulk Volume,0]

Value : SO4 [0,bioreactor6,Bulk Volume,0]

Value : SO4 [0,bioreactor7,Bulk Volume,0]

Value : SO4 [0,bioreactor8,Bulk Volume,0]

Value : SO4 [0,bioreactor9,Bulk Volume,0]

VFAt:

Description:

Abscissa: Time

Title: Total VFA

Abscissa Label: Time/ days

Ordinate Label: g VFA as COD/m³

Curves:

Type : Variable [CalcNum,Comp.,Zone,Time/Space]

Value : VFAt [0,bioreactor1,Bulk Volume,0]

APPENDIX D

The tables that make up this appendix were compiled as a result of the extensive literature survey. The kinetic constants published in the literature have been summarized and converted to a common set of units.

The process for which the kinetic constant was measured was firstly identified. This was determined from the nature of the substrate. Since a number of different compounds make up the substrates for a specific process, the various compounds had to be grouped into the following groups, consistent with the reaction used in the model (Gujer and Zehnder, 1983). These groups are defined as particulate COD, sugars and amino acids, long chain fatty acids, shorter chain volatile fatty acids (excluding acetic acid) and other intermediary fermentation products, acetic acid and hydrogen. Therefore, all rate constants relating to the hydrolysis of particulate organic matter were grouped in the table of hydrolysis rate constants (Table D1). Similarly, the various soluble components used as the substrate for the fermentation reaction are grouped as sugars and amino acids. These compounds include glucose, dextrose and sucrose as examples.

The tables include information, where available, on the conditions under which the kinetic constants were measured, or the conditions of the model in which they were used. A common set of units has been used, identical to those used in the model, and all kinetic constants, where possible, were converted to these units. Difficulties arose when the units of the yield constant were ambiguous, and no explanation was given in the literature. For this reason, the unit of the biomass concentration has been reported in the tables in the same way as was reported in the paper. The units of concentration of the substrates were converted to $\text{gCOD}\cdot\text{m}^{-3}$, while the units of time were days. For substrates such as sulfate, which by definition does not have a COD value, the units of concentration are given in $\text{mg}\cdot\text{l}^{-1}$.

As can be noted, the values of the kinetic constants vary according to the substrate used, and the temperature and pH of the system. The list of constants is by no means a review of the literature kinetic constants. Instead, it is up to the reader to choose a value of a kinetic constant for a process, that is for a specific substrate, measured under conditions as close as possible to the system for which the kinetic

constant will be used. However, there are some processes where there is a large amount of data, where two different constants are given for the same conditions. For this case, two references are given. The first, titled 'paper consulted', shows the source of the kinetic constants used for the compilation of the tables. The second, titled 'primary reference', gives the original source of the kinetic constant. If there is a large difference between two constants that were measured under the same conditions, the source paper can be consulted, and the choice of a kinetic constant can be made from that.

It can also be noted that the same initial study has been referenced by two other studies, and have reported two different values for the same constant. In cases such as this, both values have been reported. In fact, when the same reference is common to two papers, both these papers are reported.

Table D.2b: Summary of Operating and Kinetic Parameters for Fermentation/Acidogenesis

Paper Consulted	Primary Reference	Model description	K_s (gCOD.m ⁻³)	Y	u_{max} (day ⁻¹)	k	K_d (day ⁻¹)	K_f (gCOD.m ⁻³)
1 Henze and Harremoës (1983)	Ghosh and Pohland (1974)		23	0.17 gVSS.gCOD ⁻¹	30		6.1	
2 Denopoulou <i>et al.</i> (1988)	Ghosh and Pohland (1974)			0.17 gVSS.gCOD ⁻¹			6.14	
3 Jayaseelan (1997)	Mosey (1983)		680	0.12 gVSS.gCOD ⁻¹		6.67 gCOD.gVSS ⁻¹ .d ⁻¹	0.015	
4 Jayaseelan (1997)	Mosey (1983)		1270	0.12 gVSS.gCOD ⁻¹		4.65 gCOD.gVSS ⁻¹ .d ⁻¹	0.015	
5 Jayaseelan (1997)	Mosey (1983)		1580	0.12 gVSS.gCOD ⁻¹		3.85 gCOD.gVSS ⁻¹ .d ⁻¹	0.015	
6 Lettinga (1995)	Lettinga (1995)			0.085-0.14				
7 Lettinga (1995)	Lettinga (1995)			0.094				
8 Jayaseelan (1997)	Mosey (1983)		23	0.173 gVSS.gCOD ⁻¹		30 gCOD.gVSS ⁻¹ .d ⁻¹	0.8	
9 Pavlostathis and Giraldo-Gomez (1991)	Huang (1983)		527		0.323			
10 Pavlostathis and Giraldo-Gomez (1991)	Zoetemeijer <i>et al.</i> (1982)		370	0.14	0.3			
11 Pavlostathis and Giraldo-Gomez (1991)	Ghosh and Pohland (1974)		22.5	0.17 gVSS.gCOD ⁻¹	1.25		6.1	
12 Kiely <i>et al.</i> (1987)	Kiely <i>et al.</i> (1987)	uncompetitive HAC inhibition		0.176 gVSS.gCOD ⁻¹	0.3			
13 Henze and Harremoës (1983)	McCarty (1971)		192	0.15 gVSS.gCOD ⁻¹				
14 Henze and Harremoës (1983)	Ghosh and Klaus (1978)		370	0.14 gVSS.gCOD ⁻¹	7.2			
15 Pavlostathis and Giraldo-Gomez (1991)	Ghosh and Klaus (1978)		427	0.15 gVSS.gCOD ⁻¹	0.3			
16 Pavlostathis and Giraldo-Gomez (1991)	Nolte <i>et al.</i> (1985)		8					
17 Pavlostathis and Giraldo-Gomez (1991)	Nolte <i>et al.</i> (1985)		75.3			1.33 gCOD.gVSS ⁻¹ .d ⁻¹		
18 Hill and Barth (1977)	Hill and Barth (1977)	uncompetitive VFA inhibition	160	0.1875 g organism.gCOD ⁻¹	0.4	70.6 gCOD.gVSS ⁻¹ .d ⁻¹	0.025	1000 VFA
19 Buffiere <i>et al.</i> (1995)	Denaac <i>et al.</i> (1988)	Monod	140	0.036 gVSS.gCOD ⁻¹	1.2			
20 Costello <i>et al.</i> (1991)	Mosey (1983)	Non-competitive Acetic acid inhibition	24.576	0.08-0.16 gVSS.gCOD ⁻¹		0.288 gCOD.mg ⁻¹ .d ⁻¹		640
21 Denopoulou <i>et al.</i> (1988)	Zoetemeijer <i>et al.</i> (1982)			0.34				
22 Lettinga (1995)	Lettinga (1995)			0.4				
23 Lettinga (1995)	Lettinga (1995)			0.54		9.5	0.43	
24 Lettinga (1995)	Lettinga (1995)			0.17		2.5	0.79	
25 Lettinga (1995)	Lettinga (1995)			0.10-0.18		179	0.87	
26 Lettinga (1995)	Lettinga (1995)			0.12-0.17		83	6.1	
27 Lettinga (1995)	Lettinga (1995)			0.06-0.08		24-33		
28 Lettinga (1995)	Lettinga (1995)			0.13		11-19		
29 Lettinga (1995)	Lettinga (1995)			0.11		74	0.96	
30 Lettinga (1995)	Lettinga (1995)			0.21		1.6-2.2		
31 Lettinga (1995)	Lettinga (1995)			0.789		0.16	0.03	
32 Lettinga (1995)	Lettinga (1995)			0.26 gVSS.gCOD ⁻¹	1.5			21.33 HAC
33 Mioletta <i>et al.</i> (1986)	Mioletta <i>et al.</i> (1986)	uncompetitive acetic acid inhibition	277	0.21 gVSS.gCOD ⁻¹				
34 Henze and Harremoës (1983)	Sykes (1975)		200	0.04-0.2 gVSS.gCOD ⁻¹		32 gCOD.gVSS ⁻¹ .d ⁻¹		
35 Henze and Harremoës (1983)	Andrews and Duarte (1980)		24.5	0.17 gVSS.gCOD ⁻¹	0.16	65 gCOD.gVSS ⁻¹ .d ⁻¹	0.03	
36 Wu <i>et al.</i> (1998)	Andrews and Duarte (1980)		2580					
37 Wu <i>et al.</i> (1998)	Massey & Pohland (1978)							
38 Henze and Harremoës (1983)	Sykes (1975)		36.48	0.04-0.11 gVSS.gCOD ⁻¹		0.04896 gCOD.mg ⁻¹ .d ⁻¹		640
39 Henze and Harremoës (1983)	Sykes (1975)		105-3180	0.17 gVSS.gCOD ⁻¹		0.77-13.8 gCOD.gVSS ⁻¹ .d ⁻¹	0.01-0.015	
40 Costello <i>et al.</i> (1991)	Mosey (1983)		850	0.1 gVSS.gCOD ⁻¹		12 gCOD.gVSS ⁻¹ .d ⁻¹		
41 Jayaseelan (1997)	Metcalf & Eddy (1991)	Non-competitive Acetic acid inhibition						
42 Jayaseelan (1997)	Jayaseelan (1997)							

Table D.1: Summary of Operating a

	Paper Consulted	Primary Reference	Feed	Substrate
1	Shimizu <i>et al.</i> (1993)	Shimizu <i>et al.</i> (1993)	solubilised sludge	
2	Shimizu <i>et al.</i> (1993)	Shimizu <i>et al.</i> (1993)	protein	
3	Shimizu <i>et al.</i> (1993)	Shimizu <i>et al.</i> (1993)	nucleic acid	
4	Shimizu <i>et al.</i> (1993)	Shimizu <i>et al.</i> (1993)	lipid	
5	Shimizu <i>et al.</i> (1993)	Shimizu <i>et al.</i> (1993)	carbohydrate	
6	Shimizu <i>et al.</i> (1993)	Shimizu <i>et al.</i> (1993)	carbohydrate	
7	Shimizu <i>et al.</i> (1993)	Shimizu <i>et al.</i> (1993)	cellulose	
8	Gujer and Zehnder (1983)	Ghosh <i>et al.</i> (1980)	cellulose	crude cellulose
9	Gujer and Zehnder (1983)	Heukelekian <i>et al.</i> (1958)	lipids	fatty acid esters
10	Gujer and Zehnder (1983)	Sawyer and Roy (1955)	lipids	greases
11	Gujer and Zehnder (1983)	Woods and Melina (1965)	lipids	greases
12	Gujer and Zehnder (1983)	Woods and Melina (1965)	lipids	lipids
13	Shimizu <i>et al.</i> (1993)	Shimizu <i>et al.</i> (1993)	raw sludge	
14	Pavlostathis and Giraldo-Gomez (1991)	Stack & Cotta (1986)	cellulose	
15	Eastman and Ferguson (1981)	Eastman and Ferguson (1981)	raw domestic primary sludge	
16	Gujer and Zehnder (1983)	Pfeffer (1969)	domestic sludge	
17	Gujer and Zehnder (1983)	Ghosh <i>et al.</i> (1980)	proteins	
18	Gujer and Zehnder (1983)	Ghosh <i>et al.</i> (1980)	hemicellulose	
19	Henze and Harremoes (1983)	Gujer and Zehnder (1983)		
20	Henze and Harremoes (1983)	Eastman and Ferguson (1981)		
21	Pavlostathis and Giraldo-Gomez (1991)	Pavlostathis <i>et al.</i> (1988)	cellulose	
22	Gujer and Zehnder (1983)	Woods <i>et al.</i> (1965)	proteins	
23	Gujer and Zehnder (1983)	Woods <i>et al.</i> (1965)	cellulose	
24	Gujer and Zehnder (1983)	Kasper (1977)	domestic sludge	
25	Gujer and Zehnder (1983)	Pfeffer (1969)	domestic sludge	
26	Bryers (1985)	Hamer <i>et al.</i> (1985)	biomass particulates	
27	Gujer and Zehnder (1983)	Eastman and Ferguson (1981)	domestic sludge	
28	Gujer and Zehnder (1983)	Eastman and Ferguson (1981)	domestic sludge	
29	Gujer and Zehnder (1983)	Eastman and Ferguson (1981)	domestic sludge	
30	Ellosov and Argaman (1995)	Ellosov and Argaman (1995)	degradable primary VSS	
31	Hamelers <i>et al.</i> (1998)	ten Brummeler (1991)	Organic Fraction of Solids municipal waste	
32	Pavlostathis and Giraldo-Gomez (1991)	Doyle <i>et al.</i> (1983)	corn stover	
33	Pavlostathis and Giraldo-Gomez (1991)	Doyle <i>et al.</i> (1983)	corn stover	
34	Pavlostathis and Giraldo-Gomez (1991)	Doyle <i>et al.</i> (1983)	corn stover	
35	Pavlostathis and Giraldo-Gomez (1991)	Doyle <i>et al.</i> (1983)	corn stover	
36	Pavlostathis and Giraldo-Gomez (1991)	Nagase & Matsuo (1982)	casein	
37	Pavlostathis and Giraldo-Gomez (1991)	Nagase & Matsuo (1982)	gelatin	
38	Pavlostathis and Giraldo-Gomez (1991)	Greco <i>et al.</i> (1983)	zein	
39	Pavlostathis and Giraldo-Gomez (1991)	Gujer & Zehnder (1983)	mixed primary and waste activated sludge	
40	Pavlostathis and Giraldo-Gomez (1991)	Gujer & Zehnder (1983)	mixed primary and waste activated sludge	
41	Pavlostathis and Giraldo-Gomez (1991)	Pfeffer (1974)	domestic refuse	
42	Pavlostathis and Giraldo-Gomez (1991)	Pfeffer (1974)	domestic refuse	
43	Pavlostathis and Giraldo-Gomez (1991)	Foree & McCarty (1969)	algae degradation by MPB and SRB	
44	Pavlostathis and Giraldo-Gomez (1991)	O'Rourke (1968)	Municipal raw sewage protein	
45	Pavlostathis and Giraldo-Gomez (1991)	O'Rourke (1968)	Municipal raw sewage cellulose	
46	Pavlostathis and Giraldo-Gomez (1991)	O'Rourke (1968)	Municipal raw sewage lipids	
47	Pavlostathis and Giraldo-Gomez (1991)	O'Rourke (1968)	Municipal raw sewage total COD	
48	Pavlostathis and Giraldo-Gomez (1991)	Ghosh (1981)	Municipal raw sewage activated sludge	
49	Pavlostathis and Giraldo-Gomez (1991)	Gujer & Zehnder (1983)	Complex biopolymers lipids	
50	Pavlostathis and Giraldo-Gomez (1991)	Gujer & Zehnder (1983)	Complex biopolymers protein	
51	Pavlostathis and Giraldo-Gomez (1991)	Gujer & Zehnder (1983)	Complex biopolymers cellulose	
52	Pavlostathis and Giraldo-Gomez (1991)	Gujer & Zehnder (1983)	Complex biopolymers hemicellulose	

Table D.2a: Summary of Operating and Kinetic Parameters for Fermentation/Acidogenesis

Paper Consulted	Primary Reference	Feed	Substrate	Mode of Operation	pH	HRT (days)	Temp. (°C)	Operational Parameters	
								Culture	
1 Henze and Harremoës (1983)	Groth and Pohland (1974)		dextrose				37		mixed anaerobic
2 Denopoulou <i>et al.</i> (1988)	Groth and Pohland (1974)		dextrose						
3 Jeyaseelan (1997)	Mosey (1983)		fatty acid				36		
4 Jeyaseelan (1997)	Mosey (1983)		fatty acid				25		
5 Jeyaseelan (1997)	Mosey (1983)		fatty acid				20		
6 Lettinga (1995)	Lettinga (1995)		gelatin	Dispersed culture CSTR					
7 Lettinga (1995)	Lettinga (1995)		gelatin	Dispersed culture UASB					
8 Jeyaseelan (1997)	Mosey (1983)		glucose	continuous			37		
9 Pavlostathis and Gralido-Gomez (1991)	Huang (1983)		glucose	continuous			37		
10 Pavlostathis and Gralido-Gomez (1991)	Zoetemeyer <i>et al.</i> (1982)		glucose	continuous			37		
11 Pavlostathis and Gralido-Gomez (1991)	Groth and Pohland (1974)		glucose	continuous			36.5		
12 Kelly <i>et al.</i> (1997)	Kelly <i>et al.</i> (1997)	primary sewage sludge/OFMSW	glucose	CSTR	7.75		36		theoretical model
13 Henze and Harremoës (1983)	McCarty (1971)		glucose	batch			35		glucose enrichment
14 Henze and Harremoës (1983)	Groth and Klass (1978)		glucose	batch			35		
15 Pavlostathis and Gralido-Gomez (1991)	Groth and Klass (1978)		glucose	continuous			35		
16 Pavlostathis and Gralido-Gomez (1991)	Nolke <i>et al.</i> (1985)		glucose	continuous			35		
17 Pavlostathis and Gralido-Gomez (1991)	Nolke <i>et al.</i> (1985)		glucose	continuous			35		
18 Hill and Barth (1977)	Hill and Barth (1977)	raw animal waste	glucose	semicontinuous		15, 30, 45	35		mixed anaerobic
19 Buffere <i>et al.</i> (1995)	Derré <i>et al.</i> (1988)	Glucose	glucose	FB Biofilm			25		Mixed
20 Costello <i>et al.</i> (1991)	Mosey (1983)	Glucose	glucose	High Rate Continuous					Mixed
21 Denopoulou <i>et al.</i> (1988)	Zoetemeyer <i>et al.</i> (1982)		glucose						
22 Lettinga (1995)	Lettinga (1995)		glucose	Acid producing sludge					
23 Lettinga (1995)	Lettinga (1995)		glucose	Acid producing sludge					
24 Lettinga (1995)	Lettinga (1995)		glucose	Mixed culture					
25 Lettinga (1995)	Lettinga (1995)		glucose	Mixed culture					
26 Lettinga (1995)	Lettinga (1995)		glucose	Dispersed culture CSTR					
27 Lettinga (1995)	Lettinga (1995)		glucose	Dispersed culture UASB					
28 Lettinga (1995)	Lettinga (1995)		glucose	Aggregates UASB					
29 Lettinga (1995)	Lettinga (1995)		glucose	Aggregates gas lift					
30 Lettinga (1995)	Lettinga (1995)		glucose	Granular sludge 1 step UASB					
31 Lettinga (1995)	Lettinga (1995)		glucose	Granular sludge 2 step UASB					
32 Lettinga (1995)	Lettinga (1995)		glucose						
33 Mioletta <i>et al.</i> (1986)	Mioletta <i>et al.</i> (1986)		glucose						theoretical
34 Henze and Harremoës (1983)	Sykes (1975)		glucose						
35 Henze and Harremoës (1983)	Andrews and Duarte (1980)		glucose						
36 Wu <i>et al.</i> (1998)			glucose						
37 Wu <i>et al.</i> (1998)	Massey & Pohland (1978)		glucose						
38 Henze and Harremoës (1983)	Sykes (1975)		hexose						
39 Henze and Harremoës (1983)	Sykes (1975)		hexose						
40 Costello <i>et al.</i> (1991)	Mosey (1983)	Glucose	Lactate	High Rate Continuous					Mixed
41 Jeyaseelan (1997)	Metcalfe & Eddy (1991)		lipids						
42 Jeyaseelan (1997)	Jeyaseelan (1997)		lipids						

Parameters for Anaerobic Oxidation

Parameters		Kinetic Parameters					
Reaction	Temp. (°C)	Model description	K_s (gCOD.m ⁻³)	Y (gVSS.gCOD ⁻¹)	U_{max} (day ⁻¹)	k (gCOD.gVSS ⁻¹ .d ⁻¹)	k_d (day ⁻¹)
	37	Monod	1816	0.11	0.56		0.01
	37		1816	0.11	0.55	5	0.01
	37		105	0.11	0.105	0.95	0.01
	37	Monod	105	0.11	0.11		0.01
	37	Monod	3180	0.11	0.45		0.01
	37		3180	0.11	0.44	4	0.01
	37	Monod	143	0.11	0.12		0.01
	37		143	0.11	0.11	1	0.01
	37	Monod	417	0.11	0.1		0.01
	37		417	0.11	0.085	0.77	0.01
	35	Monod	2000	0.04	0.25		0.015
	35		2000	0.04	0.252	6.67	0.015
	25	Monod	3720	0.04	0.17		0.015
	25		3720	0.04	0.171	4.65	0.015
	20	Monod	4620	0.04	0.14		0.015
	20		4620	0.04	0.139	3.85	0.015

Kinetic Parameters for Acetogenesis

Kinetic Parameters							
μ (d^{-1})	K_s (gCOD.m ⁻³)	Y (gVSS.gCOD ⁻¹)	u_{max} (day ⁻¹)	k (gCOD.gVSS ⁻¹ .d ⁻¹)	k_d (day ⁻¹)	K_i (gCOD.m ⁻³)	maintenance (gCOD.gVSS ⁻¹ .d ⁻¹)
	298		0.86				
	168	0.019		86.2 gCOD.g ⁻¹ .d ⁻¹	0.093		
	0.08	7.52	0.37		0.027		
	13	0.047	0.354	8.1	0.027		
	5	0.047		15.6	0.027		
	42	0.022		7.96 gCOD.g ⁻¹ .d ⁻¹	0.005		
	9	0.047		15.6 gCOD.g ⁻¹ .d ⁻¹	0.027		
			0.36				
	500	0.029	0.3696				
	13.28	0.004 mg.gCOD ⁻¹		0.0416 gCOD.mg ⁻¹ .d ⁻¹		1920	
	100		0.25				
	89		0.32				
	45.45		0.32				
	5.28	0.027 g dry cell.gCOD ⁻¹	2.304				3.456
	> 96		8.04				
	33.4		0.29				
	39.6		0.26				
	83.48		0.13				
	240		16.8				
		0.055 g.gCOD ⁻¹					
	12						
	800	1.568 g biomass.gCOD ⁻¹	0.08		0.01		
	32.9	0.012		37 gCOD.g ⁻¹ .d ⁻¹	0.105		
	16.65	0.066 g cell.gCOD ⁻¹	0.1296				
	500	0.066 g cell.gCOD ⁻¹	1.2				
	378		0.274				
	0.536	4.7	0.31		0.01		
			0.192				
			0.096				
	48.4		0.408				
	247	0.018	0.16		0.018	215 H ₂ S	
	15	0.043		6.46 gCOD.g ⁻¹ .d ⁻¹	0.092		
	48	0.042		9.6 gCOD.g ⁻¹ .d ⁻¹	0.01		
	60	0.042	0.313	7.7	0.01		
	17		0.13				
	500		1.2				
	32	0.042		9.6	0.01		
	2.196	2.8	0.155				
	246	0.025	0.115	6.2			
	10.23	5.72	0.36		0.04		
	1145	0.051	0.358	7.8	0.04		
	613	0.051		9.8	0.04		
			0.408				
			0.1296-1.2				
	800	0.014	0.3096				
	59.36	0.0033 mg.gCOD ⁻¹		0.0179 gCOD.mg ⁻¹ .d ⁻¹		192	
	27	0.042		3.5	0.021	25 H ₂ S	
	51.5		0.05				
	51.5		0.05				
		0.079 g.gCOD ⁻¹					
	500	0.029 g biomass.gCOD ⁻¹	0.23		0.01		
	166	0.03		17.1 gCOD.g ⁻¹ .d ⁻¹	0.099		
	166	0.03	0.414	17.1	0.099		
		0.03		17	0.099		
		0.015-0.025			0.02		
		0.064		2.85	0.06		

Parameters for Acetogenic Sulfidogenesis

Operational Parameters					
S (ppm)	Mode of Operation	pH	HRT (days)	Temp. (°C)	Culture
	lab scale sulfate adapted				
	lab scale non-sulfate adapted				
	full scale sulfate adapted				
	chemostat	7	2.0833	30	<i>Desulfovibrio postgatei</i> D.A41
	chemostat	7	2.0833	30	<i>Desulfovibrio propionicus</i> NS.P31
	chemostat	7	2.0833	30	<i>Desulfovibrio baculatus</i> H.L21
	batch and chemostat	7.1	0.36 - 4.52	28	<i>Desulfovibrio propionicus</i>
	batch and chemostat	7.1	0.91 - 1.77	28	<i>Desulfovibrio vulgaris</i> Marburg
	batch and chemostat	7.1	0.91 - 1.77	28	<i>Desulfovibrio</i> sp.
	lab scale sulfate adapted				
	lab scale non-sulfate adapted				
	full scale sulfate adapted				
100	fluidised bed	7.0 and 7.2		37	<i>Desulfovibrio</i> sp. strain L1
	batch and chemostat	7		35	<i>Desulfovibrio Desulfuricans</i> (ATCC 5575)
	batch and chemostat	7		30	<i>Desulfovibrio vulgaris</i> Hildenborough (NCIB 8303)
1000	Pkd Bed	6.6	0.27 - 0.39	25	<i>Desulfovibrio desulfuricans</i>
		7			<i>Desulfovibrio vulgaris</i>
15000		6.6			<i>Desulfovibrio</i> sp.
					<i>Desulfovibrio vulgaris</i>
					<i>Desulfotomaculum orientis</i>
	chemostat	7		43	<i>Desulfovibrio Desulfuricans</i> (ATCC 5575)
	chemostat	7		35	<i>Desulfovibrio Desulfuricans</i> (ATCC 5575)
	batch	6.0 - 8.5		37	<i>Desulfovibrio desulfuricans</i> (ATCC 7757)
		7		35	<i>Desulfovibrio desulfuricans</i> (ATCC 7757)
1000	batch and chemostat			35+-1	
1000	batch				
	full scale sulfate adapted				
	CSTR			35	
	batch and chemostat	7		30	<i>Desulfovibrio vulgaris</i> Hildenborough (NCIB 8303)
	chemostat	7		43	<i>Desulfovibrio Desulfuricans</i> (ATCC 5575)
	chemostat	7		35	<i>Desulfovibrio Desulfuricans</i> (ATCC 5575)
	batch	7.1+-0.5		30	<i>Desulfovibrio salexigens</i> marine sediment
	batch	7.1+-0.4		30	<i>Desulfovibrio sapovorans</i> fresh sediment
	batch	7.1+-0.3		30	<i>Desulfovibrio vulgaris</i> (Hildenborough) fresh sediment
	batch	7.1+-0.2		30	<i>Desulfovibrio vulgaris</i> (Marburg) fresh sediment
					<i>Desulfovibrio sapovorans</i> (DSM 2055)
					<i>Desulfococcus multivorans</i> (DSM 2059)
					<i>Desulfovibrio propionicus</i> (DSM 2032)

Parameters for Acetogenic Sulfidogenesis

Kinetic Parameters						
S (gCOD.m ⁻³)	Y	u_{max} (day ⁻¹)	k	k_d (day ⁻¹)	K_i (gCOD.m ⁻³)	maintenance (gCOD.g cells ⁻¹ .d ⁻¹)
5.455		0.15				
41.82		0.15				
72.73		0.13				
	0.031 g C.gCOD ⁻¹	3.12				
	0.01 g C.gCOD ⁻¹	1.92				
	0.016 g C.gCOD ⁻¹	2.4				
0.51	0.057 g dry cell.gCOD ⁻¹	1.152				2.0736
0.557	0.033 g dry cell.gCOD ⁻¹	1.392				9.91
1.344		2.52				
62.61		0.22				
62.61		0.19				
77.22		0.35				
144		6				
2.51		4.8			250 mg H ₂ S/l	
	0.07 g.gCOD ⁻¹					
1.49		8.88				
	0.127 g cells.gCOD ⁻¹					
	0.149 g cells.gCOD ⁻¹	optimum				
	0.12 gVSS.gCOD ⁻¹					
	0.04 gVSS.gCOD ⁻¹					
10.67	0.03 g cells.gCOD ⁻¹	13.2				7.168
2.35	0.0225 g cells.gCOD ⁻¹	8.88				11.52
	6.28 10 ¹³ cells /mol SO ₄					
2.4			4.5		many values for the two species	
7.9			3.3 gCOD.gVSS ⁻¹ .d ⁻¹	0.021	194 mg H ₂ S/l	
41	0.032 gVSS.gCOD ⁻¹	3.65				
51.46		0.81			285 mg H ₂ S/l	
295	0.035			0.018		
	0.126 g.gCOD ⁻¹					
	0.159 g cells.gCOD ⁻¹	8.448				50.688
	0.188 g cells.gCOD ⁻¹	8.256				30.72
	0.125 g dry wt.g SO ₄ ⁻¹		0.006 gCOD.mg dry wt. ⁻¹ .d ⁻¹			
	0.115 g dry wt.g SO ₄ ⁻¹		0.0018 gCOD.mg dry wt. ⁻¹ .d ⁻¹			
			0.0025 gCOD.mg dry wt. ⁻¹ .d ⁻¹			
	0.141 g dry wt.g SO ₄ ⁻¹		0.0035 gCOD.mg dry wt. ⁻¹ .d ⁻¹			
76.36		1.5				
146		0.35				
5.675		2.75				

68	Henze and Hammoes (1983)	acetate and sulfate	continuous batch	30	model acetate enrichment
69	Henze and Hammoes (1983)	raw animal waste	continuous batch	30	mixed
70	Henze and Hammoes (1983)	raw animal waste	continuous batch	30	acetate enrichment
71	Henze and Hammoes (1983)	raw animal waste	continuous batch	30	mixed culture
72	Henze and Hammoes (1983)	raw animal waste	continuous batch	30	mixed culture
73	Henze and Hammoes (1983)	raw animal waste	continuous batch	30	<i>Methanobacterium</i> sp.
74	Pavlostathis and Gralbo-Gomez (1991)	raw animal waste	continuous batch	30	<i>Methanosarcina barkeri</i>
75	Pavlostathis and Gralbo-Gomez (1991)	raw animal waste	continuous batch	30	fixed bed model
76	Pavlostathis and Gralbo-Gomez (1991)	raw animal waste	continuous batch	25	mixed anaerobic
77	Yoda <i>et al.</i> (1987)	raw animal waste	continuous batch	25	mixed culture
78	Joyaseelan (1997)	raw animal waste	continuous batch	25	acetate enrichment
79	Gujer and Zehnder (1983)	raw animal waste	continuous batch	20	mixed culture
80	Henze and Hammoes (1983)	raw animal waste	continuous batch	20	Mixed
81	Henze and Hammoes (1983)	raw animal waste	continuous batch	20	Mixed
82	Hill and Barn (1977)	raw animal waste	continuous batch	20	Mixed
83	Pavlostathis and Gralbo-Gomez (1991)	raw animal waste	continuous batch	20	methane phase
84	Joyaseelan (1997)	raw animal waste	continuous batch	20	mixed anaerobic
85	Henze and Hammoes (1983)	raw animal waste	continuous batch	20	mixed anaerobic
86	Pavlostathis and Gralbo-Gomez (1991)	raw animal waste	continuous batch	20	mixed anaerobic
87	Andrews and Graef (1971)	raw animal waste	continuous batch	20	theoretical
88	Buttore <i>et al.</i> (1995)	raw animal waste	continuous batch	20	model/mixed culture
89	Costello <i>et al.</i> (1981)	raw animal waste	continuous batch	20	model
90	Halper and Pohland (1968)	raw animal waste	continuous batch	20	Methanobrix pure culture
91	Henze and Hammoes (1983)	raw animal waste	continuous batch	20	Methanobrix pure culture
92	Henze and Hammoes (1983)	raw animal waste	continuous batch	20	Methanobrix pure culture
93	Henze and Hammoes (1983)	raw animal waste	continuous batch	20	Methanobrix pure culture
94	Henze and Hammoes (1983)	raw animal waste	continuous batch	20	Methanobrix pure culture
95	Henze and Hammoes (1983)	raw animal waste	continuous batch	20	Methanobrix pure culture
96	Henze and Hammoes (1983)	raw animal waste	continuous batch	20	Methanobrix pure culture
97	Isa <i>et al.</i> (1988)	raw animal waste	continuous batch	20	Methanobrix pure culture
98	Isa <i>et al.</i> (1988)	raw animal waste	continuous batch	20	Methanobrix pure culture
99	Joyaseelan (1997)	raw animal waste	continuous batch	20	Methanobrix pure culture
100	Lettinga (1995)	raw animal waste	continuous batch	20	Methanobrix pure culture
101	Lettinga (1995)	raw animal waste	continuous batch	20	Methanobrix pure culture
102	Lettinga (1995)	raw animal waste	continuous batch	20	Methanobrix pure culture
103	Lettinga (1995)	raw animal waste	continuous batch	20	Methanobrix pure culture
104	Lettinga (1995)	raw animal waste	continuous batch	20	Methanobrix pure culture
105	Lettinga (1995)	raw animal waste	continuous batch	20	Methanobrix pure culture
106	Lettinga (1995)	raw animal waste	continuous batch	20	Methanobrix pure culture
107	Mallachou and Pralain (1996)	raw animal waste	continuous batch	20	Methanobrix pure culture
108	Moletta <i>et al.</i> (1988)	raw animal waste	continuous batch	20	Methanobrix pure culture
109	O'Flaherty <i>et al.</i> (1998)	raw animal waste	continuous batch	20	Methanobrix pure culture
110	O'Flaherty <i>et al.</i> (1998)	raw animal waste	continuous batch	20	Methanobrix pure culture
111	O'Flaherty <i>et al.</i> (1998)	raw animal waste	continuous batch	20	Methanobrix pure culture
112	Oude Elferink <i>et al.</i> (1994)	raw animal waste	continuous batch	20	Methanobrix pure culture
113	Oude Elferink <i>et al.</i> (1994)	raw animal waste	continuous batch	20	Methanobrix pure culture
114	Oude Elferink <i>et al.</i> (1994)	raw animal waste	continuous batch	20	Methanobrix pure culture
115	Oude Elferink <i>et al.</i> (1994)	raw animal waste	continuous batch	20	Methanobrix pure culture
116	Oude Elferink <i>et al.</i> (1994)	raw animal waste	continuous batch	20	Methanobrix pure culture
117	Oude Elferink <i>et al.</i> (1994)	raw animal waste	continuous batch	20	Methanobrix pure culture
118	Oude Elferink <i>et al.</i> (1994)	raw animal waste	continuous batch	20	Methanobrix pure culture
119	Oude Elferink <i>et al.</i> (1994)	raw animal waste	continuous batch	20	Methanobrix pure culture
120	Wu <i>et al.</i> (1998)	raw animal waste	continuous batch	20	Methanobrix pure culture
121	Wu <i>et al.</i> (1998)	raw animal waste	continuous batch	20	Methanobrix pure culture
122	Wu <i>et al.</i> (1998)	raw animal waste	continuous batch	20	Methanobrix pure culture
123	Wu <i>et al.</i> (1998)	raw animal waste	continuous batch	20	Methanobrix pure culture
124	Wu <i>et al.</i> (1998)	raw animal waste	continuous batch	20	Methanobrix pure culture
125	Joyaseelan (1997)	raw animal waste	continuous batch	20	Methanobrix pure culture
126	O'Flaherty <i>et al.</i> (1998)	raw animal waste	continuous batch	20	Methanobrix pure culture
127	O'Flaherty <i>et al.</i> (1998)	raw animal waste	continuous batch	20	Methanobrix pure culture
128	Wu <i>et al.</i> (1998)	raw animal waste	continuous batch	20	Methanobrix pure culture

15	30, 45				
6 - 8					
120					
1.52					

Author(s) (Year)	Microorganism	Substrate	Yield (g)	Yield (g COD/g)	Yield (g cells/g COD)	Yield (g COD/g ¹ d ¹)	Yield (g COD/g ¹ d ¹)	Yield (g COD/g ¹ d ¹)	Yield (g COD/g ¹ d ¹)
67 Henze and Harremoens (1983)	<i>Monod</i>	uncompetitive VFA and ammonia inhibition	200	0.045-0.055	0.26	0.01-0.02			
68 Henze and Harremoens (1983)	<i>Monod</i>	uncompetitive VFA and ammonia inhibition	10	0.07-0.09	0.275	0.054	5.1		
69 Henze and Harremoens (1983)	<i>Monod</i>	uncompetitive VFA and ammonia inhibition	333	0.03-0.04	0.28	0.02	2.6-5.1		
70 Henze and Harremoens (1983)	<i>Monod</i>	uncompetitive VFA and ammonia inhibition				0.01	28		
71 Henze and Harremoens (1983)	<i>Monod</i>	uncompetitive VFA and ammonia inhibition				0.037	4.8		
72 Henze and Harremoens (1983)	<i>Monod</i>	uncompetitive VFA and ammonia inhibition				0.011			
73 Henze and Harremoens (1983)	<i>Monod</i>	uncompetitive VFA and ammonia inhibition							
74 Pavlostathis and Girardo-Gomez (1981)	<i>Monod</i>	uncompetitive VFA and ammonia inhibition	356	0.054	0.24	0.04			
75 Pavlostathis and Girardo-Gomez (1981)	<i>Monod</i>	uncompetitive VFA and ammonia inhibition	11	0.02	0.25	0.05	5		300 mg VFA/l, 5 mg NH ₄ -N/l
76 Pavlostathis and Girardo-Gomez (1981)	<i>Monod</i>	uncompetitive VFA and ammonia inhibition	192	0.01	0.26	0.011	4.7		
77 Yoda et al. (1987)	<i>Monod</i>	uncompetitive VFA and ammonia inhibition	333	0.054	0.24	0.037	4.8		
78 Jayswal (1983)	<i>Monod</i>	uncompetitive VFA and ammonia inhibition	14.53	3.2	0.24	0.011			
79 Gujer and Zahradk (1983)	<i>Monod</i>	uncompetitive VFA and ammonia inhibition	950						
80 Henze and Harremoens (1983)	<i>Monod</i>	uncompetitive VFA and ammonia inhibition	869						
81 Henze and Harremoens (1983)	<i>Monod</i>	uncompetitive VFA and ammonia inhibition	2400						
82 Hill and Barth (1977)	<i>Monod</i>	uncompetitive VFA and ammonia inhibition	2.13	0.0003 mol/gCOD ¹	0.4	0.04	2.8		42.7 mg VFA/l
83 Pavlostathis and Girardo-Gomez (1981)	<i>Monod</i>	uncompetitive VFA and ammonia inhibition	237	0.029	0.3398				
84 Jayswal (1987)	<i>Monod</i>	uncompetitive VFA and ammonia inhibition	184.48	0.0023 mg/gCOD ¹	0.43				0.01152 gCOD.mg ¹ .d ¹
85 Henze and Harremoens (1983)	<i>Monod</i>	uncompetitive VFA and ammonia inhibition	395						
86 Pavlostathis and Girardo-Gomez (1981)	<i>Monod</i>	uncompetitive VFA and ammonia inhibition	2	0.06	0.4	0.04			
87 Andrews and Great (1971)	<i>Monod</i>	uncompetitive VFA and ammonia inhibition	8-80	0.039	0.4	0.02			
88 Buffers et al. (1995)	<i>Monod</i>	uncompetitive VFA and ammonia inhibition	2	0.06	0.24				
89 Costello et al. (1991)	<i>Monod</i>	uncompetitive VFA and ammonia inhibition	2	0.04					
90 Harper and Poulard (1986)	<i>Monod</i>	uncompetitive VFA and ammonia inhibition	2	0.04					
91 Henze and Harremoens (1983)	<i>Monod</i>	uncompetitive VFA and ammonia inhibition	2	0.04					
92 Henze and Harremoens (1983)	<i>Monod</i>	uncompetitive VFA and ammonia inhibition	70	0.04					
93 Henze and Harremoens (1983)	<i>Monod</i>	uncompetitive VFA and ammonia inhibition	400	0.03	0.037				
94 Henze and Harremoens (1983)	<i>Monod</i>	uncompetitive VFA and ammonia inhibition	28	0.038	0.138				
95 Henze and Harremoens (1983)	<i>Monod</i>	uncompetitive VFA and ammonia inhibition	3.2	0.769	0.1				110 mg H ₂ S/l
96 Henze and Harremoens (1983)	<i>Monod</i>	uncompetitive VFA and ammonia inhibition	37.33	0.18-0.023	0.1				42.87 mg H ₂ S/l
97 Isa et al. (1988)	<i>Monod</i>	uncompetitive VFA and ammonia inhibition	37.33	0.023	0.1				
98 Isa et al. (1988)	<i>Monod</i>	uncompetitive VFA and ammonia inhibition	14.83	0.035	0.08				
99 Jayswal (1987)	<i>Monod</i>	uncompetitive VFA and ammonia inhibition	0.32	0.03 - 0.053 g cells/gCOD ¹	0.46-0.69				
100 Lettinga (1995)	<i>Monod</i>	uncompetitive VFA and ammonia inhibition		0.025 g cells/gCOD ¹	0.5				
101 Lettinga (1995)	<i>Monod</i>	uncompetitive VFA and ammonia inhibition		0.030313 g cells/gCOD ¹	0.49-0.52				
102 Lettinga (1995)	<i>Monod</i>	uncompetitive VFA and ammonia inhibition		0.030313 g cells/gCOD ¹	0.53				
103 Lettinga (1995)	<i>Monod</i>	uncompetitive VFA and ammonia inhibition		0.0172 - 0.022 g cells/gCOD ¹	0.08-0.29				
104 Lettinga (1995)	<i>Monod</i>	uncompetitive VFA and ammonia inhibition		0.0172 - 0.022 g cells/gCOD ¹	0.19				
105 Lettinga (1995)	<i>Monod</i>	uncompetitive VFA and ammonia inhibition		0.0172 - 0.022 g cells/gCOD ¹	0.21-0.69				
106 Lettinga (1995)	<i>Monod</i>	uncompetitive VFA and ammonia inhibition		0.0172 - 0.022 g cells/gCOD ¹	0.19				
107 Malachukwu and Pardon (1996)	<i>Monod</i>	uncompetitive VFA and ammonia inhibition		0.0172 - 0.022 g cells/gCOD ¹	0.21-0.69				
108 Molesta et al. (1988)	<i>Monod</i>	uncompetitive VFA and ammonia inhibition		0.0172 - 0.022 g cells/gCOD ¹	0.19				
109 O'Flaherty et al. (1998)	<i>Monod</i>	uncompetitive VFA and ammonia inhibition		0.0172 - 0.022 g cells/gCOD ¹	0.21-0.69				
110 O'Flaherty et al. (1998)	<i>Monod</i>	uncompetitive VFA and ammonia inhibition		0.0172 - 0.022 g cells/gCOD ¹	0.19				
111 O'Flaherty et al. (1998)	<i>Monod</i>	uncompetitive VFA and ammonia inhibition		0.0172 - 0.022 g cells/gCOD ¹	0.21-0.69				
112 Oude Elferink et al. (1994)	<i>Monod</i>	uncompetitive VFA and ammonia inhibition		0.0172 - 0.022 g cells/gCOD ¹	0.19				
113 Oude Elferink et al. (1994)	<i>Monod</i>	uncompetitive VFA and ammonia inhibition		0.0172 - 0.022 g cells/gCOD ¹	0.21-0.69				
114 Oude Elferink et al. (1994)	<i>Monod</i>	uncompetitive VFA and ammonia inhibition		0.0172 - 0.022 g cells/gCOD ¹	0.19				
115 Oude Elferink et al. (1994)	<i>Monod</i>	uncompetitive VFA and ammonia inhibition		0.0172 - 0.022 g cells/gCOD ¹	0.21-0.69				
116 Oude Elferink et al. (1994)	<i>Monod</i>	uncompetitive VFA and ammonia inhibition		0.0172 - 0.022 g cells/gCOD ¹	0.19				
117 Oude Elferink et al. (1994)	<i>Monod</i>	uncompetitive VFA and ammonia inhibition		0.0172 - 0.022 g cells/gCOD ¹	0.21-0.69				
118 Oude Elferink et al. (1994)	<i>Monod</i>	uncompetitive VFA and ammonia inhibition		0.0172 - 0.022 g cells/gCOD ¹	0.19				
119 Oude Elferink et al. (1994)	<i>Monod</i>	uncompetitive VFA and ammonia inhibition		0.0172 - 0.022 g cells/gCOD ¹	0.21-0.69				
120 Wu et al. (1998)	<i>Monod</i>	uncompetitive VFA and ammonia inhibition	830	0.01-0.054	0.55				
121 Wu et al. (1998)	<i>Monod</i>	uncompetitive VFA and ammonia inhibition	650	0.01-0.054	0.15				
122 Wu et al. (1998)	<i>Monod</i>	uncompetitive VFA and ammonia inhibition	180	0.01-0.054	0.15				
123 Wu et al. (1998)	<i>Monod</i>	uncompetitive VFA and ammonia inhibition	720	0.01-0.054	0.15				
124 Wu et al. (1998)	<i>Monod</i>	uncompetitive VFA and ammonia inhibition	512	0.01-0.054	0.15				
125 Jayswal (1997)	<i>Monod</i>	uncompetitive VFA and ammonia inhibition	11-421	0.01-0.054	0.15				
126 O'Flaherty et al. (1998)	<i>Monod</i>	uncompetitive VFA and ammonia inhibition	119-47	0.01-0.054	0.15				
127 O'Flaherty et al. (1998)	<i>Monod</i>	uncompetitive VFA and ammonia inhibition	27-73	0.01-0.054	0.15				
128 Wu et al. (1998)	<i>Monod</i>	uncompetitive VFA and ammonia inhibition	640	0.01-0.054	0.15				

Parameters for Acetoclastic Sulfidogenesis

Operational Parameters				
Mode of Operation	pH	HRT (days)	Temp. (°C)	Culture
Batch+Chemostat	7	10	35	Mixed
Batch+Chemostat	7	10	35	<i>Desulfobacter postgatei</i>
Batch+Chemostat	7	10	35	<i>Desulfobacter postgatei</i>
Batch+Chemostat	7	10	35	SRB Biofilm
Batch+Chemostat	7	10	35	SRB
			35	
Batch and continuous			31	
Biofilm	7.0±0.1		30	
Chemostat - sulfate limiting	7.2	4.16667	30	<i>Desulfobacter postgatei</i> (DSM 2034)
Chemostat - acetate limiting	7.2	4.16667	30	<i>Desulfobacter postgatei</i> (DSM 2034)
			30	<i>Desulfobacter postgatei</i>
			30	<i>Desulfobacter postgatei</i>
			30	<i>Desulfobacter postgatei</i>
			30	<i>Desulfobacter postgatei</i>
Batch and continuous			25	
Batch and continuous			20	
				Digester sludge
				<i>Desulfobacter postgatei</i>
				<i>Desulfobacter postgatei</i>
Batch				<i>Desulfobacter postgatei</i>
				<i>Desulfobacter curvatus</i>
				<i>Desulfobacter latus</i>
				<i>Desulfobacter hydrogenophilus</i>
				<i>Desulfotomaculum acetoxidans</i>
				<i>Desulfobacterium</i> sp.
CSTR			35	
Chemostat - sulfate limiting	7.2	4.16667	30	<i>Desulfobacter postgatei</i> (DSM 2034)
Chemostat - acetate limiting	7.2	4.16667	30	<i>Desulfobacter postgatei</i> (DSM 2034)
Batch	7.2	4.16667	30	<i>Desulfobacter postgatei</i> (DSM 2034)
				<i>Desulfobacter postgatei</i> (DSM 2034)
				<i>Desulfotomaculum acetoxidans</i> (DSM 771)
				<i>Desulfonema magnum</i> (DSM 2077)

Parameters for Acetoclastic Sulfidogenesis

Kinetic Parameters						
K_s (g sulfate.m ⁻³)	K_s (gCOD.m ⁻³)	Y (gVSS.gCOD ⁻¹)	U_{max} (day ⁻¹)	k (gCOD.gVSS ⁻¹ .d ⁻¹)	k_d (day ⁻¹)	K_i (gCOD.m ⁻³)
	10.13 12.8			0.004832 gCOD.mg cells ⁻¹ .d ⁻¹ 0.000992 gCOD.mg cells ⁻¹ .d ⁻¹ 0.00256 gCOD.mg cells ⁻¹ .d ⁻¹		
	108.8 0.896 6.08 10.13	5.64 10 ⁻⁵ mg .gCOD ⁻¹ 0.0094 g cell COD .gCOD ⁻¹ 0.061 g .gCOD ⁻¹ 0.015 g .gCOD ⁻¹	0.015	8.3 gCOD.g cells ⁻¹ .d ⁻¹ 0.992 gCOD.g cells ⁻¹ .d ⁻¹ 0.0047616gCOD.g dry wt. ⁻¹ .d ⁻¹ 0.0049152 gCOD.g dry wt. ⁻¹ .d ⁻¹	0.0016	
	4.1 4.9 4.8 12.8 98.13 266.67	0.068 g .gCOD ⁻¹	0.72	4.76 gCOD.g cells ⁻¹ .d ⁻¹ 4.92 gCOD.g cells ⁻¹ .d ⁻¹ 4.832 gCOD.g cells ⁻¹ .d ⁻¹		
	13 4	0.061g .gCOD ⁻¹ 0.061g .gCOD ⁻¹ 0.05	8.3	7.1 gCOD.g cells ⁻¹ .d ⁻¹ 5 gCOD.g cells ⁻¹ .d ⁻¹		
	50	0.023		4.6	0.013	8 mg H ₂ S/l
		0.0672 - 0.075 g .gCOD ⁻¹	0.72-1.11	4.88 gCOD.g cells ⁻¹ .d ⁻¹		
			0.79 0.79 0.92			
		0.0875 g .gCOD ⁻¹	0.65-1.39			
19.2	24	0.041	<<0.7 0.51		0.025	285 mg H ₂ S/l
20	12.8		0.93			
40	106.67		1.5			
45	128		0.43			

Parameters for Hydrogenotrophic Sulfidogenesis

Operational Parameters					
Sulfate (ppm)	Mode of Operation	pH	HRT (days)	Temp. (°C)	Culture
100-3000	lab scale non-sulfate adapted	6.5		25 and 35	
	full scale sulfate adapted				
	UASB				
3850	batch			37	<i>Desulfovibrio vulgaris</i>
3850	batch			37	<i>Desulfovibrio desulfuricans</i>
3850	batch			37	<i>Desulfovibrio desulfuricans</i> G11
3850	batch			37	<i>Desulfovibrio desulfuricans</i> PS1
3850	batch			37	<i>Desulfovibrio desulfuricans</i> DG2
3850	batch			37	<i>Desulfovibrio</i> G11
3850	batch			37	<i>Desulfovibrio</i> PS1
3850	batch			37	<i>Desulfovibrio</i> DG2
3850	batch			37	<i>Desulfovibrio desulfuricans</i>
3850	batch			37	<i>Desulfovibrio vulgaris</i>
3850	batch			37	<i>Desulfovibrio</i> G11
3850	batch			37	<i>Desulfovibrio</i> G11
3850	batch			37	sulfate reducers <i>Desulfovibrio vulgaris</i> <i>Desulfovibrio vulgaris</i> <i>Desulfovibrio vulgaris</i> Lake sediment
120	batch				<i>Desulfovibrio strain</i> G11 <i>Desulfovibrio strain</i> PS1 <i>Desulfovibrio strain</i> DG2 <i>Desulfovibrio vulgaris strain</i> <i>Desulfovibrio vulgaris</i> (Marburg) <i>Desulfovibrio vulgaris</i> (Madison) <i>Desulfovibrio desulfuricans strain</i> <i>Desulfovibrio desulfuricans</i> BZS <i>Desulfovibrio desulfuricans strain</i> <i>Desulfovibrio desulfuricans strain</i> <i>Desulfovibrio desulfuricans strain</i> <i>Desulfobacter hydrogenophilus</i> <i>Desulfobacterium autotrophicum</i> <i>Desulfobulbus propionicus</i> 1p3 <i>Desulfobulbus propionicus</i>
	CSTR			35	
	chemostat		6.25	35	<i>Desulfovibrio vulgaris</i> (Marburg) <i>Desulfovibrio vulgaris</i> (DSM 2119)

Parameters for Hydrogenotrophic Sulfidogenesis

Kinetic Parameters

μ (d ⁻¹)	K_s (g sulfate.m ⁻³)	K_s (gCOD.m ⁻³)	Y (gVSS.gCOD ⁻¹)	u_{max} (day ⁻¹)	k (gCOD.gVSS ⁻¹ .d ⁻¹)	K_j (day ⁻¹)	K_i (gCOD.m ⁻³)
	15	0.0168		1.12			
	12	0.016		3.17			
		0.03			1.792 gCOD.g ⁻¹ .d ⁻¹		
		0.029			0.63 gCOD.g ⁻¹ .d ⁻¹		
		0.018			2.03 gCOD.g ⁻¹ .d ⁻¹		
		0.011			1.27 gCOD.g ⁻¹ .d ⁻¹		
		0.022			1.27 gCOD.g ⁻¹ .d ⁻¹		
					0.54 gCOD.g ⁻¹ .d ⁻¹		
					0.0025 gCOD.g protein ⁻¹ .d ⁻¹		
					0.0025 gCOD.g protein ⁻¹ .d ⁻¹		
					0.00108 gCOD.g protein ⁻¹ .d ⁻¹		
					0.004055 gCOD.g protein ⁻¹ .d ⁻¹		
					0.00136 gCOD.g protein ⁻¹ .d ⁻¹		
		0.0667	0.044 g protein.gCOD ⁻¹	1.5696			
		0.0387	0.062 g protein.gCOD ⁻¹	1.1688			
		0.0528	5.31 g protein.gCOD ⁻¹	1.368	0.0025 gCOD.g protein ⁻¹ .d ⁻¹		
			0.086 g cells.gCOD ⁻¹	optimum			
			0.09	3.6			
			0.15	5			
	0.001atm						
	1.6.10 ⁻⁴ atm		0.041		4.4	0.013	140 mg H ₂ S/l
	0.0384-0.0672		0.0875 - 0.125 g cells.gCOD ⁻¹	1.2-1.6	1.4976 gCOD.g ⁻¹ .d ⁻¹		
					1.4976 gCOD.g ⁻¹ .d ⁻¹		
					0.52992 gCOD.g ⁻¹ .d ⁻¹		
					0.6912 gCOD.g ⁻¹ .d ⁻¹		
			0.069 - 0.16 g cells.gCOD ⁻¹	3.6-5.5			
			0.037 - 0.069 g cells.gCOD ⁻¹	0.7-5.5			
					2.02752 gCOD.g ⁻¹ .d ⁻¹		
			0.119 g cells.gCOD ⁻¹	2.6			
				2.8-4.3			
				0.98			
				0.83-1.04			
				1.66			
				0.23-0.59			
	0.9	0.05	0.077	5		0.03	550 mg H ₂ S/l
		0.0208					
	0.5	0.032		4.22			

Parameters for Other Miscellaneous Reactions

		Kinetic Parameters				
Culture	Model description	V_{max} (gCOD.m ⁻³ .d ⁻¹)	K_s (g sulfate.m ⁻³)	K_s (gCOD.m ⁻³)	Y (g cell COD.gCOD ⁻¹)	k (gCOD.g ⁻¹ .d ⁻¹)
		1120			0.719	
	Monod	417		770		
		1440		8.01	0.113	
		960		3.84	0.06	
<i>Mosarcina</i> sp.	Monod	1440		8010		
		688.644			0.230017	
mem from raw sewage	Michaelis- Menten		0.1344			1.728

Parameters for Other Miscellaneous Reactions

Kinetic Parameters						
Culture	Model description	V_{max} (gCOD.m ⁻³ .d ⁻¹)	K_s (g sulfate.m ⁻³)	K_s (gCOD.m ⁻³)	Y (g cell COD.gCOD ⁻¹)	k (gCOD.g ⁻¹ .d ⁻¹)
<i>Mycobacterium</i> sp.	Monod	1120			0.719	
		417		770		
	Monod	1440		8.01	0.113	
		960		3.84	0.06	
		1440		8010		
688.644			0.230017			
em from raw sewage	Michaelis- Menten		0.1344			1.728

Parameters for Hydrogenotrophic Sulfidogenesis

Kinetic Parameters

μ (d ⁻¹)	K_s (g sulfate.m ⁻³)	K_s (gCOD.m ⁻³)	Y (gVSS.gCOD ⁻¹)	U_{max} (day ⁻¹)	k (gCOD.gVSS ⁻¹ .d ⁻¹)	k_d (day ⁻¹)	K_i (gCOD.m ⁻³)
	15	0.0168		1.12			
	12	0.016		3.17			
		0.03			1.792 gCOD.g ⁻¹ .d ⁻¹		
		0.029			0.63 gCOD.g ⁻¹ .d ⁻¹		
		0.018			2.03 gCOD.g ⁻¹ .d ⁻¹		
		0.011			1.27 gCOD.g ⁻¹ .d ⁻¹		
		0.022			1.27 gCOD.g ⁻¹ .d ⁻¹		
					0.54 gCOD.g ⁻¹ .d ⁻¹		
					0.0025 gCOD.g protein ⁻¹ .d ⁻¹		
					0.0025 gCOD.g protein ⁻¹ .d ⁻¹		
					0.00108 gCOD.g protein ⁻¹ .d ⁻¹		
					0.004055 gCOD.g protein ⁻¹ .d ⁻¹		
					0.00136 gCOD.g protein ⁻¹ .d ⁻¹		
		0.0667	0.044 g protein.gCOD ⁻¹	1.5696			
		0.0387	0.062 g protein.gCOD ⁻¹	1.1688			
		0.0528	5.31 g protein.gCOD ⁻¹	1.368	0.0025 gCOD.g protein ⁻¹ .d ⁻¹		
			0.086 g cells.gCOD ⁻¹	optimum			
			0.09	3.6			
			0.15	5			
		0.001atm					
		1.6.10-4 atm	0.041		4.4		0.013
		0.0384-0.0672	0.0875 - 0.125 g cells.gCOD ⁻¹	1.2-1.6	1.4976 gCOD.g ⁻¹ .d ⁻¹		140 mg H ₂ S/l
					1.4976 gCOD.g ⁻¹ .d ⁻¹		
					0.52992 gCOD.g ⁻¹ .d ⁻¹		
					0.6912 gCOD.g ⁻¹ .d ⁻¹		
			0.069 - 0.16 g cells.gCOD ⁻¹	3.6-5.5			
			0.037 - 0.069 g cells.gCOD ⁻¹	0.7-5.5			
			0.119 g cells.gCOD ⁻¹	2.6	2.02752 gCOD.g ⁻¹ .d ⁻¹		
				2.8-4.3			
				0.98			
				0.83-1.04			
				1.66			
				0.23-0.59			
	0.9	0.05	0.077	5		0.03	550 mg H ₂ S/l
		0.0208					
	0.5	0.032		4.22			

Parameters for Hydrogenotrophic Sulfidogenesis

Operational Parameters

Sulfate (ppm)	Mode of Operation	pH	HRT (days)	Temp. (°C)	Culture
100-3000	lab scale non-sulfate adapted full scale sulfate adapted UASB			25 and 35 37 37 37 37 37	<i>Desulfovibrio vulgaris</i> <i>Desulfovibrio desulfuricans</i> <i>Desulfovibrio desulfuricans</i> G11 <i>Desulfovibrio desulfuricans</i> PS1 <i>Desulfovibrio desulfuricans</i> DG2
3850	batch			37	<i>Desulfovibrio</i> G11
3850	batch			37	<i>Desulfovibrio</i> PS1
3850	batch			37	<i>Desulfovibrio</i> DG2
3850	batch			37	<i>Desulfovibrio desulfuricans</i>
3850	batch			37	<i>Desulfovibrio vulgaris</i>
3850	batch			37	<i>Desulfovibrio</i> G11
3850	batch			37	<i>Desulfovibrio</i> G11
3850	batch	6.5		37	sulfate reducers <i>Desulfovibrio vulgaris</i> <i>Desulfovibrio vulgaris</i> <i>Desulfovibrio vulgaris</i> Lake sediment
120	batch				<i>Desulfovibrio strain</i> G11 <i>Desulfovibrio strain</i> PS1 <i>Desulfovibrio strain</i> DG2 <i>Desulfovibrio vulgaris strain</i> <i>Desulfovibrio vulgaris</i> (Marburg) <i>Desulfovibrio vulgaris</i> (Madison) <i>Desulfovibrio desulfuricans strain</i> <i>Desulfovibrio desulfuricans</i> BZS <i>Desulfovibrio desulfuricans strain</i> <i>Desulfovibrio desulfuricans strain</i> <i>Desulfobacter hydrogenophilus</i> <i>Desulfobacterium autotrophicum</i> <i>Desulfobulbus propionicus</i> 1p3 <i>Desulfobulbus propionicus</i>
	CSTR chemostat		6.25	35 35	<i>Desulfovibrio vulgaris</i> (Marburg) <i>Desulfovibrio vulgaris</i> (DSM 2119)

Parameters for Acetoclastic Sulfidogenesis

Kinetic Parameters

K_s (g sulfate.m ⁻³)	K_s (gCOD.m ⁻³)	Y (gVSS.gCOD ⁻¹)	U_{max} (day ⁻¹)	k (gCOD.gVSS ⁻¹ .d ⁻¹)	k_d (day ⁻¹)	K_i (gCOD.m ⁻³)
	10.13 12.8			0.004832 gCOD.mg cells ⁻¹ .d ⁻¹ 0.000992 gCOD.mg cells ⁻¹ .d ⁻¹ 0.00256 gCOD.mg cells ⁻¹ .d ⁻¹		
	108.8 0.896 6.08 10.13	5.64 10 ⁻⁵ mg .gCOD ⁻¹ 0.0094 g cell COD .gCOD ⁻¹ 0.061 g .gCOD ⁻¹ 0.015 g .gCOD ⁻¹	0.015	8.3 gCOD.g cells ⁻¹ .d ⁻¹ 0.992 gCOD.g cells ⁻¹ .d ⁻¹ 0.0047616gCOD.g dry wt. ⁻¹ .d ⁻¹ 0.0049152 gCOD.g dry wt. ⁻¹ .d ⁻¹ 4.76 gCOD.g cells ⁻¹ .d ⁻¹ 4.92 gCOD.g cells ⁻¹ .d ⁻¹ 4.832 gCOD.g cells ⁻¹ .d ⁻¹	0.0016	
	4.1 4.9 4.8 12.8 98.13 266.67	0.068 g .gCOD ⁻¹ 0.061g .gCOD ⁻¹ 0.061g .gCOD ⁻¹ 0.05	0.72 8.3	7.1 gCOD.g cells ⁻¹ .d ⁻¹ 5 gCOD.g cells ⁻¹ .d ⁻¹		
	13 4					
	50	0.023		4.6	0.013	8 mg H ₂ S/l
		0.0672 - 0.075 g .gCOD ⁻¹	0.72-1.11	4.88 gCOD.g cells ⁻¹ .d ⁻¹		
			0.79 0.79 0.92			
		0.0875 g .gCOD ⁻¹	0.65-1.39			
19.2	24	0.041	<<0.7 0.51		0.025	285 mg H ₂ S/l
20	12.8		0.93			
40	106.67		1.5			
45	128		0.43			

Parameters for Acetoclastic Sulfidogenesis

Operational Parameters				
Mode of Operation	pH	HRT (days)	Temp. (°C)	Culture
Batch+Chemostat	7	10	35	Mixed
Batch+Chemostat	7	10	35	<i>Desulfobacter postgatei</i>
Batch+Chemostat	7	10	35	<i>Desulfobacter postgatei</i>
Batch+Chemostat	7	10	35	SRB Biofilm
Batch+Chemostat	7	10	35	SRB
			35	
Batch and continuous			31	
Biofilm	7.0±0.1		30	
Chemostat - sulfate limiting	7.2	4.16667	30	<i>Desulfobacter postgatei</i> (DSM 2034)
Chemostat - acetate limiting	7.2	4.16667	30	<i>Desulfobacter postgatei</i> (DSM 2034)
			30	<i>Desulfobacter postgatei</i>
			30	<i>Desulfobacter postgatei</i>
			30	<i>Desulfobacter postgatei</i>
			30	<i>Desulfobacter postgatei</i>
Batch and continuous			25	
Batch and continuous			20	
				Digester sludge
				<i>Desulfobacter postgatei</i>
				<i>Desulfobacter postgatei</i>
Batch				<i>Desulfobacter postgatei</i>
				<i>Desulfobacter curvatus</i>
				<i>Desulfobacter latus</i>
				<i>Desulfobacter hydrogenophilus</i>
				<i>Desulfotomaculum acetoxidans</i>
				<i>Desulfobacterium</i> sp.
DCSTR			35	
Chemostat - sulfate limiting	7.2	4.16667	30	<i>Desulfobacter postgatei</i> (DSM 2034)
Chemostat - acetate limiting	7.2	4.16667	30	<i>Desulfobacter postgatei</i> (DSM 2034)
Batch	7.2	4.16667	30	<i>Desulfobacter postgatei</i> (DSM 2034)
				<i>Desulfobacter postgatei</i> (DSM 2034)
				<i>Desulfotomaculum acetoxidans</i> (DSM 771)
				<i>Desulfonema magnum</i> (DSM 2077)

Parameters for Acetogenic Sulfidogenesis

Kinetic Parameters						
μ (day ⁻¹)	Y	U_{max} (day ⁻¹)	k	k_d (day ⁻¹)	K_i (gCOD.m ⁻³)	maintenance (gCOD.g cells ⁻¹ .d ⁻¹)
5.455		0.15				
41.82		0.15				
72.73		0.13				
	0.031 g C.gCOD ⁻¹	3.12				
	0.01 g C.gCOD ⁻¹	1.92				
	0.016 g C.gCOD ⁻¹	2.4				
0.51	0.057 g dry cell.gCOD ⁻¹	1.152				2.0736
0.557	0.033 g dry cell.gCOD ⁻¹	1.392				9.91
1.344		2.52				
62.61		0.22				
62.61		0.19				
77.22		0.35				
144		6				
2.51		4.8			250 mg H ₂ S/l	
	0.07 g.gCOD ⁻¹					
1.49		8.88				
	0.127 g cells.gCOD ⁻¹					
	0.149 g cells.gCOD ⁻¹	optimum				
	0.12 gVSS.gCOD ⁻¹					
	0.04 gVSS.gCOD ⁻¹					
10.67	0.03 g cells.gCOD ⁻¹	13.2				7.168
2.35	0.0225 g cells.gCOD ⁻¹	8.88				11.52
	6.28 10 ¹³ cells /mol SO ₄					
2.4			4.5		many values for the two species	
7.9						
41	0.032 gVSS.gCOD ⁻¹		3.3 gCOD.gVSS ⁻¹ .d ⁻¹	0.021	194 mg H ₂ S/l	
51.46		3.65				
295	0.035	0.81		0.018	285 mg H ₂ S/l	
	0.126 g.gCOD ⁻¹					
	0.159 g cells.gCOD ⁻¹	8.448				50.688
	0.188 g cells.gCOD ⁻¹	8.256				30.72
	0.125 g dry wt.g SO ₄ ⁻¹		0.006 gCOD.mg dry wt. ⁻¹ .d ⁻¹			
	0.115 g dry wt.g SO ₄ ⁻¹		0.0018 gCOD.mg dry wt. ⁻¹ .d ⁻¹			
			0.0025 gCOD.mg dry wt. ⁻¹ .d ⁻¹			
	0.141 g dry wt.g SO ₄ ⁻¹		0.0035 gCOD.mg dry wt. ⁻¹ .d ⁻¹			
76.36		1.5				
146		0.35				
5.675		2.75				

Parameters for Acetogenic Sulfidogenesis

Operational Parameters					
S (ppm)	Mode of Operation	pH	HRT (days)	Temp. (°C)	Culture
	lab scale sulfate adapted				
	lab scale non-sulfate adapted				
	full scale sulfate adapted				
	chemostat	7	2.0833	30	<i>Desulfobacter postgatei</i> D.A41
	chemostat	7	2.0833	30	<i>Desulfobulbus propionicus</i> NS.P31
	chemostat	7	2.0833	30	<i>Desulfovibrio baculatus</i> H.L21
	batch and chemostat	7.1	0.36 - 4.52	28	<i>Desulfobulbus propionicus</i>
	batch and chemostat	7.1	0.91 - 1.77	28	<i>Desulfovibrio vulgaris</i> Marburg
	batch and chemostat	7.1	0.91 - 1.77	28	<i>Desulfovibrio</i> sp.
	lab scale sulfate adapted				
	lab scale non-sulfate adapted				
	full scale sulfate adapted				
100	fluidised bed	7.0 and 7.2		37	<i>Desulfovibrio</i> sp. strain L1
	batch and chemostat	7		35	<i>Desulfovibrio Desulfuricans</i> (ATCC 5575)
	batch and chemostat	7		30	<i>Desulfovibrio vulgaris</i> Hildenborough (NCIB 8303)
20	Pkd Bed	6.6	0.27 - 0.39	25	<i>Desulfovibrio desulfuricans</i>
		7			<i>Desulfovibrio vulgaris</i>
15000		6.6			<i>Desulfovibrio</i> sp.
					<i>Desulfovibrio vulgaris</i>
					<i>Desulfotomaculum orientis</i>
	chemostat	7		43	<i>Desulfovibrio Desulfuricans</i> (ATCC 5575)
	chemostat	7		35	<i>Desulfovibrio Desulfuricans</i> (ATCC 5575)
	batch	6.0 - 8.5		37	<i>Desulfovibrio desulfuricans</i> (ATCC 7757)
		7		35	<i>Desulfovibrio desulfuricans</i> (ATCC 7757)
100	batch and chemostat			35+-1	
20	batch				
	full scale sulfate adapted				
	CSTR			35	
	batch and chemostat	7		30	<i>Desulfovibrio vulgaris</i> Hildenborough (NCIB 8303)
	chemostat	7		43	<i>Desulfovibrio Desulfuricans</i> (ATCC 5575)
	chemostat	7		35	<i>Desulfovibrio Desulfuricans</i> (ATCC 5575)
	batch	7.1+-0.5		30	<i>Desulfovibrio saloxigens</i> marine sediment
	batch	7.1+-0.4		30	<i>Desulfovibrio sapovorans</i> fresh sediment
	batch	7.1+-0.3		30	<i>Desulfovibrio vulgaris</i> (Hildenborough) fresh sediment
	batch	7.1+-0.2		30	<i>Desulfovibrio vulgaris</i> (Marburg) fresh sediment
					<i>Desulfovibrio sapovorans</i> (DSM 2055)
					<i>Desulfococcus multivorans</i> (DSM 2059)
					<i>Desulfobulbus propionicus</i> (DSM 2032)

Kinetic Parameters for Acetogenesis

Kinetic Parameters							
$\mu^{-1} \cdot d^{-1}$	K_s (gCOD.m ⁻³)	Y (gVSS.gCOD ⁻¹)	u_{max} (day ⁻¹)	k (gCOD.gVSS ⁻¹ .d ⁻¹)	k_d (day ⁻¹)	K_i (gCOD.m ⁻³)	maintenance (gCOD.gVSS ⁻¹ .d ⁻¹)
	298		0.86				
	168	0.019		86.2 gCOD.g ⁻¹ .d ⁻¹	0.093		
	0.08	7.52	0.37		0.027		
	13	0.047	0.354	8.1	0.027		
	5	0.047		15.6	0.027		
	42	0.022		7.96 gCOD.g ⁻¹ .d ⁻¹	0.005		
	9	0.047		15.6 gCOD.g ⁻¹ .d ⁻¹	0.027		
			0.36				
	500	0.029	0.3696				
	13.28	0.004 mg.gCOD ⁻¹		0.0416 gCOD.mg ⁻¹ .d ⁻¹		1920	
	100		0.25				
	89		0.32				
	45.45		0.32				
	5.28	0.027 g dry cell.gCOD ⁻¹	2.304				3.456
	> 96		8.04				
	33.4		0.29				
	39.6		0.26				
	83.48		0.13				
	240		16.8				
		0.055 g.gCOD ⁻¹					
	12						
	800	1.568 g biomass.gCOD ⁻¹	0.08		0.01		
	32.9	0.012		37 gCOD.g ⁻¹ .d ⁻¹	0.105		
	16.65	0.066 g cell.gCOD ⁻¹	0.1296				
	500	0.066 g cell.gCOD ⁻¹	1.2				
	378		0.274				
	0.536	4.7	0.31		0.01		
			0.192				
			0.096				
	48.4		0.408				
	247	0.018	0.16		0.018	215 H ₂ S	
	15	0.043		6.46 gCOD.g ⁻¹ .d ⁻¹	0.092		
	48	0.042		9.6 gCOD.g ⁻¹ .d ⁻¹	0.01		
	60	0.042	0.313	7.7	0.01		
	17		0.13				
	500		1.2				
	32	0.042		9.6	0.01		
	2.196	2.8	0.155				
	246	0.025	0.115	6.2			
	10.23	5.72	0.36		0.04		
	1145	0.051	0.358	7.8	0.04		
	613	0.051		9.8	0.04		
			0.408				
			0.1296-1.2				
	800	0.014	0.3096				
	59.36	0.0033 mg.gCOD ⁻¹		0.0179 gCOD.mg ⁻¹ .d ⁻¹		192	
	27	0.042		3.5	0.021	25 H ₂ S	
	51.5		0.05				
	51.5		0.05				
		0.079 g.gCOD ⁻¹					
	500	0.029 g biomass.gCOD ⁻¹	0.23		0.01		
	166	0.03		17.1 gCOD.g ⁻¹ .d ⁻¹	0.099		
	166	0.03	0.414	17.1	0.099		
		0.03		17	0.099		
		0.015-0.025			0.02		
		0.064		2.85	0.06		

Parameters for Anaerobic Oxidation

Parameters		Kinetic Parameters					
Reaction	Temp. (°C)	Model description	K_s (gCOD.m ⁻³)	Y (gVSS.gCOD ⁻¹)	U_{max} (day ⁻¹)	k (gCOD.gVSS ⁻¹ .d ⁻¹)	K_d (day ⁻¹)
	37	Monod	1816	0.11	0.56		0.01
	37		1816	0.11	0.55	5	0.01
	37		105	0.11	0.105	0.95	0.01
	37	Monod	105	0.11	0.11		0.01
	37	Monod	3180	0.11	0.45		0.01
	37		3180	0.11	0.44	4	0.01
	37	Monod	143	0.11	0.12		0.01
	37		143	0.11	0.11	1	0.01
	37	Monod	417	0.11	0.1		0.01
	37		417	0.11	0.085	0.77	0.01
	35	Monod	2000	0.04	0.25		0.015
	35		2000	0.04	0.252	6.67	0.015
	25	Monod	3720	0.04	0.17		0.015
	25		3720	0.04	0.171	4.65	0.015
	20	Monod	4620	0.04	0.14		0.015
	20		4620	0.04	0.139	3.85	0.015

Table D.2b: Summary of Operating and Kinetic Parameters for Fermentation/Acidogenesis

Paper Consulted	Primary Reference	Model description	Kinetic Parameters					
			K_s (gCOD.m ⁻³)	Y	u_{max} (day ⁻¹)	k	K_d (day ⁻¹)	K_i (gCOD.m ⁻³)
1 Henze and Harremoës (1983)	Ghosh and Pohland (1974)		23	0.17 gVSS.gCOD ⁻¹	30		6.1	
2 Denopoulou <i>et al.</i> (1988)	Ghosh and Pohland (1974)			0.17 gVSS.gCOD ⁻¹			6.14	
3 Jeyaseelan (1997)	Mosey (1983)		680	0.12 gVSS.gCOD ⁻¹			0.015	6.87 gCOD.gVSS ⁻¹ .d ⁻¹
4 Jeyaseelan (1997)	Mosey (1983)		1270	0.12 gVSS.gCOD ⁻¹			0.015	4.85 gCOD.gVSS ⁻¹ .d ⁻¹
5 Jeyaseelan (1997)	Mosey (1983)		1580	0.12 gVSS.gCOD ⁻¹			0.015	3.85 gCOD.gVSS ⁻¹ .d ⁻¹
6 Lettinga (1995)	Lettinga (1995)			0.085-0.14				
7 Lettinga (1995)	Lettinga (1995)			0.094				
8 Jeyaseelan (1997)	Mosey (1983)		23	0.173 gVSS.gCOD ⁻¹			0.8	30 gCOD.gVSS ⁻¹ .d ⁻¹
9 Pavlostathis and Giraldo-Gomez (1991)	Huang (1983)		527		0.323			
10 Pavlostathis and Giraldo-Gomez (1991)	Zoetmeyer <i>et al.</i> (1982)		370	0.14	0.3			
11 Pavlostathis and Giraldo-Gomez (1991)	Ghosh and Pohland (1974)		22.5	0.17 gVSS.gCOD ⁻¹	1.25		6.1	
12 Kiely <i>et al.</i> (1997)	Kiely <i>et al.</i> (1997)	uncompetitive HAC inhibition		0.176 gVSS.gCOD ⁻¹	0.3			
13 Henze and Harremoës (1983)	McCarty (1971)		192	0.15 gVSS.gCOD ⁻¹				
14 Henze and Harremoës (1983)	Ghosh and Klaus (1978)		370	0.14 gVSS.gCOD ⁻¹	7.2			
15 Pavlostathis and Giraldo-Gomez (1991)	Ghosh and Klaus (1978)		427	0.15 gVSS.gCOD ⁻¹	0.3			
16 Pavlostathis and Giraldo-Gomez (1991)	Neilke <i>et al.</i> (1985)		8					1.33 gCOD.gVSS ⁻¹ .d ⁻¹
17 Pavlostathis and Giraldo-Gomez (1991)	Neilke <i>et al.</i> (1985)		75.3					70.6 gCOD.gVSS ⁻¹ .d ⁻¹
18 Hill and Barth (1977)	Hill and Barth (1977)	uncompetitive VFA inhibition	160	0.1875 g organism.gCOD ⁻¹	0.4		0.025	1000 VFA
19 Buffiere <i>et al.</i> (1995)	Denac <i>et al.</i> (1988)	Monod	140	0.036 gVSS.gCOD ⁻¹	1.2			640
20 Costello <i>et al.</i> (1991)	Mosey (1983)	Non-competitive Acetic acid inhibition	24 576	0.08 - 0.16 gVSS.gCOD ⁻¹				
21 Denopoulou <i>et al.</i> (1988)	Zoetmeyer <i>et al.</i> (1982)			0.34				
22 Lettinga (1995)	Lettinga (1995)			0.4				
23 Lettinga (1995)	Lettinga (1995)			0.54			0.43	9.5
24 Lettinga (1995)	Lettinga (1995)			0.17			0.79	2.5
25 Lettinga (1995)	Lettinga (1995)			0.10-0.18			0.87	179
26 Lettinga (1995)	Lettinga (1995)			0.12-0.17			6.1	63
27 Lettinga (1995)	Lettinga (1995)			0.06-0.08				24-33
28 Lettinga (1995)	Lettinga (1995)			0.13				11-19
29 Lettinga (1995)	Lettinga (1995)							74
30 Lettinga (1995)	Lettinga (1995)			0.11				0.4
31 Lettinga (1995)	Lettinga (1995)			0.21				1.6-2.2
32 Molella <i>et al.</i> (1986)	Lettinga (1995)			0.769				0.16
33 Henze and Harremoës (1983)	Molella <i>et al.</i> (1986)	uncompetitive acetic acid inhibition	277	0.26 gVSS.gCOD ⁻¹	1.5		0.03	
34 Henze and Harremoës (1983)	Sykes (1975)		200	0.21 gVSS.gCOD ⁻¹	0.16		0.03	
35 Henze and Harremoës (1983)	Andrews and Duarte (1980)		24.5					32 gCOD.gVSS ⁻¹ .d ⁻¹
36 Wu <i>et al.</i> (1998)	Wu <i>et al.</i> (1998)		2580					65 gCOD.gVSS ⁻¹ .d ⁻¹
37 Wu <i>et al.</i> (1998)	Wu <i>et al.</i> (1998)			0.04 - 0.2 gVSS.gCOD ⁻¹				
38 Henze and Harremoës (1983)	Massey & Pohland (1978)			0.17 gVSS.gCOD ⁻¹				
39 Henze and Harremoës (1983)	Sykes (1975)							
40 Costello <i>et al.</i> (1991)	Sykes (1975)							
41 Jeyaseelan (1997)	Mosey (1983)	Non-competitive Acetic acid inhibition	36.48	0.04 - 0.11 gVSS.gCOD ⁻¹			0.01 - 0.015	0.04896 gCOD.mg ⁻¹ .d ⁻¹
42 Jeyaseelan (1997)	Metcalf & Eddy (1981)		105 - 3180	0.1 gVSS.gCOD ⁻¹				0.77 - 13.8 gCOD.gVSS ⁻¹ .d ⁻¹
	Jeyaseelan (1997)		850					12 gCOD.gVSS ⁻¹ .d ⁻¹

Table D.1: Summary of Operating a

	Paper Consulted	Primary Reference	Feed	Substrate
1	Shimizu <i>et al.</i> (1993)	Shimizu <i>et al.</i> (1993)	solubilised sludge	
2	Shimizu <i>et al.</i> (1993)	Shimizu <i>et al.</i> (1993)	protein	
3	Shimizu <i>et al.</i> (1993)	Shimizu <i>et al.</i> (1993)	nucleic acid	
4	Shimizu <i>et al.</i> (1993)	Shimizu <i>et al.</i> (1993)	lipid	
5	Shimizu <i>et al.</i> (1993)	Shimizu <i>et al.</i> (1993)	carbohydrate	
6	Shimizu <i>et al.</i> (1993)	Shimizu <i>et al.</i> (1993)	carbohydrate	
7	Shimizu <i>et al.</i> (1993)	Shimizu <i>et al.</i> (1993)	cellulose	
8	Gujer and Zehnder (1983)	Ghosh <i>et al.</i> (1980)	cellulose	crude cellulose
9	Gujer and Zehnder (1983)	Heukelekian <i>et al.</i> (1958)	lipids	fatty acid esters
10	Gujer and Zehnder (1983)	Sawyer and Roy (1955)	lipids	greases
11	Gujer and Zehnder (1983)	Woods and Melina (1965)	lipids	greases
12	Gujer and Zehnder (1983)	Woods and Melina (1965)	lipids	lipids
13	Shimizu <i>et al.</i> (1993)	Shimizu <i>et al.</i> (1993)	raw sludge	
14	Pavlostathis and Giraldo-Gomez (1991)	Stack & Cotta (1986)	cellulose	
15	Eastman and Ferguson (1981)	Eastman and Ferguson (1981)	raw domestic primary sludge	
16	Gujer and Zehnder (1983)	Pfeffer (1969)	domestic sludge	
17	Gujer and Zehnder (1983)	Ghosh <i>et al.</i> (1980)	proteins	
18	Gujer and Zehnder (1983)	Ghosh <i>et al.</i> (1980)	hemicellulose	
19	Henze and Harremoës (1983)	Gujer and Zehnder (1983)		
20	Henze and Harremoës (1983)	Eastman and Ferguson (1981)		
21	Pavlostathis and Giraldo-Gomez (1991)	Pavlostathis <i>et al.</i> (1988)	cellulose	
22	Gujer and Zehnder (1983)	Woods <i>et al.</i> (1965)	proteins	
23	Gujer and Zehnder (1983)	Woods <i>et al.</i> (1965)	cellulose	
24	Gujer and Zehnder (1983)	Kasper (1977)	domestic sludge	
25	Gujer and Zehnder (1983)	Pfeffer (1969)	domestic sludge	
26	Bryers (1985)	Hamer <i>et al.</i> (1985)	biomass particulates	
27	Gujer and Zehnder (1983)	Eastman and Ferguson (1981)	domestic sludge	
28	Gujer and Zehnder (1983)	Eastman and Ferguson (1981)	domestic sludge	
29	Gujer and Zehnder (1983)	Eastman and Ferguson (1981)	domestic sludge	
30	Eliosov and Argaman (1995)	Eliosov and Argaman (1995)	degradable primary VSS	
31	Hamelers <i>et al.</i> (1998)	ten Brummeler (1991)	Organic Fraction of Solids municipal waste	
32	Pavlostathis and Giraldo-Gomez (1991)	Doyle <i>et al.</i> (1983)	corn stover	
33	Pavlostathis and Giraldo-Gomez (1991)	Doyle <i>et al.</i> (1983)	corn stover	
34	Pavlostathis and Giraldo-Gomez (1991)	Doyle <i>et al.</i> (1983)	corn stover	
35	Pavlostathis and Giraldo-Gomez (1991)	Doyle <i>et al.</i> (1983)	corn stover	
36	Pavlostathis and Giraldo-Gomez (1991)	Nagase & Matsuo (1982)	casein	
37	Pavlostathis and Giraldo-Gomez (1991)	Nagase & Matsuo (1982)	gelatin	
38	Pavlostathis and Giraldo-Gomez (1991)	Greco <i>et al.</i> (1983)	zein	
39	Pavlostathis and Giraldo-Gomez (1991)	Gujer & Zehnder (1983)	mixed primary and waste activated sludge	
40	Pavlostathis and Giraldo-Gomez (1991)	Gujer & Zehnder (1983)	mixed primary and waste activated sludge	
41	Pavlostathis and Giraldo-Gomez (1991)	Pfeffer (1974)	domestic refuse	
42	Pavlostathis and Giraldo-Gomez (1991)	Pfeffer (1974)	domestic refuse	
43	Pavlostathis and Giraldo-Gomez (1991)	Foree & McCarty (1969)	algae degradation by MPB and SRB	
44	Pavlostathis and Giraldo-Gomez (1991)	O'Rourke (1968)	Municipal raw sewage protein	
45	Pavlostathis and Giraldo-Gomez (1991)	O'Rourke (1968)	Municipal raw sewage cellulose	
46	Pavlostathis and Giraldo-Gomez (1991)	O'Rourke (1968)	Municipal raw sewage lipids	
47	Pavlostathis and Giraldo-Gomez (1991)	O'Rourke (1968)	Municipal raw sewage total COD	
48	Pavlostathis and Giraldo-Gomez (1991)	Ghosh (1981)	Municipal raw sewage activated sludge	
49	Pavlostathis and Giraldo-Gomez (1991)	Gujer & Zehnder (1983)	Complex biopolymers lipids	
50	Pavlostathis and Giraldo-Gomez (1991)	Gujer & Zehnder (1983)	Complex biopolymers protein	
51	Pavlostathis and Giraldo-Gomez (1991)	Gujer & Zehnder (1983)	Complex biopolymers cellulose	
52	Pavlostathis and Giraldo-Gomez (1991)	Gujer & Zehnder (1983)	Complex biopolymers hemicellulose	

Table D.2a: Summary of Operating and Kinetic Parameters for Fermentation/Acidogenesis

	Paper Consulted	Primary Reference	Feed	Operational Parameters					
				Substrate	Mode of Operation	pH	HRT (days)	Temp. (°C)	Culture
1	Henze and Harremoës (1983)	Ghosh and Portland (1974)		dextrose				37	mixed anaerobic
2	Denopoulou <i>et al.</i> (1988)	Ghosh and Portland (1974)		dextrose					
3	Jeyaseelan (1997)	Mosny (1983)		fatty acid				35	
4	Jeyaseelan (1997)	Mosny (1983)		fatty acid				25	
5	Jeyaseelan (1997)	Mosny (1983)		fatty acid				20	
6	Lettinga (1995)	Lettinga (1995)		gelatin	Dispersed culture CSTR				
7	Lettinga (1995)	Lettinga (1995)		gelatin	Dispersed culture UASB				
8	Jeyaseelan (1997)	Mosny (1983)		glucose	continuous			37	
9	Pavlostathis and Gralido-Gomez (1991)	Huang (1983)		glucose	continuous			37	
10	Pavlostathis and Gralido-Gomez (1991)	Zoetemeijer <i>et al.</i> (1982)		glucose	continuous			36.5	
11	Pavlostathis and Gralido-Gomez (1991)	Ghosh and Portland (1974)		glucose	CSTR			36	
12	Kelly <i>et al.</i> (1997)	Kelly <i>et al.</i> (1997)	primary sewage sludge/OFMSW	glucose		7.75		35	theoretical/model
13	Henze and Harremoës (1983)	McCarty (1971)		glucose				35	glucose enrichment
14	Henze and Harremoës (1983)	Ghosh and Klass (1978)		glucose	batch			35	
15	Pavlostathis and Gralido-Gomez (1991)	Ghosh and Klaus (1978)		glucose	continuous			35	
16	Pavlostathis and Gralido-Gomez (1991)	Nolke <i>et al.</i> (1985)		glucose	continuous			35	
17	Pavlostathis and Gralido-Gomez (1991)	Nolke <i>et al.</i> (1985)		glucose	continuous			35	
18	Hill and Barth (1977)	Hill and Barth (1977)	raw animal waste	glucose	semicontinuous			25	mixed anaerobic
19	Buffere <i>et al.</i> (1995)	Derat <i>et al.</i> (1988)	Glucose	glucose	FB Biofilm		15, 30, 45		Mixed
20	Costello <i>et al.</i> (1991)	Mosny (1983)	Glucose	glucose	High Rate Continuous				Mixed
21	Denopoulou <i>et al.</i> (1988)	Zoetemeijer <i>et al.</i> (1982)		glucose					
22	Lettinga (1995)	Lettinga (1995)		glucose	Acid producing sludge				
23	Lettinga (1995)	Lettinga (1995)		glucose	Acid producing sludge				
24	Lettinga (1995)	Lettinga (1995)		glucose	Mixed culture				
25	Lettinga (1995)	Lettinga (1995)		glucose	Mixed culture				
26	Lettinga (1995)	Lettinga (1995)		glucose	Dispersed culture CSTR				
27	Lettinga (1995)	Lettinga (1995)		glucose	Dispersed culture UASB				
28	Lettinga (1995)	Lettinga (1995)		glucose	Aggregates UASB				
29	Lettinga (1995)	Lettinga (1995)		glucose	Aggregates gas lift				
30	Lettinga (1995)	Lettinga (1995)		glucose	Granular sludge 1 step UASB				
31	Lettinga (1995)	Lettinga (1995)		glucose	Granular sludge 2 step UASB				
32	Lettinga (1995)	Lettinga (1995)		glucose					
33	Medetta <i>et al.</i> (1986)	Medetta <i>et al.</i> (1986)		glucose					theoretical
34	Henze and Harremoës (1983)	Sykes (1975)		glucose					
35	Henze and Harremoës (1983)	Andrews and Duarte (1980)		glucose					
36	Wu <i>et al.</i> (1998)			glucose					
37	Wu <i>et al.</i> (1998)			glucose					
38	Henze and Harremoës (1983)	Sykes (1975)		hexose					
39	Henze and Harremoës (1983)	Sykes (1975)		hexose					
40	Costello <i>et al.</i> (1991)	Mosny (1983)	Glucose	Lactate	High Rate Continuous				Mixed
41	Jeyaseelan (1997)	Medcalf & Eddy (1991)		lipids					
42	Jeyaseelan (1997)	Jeyaseelan (1997)		lipids					

